Methanol oxidation on transition elements oxides

Abdulmohsen Alshehri

School of Chemistry, Cardiff University

PhD Thesis 2013

Abstract

Methanol oxidation to formaldehyde is one of the most important industries in our lives; the reaction occurs on catalyst surface in heterogeneous catalysis. Iron molybdate is the current selective catalyst. However, molybdenum volatilises during methanol oxidation and leaving the catalyst with a low molybdenum ratio, which deactivates the catalyst, a 2.2 Mo: 1Fe iron molybdate catalyst was used instead the stoichiometric catalyst, while yield of formaldehyde cannot be 100%. The goal of this study is to find more selective and more productive catalyst than iron molybdate catalyst, the first step is to find another transition element as selective as molybdenum, because molybdenum is the selective part, and iron is the active part, the resulting iron molybdate catalyst is a selective catalyst to formaldehyde near molybdenum and active near iron. Experimentally, catalysts were prepared using co-precipitation method, however, some doped catalysts were papered by incipient wetness impregnation, also sol-immobilization was used to prepare nano-gold particles on the surfaces of few supports. Catalysts characterizations were carried out within several techniques for the surface analysis (XPS) and bulk analysis (XRD), also the surface area was measured by BET equipment. Raman too was used in this study, while micro-reactor was the reactor to determine selectivity and activity of each catalyst. When molybdenum replaced by vanadium, the catalyst yielded 100% formaldehyde at 200 ^{o}C; moreover, tungsten was selective. Likewise, iron was replaced by other active metals such as manganese, copper and bismuth, which are active. Nano-gold improved activity when doped on molybdenum oxide and iron molybdate supports.

Acknowledgment

By the name of Allah, the most gracious and the most merciful, I thank him for his goodness. Then I thank my wife who helped me throughout my study, also I thank my mother, my father, my friends and all other were supporting me during my study. Thanks to my supervisors Mike Bowker and Albert Carley.

I thank King Abdulaziz University in Saudi Arabia, The royal embassy of Saudi Arabia and Saudi Arabian cultural bureau in London for their found and support.

I thank Cardiff University, that give me a chance to study this course, and allow me to use all facilities in or out the university during my study.

Contents

1. Introduction

1.1 Heterogeneous Catalysis

A catalyst is a substance that accelerates the rate of a reaction to occur faster than an uncatalysed reaction, but it does not convert, or chemically change, at the end of the reaction, or appear in the overall reaction equilibrium composition. Catalysis is the process whereby reactions are accelerated through the effects of a catalyst. Heterogeneous catalysis occurs when the catalyst and the reactants are different in phases. Solid catalyst and gaseous reactants are the most commonly used in heterogeneous catalysis. The exhaust catalytic gas system in automobile is an example of a heterogeneous catalytic system.

A catalyst simply provides a lower energy path for molecules to break and reform their bonds, as is required for a chemical reaction. It lowers the level of activation energy (ΔEg) that is necessary to break bonds, and then reacts to products by making new bonds [1].

1.1.1 Importance of catalysis

Catalysis is an important field for modern industry and economy, as well as for the environment and health. Approximately 90% of chemicals and materials are produced using catalysis, which saves energy that would be consumed in industry, and helps the economies of chemical exporting countries.

The most well-known example of how catalysis protects our environment is in cars. Each car is built with a catalytic exhaust to convert and reduce pollutants such as NO, which are emitted by cars and would otherwise damage the environment. All living matter vitalises enzymatic catalysis, including photosynthesis. This is a process for gaining energy from light, where photons are absorbed by chlorophyll and the energy is stored as separated charges. Then a number of enzymes work as catalysts to produce sugar, which is the chemical energy source.

In recent times, catalysis has become more important in further applications. It is used in oil cracking with wide range products. Furthermore, in

the future catalysis will be needed for finding new ways to produce chemicals from alternative sources, finding new alternative energy sources and engaging more in environment protection.[1]

1.1.2 Catalytic cycle

The oxidation of carbon monoxide demonstrates the formation of products from the heterogeneous catalytic reaction of a solid-gas system as in Fig. 1.1, and this reaction takes place in automobile exhaust catalysis (Pt catalysts, invented by Eugene Houdry in1950). Molecules from the gas phase adsorb on a metal surface; molecules bond with the surface in molecular form; and then the adsorbed oxygen molecules dissociate into atoms, but the CO does not dissociate because of its high internal bond strength (1076 KJ/mol), compared with oxygen (500 KJ/mol). The next step is that the oxygen atoms react with the CO to form carbon monoxide, which is the adsorbed product. The rate-determining step is the surface reaction step: the product, which is carbon dioxide in this reaction, is desorbed from the surface into the gas phase.

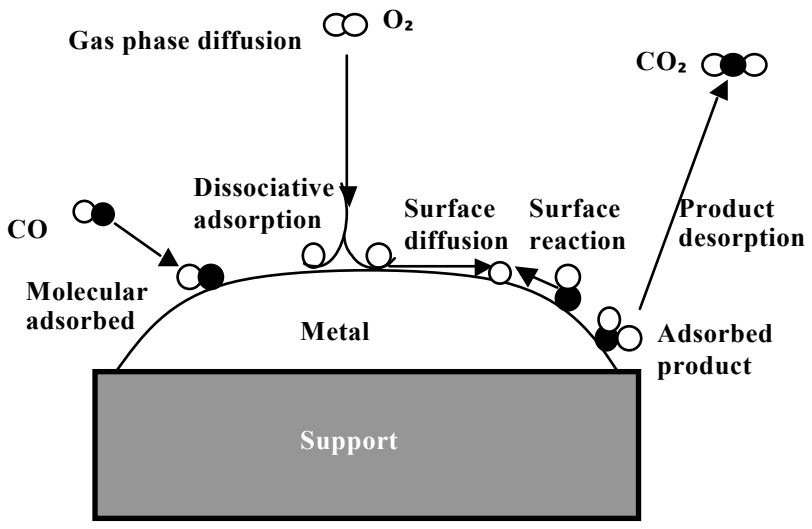

Fig. 1.1 Solid surface- gas reactants heterogeneous catalytic system.

In the gas phase, the reaction activation energy, ΔEg, is high, as in Fig. 1.2. Before it can make new bonds, a large amount of energy needs to be spent to break the reactant bonds. On the catalyst surface, reacting molecules are

stabilised during the reaction because of the bonding sites on the catalyst; that provides lower energy for the molecules to break and reform their bonds, and this bonding stabilises the intermediates in the reactions.

Consequently, activation barriers in a catalysed reaction are lower than in an uncatalysed one, and the reaction is accelerated. A catalyst lowers the activation barriers to increase the reaction rate and speeds the approach to equilibrium without affecting the equilibrium concentration.[1,2]

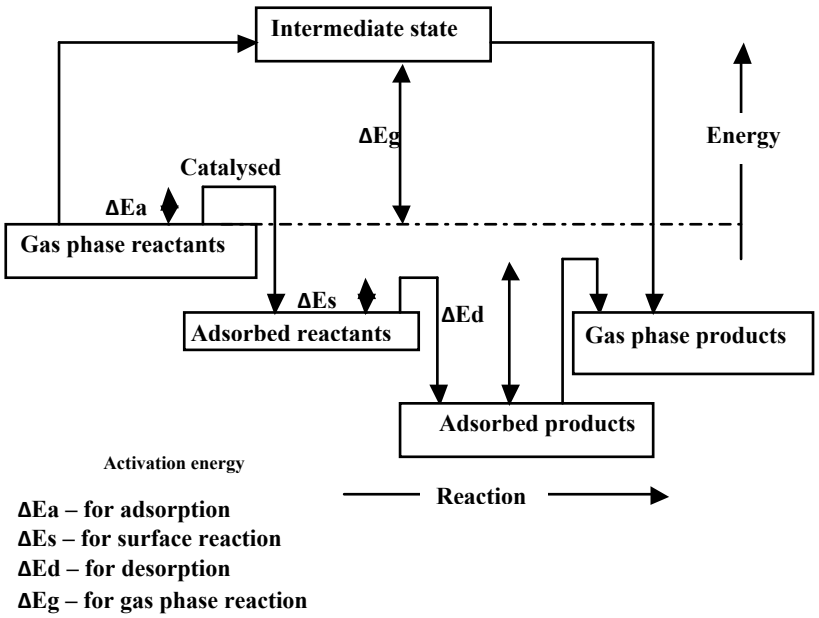

Fig. 1.2 Activation energies and catalytic reaction.

1.1.3 Adsorption on a surfaces

Fig. 1.1 shows that adsorption is the first reactive step in the heterogeneous catalytic cycle. There are two types of adsorption: physical adsorption and chemical adsorption. Physical adsorption occurs between all gases and all solids; it does not form a real chemical bond between molecules and surface, though, and is caused by van der Waals forces. Chemical adsorption, which is also called chemisorption (Newns-Anderson)[44,45], is a stronger adsorption, which is caused by breaking and weakening the molecules' bonds to make a new bond between the adsorbate and the surface.

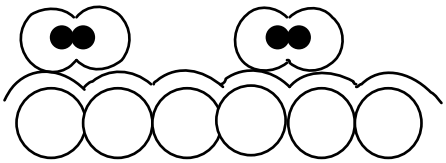

Fig. 1.3 Physical adsorption on a surface

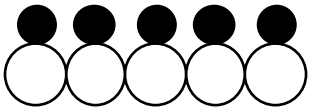

1.4 Chemical adsorption on a surface

In principle, physical adsorption appears when a molecule approaches a surface, attracted by van der Waals forces, which to essentially caused by electrostatic polarisation between the molecule and the surface. As the molecule approaches nearer to the surface, as shown in Fig. 1.3, repulsion occurs owing to the nearness of the outer electronic orbital of the surface and the molecule. As a result, only a low energy level is needed to accommodate the molecule; and the heat of adsorption, ΔH(p), is low (~20 KJ/mol). It is a weak adsorption; because the molecule is distant from the surface in comparison with chemical adsorption (figure 1.4), as can be seen in Fig 1.5. Frenkel's equation (Frenkel, 1924) can be used to approximate the time that the molecule stays adsorbed on the surface, $\tau = \tau_o e^{[E/RT]}$, where τ is the surface lifetime, τ_o is the lifetime of the surface vibration ($\sim 10^{-13}$ s) and the adsorption energy is E.

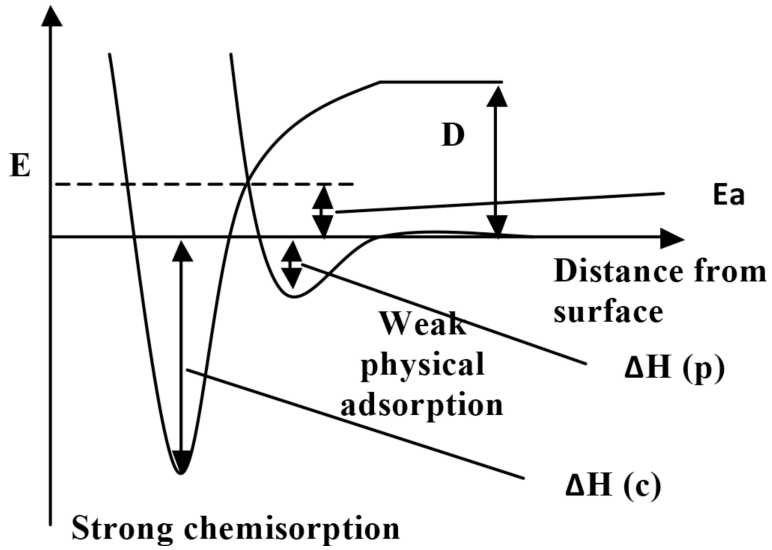

Figure 1.5 Lennard Jones-type description of adsorption energetics [2]

Chemical adsorption creates a real bond with the surface. Fig 1.4 shows that the molecule has to be close to the surface. Fig 1.5 shows the gas phase dissociation energy (D), when the molecule approaches the surface the potential energy falls to a deep minimum at a close distance from the surface, and the heat

of chemical adsorption, ΔH (c), is much higher than the heat of physical adsorption ΔH (c).[1, 2]

It is recognised that a catalyst affects the rate of a reaction; it lowers the activation energy of the reaction, and makes a new pathway with lower energy by bonding the reactant molecules to the surface to reach a more stable state. A catalyst increases the rate of a reaction, for example:

$$\mathbf{A + B \rightleftharpoons C + D} \qquad \textbf{(Eq 1.1)}$$

The rate of this reaction is:

$$-\frac{\mathbf{d[A]}}{\mathbf{dt}} = \mathbf{k[A]^n\,[B]^m}$$

Where $\mathbf{k = A\ exp^{(-E\ /\ RT)}}$, and, from Fig 1.2, E is the activation energy of the reaction in the gas phase at T temperature.

Hence, the reaction rate is increased by reducing ΔEg or increasing factor (**a**). In a catalysed reaction, both A and B are adsorbed on the surface and need lower energy to react, to products bonded to the surface. To summarise, heterogeneous catalysis is mainly the study of gas molecules adsorbed on a catalyst surface, and the behaviour of a catalyst in a particular reaction.[1,2]

1.2 The selective oxidation of methanol

This section gives a short introduction to methanol, formaldehyde and formaldehyde production, either by oxidation or by oxidative dehydrogenation. It will show a thermal study for reactions may occur ether desired or as side reaction and determining the favoured reaction. The current catalyst of methanol oxidation will be illustrated in terms of industrial plant and processes.

1.2.1 Methanol properties

Methanol, CH_3OH, is colourless, volatile and flammable, with a distinctive odour; it has an molecular mass of 32.04 g mol^{-1} and a density of

0.7918 g cm^{-3}. The boiling point of alcohols is higher compared with alkalines owing to the positivity of –OH, as polarised hydrogen is attracted to negative polarised oxygen in another molecule, and causes a weak force that leads to extra energy, which has to be overcome to let the molecules in the liquid phase evaporate. Methanol boils at 65°C and melts at -97.8°C; it is soluble in water. Methanol is a water derivative with one –H molecule replaced by a $–CH_3$ one, with a tetrahedral angle of 109°. Methanol is a weak acid with 15.5 pKa, which is similar to water's pKa of 15.7. However, methanol's acidity is greater than methane's because of the strong electronegativity of the oxygen attached to the proton, which stabilises the negative charge of the alkoxide ion. It is also a weak base, as a strong acid protonates the hydroxyl group, making an alkyloxonium ion. A substance with a Lewis acidity accepts an electron pair, whereas a Lewis base is a material that donates a pair of electrons. When a substance has a polar bond to hydrogen, either a low energy orbital or a vacant orbital, it becomes a Lewis acid. For example, methanol is a proton donor, as in Eq 1.2:

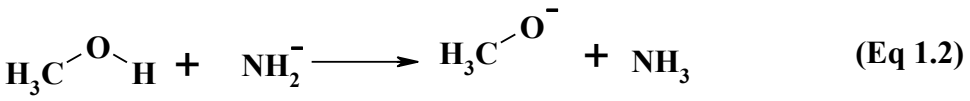

(Eq 1.2)

Methanol can also be a Lewis base, when the methanol has a lower acidity and is protonated by the higher acidity reactants of the electron donors, as in catalytic reactions:

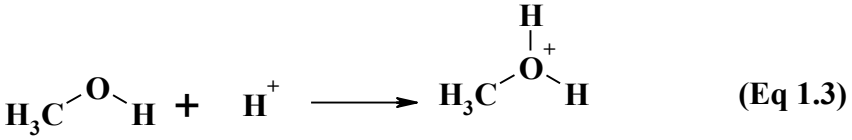

(Eq 1.3)

Alcohols dehydrate by removing the water group from their molecules, and then converting the alcohols to ethers in a strong acid or a catalysed acid. However, the case with methanol is firstly protonation of methanol in acidic conditions, and then another methanol molecule would attack the protonated methanol to eliminate the H_2O and form dimethyl ether.

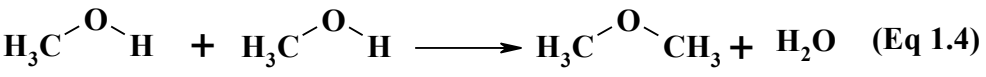

(Eq 1.4)

Methanol can be oxidised to formaldehyde, and further oxidation leads to the formation of formic acid or even full oxidation to carbon dioxide.[3,4,5]

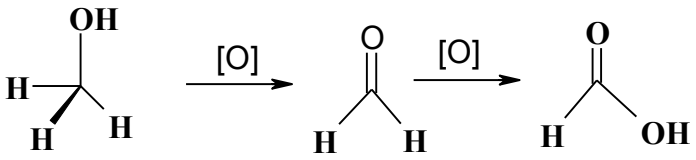

(Eq 1.5)

Methanol can be produced in many ways, owing to the improvements in methanol synthesis technology since it was first introduced by BASF in 1923. Hydrogenation of carbon monoxide mixture with CO_2 can be catalysed by ZnO-Cr_2O_3 at pressure of 240–300 bars and 350–400°C temperature on a large scale. Methanol formation is:

$$CO + CO_2 + 2H_2 \rightarrow CH_3OH \qquad (\Delta H_{298} = -91\ KJ/mol) \quad \textbf{(Eq 1.6a)}$$

$$CO_2 + 3H_2 \rightarrow CH_3OH + H_2O \qquad (\Delta H_{298} = -49\ KJ/mol) \quad \textbf{(Eq 1.6b)}$$

A mixed catalyst of copper, zinc oxide and alumina was later developed, replacing the zinc chromate to produce methanol from hydrogen and carbon monoxide at 250–280°C and pressure of 60–80 bars.

$$CH_4 + H_2O \rightarrow CO + 3H_2 \qquad (\Delta H_{298} = 206.1KJ/mol) \qquad \textbf{(Eq 1.7)}$$

$$CO + H_2O \rightarrow CO_2 + H_2 \qquad (\Delta H_{298} = -40.1\ KJ/mol) \qquad \textbf{(Eq 1.8)}$$

$$CO_2 + H_2 \rightarrow CH_3OH + H_2O \qquad (\Delta H_{298} = 40.9\ KJ/mol) \qquad \textbf{(Eq1.9)}$$

Steam methane reforming (SMR) is applied to methanol synthesis. In fact, SMR is an endothermic reaction on an Ni-based catalyst. The reaction operates at 900°C and pressure of 70 bar. However, the stoichiometry of methanol synthesis has to be adjusted by increasing the H_2/CO ratio. H_2O and CO are reacted within water gas shift reaction to give CO_2 and H_2. The ideal H_2/CO is near ~2[8,9].

Methanol is used in many applications; and the most important use is the production of other chemicals. It is the feedstock of formaldehyde and also produces dimethyl ether. Methanol is used in fuel cells for electricity generation at low temperatures and low pressure. In 2005 Toshiba produced a fuel cell with

direct methanol fuel cell (DMFC) technology. It is the smallest available fuel cell (22 x 56 x 4.6 mm), so it can be used to generate power for even small electrical devices, like laptops and mobile phones. It is an alternative renewable source as it can be produced from wood or bio-alcohol to operate cars and engines instead of petroleum, for example, in drag cars and Indy cars in the USA.[6,7,8]

1.2.2 Formaldehyde properties

Formaldehyde, H_2CO, is also called methanal, , it is a colourless gas with a pungent odour, and it melts at -92°C and boils at -21°C. It appears in two polymerised forms as a solid. The first contains four carbon atoms, each bonded to two oxygen and two hydrogen atoms, as shown in Fig 1.7. The other polymerised formaldehyde is polyhydroxyaldehydes, which contains six carbon atoms and a four-hydroxyl group, as shown in Fig 1.8.

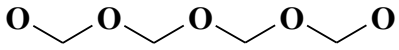

Polymethylenes

Fig 1.7 Polymethylenes

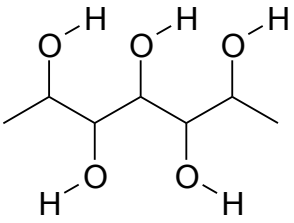

Polyhydroxyaldehdyes

Fig 1.8 Polyhydroxyaldehdyes

There is a bond polarity effect on aldehyde that is caused by the polarised bond between oxygen and carbon, C==O, where carbon is a Lewis acid by reason of its electrophilic negative and positive polarisation. The carbonyl oxygen behaves as a Lewis base and has a nucleophile with negative polarisation. Aldehydes can be easily converted to carboxylic acid by oxidation, because the hydrogen can be removed in the oxidation reaction.

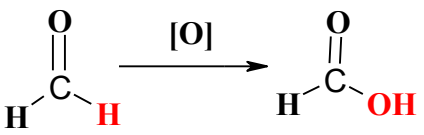

Formaldehyde **Formic acid**

Eq 1.10

Aldehydes are easily reduced to alcohol by carbonyl reduction, which involves adding a nucleophilic like hydride. The negatively charged hydride ion forms an alkoxide ion under basic conditions. The alkoxide ion is an intermediate stage before it is protonated to be alcohol, as shown in Eq 1.11.

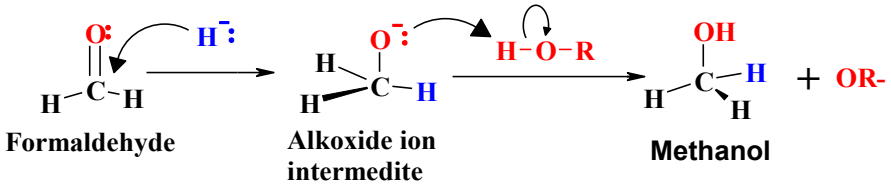

Eq 1.11

The nuclephilic addition of water to aldehydes forms carbonyl hydrates, also called germinal (gem) diols. Gem produces aldehyde again by eliminating water and creating equilibrium between the hydrates and aldehydes (Eq 1.12). Formaldehyde in its aqueous solution prefers to be in hydrate form more than in aldehyde form, where formaldehyde aqueous solution consists of only 0.1% aldehyde and 99.9% hydrate.[7]

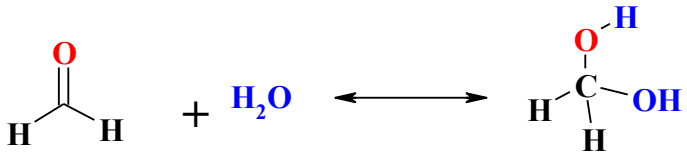

Eq 1.12

Formaldehyde **Carbonyl hydrate(gem diol)**

Methanol is the only feedstock for formaldehyde in the industrial production of formaldehyde. There are two manufacturing catalytic reactions for formaldehyde. One is oxidation of methanol on a mixture of iron and molybdenum, which is called iron molybdate. In this reaction methanol is adsorbed on the surface of the iron molybdate, and reacts with lattice oxygen to form formaldehyde and water at a temperature of 350°C (Eq 1.13), then oxygen gas reoxidized the surface.

$$CH_3OH_{(g)} + \tfrac{1}{2}\, O_{2(g)} \rightarrow HCHO_{(g)} + H_2O_{(g)} \quad (\Delta H_{298} = -156\ KJ/mo) \quad \textbf{(Eq 1.13)}$$

The other way of producing formaldehyde is by dehydrogenation of the methanol in an endothermic reaction. The reaction takes place at a higher temperature than the oxidation reaction, at approximately 600°C, and on a larger scale silver catalysts (Eq 1.14).

$$CH_3OH_{(g)} \rightarrow HCHO_{(g)} + H_{2(g)} \quad (\Delta H = +80\ KJ.\ mol^{-1)}\ (Eq\ 1.14)$$

Formaldehyde is a raw material that is used worldwide in more than 40 products. It is important in the production of resins and polymers, adhesives, and thermoset plastic. It is also used in residential construction, automobiles, civilian and military aircraft and health care. It kills most bacteria and viruses, including the unwanted viruses in vaccines production. Its derivatives are used in creams and beauty products, as an embalming agent, as a fixative for microscopy, and in dentistry [9]. Some examples of formaldehyde's derivatives are in Table 1.1:

Derivative	Properties	Brief summary of use
(UF) Urea formaldehyde	Resins, thermoset, high tensile strength, low water absorption, high surface hardness	Adhesives, decorative laminates, paper, wood glue
(UFFI) Urea formaldehyde foam insulation	Mix of urea formaldehyde and foam	Building walls, saving energy
(MF) Melamine formaldehyde resin	Thermoset plastic, strong	Kitchen, countertops, laminate floors, furniture
(PF) Phenol formaldehyde resin	Thermoset resin, produced from phenol and formaldehyde	Circuit boards, lab benchtops, adhesives, fibreglass, micro-balloons for density control
(POM) Polyoxymethylene	Thermo plastic, high strength and low coefficient of friction	Valves, screws, springs, TVs, other electronic devices
(MDI) Methylene diphenyl diisocyanate	Reacts with polyols to give polyurethane	Thermal insulators, adhesives, high strength glue

Table 1.1 Derivatives of formaldehyde and their uses

1.2.3 Methanol oxidation selectivity

Methanol is converted to formaldehyde in heterogeneous catalysed reactions, the oxidation of methanol over an iron molybdate catalyst. Methanol molecule reacts with the catalyst surface and forms a methoxy group. This happens by losing one hydrogen atom to make the hydroxyl group, causing another hydrogen atom to be subtracted that methoxy group by neighbouring terminal oxygen, leading to the formation of formaldehyde. The formaldehyde molecule then desorbs; and water forms and desorbs. The consumed oxygen from the surface will be occupied from the gas phase.

Methanol collides with the surface of the catalyst and sticks to it for a short time, when the binding energy barrier has been overcome, the methanol binds to the surface chemically and behaves as a Lewis acid by donating one proton from its hydroxyl group. Once the hydrogen reacts with the terminal oxygen of the metal surface, the methoxy bonds to the Mo of the iron molybdate surface (Eq 1.15)[10].

$$CH_3OH_{(g)} + O_{(t)} \rightarrow CH_3O_{(a)} + OH_{(a)} \qquad \textbf{(Eq 1.15)}$$

(O_t = terminal oxygen)

After adsorption of the methanol, the Mo is reduced to a 5+ oxidation state, an intermediate state as illustrated in Scheme 1.1. The bridging oxygen will attack the bonded methoxy and take one hydrogen atom to form another hydroxyl, as shown in Eq 1.16[11].

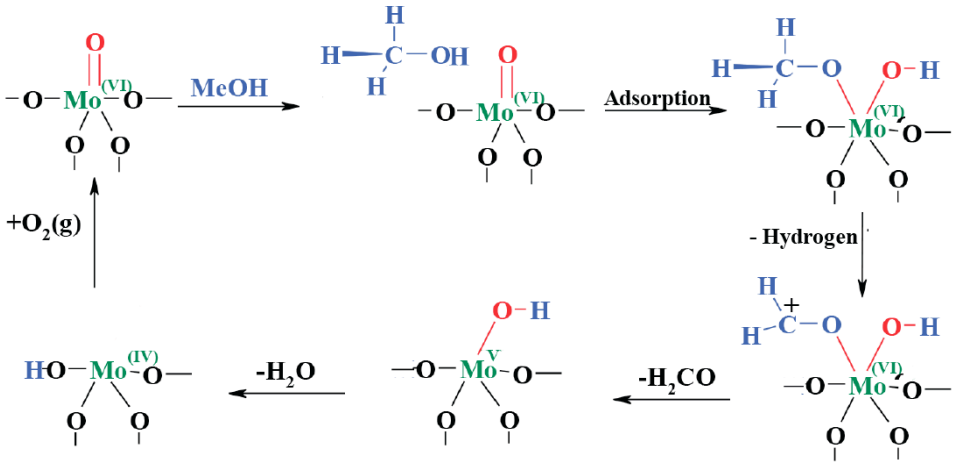

Scheme 1.1 Molybdenum oxidation states during methanol oxidation

$$CH_3O_{(adsorbed)} + O_{(bridging)} \rightarrow H_2CO_{(gas)} + OH_{(adsorbed)} \quad \textbf{(Eq 1.16)}$$

Mo is in its 4+ oxidation state; later, the formaldehyde desorbs and water is formed, as in Eq 1.17. At the end there is one surface oxygen from the two hydroxyls, the other having been replaced by anion vacancy, which is then reoxidised by ether oxygen from the bulk lattice, as in Eq 1.18, or by consuming oxygen gas, as in Eq 1.19.

$$2OH_{(adsorbed)} \rightarrow H_2O_{(gas)} + O_{(surface)} + V_{(surface)} \quad \textbf{(Eq 1.17)}$$

$$V_{(surface)} + O_{(lattice)} \rightarrow V_{(lattice)} + O_{(surface)} \quad \textbf{(Eq 1.18)}$$

$$2V_{(surface)(s)} + O_{2(gas)} \rightarrow 2\ O_{(surface)} \quad \textbf{(Eq 1.19)}$$

Carbon monoxide is one of methanol's oxidation products, when methanol reacts with the metal surface oxygen, forming formaldehyde, which later reacts with the extra bridging oxygen and reforms CO and water, as shown in Eq 1.20. CO is produced during the formation of formaldehyde. As more formaldehyde is produced, the amount of carbon monoxide increases. Carbon monoxide can also be produced by dehydrogenation of methanol, which is an endothermic reaction, as shown in Eq 1.21.

$$CH_2O_{(adsorbed)} + O_{(bridging)} \rightarrow CO_{(gas)} + H_2O_{(gas)} + V_{(surface)} \quad \textbf{(Eq 1.20)}$$

$$CH_3OH \rightarrow CO + 2\ H_2 \qquad \Delta H = +88\ KJ/mol \quad \textbf{(Eq 1.21)}$$

Another possible side reaction is the formation of HCOOH bonded to the surface, which either dehydrates to carbon monoxide and water, or oxidises and burns to carbon dioxide and water, as an Eq 1.22 and Eq 1.23.

$$HCOOH_{(adsorbed)} \rightarrow CO_{(gas)} + H_2O_{(gas)} \quad \textbf{(Eq 1.22)}$$

$$HCOOH_{(adsorbed)} + O_{(surface)} \rightarrow CO_{2(gas)} + H_2O_{(gas)} \quad \textbf{(Eq 1.23)}$$

Dimethyl ether is the dehydration product of methanol, which is formed by eliminating the water molecule from the two methanol molecules reacting on the metal surface. The reaction usually occurs at a low temperature at low conversion of methanol. The reason behind this is that the Lewis acidity site of the catalyst is used to oxidise the methanol. According to the Lewis acidity rule, the methanol will be a Lewis base and donate the electron pair to the surface, which is then protonated with another methanol molecule on the surface and reforms CH_3OCH_3 and water, as shown in Eq 1.24.

$$\mathbf{2CH_3OH_{(g)} \rightarrow CH_3OCH_{3(g)} + H_2O_{(g)}} \qquad \textbf{(Eq 1.24)}$$

Methane can be produced in a side reaction of methanol oxidation over some catalyst. The hydrogenation of methanol generates CH_4 and oxygen, as in Eq 1.25. It is an endothermic reaction.[10,11]

$$\mathbf{CH_3OH_{(g)} \rightarrow CH_{4(g)} + 1/2O_{2(g)}} \qquad \mathbf{\Delta H = +27\ kJ/mol} \qquad \textbf{(Eq 1.25)}$$

1.2.4 Thermodynamics and reaction favourability

Thermodynamics is the field that demonstrates reaction favourable pathways, affected by energetics of reactant and products and the change of heat. Enthalpy change, ΔH, is how much heat is involved in a chemical system and chemical reaction. The enthalpy change for a reaction is difference in enthalpy between the products and the reactants, depending on temperature and pressure. Eq 1.26 calculates H, where U is the internal energy, P is pressure and V is volume.

$$\mathbf{H = U + PV} \qquad \textbf{(Eq 1.26)}$$

The enthalpy change of a reaction could be determined over standard conditions of 298.15 Kelvin and 1 bar; which gives the symbol ΔH^o. Positivity of enthalpy change means that a reaction is endothermic, whereas negativity means

that a reaction is exothermic. An example is in Eq 1.27, where ΔH^{o}_{p} is enthalpy for products (C) and ΔH^{o}_{r} is enthalpy for reactants (A+B), at 298 K.

$$\mathbf{A + B \rightarrow C} \qquad \textbf{(Eq 1.27)}$$

$$\mathbf{\Delta H^{o} = \Delta H^{o}_{p} - \Delta H^{o}_{r}} \qquad \textbf{(Eq 1.28)}$$

At a different temperature, the C_p constant is heat capacity at constant pressure, which is the required heat to raise the temperature for 1 mole of substance, so the enthalpy increases by increase of temperature, as shown in Eq 1.29.

$$\mathbf{d}\boldsymbol{H} = \mathbf{C_p}\ \mathbf{d}\boldsymbol{T} \qquad \textbf{(Eq 1.29)}$$

There are reactions that occur with no change of internal energy, in other words, without heat change. There is another factor that drives the reaction route, which is entropy, or randomness and disorder of the reaction. An increase of entropy means an increase in spontaneous processes. The entropy can be calculated as shown in Eq 1.30, where ΔS is the change in entropy from the initial state to the final state, and heat is added to the reaction reversibly at a temperature T.

$$\mathbf{\Delta S = q_{rev} / T} \qquad \textbf{(Eq 1.30)}$$

The change in entropy is calculated at absolute conditions at a temperature of 0 Kelvin. The third law of thermodynamics says that entropy for a perfect crystal is zero at a temperature of 0 Kelvin. Entropy can also be found at standard conditions of 1 bar pressure and 298.15 Kelvins of temperature, ΔS° entropy for a chemical reaction means the difference in entropies between the products and the reactants at standard conditions (298K, 1bar); it is shown in Eq 1.31 and Eq1.32, where ΔS^{o}_{p} is product entropy and S^{o}_{r} is reactants entropy ($S^{o}_{r(A)} + S^{o}_{r(B)}$).

$$A + B \rightarrow C \qquad \textbf{(Eq 1.31)}$$

$$\Delta S^o = \Delta S^o_p - S^o_r \qquad \textbf{(Eq 1.32)}$$

Over the range of temperature, ΔC_p, the heat capacity can be calculated, for example from T_1 to T_2, so the entropy will change from ΔS_{T1} to ΔS_{T2}, as shown in Eq 1.33.

$$\Delta S_{T2} = \Delta S_{T1} + \Delta C_p \ln (T_2 / T_1) \qquad \textbf{(Eq 1.33)}$$

Gibbs free energy

Free energy is the relation between the energy change given by a change of enthalpy and disorder achievement by a change of entropy. Free energy can be negative, which denotes a spontaneous reaction. When it is positive it is non-spontaneous. Eq 1.34 shows the relationship between free energy, enthalpy, entropy and temperature.

$$G = H - TS \qquad \textbf{(Eq 1.34)}$$

The free energy of a chemical reaction means the difference between products' free energy and reactants' free energy. At standard conditions, which are 298.15 Kelvins and 1 bar, Eq 1.35 and Eq 1.36 are examples of Gibbs free energy, where ΔG^o_p is product Gibbs free energy and G^o_r is reactants Gibbs free energy ($G^o_{r(A)} + G^o_{r(B)}$).

$$A + B \rightarrow C \qquad \textbf{(Eq 1.35)}$$

$$\Delta G^o = \Delta G^o_p - G^o_r \qquad \textbf{(Eq 1.36)}$$

Table 1.2 shows the thermodynamics of various reactions, depending on free energy and temperature. When a reaction is exothermic and has increased

entropy, then the reaction is product-favoured, and the increase of temperature increases the free energy of the reaction. When a reaction is endothermic and entropy decreases, it leads to a reactant-favoured reaction. However, in the case of exothermic reaction with decreased entropy, the Gibbs free energy value depends on the temperature, which may increase $-T\Delta S > 0$, whereas in an endothermic reaction with increased entropy the temperature will decrease $-T\Delta S < 0$, and Gibbs free energy will be more negative.

ΔH	ΔS	ΔG	Reaction status
Exothermic(-)	**Increase (+)**	**Negative (-)**	**Spontaneous**
Endothermic(+)	**Decrease (-)**	**Positive (+)**	**Non-spontaneous**
Exothermic(-)	**Decrease (-)**	**Varies dependent**	**Depends on T**
Endothermic(+)	**Increase (+)**	**Varies dependent**	**Depends on T**

Table 1.2 Thermodynamics of various reactions

$$(d\Delta G/dT)_p = -\Delta S \qquad \textbf{(Eq 1.37)}$$

At constant pressure dp = 0, Eq 1.37 shows the dependence of Gibbs free energy on temperature. The rule is that with an increase of temperature the Gibbs free energy depends on signs.[12]

Thermochemistry and adsorption

Adsorption is a chemical process that involves either a real bond between the adsorbent and the adsorbate, or just a weak interaction caused by van der Waals forces. Adsorption, as illustrated in section one, mainly decreases the energy barrier of reactant chemicals after being adsorbed and bonded to the surface and then reacts and converts to products. Thus, adsorption depends on enthalpy, entropy and Gibbs free energy; it involves change of heat. In the gas-solid system adsorption is an exothermic reaction, and the heat is related to the coverage of gas on the surface. The heat of adsorption is determined using a calorimeter, as shown in Eq 1.38, where *n* is the number of gas mole adsorbed, ΔH_a is the heat involved, and q is the heat of the adsorption at a constant volume.

$$q = (\Delta H_a/n)_V \quad \text{(Eq 1.38)}$$

$$A_{(g)} + S \rightarrow A\text{-}S \quad \text{(Eq 1.39)}$$

$$\Delta G^\circ = \Delta H^\circ - T\Delta S^\circ = -RT \log K^\circ \quad \text{(Eq 1.40)}$$

The heat of adsorption depends on the coverage; an example is shown in Eq 1.39 and Eq 1.40, where S is the surface site, A is the gas, which would adsorb, and K° is the equilibrium constant. The occurrence of adsorption also depends on the entropy of the surface. Afterwards, gas may dissociate and react adsorbed products, and the products are then desorbed.

Methanol oxidation thermodynamics

Equation	ΔH kJ/mol	ΔS kJ/mol	ΔG kJ/mol
$CH_3OH_{(g)} + 1/2\ O_{2\ (g)} \rightarrow HCHO_{(g)} + H_2O_{(g)}$	-164	-72	-123
$CH_3OH_{(g)} \rightarrow HCHO_{(g)} + H_{2(g)}$	+80	-122	+145
$CH_3OH_{(g)} \rightarrow CO + 2\ H_2$	+88	-245	+218
$CH_3OH_{(g)} + O_{2(g)} \rightarrow CO_{(g)} + 2H_2O_{(g)}$	-400	-145	-389
$CH_3OH_{(g)} + 3/2\ O_{2(g)} \rightarrow CO_{2(g)} + 2H_2O_{(g)}$	-707	-55	-688
$2CH_3OH_{(g)} \rightarrow CH_3OCH_{3(g)} + H_2O_{(g)}$	-27	+15	-34
$CH_3OH_{(g)} \rightarrow CH_{4(g)} + 1/2\ O_{2(g)}$	+124	-53	+153

Table 1. 3 Thermodynamic data for reactions at 250°C

Table 1.3 shows that dehydrogenation reactions are endothermic reactions, methanol is dehydrogenated to formaldehyde and hydrogen over a silver oxide catalyst, and a large amount of energy is consumed to feed the reaction. The oxidation reaction is catalysed by an iron molybdate, the most favoured reaction is the combustion of methanol to either carbon monoxide or carbon dioxide, or both. However, formaldehyde is produced by the oxidation of methanol, which refers to the catalyst surface behaviour that creates the pathway for making a methoxy group on the surface and lets formaldehyde form.

Dimethyl ether is an exothermic reaction with positive entropy; dimethyl ether may form without heat being added, even at low temperatures, because of its spontaneity, as seen in Table 1.3. It cannot be the main product because production of formaldehyde has more free energy at high temperatures. However, some catalysts behave as a Lewis acid and protonate methanol to remove the water and form dimethyl ether, even at high temperatures. At high temperatures, carbon monoxide and carbon dioxide join to fully combust the methanol. Nevertheless, some catalysts just burn methanol to carbon dioxide at low temperatures, with 100% yield to carbon dioxide.[13,14]

1.3 Industrial process

There are two industrial plants for producing formalin, according to the catalyst used. Rich methanol, mixed with air (50%v/v), is passed over a silver catalyst, where as the iron molybdate process limited concentration of methanol (6.7-36.5 vol. % in air) and air. Oxidative dehydrogenation over a silver catalyst operates at a high temperature, up to 600°C, and 75% of methanol conversion, and 89% formaldehyde selectivity. The rest of the un-reacted methanol is recycled. However, silver as a catalyst is sensitive in terms of contamination by methanol. Iron molybdate, on the other hand, operates at the lower temperature of 350°C, yielding 95% formaldehyde with 99% conversion of the methanol. Nonetheless, using iron molybdate costs less than using a silver oxide. Nowadays, both iron molybdate and silver catalysts are used in formalin production plants.

1.3.1 Industrial plant

An industrial Formaldehyde plant has two major designs, depending on whether it is for the dehydrogenation or oxidation process. For an oxidation reaction, the plant contains mainly a reactor, a vaporiser, a condenser and two absorbers in addition to a formalin tank. The reactor holds up to 16,000 reactor tubes. Each tube is 12 to 14 metres in length, and contains an inert ceramic ring layer to heat the gases. The next layer has a mix of the inert ceramic and the catalyst to stop the hotspot temperature, which will deactivate the catalyst in the next layer. Then comes a pure layer of the catalyst; and the last layer is inert, for products cooling. The vaporiser is to vaporise the injected methanol with air and

push the mix to the reactor. The absorbers allow the separation of formalin, by absorbing the formaldehyde into the process water where the pipeline between the reactor and the absorber is heated to avoid the polymerisation of formaldehyde, and then formalin is stored. Heat is adjusted and controlled using HTF, heat transfer fluid. Dowtherm oil is used to transfer heat and adjust the temperature in the range of 250°C to 320°C. The temperature of the reactor is recorded with a series of thermocouples.

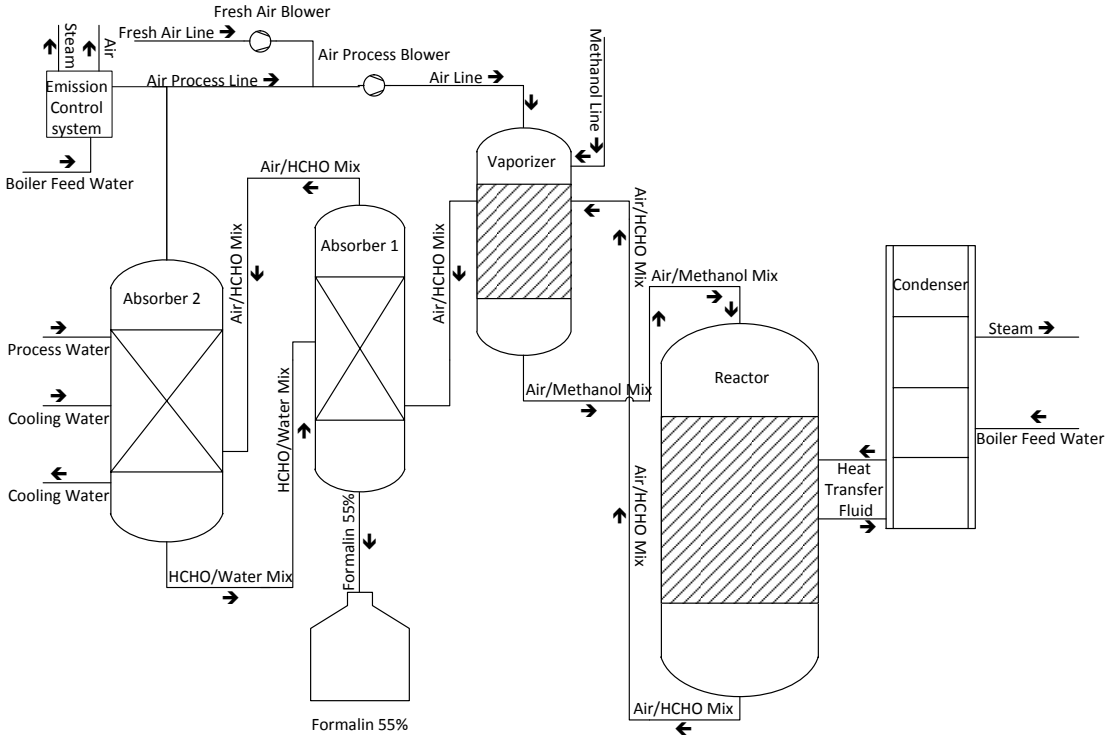

Scheme 1.2 Formaldehyde production plant

Air is compressed into the system using blowers and mixed with recycled air to reach a gas mixture of 11% O_2. The gas mixture flows into the vaporiser where the balance of methanol is sprayed and vaporised, and then the methanol/gas flows at pressure of 1.4 bar to the reactor. The methanol/gas enters the reactor tubes and is heated by the first inert ceramic ring. The second layer controls its temperature, and the third layer is where the pure catalyst reacts. Products pass through a further inert ring to reduce the products' temperature. As with the earlier description of heat control, any further increase of the system temperature is caused by the exothermic reaction that will be transferred to the

condenser. Products leave the reactor and pass outside the vaporiser, outside of the incoming methanol. The products' pipes are heated to avoid polymerisation of the formaldehyde; then the formaldehyde is absorbed into the process water in absorber 1, the result is reabsorbed by absorber 2, and the formalin is transferred to be stored. The production per ton contains 93% of formaldehyde; the rest is a mix of CO, unconverted methanol, CO_2, dimethyl ether and formic acid. One metric ton consumes approximately 425 kg of methanol, 55–65 K Wh electricity, 0.03–0.05 kg of catalyst and 400 kg of process water. 450-700 kg of steam is produced per metric ton, it may sell up to 6000 Great Britain Pound.

1.3.2 Current catalyst in industrial process

The current industrial catalyst is about 2.1Mo:1Fe iron molybdate, which has more of a ratio of the molybdenum element than the stoichiometric (1.5Mo:1Fe) $Fe_2(MoO_4)_3$, the ratio of which is required to avoid combustion of the methanol to CO_2. The reason behind this is that Mo tends to segregate on the surface, which makes the iron molybdate selective to formaldehyde. Iron is in the bulk: when the iron molybdate has iron on the surface, CO_2 production will be too high, and when iron molybdate loses Mo from the surface, the selectivity to formaldehyde reduces. Basically, Mo is lost from the surface by changes in the oxidation state. This is caused by reduction of the iron molybdate after it has been used several times, when the Fe reacts with the Mo and forms $FeMoO_4$ and other, less reactive phases.

Iron molybdate is industrially prepared by the coprecipitation method, in which ammonium heptamolybdate $(NH_4)_6Mo_7O_{24}$ is mixed with iron chloride, $FeCl_3$, in solution, and then the pH of the solution is altered until a precipitate forms. The precipitate is then filtered and dried. A binding agent is added to the dried mix to help in pelletising, and the last step is the calcination of the catalysts' pellets. Iron molybdate has been studied after industrial use, as the surface area of the catalyst decreases along the tube. The selectivity of the catalyst is lowest at the hotspot point, while its activity above or below is similar. Selectivity is higher below the hotspot; whereas above this point the selectivity decreases.[6,15]

1.4 Metal oxides in catalysis

There is growing usage of metal oxides in catalysis, especially in heterogeneous catalysis, where the catalyst is economically important for chemical production. Metal oxides are good because of their surface properties, as they have a wide range of catalyst electronic structures and oxidation states, which are useful for controlling the selectivity of the desired production.

1.4.1 Properties of metal oxides

Metals are the transition elements in block d of the periodic table, from group 3 to group 12, where they have incomplete electron filling in atomic d orbital. The incomplete d orbital enables the transition element atoms to share their electrons by donating or accepting electrons from other atoms. Transition elements are recognised by having several oxidation states, for example iron is +3 and +2. This variety of oxidation state is related to the unpaired electrons in the d orbital, which allows metals easily to lose or share electrons. However, some of the metals have one oxidation state, where the majority of elements in block d have multiple oxidation states, especially those in the middle of the block, for example, manganese has -1, -2, +1, +2, +3, +4, +5, +6 and +7 oxidation states. Also, metals compounds are paramagnetic when their electrons are unpaired in the d orbital. Most metal compounds have a high density, boiling point and melting point owing to their metal-metal bond, beside their conductivity and optical absorption.

Metals join with oxygen to form metal oxides in many different types of chemical bond, starting from the ionic model to the high covalent model, forming simple oxides, like CuO, to more complex metal oxides, like $FeVO_4$. Their properties depend on their electronic structure, which affect their magnetic and spectroscopic properties. Bulk structures of transition metal oxides are described by their crystallography, examples to metal oxides structures are rock salt; corundum, rutile and spinel. This gives an idea of the oxide structure compared with its properties. For example, iron oxide has many different structures: α-Fe_2O_3 is a corundum structure, with closely-packed hexagonal oxygen layers, and with two-thirds of the octahedra filled and empty tetrahedral. Another structure of

iron oxide is spinel, where the two iron oxidation states (Fe^{2+}, Fe^{3+}) are involved to form Fe_3O_4, with half the octahedral and half the tetrahedra filled. Another spinel structure is γ-Fe_2O_3, and this gives an idea of how oxides are different in their structure, even one metal oxide, like iron oxide.One metal oxide property is that the metal oxidation state can be changed: for instance, molybdenum oxide MoO_3 can be changed to Mo^{5+} as an intermediate state or can be further reduced to Mo^{4+}. This property of easy oxidation and reduction by formation of an intermediate state is important in catalytic reactions. The structure of oxide can be determined by X-ray diffraction for bulk structures, whereas the surface structure of macroscopic crystals can be determined by low energy electron diffraction (LEED).

The surfaces of oxide are part of the whole oxide structure. However, the surface and near-surface region are changed to form the surface of an oxide, where the rules of forming a surface from bulk is by cleavage to draw the crystal plane. Then the atoms rearrange themselves and form a stable state by lowering the surface Gibbs energy. However, not all oxide crystals cleave. For example, α-Fe_2O_3, hamatite, has a corundum bulk structure, and its surface has (0001), (1011) and (1012) planes from the growth of single crystals at specific pressure and temperature. In reconstructing the surface, there is the possibility of losing some oxygen atoms, which leads to cation reduction on the surface.[16,17]

There are some oxides that are supported by other materials to improve some of their properties. Either an oxide is a monolayer stuck on another oxide support surface or it has further oxide growth on the support surface, where the support behaves as oxide bulk and the surface is oxidised to cover that support. This enables control of the catalyst selectivity to the desired products. For example, vanadium oxide, V_2O_5, has a surface plane of (010), but when it is supported by TiO_2 it shows a plane of (001), and the $[VO_4]^{n-}$ group exists on the titanium surface. As Fig 1.9 shows, each vanadium is surrounded by 5 oxygen atoms, with two in the V=O group, which is not the same as the vanadium oxide surface or bulk. This unique structure can be determined by Raman shifts; V=O shifts increase in this structure as its peak intensity increases.

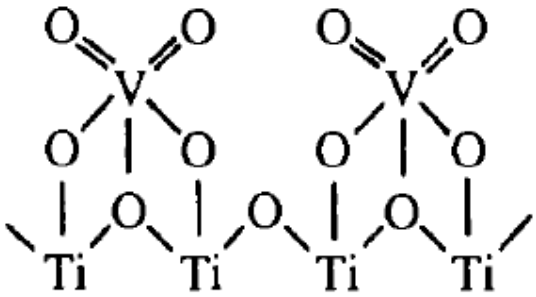

Fig 1.9 Monovandate on anatase[19]

There are some factors that make the surface structure different from the bulk structure; they are the surface tension or Gibbs energy of the oxide components. The adsorbate has an effect on the surface as it lowers the surface energy of that solid. Another factor is the adsorption reaction, which causes the formation of other compounds in different stoichiometry compared to the bulk, either by reduction or oxidation of the surface components. The surface electronic structure may separate from the bulk electronic structure because of the surface appearance. This electronic structure is called a surface state, and the surface state is not fully filled with electrons. They interact with the molecules by electronic donation and acceptance between them. or even the molecule reach close to surface empty conduction band build pair of states allowing to donate or accept electrons between them. The surface state is affected by many factors, including the ionicity of the oxide, the ions' positions, the rearrangement of the surface and the change in its structure. This shows that the surface is different from its bulk, when the oxygen leaves the surface or when the surface reduction changes the surface electronic structure.

The surface of a metal oxide is determined to be unsaturated compared with its bulk, as the bulk contains metals and oxygen in order to be fully saturated, whereas the surface rearrangement involves breaking the bonds and more free bonds, in other words, the surface ions have less neighbour ions than the fully packed bulk, which leads the surface to be unsaturated. The surface unsaturated sites interact with the atmospheric molecules and bind with them to be saturated, which is the reason behind the adsorption of gas molecules on the surface. The surface binds to gaseous molecule like water, CO, CO_2, NO; these molecules are strongly bonded to the surface, and the surface may not be able to bond with

another molecule or host more adsorbate. However, the surface of an oxide can be treated to clean it of the adsorbed water or other adsorbed vapours by heating the surface to a high temperature, up to 400^{o}C, so that the surface will again be unsaturated and ready to interact with other gas molecules to act as base or acid sites by denoting or accepting electrons.

The catalytic properties of the oxide surface are illustrated by its ability to bond with a gas molecule in a gas-solid system, where the gas is chemically or physically bonded to that surface in many types of adsorption. The first type includes non-dissociative adsorption of the molecules on the surface, by making a covalent of σ-bond or π-bond in a single surface ion. The dissociative molecule is adsorbed on the surface and separated into two parts with a pair of charged sites on that surface. For example, the dissociation of water, which gives hydroxyl groups bonded to cation sites and hydrogen allows while migrate to oxygen lattice sites to make another hydroxyl group. Furthermore, the adsorption may involve an electronic transfer between the adsorbed molecules and the surface. This type of adsorption reduces or oxidises the oxide surface because of the release or capture of electrons. However, the reduction or oxidation of the surface can even include oxygen or proton transfer from the surface to an adsorbate. Thus, the properties of the oxide surface make oxides important tools for heterogeneous catalytic reaction, where the catalytic reaction can be controlled when these properties are understood.[18,19]

1.4.2 Heterogeneous catalytic oxidation by metal oxide

As illustrated earlier, the main player of the heterogeneous catalytic reaction is the surface, where the molecules first interaction with the surface, and may dissociate or react with other adsorbed molecules on the surface. For an oxidation reaction, molecules are dissociatively adsorbed, and may react with the lattice oxygen. The oxidation reaction is affected by the oxidation state of the catalyst, where the surface would be reduced by changing its oxidation state as a result of the oxygen lattice missing from its structure. Later, fast reoxidation will occur to replace the missed oxygen, either from the bulk or from the atmospheric oxygen.

The way of choosing an oxide starts from the method used in preparation and its thermal treatment, as a catalyst can be prepared through many different methods, with different levels of heat and pressure. Some of the methods for catalyst preparation are co-precipitation, gel formation, and complexion, where the first step is to separate the metal ions from the precursor solution at specific temperature, oxygen pressure and pH. This results in a precipitate being formed, which then can be washed, dried and calcined. Furthermore, there are several steps of treatment, like catalyst activation using microwave and ultrasonic waves, and promotion using alkali or alkaline. A catalyst can be supported to increase the surface area; especially in an oxidation reaction where the reaction heat can be high enough to cause sintering and deactivate the catalyst. The methods commonly used are impregnation and sol-immobilization. The preparation method is an important tool in catalyst performance; it controls the surface properties of the catalyst, its selectivity, reactivity, thermal characteristics, stability, morphology, mechanical strength, and its cost.

An oxidation reaction means inserting oxygen into a molecule. where the catalyst is selective to oxidize molecule like an alcohol to either partial oxidation to aldehyde or fully oxidation to CO and CO_2, and the catalyst selectivity to products is different from catalyst to another, This can be explained through the formation of an intermediate compounds that formed on the surface. For example, methanol is converted to formaldehyde, where an intermediate methoxy group is formed on the catalyst's surface before it decomposes. The density of the active oxygen affects the selectivity, as too many active oxygen ions would lead to over oxidation to undesired products, and the low density of the active oxygen makes the catalyst inactive. The catalyst acidity may change the selectivity to undesired products [20,21].

1.5 Nanotechnology in catalysis.

Nano refers to the scale unit of 10^{-9} m; this small scale is used as a new technology and method for prodiction materials, devices and systems in general. Nanoscience is related to nanoscale study, and it determines the nanoscale impact on systems, whether molecules or devices and machines, whereas nanotechnology is the method used to apply that science in human life by

developing and controlling nanosystems, and their novel properties. Nanotechnology is new and important in many fields and it has applications in medicine, engineering and natural science.

1.5.1 Nanocatalysis.

Chemical nanotechnology is about materials in their nanosystems, which show other properties compared with the larger scale systems. Nanoparticles have different properties compared with the larger particles, that is, different atom arrangements, electronic structure, reactivity, conductivity and magnetic properties. The proof of the size dependence of properties is to measure the bulk properties and then measure them when their sized is reduced to nanoparticles. The smallest nanoparticles are in a face-centred cubic (FCC) structure, which is a centred atom (black circle) surrounded by 12 atoms (white circle), as in Fig 1.10. This is an example of how crystals start and grow for FCC nanoparticles. If another layer is added to this layer, containing 42 atoms, so, the structure contains 55 atoms, which is called the structural magic number for "n" layers ($N=1/3[10n^3 - 15n^2 + 11n - 3]$), and N=1, 13, 55, 147,…, to large nanoparticles. For example, Au_{55} has pure FCC nanoparticles and is very reactive with a short lifetime, which can be stabilised by adding other ligand atoms between its atoms, like $Au_{55}(PPh_3)_{12}Cl_6$. In Fig 1.10, there are 12 atoms on the surface and one atom is centred, which means that around 92.3% of the atoms are on the surface. That percentage decreases with larger particles, as the number of surface atoms is $N_{surf} = 10n^2 - 20n + 12$. For example, N surface for 55 atoms in the FCC nanoparticles is 42 atoms, so 76.4% of atoms are on the surface, for one layer is 100% atoms are in the surface[22].

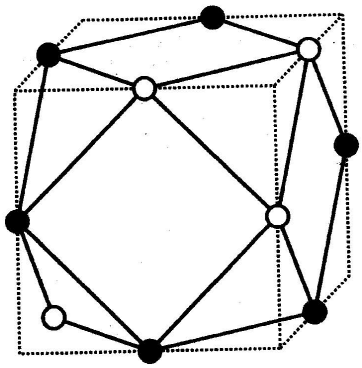

Fig 1.10 FCC nanoparticles structure[22]

Nanoparticles are characterised as high surface materials and their surface atoms are all ready to react with molecules, though they tend to sinter together to form larger particles affected. The most common preparation method of nanoparticles is bing supported for catalytic reaction. Nanoparticle properties start from the surfaces. The surface energy of nanoparticles is greater than that of larger particles, which then affects the surface stress and the lattice parameter, so nanoparticles prefer to be in core spherical particles, and their equilibrium shape is as shown in Fig 1.11 below, where (a) is an icosahedron, (b) is a truncated octahedron, and (c) is a decahedron. Nanoparticles commonly tend to be icosahedron shaped as it involves more edge sites, as with the decahedron. However, the smallest energy planes are (100) and (111), and can be found in the truncated octahedron shape.

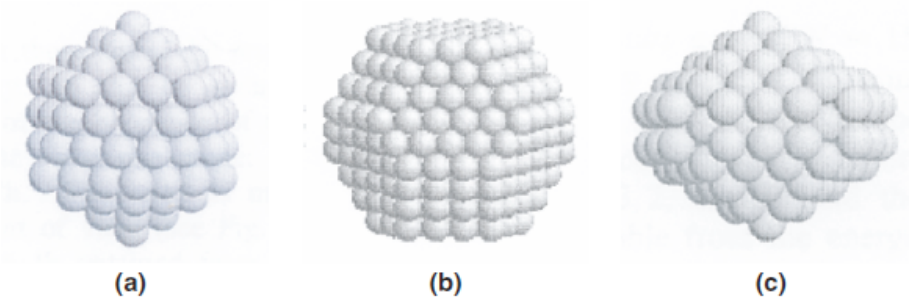

Fig 1.11 Nanoparticles stable shapes[23]

Supported nanoparticles are affected by interaction with support particles, as described by the Wulff-Kaichew theorem ($\Delta h/h_s = \beta/\Upsilon$), where Δh is the work needed to split the supported particles from the support surface, β is the adhesion energy, h_s is the plane central distance, and Υ is the surface energy. So, stronger interaction between supported particles and the support surface particles tends to form flatter particles on the support. However, particles sizes are also affected by many other factors, for example, temperature.[23]

The melting point is also changed as the particle size changes compared with bulk materials. As the particle size decreases, its melting point decreases as well. This is described using Pawlow's law in Eq 1.41, where T is the melting point of the crystal and T_m is the bulk melting point, γ is the surface energy for solid and liquid (as denoted 's' for solid and 'l' for liquid), ρ is the density of solid and liquid (also noted as 's' for solid and 'l' for liquid), L is the fusion heat and R is the crystal radius. Most nanomaterials show melting point depression

caused by the increase of their surface to volume ratio. This is the reason behind the change in their thermal properties, which is not the same case for bulk materials. As an example of that, gold nanoparticles melt at approximately 300^{o}C for 2.5 nm particles, whereas bulk gold has a melting point of 1064.18^{o}C.

$$\frac{T}{T_m} = 1 - \frac{2\left(\gamma_s \rho_s^{-2/3} - \gamma_l \rho_l^{-2/3}\right)}{LR\,\rho_s^{1/3}} \qquad \text{Eq 1.41}$$

The electronic structure of bulk materials determines their solid properties, but for small nanoparticles it is different, as most of the particle atoms are located on the surface. The width of valence band is reduced and its gravity centre moves toward Fermi level, as a result of low coordination, especially in the edge atoms like atoms in the corners, and that increases the localization of the valence band, where the shift of d band centre to Fermi level decreases the dissociation barrier of the adsorbed energy and also increases its adsorption energy.

In catalysis, the most important aspect of a catalyst is its reactivity in terms of how selective and active the catalyst is. It is well known that nanoparticles are active materials in catalytic processes, as their molecules interact more than those in bulk materials, and they are active at low temperature in most cases. Nanoparticle reactivity is changed by many factors. Where a support is involved in the molecule adsorption, the molecules are adsorbed physically and then adsorbed chemically on the catalyst. In other words, the support can make the catalyst more active for the adsorption reaction. Another factor is morphology. For reduction of NO by CO on Pd/MgO, three catalysts were chosen to determine the morphology effect. The largest was the least reactive, although the middle size particle was more active than the smallest particle. The reason behind this was that the large size has many (100) planes, which are less reactive than the (111) planes in the middle size particle, which has a truncated octahedron shape with (111) and (100) planes; whereas the smallest particle has (111) planes and the edge sites effect is not seen in small particle size. The effect of the edge sites is by their low coordination compared

with other sites, which moves the d states close to the Fermi level, and increases the adsorption energy as well as reducing the dissociation barrier.[24]

1.5.2 Catalysis by nano-gold.

Nanoparticles of gold were first prepared by Faraday in 1857, by reducing an aqueous solution of $AuCl^-_4$ with phosphorus in carbon disulfide (CS_2). However, nanoparticle gold is prepared using the verity method in recent papers. It is prepared as protected nanoparticles to make monolayer on support from colloidal solution, $HAuCl_4$ is an aqueous solution and is protected by tetra octyl ammonium bromide to protect the particles size from 1–5 nm. It is reduced in the presence of the surfactant by sodium borohydride ($NaBH_4$) as reduction agents, as in Fig. 1.13. However, in sol-immobilization, the phase-transfer agent is polyvinyl alcohol (PVA), which is then filtered and washed using a sol-gel filter.

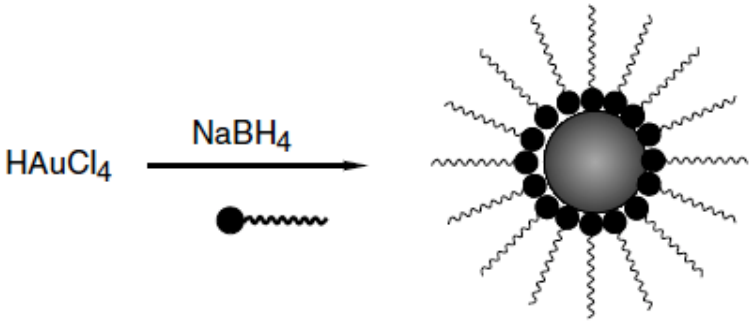

Fig 1.13 Protected transfer of gold nanoparticles[25]

There are many tools used for the characterisation of gold nanoparticles; Uv/Vis absorption spectroscopy is one of the important techniques for nanoparticles. It determines particle size and shape through the surface plasmon resonance; it measures the frequency of the plasmon absorption band (ω_p), where $\omega_p = \pi Ne^2/m$, N is the free electron density, (e) is the electron charge and (m) is the mass; and it is an excitation of the conduction band electrons by electromagnetic radiation, which is a collective oscillation of valence electrons. Furthermore, the structure of the gold particles is determined by X-ray diffraction (XRD), transmission electron microscopy (TEM), atomic force microscopy (AFM) and scanning tunnelling microscope (STM), whereas the surface components and oxidation state are determined by X-ray photoelectron

spectroscopy. Moreover, IR is a powerful technique for adsorbate in the surface; it is commonly used for in-situ analysis.

In heterogeneous catalysis, gold was known as an inactive catalyst. However, it was later discovered that nanoparticles of gold on support are very active at low temperature for CO oxidation. Nanoparticles gold was reported by Hutchings[26] to be a good catalyst for ethyne hydrochlorination at a low temperature, near to 180^{o}C, which makes it a better catalyst than mercury supported on chloride catalysts, as the nano-gold catalyst is less poisoned by reactants. Further treatment of NO has been applied to avoid the catalyst being deactivated at temperatures higher than 100^{o}C.

Likewise, nano-gold is an effective catalyst in oxidation reactions. The oxidation of CO on supported gold nano-crystals shows enormous activity. The temperature of the reaction is less than 0^{o}C, as was first discovered by Haruta.[26] However, nano-Au/ZnO is an example of a very reactive catalyst for CO oxidation. Another catalyst is nano-Au/α-Fe_2O_3, which is used for CO oxidation at low temperatures, close to 25^{o}C. From this, it can be recognised that supporting nanoparticles of gold with an oxide makes it a very active catalyst at low temperature, where the activity enhanced by the gold nanoparticles is attached to the support. Furthermore, the oxidation reaction of the nano-gold supported catalyst is active for alcohols, alkanes, alkenes and even hydrogen oxidation to hydrogen peroxide.

There is a huge debate about the calculation and experimental determination of gold nanoparticle structures. The most well-known structure is shown in Fig 1.14, where (a) is a truncated octahedron, (b) is an icosahedron, (c) is a Marks decahedron and (d) is a cub-octahedron. The most common structures are the truncated octahedron and the decahedron (Marks), although the rest of the structures are active in some cases. For example, Au/MgO has an icosahedron structure and Au/TiO is a cub-octahedron. However, their two-dimensional structure is far from the FCC structure. It is too small, with particles normally 2 nm and less, and has fewer layers (a monolayer or two layers). These catalysts are very active, like those used for CO oxidation.[27]

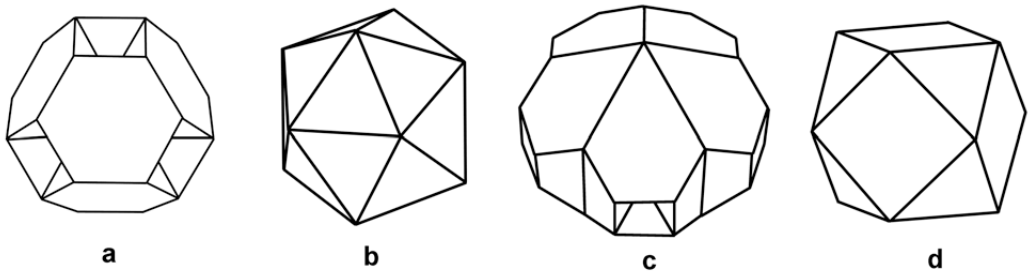

Fig 1.14 Gold nanoparticles shapes[27]

1.6 Iron molybdate and relative oxides

The current catalyst for methanol oxidation is iron molybdate, $Fe_2(MoO_4)_3$, as illustrated earlier in this chapter, which is the most selective catalyst to formaldehyde. It yields 90% formaldehyde, and the rest is dimethyl ether at low temperature. Iron oxide catalyst is a combustor catalyst, and methanol is converted to CO_2 during any conversion, even at low temperature. However, it is active catalyst and converts methanol at approximately 180^{o}C. The molybdenum oxide catalyst is selective to formaldehyde near to 100%, but the catalyst is not very active. It does not convert all the methanol, even at high temperatures of 500 ^{o}C, and its selectivity to formaldehyde decreases with increasing temperature, which makes it a poor catalyst. Thus, the iron molybdate is more selective than iron oxide and more active than molybdenum oxide.[11]

There are many forms of iron oxide: haematite (α-Fe_2O_3), magnetite (Fe_3O_4), maghemite (γ-Fe_2O_3), β-Fe_2O_3, e-Fe_2O_3 and FeO; but the common catalyst is hematite. Hematite has the hexagonal close-packed structure of oxygen layers and octahedron iron atoms between two sheets of anions, with space group R3c, and close packed staking anions of ABAB[001], where the lattice parameters are a=0.5034 and c=1.3752. Methanol is adsorbed on the surface of iron oxide and dissociated to methoxy and hydroxyl groups adsorbed on the surface. Further oxidation of the methoxy group occurs by the surface oxygen bonding formate to the surface and then to CO_2. In other words, iron oxide burns methanol to give H_2, CO_2, CO, and water.[11,28]

Although the most common forms of molybdenum oxide catalysts are MoO_3 and MoO_2, they have different oxidation states, and their structures and catalytic behaviours are also different. Molybdenum trioxide is known as α-MoO_3 and β-MoO_3. The α-MoO_3 crystal structure is orthorhombic and P_{nma} spacing group, and its layers contain a molybdenum octahedral oxygen structure such as MoO_6. Each molybdenum atom is linked to common oxygen corners, common oxygen and edge oxygen. These oxygen atoms are bonded to one molybdenum (terminal oxygen), and asymmetric oxygen is bonded with two molybdenum and symmetrical bridging oxygen bonded to three molybdenum, where the lattice parameters are a=3.962, b=13.858 and c=3.607. The monoclinic β-MoO_3 has a spacing group of $P2_{1/c}$, and lattice parameters of a=7.122, b=5.374 and c=5.565, which is similar to ReO_3 and has octahedral oxygen layers. Moreover, MoO_2 is monoclinic in structure and has a $P2_{1/n}$ spacing group; its lattice parameters are a=5.607, b=4.860, c=5.537, and ß=119.37.[29]

Methanol adsorbs physically on the surface of molybdenum oxide at 23^{o}C, but the chemisorption starts at (activated adsorption) 100^{o}C leading to the making of a real molybdenum methoxy group bond (Mo-OCH_3). Then formaldehyde is formed and desorbed at approximately 250^{o}C, but there is also production of CO and CO_2 at high temperature owing to the methanol and formaldehyde being fully oxidised. However, the methanol is adsorbed weakly on the surface of molybdenum oxide, where the molybdenum catalyst contains a large (010) face, which is the best for achieving methanol oxidation to formaldehyde, but is not involved in the reaction below 100^{o}C. It contains Mo=O bonds, which become more active when the temperature increases and react with the methanol. The orthorhombic single crystal of MoO_3 shows that the main product from the (010) face is formaldehyde, and dimethyl ether is the main product of (001 + 101) faces at low temperature. Formaldehyde formation leaves the molybdenum atom in a lower oxidation state, as the oxidation process leaves the surface with one oxygen atom missing. So, Mo^{6+} will be reduced to Mo^{+5} by formaldehyde desorption, and then further reduced when water decomposes and molybdenum becomes Mo^{4+}. The end of this reaction is reoxidation of Mo^{4+} to Mo^{6+} by either the bulk oxygen or the gas-phase oxygen.[14,30,31,32] However, the MoO_2 catalyst is more active than the MoO_3 catalyst, but it is not as selective to

formaldehyde compared with MoO_3. When the MoO_2 catalyst is activated by increasing the temperature, its selectivity to formaldehyde decreases to the point that the catalyst changes its behaviour and starts to become more selective to formaldehyde. That is the point or temperature where the MoO_2 is being oxidised to MoO_3, and it confirms that MoO_3 is the selective phase, whereas MoO_2 mainly produces CO, and it is oxidised to MoO_3 in gas oxygen.[11,33]

Molybdenum oxide catalyst is the selective catalyst for methanol oxidation, but it is a poor catalyst because it does not convert all the methanol to formaldehyde. Iron molybdate is the more active catalyst and is as selective as molybdenum oxide alone. Iron molybdate's structure is described in two phases of monoclinic and orthorhombic structures; monoclinic iron molybdate has lattice parameters of a=15.73, b=9.231, and c=18.22, as in Fig 1.15(a), where the SEM image is of both monoclinic and orthorhombic structures of iron molybdate. Fig 1.15(b), however, shows orthorhombic $Fe_2(MoO_4)_3$ with lattice parameters of a=12.86, b=9.246, and c=9.333.0 Both structures are fabricated by the co-precipitation method in the aqueous phase, where the main factors are pH value, reaction temperature, concentration and reaction time. Monoclinic iron molybdate is prepared in approximately pH 1–1.65, from iron nitrate and ammonium heptamolybdate. The orthorhombic iron molybdate is prepared using the same method but the pH value is 3. However, pH is not the only factor in this method: temperature can affect it too, where decreasing the reaction temperature builds smaller particles. Another factor is the concentration of iron nitrate. The stoichiometric iron molybdate ($Fe_2(MoO_4)_3$), which has a ratio of 1Fe:1.5Mo, is built in particles sized smaller than 2.2 iron molybdate, because it has a more concentration of iron than 2.2 iron molybdate. Monoclinic iron molybdate is a pale green powder and orthorhombic is a light yellow powder. Their different properties can be obtained according to their synthesis conditions of temperature and pH value. For example, the surface area of the orthorhombic structure is 24 m^2/g, when the catalyst is prepared in pH 3 and at 140^oC; the monoclinic structure has a lower surface area using BET surface area measurements.[34]

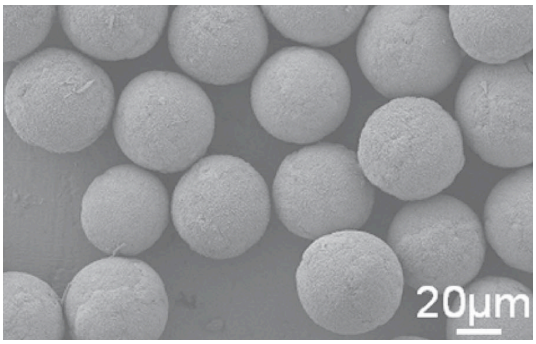

Fig 1.15(a) Monoclinic structure

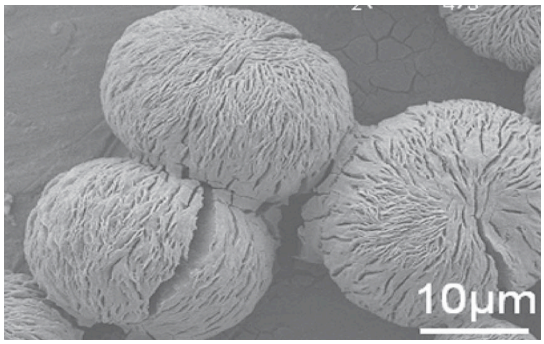

Fig 1.15(b) Orthorhombic structure

Several methods have been improved to prepare an iron molybdate catalyst rather than co-precipitation, which requires heat for the synthesis reaction and for calcination. The sol-gel method was used to prepare the iron molybdate with a chlorinated species that has an effect on the selectivity to formaldehyde but negatively affects the catalyst's activity. The catalyst was prepared in this method by dropping an iron solution on an organic acid medium containing molybdenum; no precipitate was formed, and the mix was then heated to evaporate the water. Using this method, the result is iron molybdate with a higher surface size compared with catalysts prepared by the co-precipitation method. Besides, there are other methods like the reaction of MoO_3 with Fe_2O_3 at temperature of 700^oC, or just a physical mix of these two oxides.[10]

There are two main forms of iron molybdate: ferric molybdate, $Fe_2(MoO_4)_3$, and ferrous molybdate, $FeMoO_4$. Ferric molybdate is the active catalyst for methanol oxidation, but ferrous molybdate is one of the possible compounds that appears after ferric molybdate reduction during methanol oxidation. Ferrous molybdate is formed in three structures: α-$FeMoO_4$ is a monoclinic structure with lattice parameters of a=9.807, b=8.950, c=7.659 and ß=114.02; ß-$FeMoO_4$ has lattice parameters of a=10.301, b=9.402, c=7.053, and ß=106.28; and the third structure is FeMoO4-II, which is formed at high pressure and has lattice parameters of a=4.708, b=5.701, and c=4.944.[35,36,37,38] The formation of α-$FeMoO_4$ and ß-$FeMoO_4$ during methanol oxidation depends on the temperature when the methanol contacts the catalyst to act as redox agent. α-$FeMoO_4$ is formed at temperatures below 300^oC, as it has Mo in the octahedron coordination, whereas ß-$FeMsoO_4$ is formed at temperatures above 300^oC, and

has Mo in tetrahedron. Both catalysts are reoxidized by the gas oxygen: α-$FeMoO_4$ gives MoO_3 and Fe_2O_3; whereas ß-$FeMoO_4$ gives $Fe_2(MoO_4)_3$ and Fe_2O_3.[10]

Stoichiometric ferric molybdate is the active phase for methanol oxidation, where Mo is tetrahedral and Fe is octahedral. Each FeO_6 octahedron is surrounded by six atoms, while tetrahedral MoO_4 is linked to four atoms. Each unit cell contains 16 FeO_6 and 24 tetrahedral MoO_4, and each oxygen is connected to one Fe and one Mo, where the oxygen-metal-oxygen is bonded at an angle of 109^o for tetrahedron and 90^o in the octahedron structure. However, as the catalyst changes its active phase to form other compounds, like $FeMoO_4$, which is poor for methanol oxidation to formaldehyde, to avoid deactivation of the catalyst and not be fully reduced, extra Mo is added to the catalyst above the stoichiometric ratio 1.5. There are several ratios being used in industrial plant, for example 3Mo:1Fe, in which excess Mo has an effect on the structure, as it replaces the octahedral Fe^{3+}, where the Mo tends to segregate on the surface of the iron molybdate, for both stoichiometric and Mo-rich iron molybdate. Bowker et al.[15] have studied the surface changes of the 2.2Mo:1Fe iron molybdate catalyst during methanol oxidation in aerobic and anaerobic conditions. The results obtained show the reduction of MoO_3 to MoO_2 and the appearance of α-$FeMoO_4$ beside Mo_4O_{11} (intermediate phase between MoO_3 and MoO_2) at a temperature of 250^oC. The selectivity to formaldehyde decreases from 80% to 40% and lower with the increase of temperature, which causes a full change of $Fe_2(MoO_4)_3$ and MoO_3 to Mo_4O_{11}, MoO_2, α-$FeMoO_4$, ß-$FeMoO_4$. Moreover, any excess change of Mo Fe_2O_3 to $Fe_2(MoO_4)_3$, as some confirmed that the active phase of iron molybdate catalyst is the one with ratio of Mo/Fe = 1.7 [10].

Iron molybdate was promoted by doping promoters; these promoters were added to increase the catalytic performance of iron molybdate, with elements like vanadium, tungsten, chromium, cobalt, nickel, tellurium and magnesium. For instance, Cr was doped on iron molybdate. It increases the surface area compared with the unpromoted catalysts, which leads to increase in its catalytic activity, but some papers confirmed that Cr decreases formaldehyde selectivity. However, some papers show that Cr promotion increases the catalyst selectivity, and that a Cr doped catalyst is more stable for long-term use. Tungsten was added to iron

molybdate in the co-precipitation method, the result being more active and selective than iron molybdate not promoted by WO_3. Moreover, other elements like Ni and Co when added to iron molybdate decrease its selectivity [40,10].

In the industrial application of iron molybdate, the catalyst is active up to 12 months, as iron molybdate is deactivated during this time. The result is less selectivity to formaldehyde and the production of other undesired products. The active phase of iron molybdate is the stoichiometric iron molybdate with molybdenum oxide segregated on the surface. Mo is volatised from the catalyst surface during methanol oxidation. The volatility of Mo increases with the increase of methanol concentration and the decrease of oxygen partial pressure, as methanol is separated into methoxy groups bonded to the Mo atom on the surface. Then the Mo is slowly volatised as gaseous Mo-OCH_3, and the region of the volatile Mo-OCH_3 is the hotspot. It then travels to a colder region, in which the catalyst activity and selectivity, and the mobile Mo-OCH_3 enhance other Mo sites to be volatilised as well, which can be cleaned by a methanol-He stream at 250^{o}C. FeO_x can be formed in the surface region, but the excessed Mo will recover the missed Mo sites and overcome the formation of FeO_x. During methanol oxidation that involves a reduction of the catalyst, other phases are formed rather than the active iron molybdate, like α-$FeMoO_4$, β-$FeMoO_4$, MoO_2, FeO_x and Mo_4O_{11}, where these are not the active forms for methanol oxidation to formaldehyde.[39,40,41]

Nowadays, the current selective catalyst is iron molybdate, while other catalysts are being investigated and used as selective catalysts. A silver catalyst was the selective catalyst used instead of iron molybdate. It is a pure metal of 99.99% Ag in forms like wire and fine gauze with a low surface area (0.1 m^2g^{-1}). However, 50% of commercial formaldehyde production is based on silver catalytic reaction, which involves dehydrogenation of methanol to formaldehyde and hydrogen as endothermic reaction. The next reaction is the oxidation of hydrogen to water as exothermic reaction and to boost the dehydrogenation equilibrium to formaldehyde side. A silver catalyst is 90% selective to formaldehyde, but not all the methanol reacts, as the conversion of methanol reaches 75% and the rest, the unreacted methanol, is separated and recycled.

Also, the reaction requires much more heat compared with an iron molybdate catalyst, where the reaction temperature is 580^{o}C. On silver, methanol is rich (50% v/v in air), as well as the lifetime of a silver catalyst being only several months as it can be contaminated by flow gas. Economically, a silver catalyst is flexible and easy to operate but it costs more, where it is used for large industrial plant. The presence ($O_{2(g)}$) of oxygen is important for methanol dehydrogenation to formaldehyde, as it activates the silver catalyst, and the oxygen is adsorbed weakly on the surface of the silver to make it ready for the methanol to be adsorbed. The adsorption of oxygen can be described in two ways. The first includes a weak adsorption on the surface of the silver, while the second includes absorption of the silver lattice with a strong bond. For methanol conversion to formaldehyde, the lattice oxygen is involved in the reaction, whereas the weak absorbed oxygen is responsible for CO_2 formation, as it forms HCOOH as an intermediate state that then decomposes as carbon dioxide and hydrogen.[10,42,43] More detail on individual academic contributions will be provided in the introductions to chapters 3, 4 and 5.

1.7 Aims and objectives

The first target is to scan single oxides for their selective to formaldehyde. Elements were mainly chosen in this study that are in the same regain of the periodic table in order to see: i) any elements behave similar to molybdenum and ii) to determine what reason is that makes MoO_3 selective. However, some other elements were chosen that have different properties such as their oxidation state. These single oxides date may help us to predict effective properties in the selectivity of methanol oxidation to formaldehyde. Chapter 3 contains the catalytic determination of single oxides catalysts, and comparison is made with selective catalyst, and with molybdenum oxide.

Moreover, from the single oxides work, oxides can be found to show selectivity to formaldehyde when prepared in more complex oxides, either by changing the anion or cation. The aim here was to replace Mo by other selective elements, as was discovered from their single oxide behaviour, and iron too was to be replaced by other elements that showed activity in their single oxides form. The target in Chapter 4 of using other element combustions instead of iron

molybdate is to control the selectivity and activity by making a new catalyst that is more active in converting all methanol to formaldehyde with less heat needed for the catalyst activation. This would result in reduced cost and is environmentally greener. The target of the selectivity study is to reach a better selectivity than that of iron molybdate, which is 95%.

Chapter 5 illustrates another point of study in this research, which is that doping an iron molybdate catalyst with other selective elements might improve its selectivity. Another was to to support elements on large surface area materials like carbon, as it is known that molybdenum oxide is poor in terms of activity due to its low surface area. It has a surface area of only $1 m^2 g^{-1}$, whereas iron molybdate has a surface area of 5 $m^2 g^{-1}$, and is more active than molybdenum oxide. Furthermore, nano-gold catalysts are very active catalysts, as shown in recently published papers, so it was worth testing Au doping methods for methanol oxidation to formaldehyde.

1.8 References

[1] Bowker, M. (1998). *The basis and application of heterogeneous catalysis*. Oxford University Press Inc: New York.

[2] Thomson, S.J., Webb, G. (1968). *Heterogeneous catalysis*. Oliver & Boyd: Edinburgh and London.

[3] Brown, W.H., Foote C. S., Iverson, B. L. (2205) *Organic chemistry*. Thomson books/Cole: USA.

[4] Schore, N. E., Vollhardt, K.P.C.(2002) *Organic chemistry*. W. H. Freeman and company: USA.

[5] John McMurry.(2010) *Fundamentals of organic chemistry*. Books/Cole, Cengage learning: Australia.

[6] House, Matthew Peter.(2007). *The selective oxidation of methanol over iron molybdate catalysts*. Thesis (Ph.D.) - Cardiff University.

[7] Twigg, Martyn V.(1996) *Catalyst handbook*. Manson publishing Ltd: England.

[8] Lange, J. P. (2001) Methanol synthesis: a short review of technology improvements. Catalysis today 64, 3-8.

[9]- Global Insight. March 2006.*Economic Primer on Formaldehyde*. Lexington U.S.A. Global Insight.

[10] Kiennemann, A., Soares, A. P. V., Portela, M. F.(2004) *Methanol selective oxidation to formaldehyde over iron-molybdate catalysts*. Taylor & Francis. 47:125-174.

[11]-Bowker, M., Holroyd, R., House, M., Bracey, R., Bamroongowndee, C., Carley A. and Shannon M. (2008). *The Selective Oxidation of Methanol on Iron Molybdate Catalysts*. Springer science, 48, 158-165.

[12] Price, G.(1998). *Thermodynamics of chemical processes*. Oxford University Press Inc: New York.
[13]-House, M.P., Shannon, M.D. and Bowker, M.(2008). *Surface Segregation in Iron Molybdate Catalysts*. Springer science,122, 210-213.
[14]-Bowker, M., Holroyd, R., Elliott, A., Morrall, P., Alouche, A., Entwistle, C. and Toerncrona, A.(2002). *The selective oxidation of methanol to formaldehyde on iron molybdate catalysts and on component oxides*. Plenum Publishing Corporation,83, 3-4.
[15]-Bowker, M., Carley, A. and House, M.(2007). *Selective oxidation of methanol on iron molybdate catalysts and the effects of surface reduction*. Journal of catalysis, 252, 88-96.
[16]N.N. Greenwood A Earnshaw. (1998). *Chemistry of the elements*. (2nd Ed). Butterworth-Heinemann. Oxford.
[17]P.A. Cox. (1995). *Transition metal oxides*. Clarendon, Oxford.
[18]V.E. Henrich, P.A. Cox.(1994). *The surface science of metal oxides*. Cambridge university press: Cambridge.
[19]H.H. Kung. (1989). *Transition metal oxides: surface chemistry and catalysis*. Elsevier: New York.
[20]. D.K. Chakrabarty, B. Viswanathan. (2009). *Heterogeneous catalysis*. New age science: Kent, UK.
[21]. F. Schmidt (2001). *New catalyst preparation technologies—observed from an industrial viewpoint*. Applied catalysis: 221, 15-21.
[22]Charies P., Poole Jr., Frank J. O. (2003). *Introduction to nanotechnology*. Wiley Interscience: Canada.
[23]. U. Heiz, U. Landman. (2007) *Nanocatalysis*. Springer: USA.
[24] C.P. Vinod.(2010). *Surface science as a tool for probing nanocatalysis phenomena*. Catalysis Today 154,113–117.
[25]T. Pradeep. (2007). *Nano: The essentials*. Tata McGraw Hill: New Delhi.
[26] Graham Hutchings. (2004). *New directions in gold catalysis*. Gold Bulletin 37,1–2.
[27] M.B. Cortie, E. van der Lingen. (2002). *Catalytic gold nanoparticles*. Materials Forum. 26, 1-14
[28]. R. M. Cornell, Udo Schwertmann. (2003). *The iron oxides: structure, properties, reactions, occurrences, and uses*. WILEY-VCH: Germany.
[29] T. Ressler, J. Wienold, R.E. Jentoft, T. Neisius. (2002). *Bulk structural investigation of the reduction of MoO_3 with propene and the oxidation of MoO_2 with oxygen*. Journal of catalysis: 210, 67-83.
[30] Wu-Hsun Cheng. (1996). *Methanol and formaldehyde oxidation study over molybdenum oxide*. Journal of catalysis 158, 477–485.
[31] E. Gaigneaux, H. Abdel Dayem, E. Godard, P. Ruiz.(2000). *Dynamic phenomena and catalytic reactivities of oxide surfaces*. Applied Catalysis A: General 202, 265–283.
[32] J.M. Tatibougt. (1997). *Methanol oxidation as a catalytic surface probe*. Applied Catalysis A: General 148, 213-252.
[33]. Michael Bowker, Albert F. Carley, Matthew House. (2008). *Contrasting the Behaviour of MoO3 and MoO2 for the Oxidation of Methanol*. Catal Lett. 120:34–39.
[34] Yi Ding, Shu-Hong Yu, Chen Liu, Zheng-An Zang. (2007). *3D Architectures of Iron Molybdate: Phase Selective Synthesis, Growth Mechanism, and Magnetic Properties*. Chem. Eur. J.: 13, 746 –753.

[35] Koenig, U., Morgenstern, T., Foersterling, G. (1993). *A Study of Structural Crystallography on Ternary Metal Oxides in the System Fe-Mo-O*. Materials Science Forum:133-136, 687.
[36] Fagherazzi, G., Pernicone, N. (1970). *Structural study of a methanol oxidation catalyst*. Journal of Catalysis: 16, 321-325.
[37] Rodriguez, J. A.; Hanson, J. C.; Chaturvedi, S.; Maiti, A.; Brito, J. L .(2000). *Studies on the Behavior of Mixed-Metal Oxides: Structural, Electronic, and Chemical Properties of β-$FeMoO_4$*. Journal of Physical Chemistry B: 104, 8145-8152.
[38] Sleight, A. W.; Chamberland, B. L.; Weihe r, J. F. (1968). *Magnetic, Moessbauer, and structural studies on three modifications of $FeMoO_4$*. Inorganic Chemistry: 7, 1093-1098.
[39] Arne Andersson, Magnus Hernelind, Ola Augustsson. (2006). *A study of the ageing and deactivation phenomena occurring during operation of an iron molybdate catalyst in formaldehyde production*. Catalysis today:112, 40-44.
[40] Kamalakanta Routray, Wu Zhou, Christopher J. Kiely, Wolfgang Grünert, Israel E. Wachs. (2010). *Origin of the synergistic interaction between MoO_3 and iron molybdate for the selective oxidation of methanol to formaldehyde*. Journal of catalysis: 275, 84-98.
[41] Krasimir I., Dimitar Y. D. (2010). Deactivation of an industrial iron-molybdate catalyst for methanol oxidation. Catalysis today: 154, 250-255.
[42] Israel E. Wachs. (2003).*Extending surface science studies to industrial reaction conditions: mechanism and kinetics of methanol oxidation over silver surfaces*. Surface Science: 544, 1–4.
[43] Deng, J.; Xu, X.; Wang, J.; Liao, Y.; Hong, B.(1995). *In situ surface Raman spectroscopy studies of oxygen adsorbed on electrolytic silver*. Catalysis Letters: 32, 159-170.
[44]D. M. Newns, Phys. (1969). 178, 1123.
[45] Anderson phys. (1961), 124, 41.

2. Experimental

2.1 Introduction

The experimental chapter considers the materials and analysis used in the methanol oxidation study. The first part of the chapter explains the preparation methods with regard to all the catalysts that were used in two experiments, and their reactivity using a pulsed flow reactor for each catalyst. The first experiment is Temperature Programmed Reaction (TPR), while the second experiment is the Temperature Programmed Desorption (TPD). The characterization of a limited number of catalysts is carried out by Raman spectroscopy, X-ray diffraction (XRD), X-ray photoelectron spectroscopy (XPS) and through the use BET surface area measurements.

2.2 Catalyst preparation

The catalysts in this research were prepared by more than one method as will be described in more detail for each method. Some of the materials were bought commercially from scientific research suppliers which meet the standard required for methanol oxidation.

2.2.1 Industrial catalysts

A number of single oxides were purchased from Sigma Aldrich as follows: vanadium oxide (IV) V_2O_4 (99.9%), molybdenum (IV) oxide, MnO_2 (≥99.99%), niobium (V) oxide Nb_2O_5 (99.99%), tantalum (V) oxide (99.99%), cobalt (II) oxide (99.99%), copper (I) oxide Cu_2O (≥99.99%) and rhenium (VI) oxide ReO_3 (99.99%).

2.2.2 precipitation method

Co-precipitation means the formation of a precipitate for substances under specific conditions of temperature and pH, where pH is the main factor in the formation of the precipitate. The method which was used for a single oxide starts with the soluble salt of the metal in acidified water to pH 2. The first application of this method is the preparation of manganese (III) oxide by the addition drop-

wise of solution which contains the desired amount of manganese nitrate hydrate (Aldrich=99.99%) dissolved in 50 ml water, dropped into 100 ml water acidified to pH 2. The mixture was heated up to 60 ^{o}C with stirring. With the consumption of the manganese solution, a precipitate appears. The mixture was then heated up to 90^{o}C to evaporate the water. The next step was to dry it in an oven at a temperature of 120^{o}C overnight. The last step was calcination at 500^{o}C for 48 h. The same method was used for the rest of the single oxide catalysts. However, the raw salts are different as follows: iron nitrate (Aldrich=99.99%) produced iron oxide Fe_2O_3 haematite; ammonium hepta-molybdate (Aldrich=99.98%) produced molybdenum (VI) oxide MoO_3; vanadium (V) oxide V_2O_5 was obtained from ammonium meta-vanadate (Aldrich=99.99%), chromium (III) oxide Cr_2O_3 produced from chromium nitrate none-hydrate (Sigma-Aldrich=99%); ammonium para-tungstate hydrate (Aldrich=99.99%) converted to tungsten (VI) oxide WO_3, and copper (II) oxide formed from copper nitrate hydrate (Aldrich=99.999%).

The other use of the co-precipitation method was to form complex oxide catalysts, where the stoichiometry iron molybdate $Fe_2(MoO_4)_3$ was made by iron nitrate (Aldrich=99.99%) dissolved in 50 ml of deionized water added drop-wise in a solution of ammonium hepta-molybdate (Aldrich=99.98%) and 100 ml deionized water which was then acidified to pH 2. The temperature of the reaction was 60^{o}C with stirring throughout. After the precipitate formed, the temperature was increased up to 90^{o}C for water evaporation, then the precipitate was dried overnight in an oven at 120^{o}C. The last stage was calcining at 500^{o}C to let molybdena segregate on the surface of the iron molybdate. There was also the preparation involving a further addition of molybdena on iron molybdate. The addition of molybdena depends on the ratio of iron and molybdenum chosen. The stoichiometric iron molybdate has a ratio of 1.5Mo: 1Fe, whereas the ferrous iron molybdate ($Fe_2 (MoO_4)_3$) has a 2.2Mo:1Fe ratio. The addition was to add more ammonium hepta-molybdate which reacted with same amount of iron nitrate. Iron niobate, $FeNbO_4$, was produced using the same method used for the iron molybdenum preparation, where the raw salts were iron nitrate which reacted with ammonium niobate oxalate hydrate.

More catalysts were prepared in a similar fashion to the iron molybdate preparation method, and even with more than one ratio. Iron vanadate $FeVO_4$ was prepared using a solution of the desired amount of iron nitrate with 50 ml deionized water, which was added drop-wise to a solution of the desired amount of ammonium meta-vanadate dissolved in 100 ml deionized water, after being acidified to pH 2, with stirring and heating at 60^{o}C. It was then heated to 90^{o}C, then dried overnight at 120^{o}C. The result was calcined at 500^{o}C for 48h. Iron vanadate has a 1V to 1Fe ratio in its single phase $FeVO_4$, but there are two other ratios ($FeVO_4.xV_2O_5$) which were prepared by adding more ammonium meta-vanadate to achieve a 2V: 1Fe ratio and a 3V: 1Fe ratio.

Through the same method, iron tungstate was prepared from ammonium tungstate and iron nitrate in two different ratio. The stoichiometry phase is $Fe_2(WO_4)_3$ with a ratio of 1.5W to 1Fe, although, $Fe_2(WO_4)_3$ x WO_3 has more access to tungsten oxide on the iron tungstate surface referred to by the ratio of 2.2W: 1Fe.

Furthermore, copper molybdate, $CuMoO_4$, was prepared from copper nitrate and ammonium hepta-molybdate, in the same way as the iron molybdate preparation method which was described earlier. Furthermore, the stoichiometry of copper molybdate is 1Mo:1Cu, while both 1.5Mo:1Cu and 2Mo:1Cu were tested in this study. Manganese molybdate, $MnMoO_4$, was prepared by a reaction of manganese nitrate and ammonium hept-molybdate as descried for the iron molybdate preparation method. Nevertheless, the manganese molybdate single phase was 1Mo:1Mn ratio, whereas increased amounts of molybdenum on managanese molybdate achieved ratios of 1.5Mo:1Mn and 2Mo:1Mn, both of which were tested.

2.2.3 Incipient wetness impregnation

The impregnation method is quite a common technique for heterogeneous catalyst preparation. It is one of the methods for covering the surface of a catalyst through the use of incipient wetness impregnation. Principally, the metal precursor is dissolved in an aqueous solution which is then added to support; the support has pores which will be filled by the full volume of metal solution when

added. The concentration of the surface coverage is the same as the metal precursor concentration in its solution. It is important to know the liquid volume needed to fill the support pores. The mixture of the metal precursor and the support should then be dried and calcined to evaporate any volatile substances.

The impregnation method used in this study was to take 1g of a support, for instance, iron molybdate (2.2Mo:1Fe), which was then filled by a known volume of deionized water. Any more addition of the liquid would make the iron molybdate wet. In another way, the precursor metal weight should be dissolved in a volume of water in the same way as iron molybdate is consumed from water. Furthermore, the same situation was used for carbon support and iron oxide. The precursor metals and supports which were chosen in this study are listed in table below:

Precursor	Support	Concentration	Water
WO_3	$Fe_2(MoO_4)_3$	2%	0.33 ml
V_2O_5			
$Fe_2(WO_4)_3$			
$FeVO_4$			
$CuMoO_4$			
$MnMoO_4$			
MoO_3	Carbon	6%	1.95 ml
MoO_3	Fe_2O_3	3%	0.45 ml

Table 2.1 Catalysts prepared in the lab. by impregnation

Once the volume is known with regard to filling the support pores, the next step was to determine the total surface area of the support. For example, tungsten oxide was impregnated on iron molybdate, where the surface of the iron molybdate was 5 m^2g^{-1}. So 0.25% of WO_3 was the W sites per g, and each mole has an Avogadro's number times the atomic number. The weight of W which was then needed to fill the surface was calculated from its moles. The last step of the calculation was to calculate the W weight from its raw material which was ammonium para-tungstate. Then the amount which would have to be dissolved in

0.33 ml of deionized water was calculated to add to the dry iron molybdate. The mix was dried at 120^{o}C overnight. Before using the catalyst, it was calcined at 400^{o}C for 1 hour. The same calculation was used for the rest of the impregnated catalysts in the table above, in terms of the surface area for carbon (600 m^2g^{-1}) and iron oxide (10 m^2g^{-1}).

Calculations: (Tungsten as an example)

1. W sites = (No. of W atoms in WO_3) x (Support surface area ($Fe_2(MoO_4)_3$)) x (No of sites in 1 g of support (10^{19}). So, W sites = 0.25 x 5m^2/g x 10^{19} = 1.25 x 10^{19} sites of W / 1g of $Fe_2(MoO_4)_3$ for 1 monolayers.
2. W sites 1.25 x 10^{19} x 2 (monolayers) = 2.5 x 1e^{19} W sites/ $Fe_2(MoO_4)_3$.
3. 2.5 e^{19} W sites was tungsten concentration in 0.33 ml solution, but in 5ml solution, W sites = (2.5 e^{19} x 5)/0.33 = 3.8 e^{20} W sites.
4. W moles = W sites (3.8 e^{20})/ Avogadro's constant (6.0221417930 e^{23}) = 6.31 e^{-4} mole.
5. W weight form moles = W moles (6.31 e^{-4} mole) x W molar mass (183.85 g/mole) = 0.11601 g.
6. W weight was taken as $(NH_4)_{10}(W_{12}O_{41}).\ 5H_2O$, so, weight need to be taken from $(NH_4)_{10}(W_{12}O_{41}).\ 5H_2O$ = W weight (0.11601) x $(NH_4)_{10}(W_{12}O_{41}).\ 5H_2O$ molar mass (3132.2 g/mole) / No of tungsten in ammonium paratungstate (12) = 30.2805435 g of $(NH_4)_{10}(W_{12}O_{41}).\ 5H_2O$ in 5 ml deionized water.

2.2.4 Sol-immobilization method

The sol gel method is one of the new technologies used in catalysis. It forms catalysts in nanoparticles. This means different catalytic behaviour compared to the same catalyst prepared by another method such as co-impregnation, which means that it can be more active. It is a useful method for coating an active metal solution on a support. The principle of this method is to start with a colloidal solution. This is mostly in nanoparticles which are then immobilized on a support. In this study, nano-gold particles were immobilized on two supports - molybdenum oxide and iron molybdate. In practical terms, 1% Au/MoO_3 was prepared by taking the required volume from 12.25 g ml^{-1} $HAuCl_4.3H_2O$ which then reacted with a solution of 1wt% (PVA) poly vinyl alcohol (Aldrich= 80% hydrolyzed) as it was stirred for 15 min. The volume taken from the PVA solution was (PVA (w) /Au (w)= 1.2). The next step was to

make 0.1M of fresh $NaBH_4$ solution, where the volume added from $NaBH_4$ was calculated as ($NaBH_4$ (mol)/Au (mol)=5), and the mix was continuously stirred for 30 min. Afterwards, concentrated sulphuric acid (3-5 drops) was added to the solution to acidify it to pH1. After adding the sulphuric acid, the solution was stirred continuously for 1 hour. The solution was then filtered with sufficient deionized water. The two catalyst were dried overnight at 120^{o}C and the last step was to calcine them at 400^{o}C.

2.2.5 Catalyst placing

The catalysts tested in this study were crushed and then pressed by weights of up to 10 tons, and sieved using metal sieves. The size of the sieves used were 850 micrometer at the top where the pressed powder was smashed. Underneath this was another sieve which was 600 micrometer in size. This sieve was used to collect the catalyst crystals of a size between 600 and 850 micrometers. Then the resulting material was put into a glass tube on top of quartz wool. Finally, the catalyst was then run using a Cat-lab microreactor.

2.3 The pulsed flow reactor

The pulsed flow reactor was designed by Hiden Analytical Ltd. The reactor contains two modules, The first module is the Cat-lab microreactor, and the second module is the gas analyzer (QIC-20) using a mass spectrometer. The reactor is closed, and evacuated by two rotary pumps and another turbo-pump. There is another part called the Cat-lab control rack which is linked to the first module which contains of gas panel, a furnace power control and a process control interface. The pulsed flow reactor is important for studying a reaction kinetically and its mechanisms. Looked at another way, it is an industrial plant on a small scale, which is useful in the lab. It is also useful for studying the surface of a catalyst in order, for instance, to calculate the surface area.

2.3.1 Cat-lab Micro-reactor

The Cat-lab microreactor contains two parts. The first one is the micro-reactor where is where the catalyst bed is fitted as shown in scheme 2.1. The other part contains the gas panel, the furnace power control and the process control interface. The gas panel has 8 flow channels for mixing gases, ranging

from a flow rate of 2 ml min^{-1} to 100 ml min^{-1}. It is controlled by Cat-lab software in the computer through the process control interface. The process control interface is connected to the computer using a 9-way D-type cable starting from COM-0 in the process control interface to the comms port in the computer. It allows the user to control the sample temperature and the gases flow from the Cat-lab software using Windows.

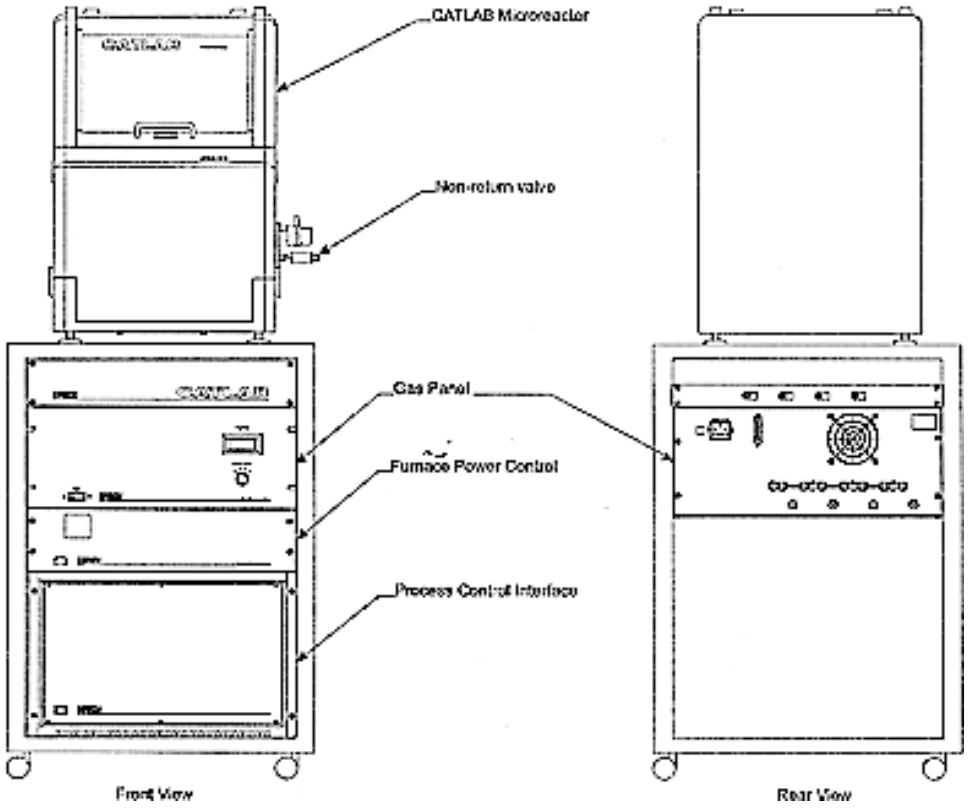

Figure 2.1 Micro-reactor module[4]

The microreactor has a catalyst bed fitted into a furnace. The catalyst bed is a long tube made of coated glass to withstand temperatures up 800^{o}C. The catalyst tube is also made of coated glass for less reactivity. It can be placed into the catalyst bed from the top, which is stopped by a point of narrow glass, as in figure 2.2. The other end of the catalyst bed is fitted down to the mass spectrometer line. However, not all of the gas flows into the mass spectrometer. The catalyst bed has a narrow mass spectrometer inlet starting just under the catalyst tube and linked to analysis line. This inlet takes small amounts of the gas while the rest is vented (Vent 1). There are three thermocouples; the first is the sample thermocouple which gets into the catalyst from the top of the reactor and gives a sample temperature read. The second thermocouple is fitted into the

furnace and is entitled the external furnace temperature thermocouple. This gives the furnace temperature reading. The third one is the sentry thermocouple, which is also fitted into the furnace. All temperature readings are transferred to the Cat-lab software in the computer through the process control interface.

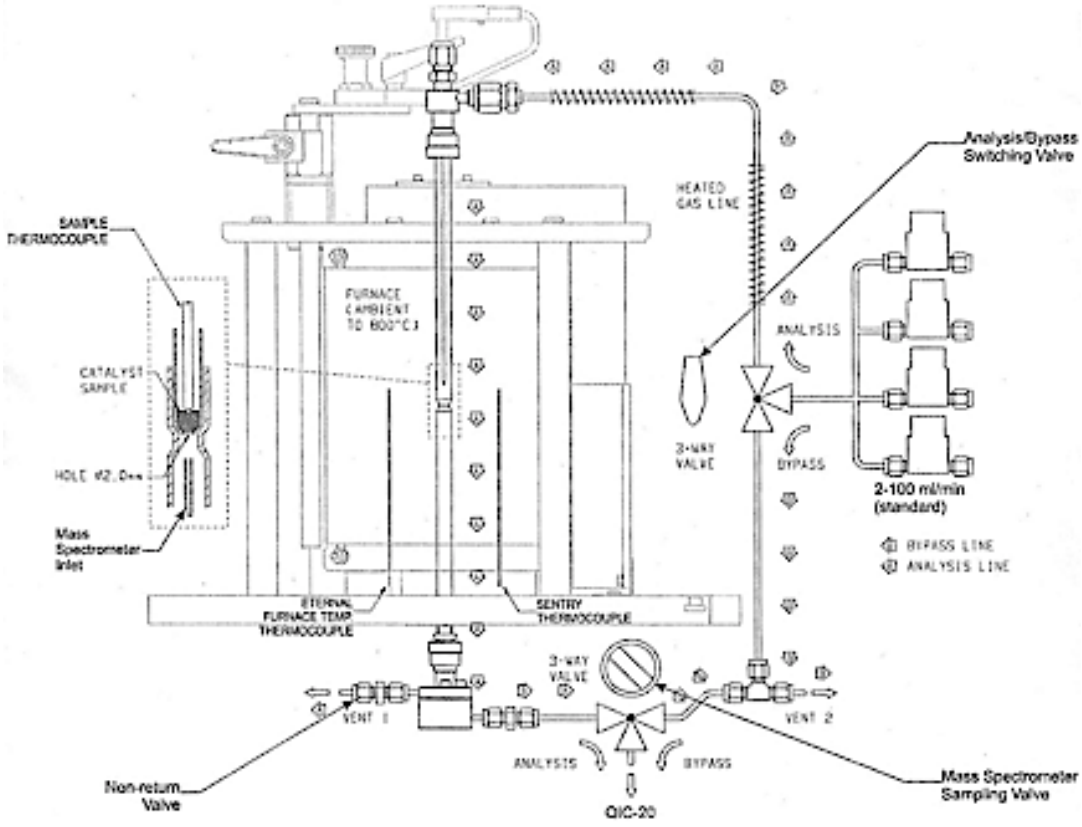

Figure 2.2 Schematic drawing of a Cat-lab microreactor[4]

As can be seen in figure 2.2, gas flows from the gas controller to the analysis/bypass switching valve (3 way valve), through the analysis line (A line, in figure 2.2) and then goes over the catalyst to the mass spectrometer through the mass spectrometer sampling valve (3 way valve). The line is heated to 60^{o}C. This valve gives an option of switching the gas line to the mass spectrometer or for the gas to be vented. Line B is the bypass line for when the gas goes either to the mass spectrometer through the mass spectrometer-sampling valve, or is to be vented.

The catalyst tube should be filled with 0.5g of a catalyst above a piece of quartz wool. As can be seen in figure 2.3, the inlet manifold assembly should be pulled up and the inlet loading clamp must be then tightened for safe sampling for when the gas has to be vented by switching the mass spectrometer sampling and the analysis/bypass (figure 2.2) valves to the bypass. Next, it is necessary to put the

catalyst tube into the catalyst bed and press it gently so as not to break the glass. The last step is to place the sample thermocouple into the catalyst tube until it reaches the catalyst crystals and screw all the nuts tight to avoid any gas leakage.

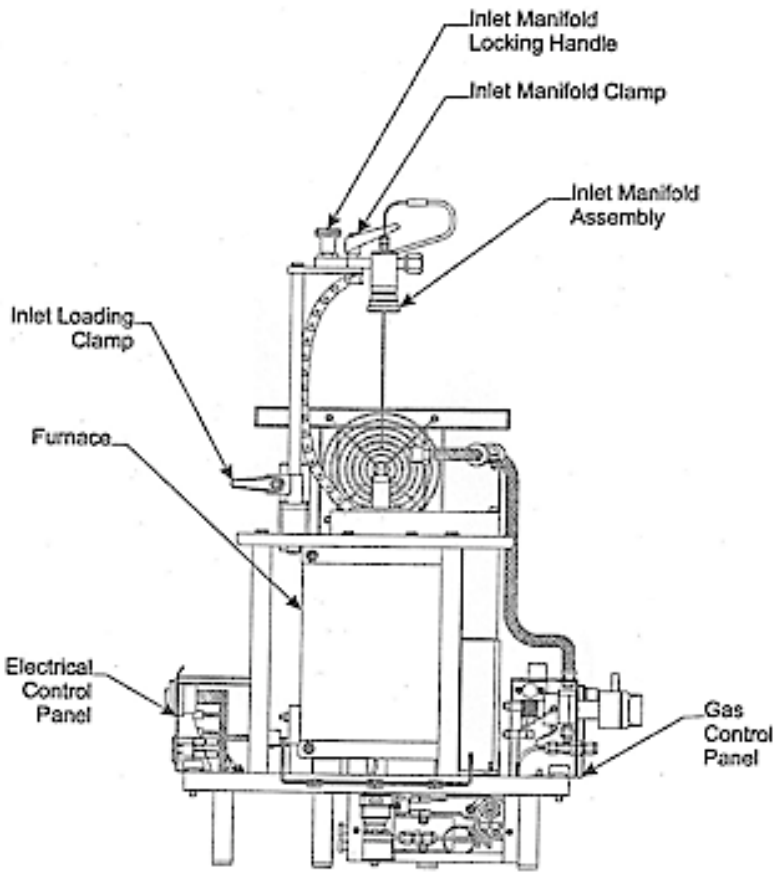

Figure 2.3 Cat-lab microreactor drawn for placing the catalyst[4]

2.3.2 Gas analysis system (QIC-20)

The gas analysis system was designed by Hiden Analytical Ltd. It is a closed box which contains a mass spectrometer, an ultra high vacuum (UHV) system, a pressure gauge and a sampling system. As can be seen in figure 2.4, there is a mass spectrometer probe, an RF head, a UHV chamber, a penning gauge head, a QIC capillary inlet, a turbo power supply, a capillary temperature controller, a penning gauge controller, a turbo interface unit and a mass spectrometer interface unit. The QIC box is built in such a way as to protect the equipment from dust with a hood from the top and a glass door to the front. It also has fans to cool it down, so that it does not reach too high a temperature,

since this would cause damage to some electronic parts. The emission is set at 1000 μA with a multiplier potential of 850 V.

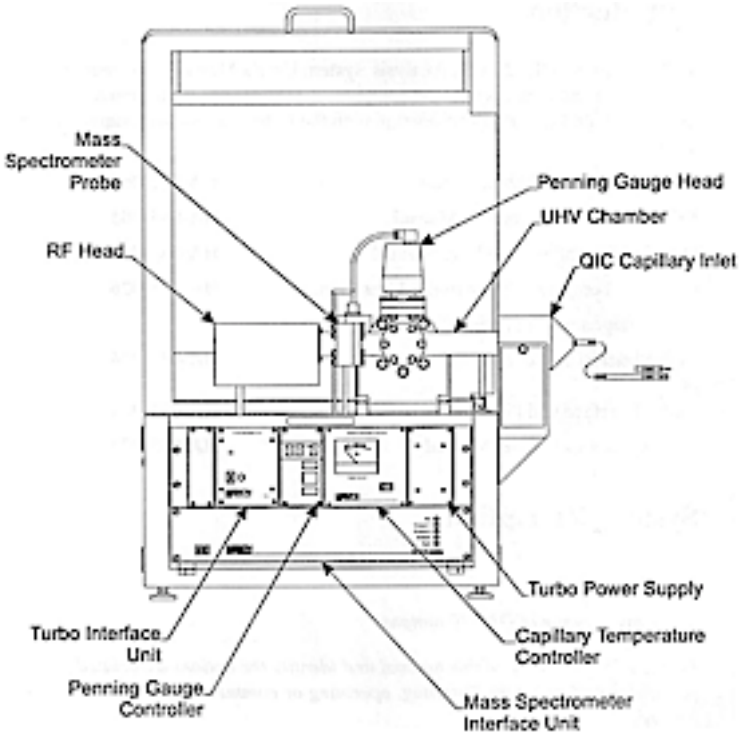

Figure 2.4 QIC 20 module[5]

Mass spectrometry is a useful technique for chemical compounds analysis which depends on the mass to charge ratio (m/z). The principle of mass spectrometer analysis is to ionize a molecule and accelerate it and separate ions by deflecting them to fly with different trajectories according to their mass-charge ratio (m/z). The quadruple mass spectrometer is one of the mass spectrometer techniques. It contains an electric field instead of a magnetic field. It contains an ion source, a single quadruple mass filter and a detector, as shown in figure 2.5. The range of masses is between 2 and 200 atomic mass units. In principle, vapours go to the ion source, which mainly has twin filaments of tungsten of 0.15 mm diameter, which generate electrons which bombard the gas particles, making them positivity charged. Then the positive ions are focused into a (z-axis) quadruple mass filter, with approximately the same potential energy. An electromagnetic field is produced by voltage being applied between two rods pairs, which are 6 mm in diameter. V is the alternating current (AC) applied to one opposing pole pair, and U is the direct current (DC) applied to the other pair.

Depending on the voltage applied, masses will be deflected according to their mass to charge ratio. They will then strike rods and will be removed by the vacuum system. However, the quadruple mass filter is less selective with heavy masses, because the electric field increases the oscillation amplitude. This may lead to ions colliding or leaving the quadruple mass filter. The amplifier (RF) is fitted to the probe (quadruple mass filter) and is connected to it via a 12-way connection; the RF head contains single conditioning electronics, a power supplier for the quadruple mass filter, and a cable connected to the RC interface unit (RC-IU) The RC -IU is connected to the computer and fully controlled by Cat-lab software. It has an automatic shutdown function for the mass spectrometer in the event of leakage or high pressure gas entering the mass spectrometer.

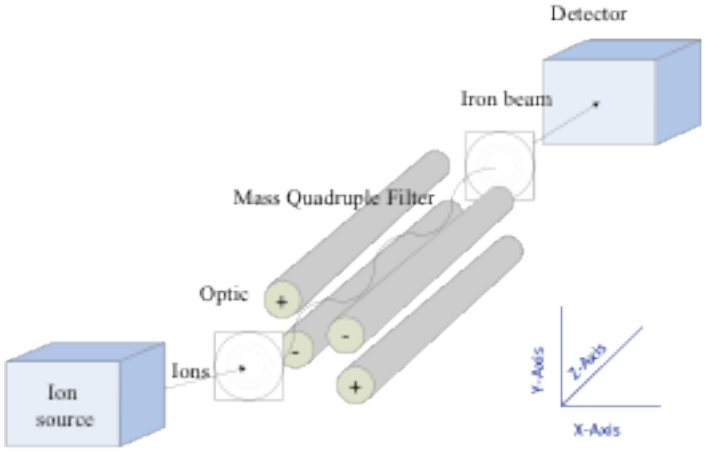

Figure 2.5 Mass quadruple filter

The mass spectrometer analysis system has to be evacuated of air and ions steams deflected by the quadruple filter, which may cause a collision with ions beam going to the detector. In general, the mass spectrometry techniques require a gas pressure lower than 10^{-6} torr. Consequently, there is another system which solves this problem in addition to the vacuum pumps. This is the fast sampling system. The fast sampling system contains a capillary inlet and a platinum orifice (see scheme 2.6). Gas goes to the QIC-20 system through a silica capillary inlet which is connected to a bypass rotary pump. This causes a pressure reduction with high velocity. Further reduction is made by the platinum orifice when gas exits the capillary line. The platinum orifice is placed at a distance of 4 mm, and

the gas passes through the orifice to the ion source which is located at a distance of 12 mm between the orifice and ion source. One of the fast capillary sampling functions is to heat the gas by heating the silica capillary (160^{o}C), the orifice and the bypass regions (120 ^{o}C).

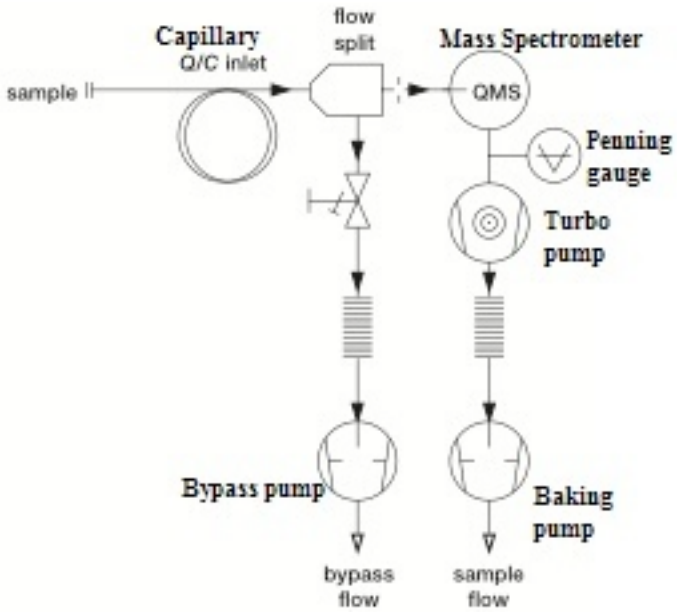

Figure 2.6 QIC-20 sampling systems[7]

There are three pumps fitted in the QIC-20. These are the turbo-molecule pump, the baking rotary pump and the by-pass rotary pump, as shown in scheme 2.6. All pumps help to remove gas and air from the mass spectrometer. The turbo-molecule pump is designed by Pfeiffer Vacuum (TMU 071), as in Figure 2.7. It contains a high vacuum flange which is connected to the ultra high vacuum chamber (H, 1), a force vacuum flange (2, V) which is connected to the baking pump, a venting valve (4, F), a remote plug (8d) and an electronic drive unit which is connected to the RC interface controller.

The principle of the vacuum pump is to pump gas particles out of the UHV chamber, and to reach a pressure lower than 10^{-6} torr. Starting from the active design which contains rotors and stators surrounded by turbine blades, each pair of rotors and stator blades forms stages. As can be seen from figure 2.8, the gas particles hit the rotor during the first stage. They will then be then forced by the first stage of the rotors and stators to the outlet, via shorter radial blades at lower stages. Then the gas will be removed by the backing rotary pump.

1 High vacuum flange
2 Fore-vacuum flange
4 Venting Valve
6 Rubber feet
8 Electronic Drive Unit TC 600
8d Remote plug

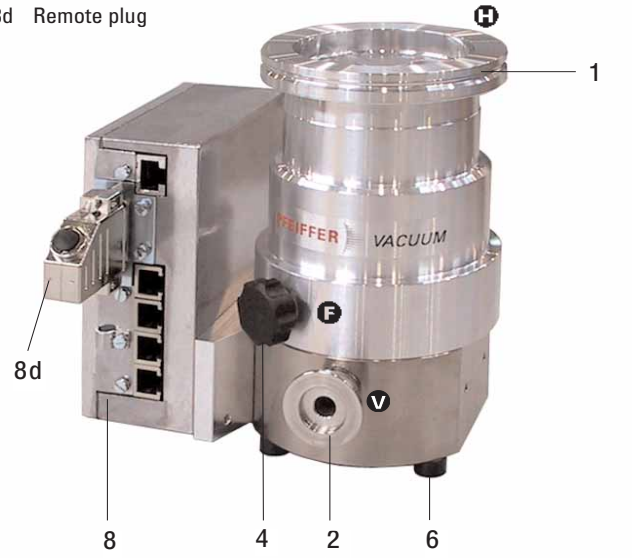

Figure 2.7 Pfeiffer turbomolecular pump[8]

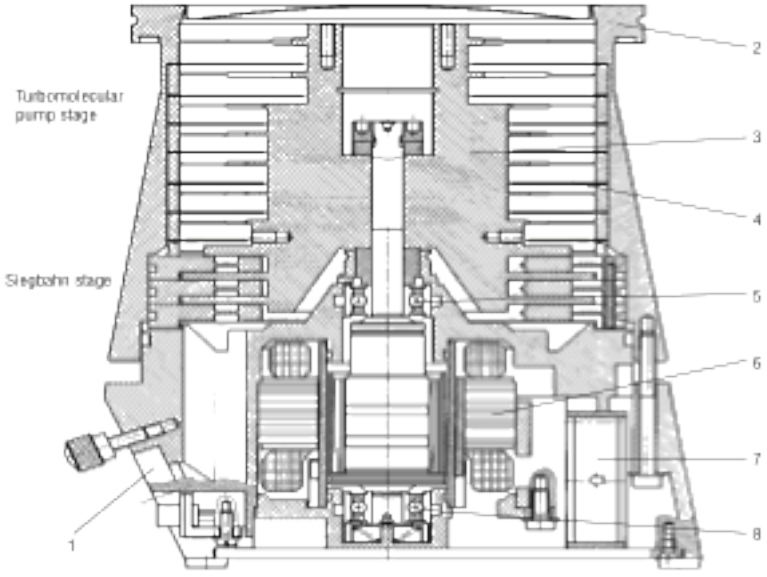

1 Vacuum port
2 High vacuum flange
3 Rotor
4 Stator
5 Bearing
6 Motor
7 Fan
8 Bearing

Figure 2.8 Vertical cross section of a turbomolecular pump[9]

Rotary vane pumps are fitted in this equipment. One is the bypass pump, while the other is the baking pump. It consists of a pumping house, rotors, oil level slide glass, a suction duct, an anti-suck-back valve, a dirt trap, an intake port, a lid of gas ballast valve, an exhaust port, an air inlet silencer, an oil filter, an exhaust valve, an exhaust duct, a gas ballast duct, an oil injection valve and a vane. It involves three vanes balanced at 120^{o}. These rotate and are forced by centrifugal force and springs. The gas enters the pumping stator house through the intake port, and will be rotated by the vanes and pushed out through exhaust port to be vented.

Pressure is measured in the QIC-20 by a Penning gauge, which is fitted on the ultra high vacuum (UHV) chamber, between the turbomolecular pump and the mass spectrometer. PFEIFFER Vacuum manufactured the penning gauge - the IKR 261 - and it is an active cold cathode with a molybdenum filament. As can be seen from figure 2.9, it contains a cathode axis and two endplates, an anode, an open cylinder, and an iron current amplifier. In principle, as the discharge is made by the electric field and the magnetic field, the gas needs be measured. It is ionized by a filament feed with 6 kV, which generates gas ions and a discharge current. The discharge current is affected by the magnetic field and will travel to the anode along a longer path. The gas ions will go to the cathode to generate an ion current. The result in terms of gas pressure is shown through an electrometer (see scheme 2.10).

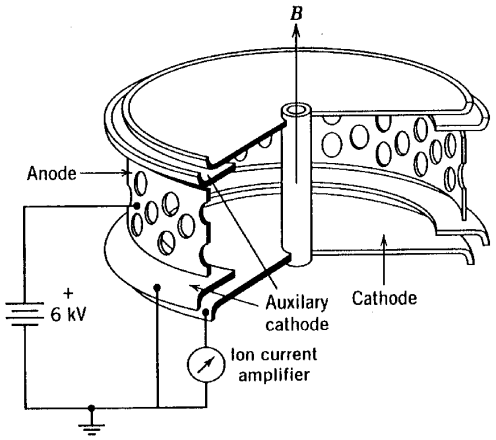

Figure 2.9 Diagram of the Penning gauge[10]

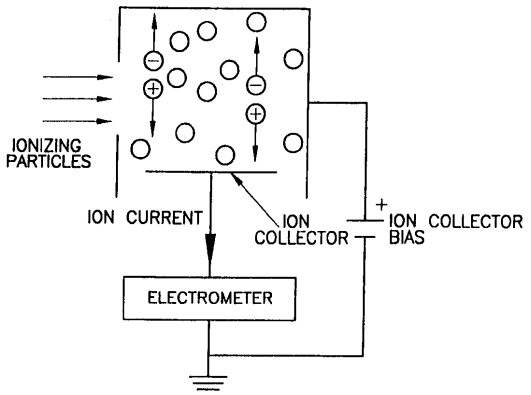

Figure 2.10 Drawing of the ionization gauge principle[10]

The QIC and the Cat-lab microreactor have to be calibrated to avoid errors in the results when using it. The calibration is used to see any reactivity in the tube used in the reactor. The tube used for the catalyst run is made from coated glass. It has a hole at the end, which must be blocked using quartz wool. Both the glass tube and the quartz wool are unreactive when there is no catalyst present.

2.3.3 TPR

The temperature programmed reaction (TPR) is an oxidation reaction in the presence of oxygen and with helium as a carrier (10% O_2/ He). The other point is to control the temperature as desired by increasing or decreasing temperature which is controlled by computer. In the TPR, the temperature rise rate was 8^oC per minute; and the range was from room temperature up to 400^oC, with the gas flowing at 30 ml min^{-1}, and the gas pressure in the cylinder was 20 bar. Methanol is in the liquid phase and has to be converted into the gas phase. This was done by injecting 1 microliter into a heated pipeline which has a flow of oxygen and the carrier gas which will carry the injected methanol to the catalyst. Methanol was injected one microliter every 2 minute. The temperature program should not start until the surface of the catalyst was covered by methanol monolayer. This can be determined when at least 5 peaks of methanol are the same in height, which means methanol is not consumed by the surface.

Practically, the catalyst is pressed and sieved between 650 and 800 micrometers in size. Then 0.5g of the catalyst is placed into the catalyst tube on top of quartz wool. Another piece of quartz wool is placed on top of the catalyst, otherwise some of the catalyst particles might be flushed out of the tube. The next step is to thermally pretreat the catalyst after conducting a check for gas leaks. The temperature of the pretreatment is 400^oC for 60 min. This is to clean the catalyst surface of volatile components. It should then be left in order to cool down. The next step is to calibrate the reactor with methanol. 1 microliter of methanol is injected every 2 minutes through the bypass line up to 5 times. When the catalyst is not involved in this step, the mass spectrometer will show the sensitivity to methanol, as it tends to vary from one experiment to another. Figure 2.11 shows

the raw data obtained from the mass spectrometer. Software is then used for better quality plotting.

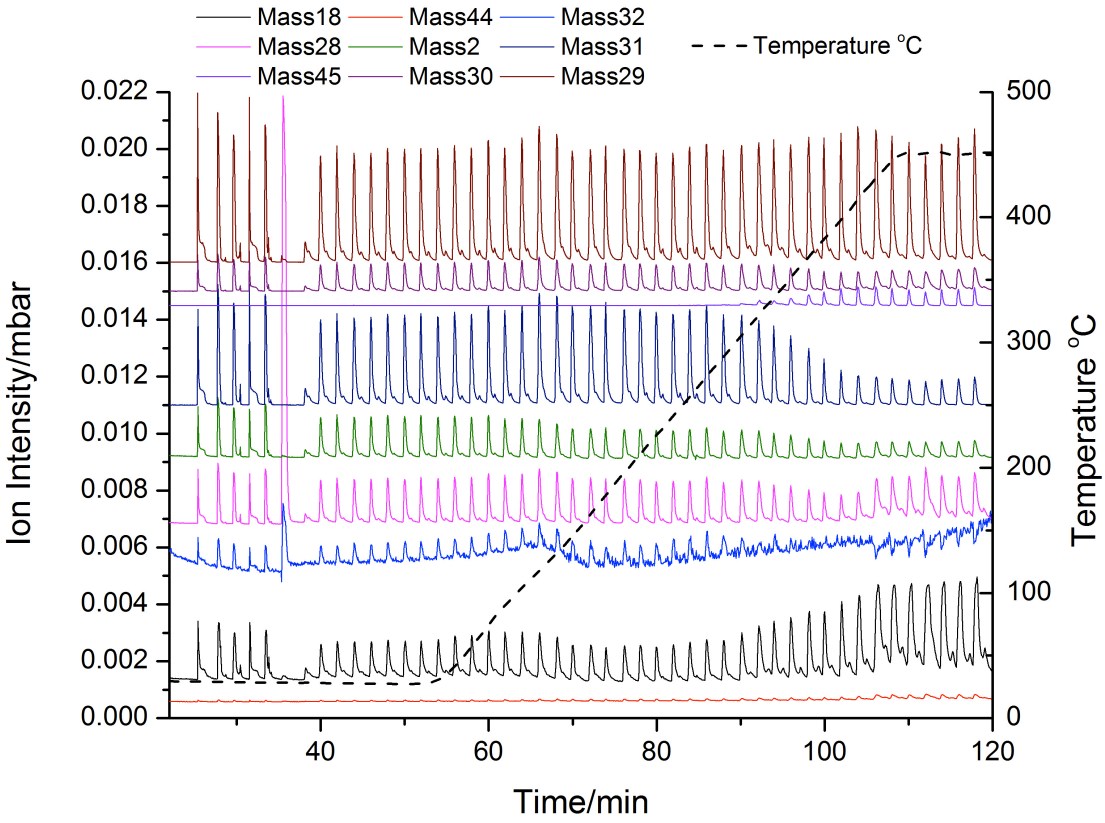

Figure 2.11 TPR raw mass spectra example

Methanol injections appear as pulses in the data chart above. The first five injections were injected in the bypass, and then the valve was switched back to pass through catalyst. The catalyst is placed on a clean surface, which has to be covered with methanol before the temperature programmed start. 12 injections were sufficient to cover the surface. Then the temperature was increased at a rate of 8°C per minute. The maximum temperature reached in this reaction was 450 °C. The masses were scanned in the mass spectrometer. These have to be chosen before the beginning of the experiment based on the literature. In the case of the methanol oxidation reaction, the masses scanned were methanol, formaldehyde, carbon monoxide, carbon dioxide, dimethyl ether, oxygen, water and hydrogen. However, other alcohols were tested in this research - ethanol, iso-propanol and n-propanol. Ethanol oxidation has other masses such as ethanol itself, ethanal and ethylene, as well as carbon monoxide, carbon dioxide, water and hydrogen. Iso-propanol oxidation involves masses of acetone, propane, propylene and iso-propanol, as well as carbon monoxide, carbon dioxide, water and hydrogen.

Nevertheless, the masses scanned for n-propanol oxidation were similar to the other alcohols for carbon monoxide, carbon dioxide, water and hydrogen, whereas n-propanol produces n-propanal, propane and propylene. More details of each product-cracking pattern will be explained later in this chapter.

Further analysis has been done by converting the pulses in Figure 2.1 to data points making curves. These curves show the selectivity of the catalyst used with each product, and how much of the reactants were converted to products. First of all, each molecule has cracking fragments in several masses analysed. For example, formaldehyde is 100% mass 29, 88.5% of mass 30, mass 28 has 30.9% of formaldehyde and others as in Table 2.2.

Compound	Cracking fractions (%)
Water	18 (100) 17 (21.1), 16 (0.9), 19 (0.5), 20 (0.3)
Carbon Monoxide	28 (100) 12 (4.7), 16 (1.7), 29 (1.2), 14 (0.8)
Carbon dioxide	44 (100), 16 (9.4), 28 (8.2), 12 (6.7)
Methanol	31 (100), 32 (71.7), 29 (42.1), 28 (9), 30 (7.8)
Oxygen	32 (100), 16 (3.6)
Formaldehyde	29 (100), 30 (66), 28 (33), 31 (3)
Dimethyl ether	45 (100), 29 (39), 15 (24), 31 (3), 43 (1)
Hydrogen	2 (100), 1 (2.1)
Ethanol	31 (100), 45 (34.4), 27 (23.9), 29 (23.4), 46 (16.5)
Ethanal	29 (100), 44 (88.3), 43 (50), 42 (14.9), 28 (9)
Iso-propanol	45 (100), 43 (19), 27 (10), 41 (7), 29 (6), 39 (5.7), 28 (5.2),
n-propanol	31 (100), 29 (17), 59 (15), 27 (14), 42 (13), 28 (10)
Acetone	43 (100), 58 (27.1), 27 (8), 42 (7), 26 (5.8), 29 (4.3)
Propylene	41 (100), 42 (69.2), 39 (60.9), 27 (24.7), 38 (14.4)
Propane	29 (100), 28 (61.5), 44 (40.2), 43 (33.6), 27 (31.6), 39 (16.5),
Propanal	29 (100), 58 (64.2), 28 (62.3), 27 (35), 57 (18.6), 26 (10.2),
Ethylene	28 (100), 27 (63.4), 26 (62.7), 25 (12.2), 14 (6.9)

Table 2.2 Cracking fractions of reactants and products - % fraction in brackets

The mass spectrometer is more complicated than just scanning masses. In the example provided earlier, carbon monoxide has 100% cracking in mass 28, so there will be a contribution in the carbon monoxide reading if there is any

production of formaldehyde at the same time. The way to avoid this is to remove formaldehyde form mass 28, which at the end gives an amount of carbon monoxide. Each pulse was converted to a digital value by calculating the peak area integrally. Consequently, the value of formaldehyde will be subtracted from the value of the mass 28 peak The remaining value is the carbon monoxide value, which can then be plotted in chart using Origin software as shown Figure 2.12.

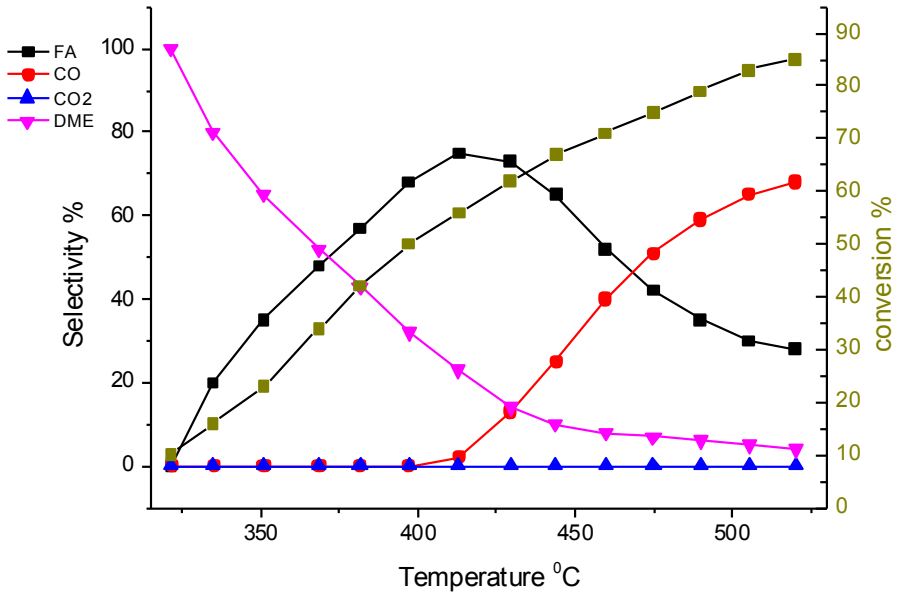

Figure 2.12 An example of selectivity and conversion chart

From Figure 2.1, methanol affects all masses even when there is no catalyst (bypass), and the temperature is low, so methanol was removed from all other masses. The next step was to remove the contribution of all masses. For example, formaldehyde has cracking in mass 28 (30.9%), and mass 28 should be carbon monoxide cracking, so formaldehyde was subtracted from mass 28 as (mass 28- (formaldehyde * 0.309) = carbon monoxide). This approach was applied to all other masses. Figure 2.2 is the final graph after analysis. It shows the conversion of the reactant on a catalyst at various temperatures. It also shows the selectivity of each product. Another analysis can be obtained from the chart. This was the yield to products, where the yield is the product of selectivity and conversion at the same temperature.

2.3.4 TPD

Temperature programmed desorption (TPD) is a useful technique in heterogeneous catalysis. It shows the preferred products for a catalyst at various temperatures. TPD was run with a helium gas flow through a catalyst at a rate of 30 ml min^{-1}. The catalyst was then filled with a sufficient volume of the reactant. In another way, methanol or other reactants were injected, with 1 microliter of the reactant being injected every 2 min. When the surface of the catalyst was covered by the reactant, the peaks remained steady, so the peaks remain the same with regard to any further injection. The next step was to allow all peaks to settle down (approx. 25 min). The TPD was then started and the temperature increased from 25°C to 400°C. The temperature rate rise was 12°C per minute, as shown in Figure 2.13. TPD can be used to determine the heat of adsorption, Redhead who has first introduced it, using its equation to calculate the heat of adsorption from desorbed peak in TPD result, where $Ed/dt = A/B\ e^{-Ed/RT}$, $A \sim 10^{13}$, B is found in the TPD spectra.

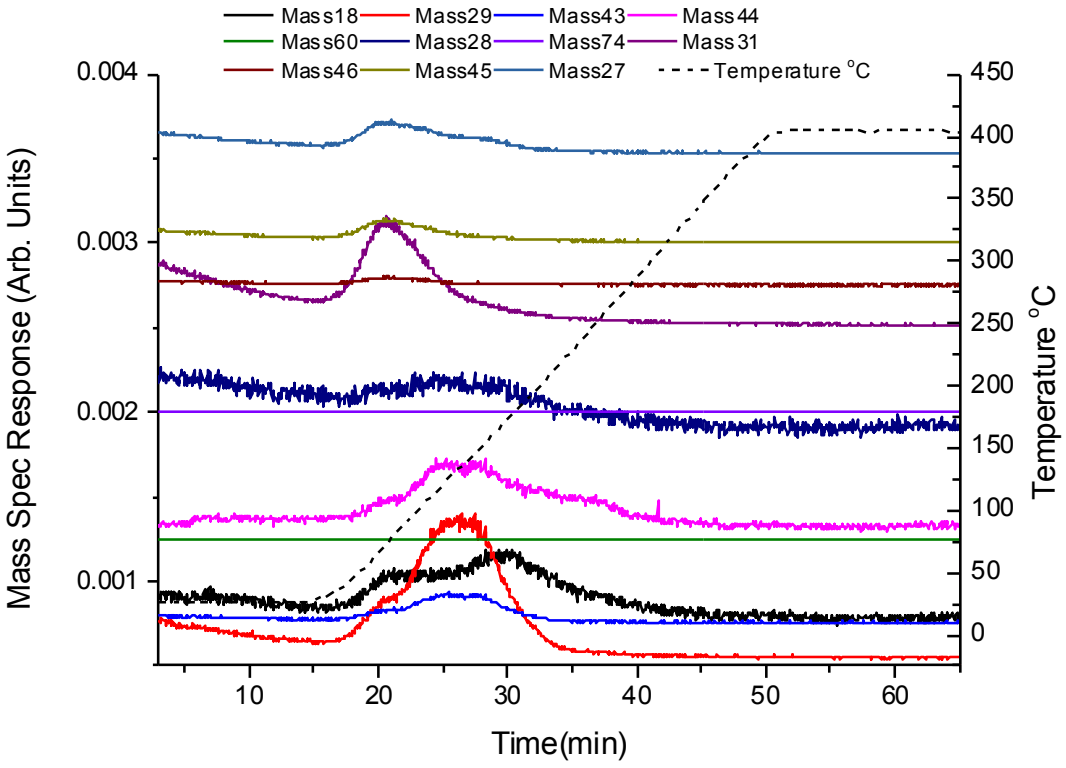

Figure 2.13 An Example of TPD result

Figure 2.13 shows the desorption of masses according to the left Y-axis, and the right Y-axis is the temperature reading as plotted as a dotted line in the graph. Both were plotted against time (min) on the X-axis. The results depend on the products which appear in the absence of oxygen. As a result, the main factor is the catalyst itself, which is the favorable reaction pathway of the oxidation reaction and donates its oxygen atoms to the products, and gives only the preferred products. TPD also explains the heat needed of desorption of each product, and how the catalyst is active with regard to each product, for example, formaldehyde desorbs by 180 ^{o}C on iron molybdate catalyst.

2.3.5 Surface area measurement

There are several techniques to measure the surface area of a catalyst. One of them is methanol coverage using a Cat-lab micro-reactor. The measurement is based on the volume of methanol which is which is needed to cover a catalyst surface, where the gas flowing was helium at a rate of 30 ml min^{-1}, and at a temperature of 25^{o}C. Once the methanol volume was known, further calculations were applied to obtain the surface area in meter square per gram.

In practical terms, methanol is injected on to the catalyst. In the first few injections there will be small peaks of methanol shown in the computer using the mass spectrometer. The methanol peaks are small because part of the methanol is consumed by the catalyst as it fills its surface and covers it. The calculations which were used to determine the surface area were used previously by the Bowker group, 2 microliters of methanol were consumed by 1g of the catalyst. It then equals 0.002 cm^3, where the mass of the methanol is the volume of the methanol (0.002 cm^3) times methanol density (0.7918 $g.cm^{-3}$), which is 0.001584 g of methanol. Then the methanol moles is 4.95 10^{-5} (mole = mass (0.001584) / molecular weight (32)), and the number of methanol sites is Avogadro's number (6.02214179 10^{23}) times methanol moles (4.95 10^{-5}), which equal 2.98 10^{19}. By assuming that every square metre of the catalyst has 1 10^{19} sites available, so the surface area of that catalyst is 2.98 $m^2.g^{-1}$. The results were compared to the BET surface area measurement (section 2.7).

2.4 Raman spectroscopy

Raman spectroscopy is useful technique to determine molecule vibrational modes. It is based on Raman scattering of monochromatic laser, where the laser interacts with molecular vibrations and then scattered, which changes the laser energy by increase or decrease, however, the scattered laser is detected to determining these shifts in energy, and gives an information in vibrations of studied molecules either solid, gas or liquid.

2.4.1 Theory

The Raman spectroscopic technique relies on scattered radiation from a molecule. It begins with a monochromic excitation source in the form of a laser. This projects photons which are used to hit the molecule. This will produce three kinds of scattered radiation, as shown in Figure 2.4. The first radiation is an elastic interaction which includes scattered photons (ν_{sc}) with an energy equal to the photon that was used to excite the molecule (ν_{ex}). This is called Rayleigh scattering ($\nu_{sc}= \nu_{ex}$), while the other two radiations are the Raman scattering. They are an inelastic scattering which involves either decreased or increased scattered photon energy, referred to as Stokes and anti-Stokes lines respectively. The Stokes line is an electron which has energy and which has left its ground state. It then returns at a level higher than its ground state,. The return involves losing less energy than the excitation energy. On the other hand, the anti-Stokes line is an electron excited in a molecule which is already excited and has left its ground state. However, the electron returns to a level lower than its ground state before it was excited. The Rayleigh scattering is filtered and the remaining Raman collected and focused in the detector. The results then appear in terms of the frequency of the scattered radiations.

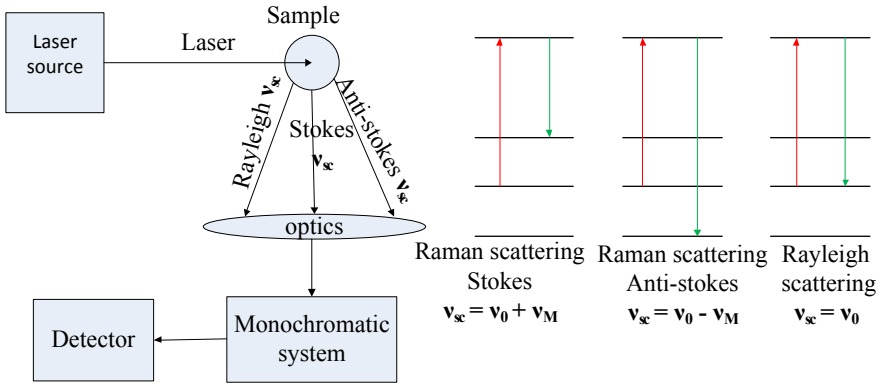

Figure 2.14 Raman spectroscopy system and theory

2.4.2 Equipment

The spectroscopy equipment that was used was a RENISHAW inVia Raman microscope. This has a green argon iron laser ($\lambda = 514$) with an output of less than 30mW. The samples used were all solid and only 0.2g of each sample was tested on an aluminum plate. The instrument was calibrated using standard silicon in a static run centered at 520 m^{-1}, with 100% power and 10-second accumulation. When repeated to five accumulations, it gives one peak at 520 cm^{-1}.

All the results were collected, and were compared to findings in the literature. Each sample was analyzed by Raman when it was fresh and after using it as a catalyst for methanol oxidation to see a difference in the structure, especially the change in the surface structure depending on the reduction of intensity of each peak.

2.5 X-ray diffraction (XRD)

X-ray diffraction is an important tool for determining the bulk structures of samples that were tested in this study. It analyzes the polycrystalline diffraction of X-rays by powders, as every material has a specific unique pattern which can be then be compared to the database and to the literature.

2.5.1 Theory

The principle of x-ray diffraction and bulk structure determination is that when an x-ray beam hits a polycrystalline sample, this sample has atoms ordered in a specific planes for each crystal, which build the unit cell with d-spacing between planes, basically, x-ray beams with known wavelength and theta angle projected onto a sample, which then will be reflected at theta angle (figure 2.15), then Bragg's law, **$(n\lambda = 2d \sin \theta)$**, is applied to determine d-spacing, where λ is the wavelength of the incident x-ray, θ is the angle between the incident ray and the reflected one, and *d* is the space between the atoms in the lattice. The plotting angular positions and intensities produce patterns that are characterization of that sample, it is a fingerprint of a powder can be compared to literature and database to determine its phases. The unit cell of atoms arrangement is defined by three-

dimensional a, b, c with interaxial angles between them as α, β and γ which illustrated in figure 2.16, which also called lattice parameters, which defines unit cell shape, for example cubic crystal has a = b = c in length, and $\alpha = \beta = \gamma = 90^{o}$. However, plane form can be determined by indices h, k, and l that cut the a, b and c axis, where h cuts a-axis, k cuts b-axis and l cuts c-axis, for example plane (200), cut a-axis in half, where parallel on b-axis and c-axis, figure 2.17 is an example of plane (100).

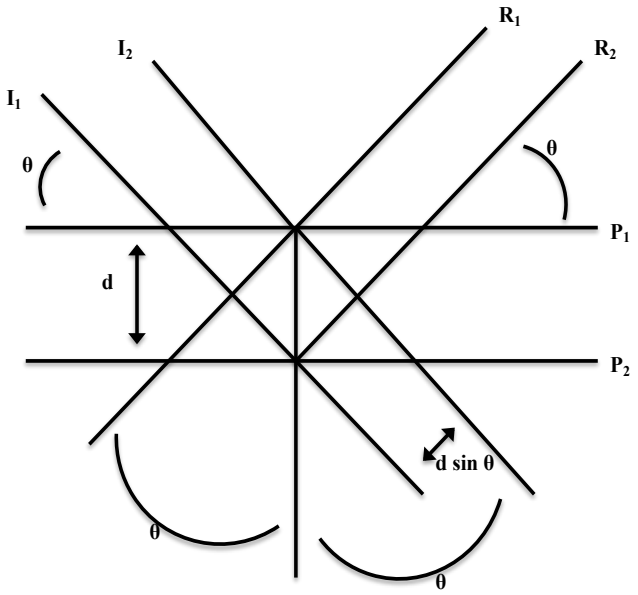

Figure 2.15 X-ray diffraction theory, where I = incident rays, R= reflected rays, d = spacing between two planes, P= planes and θ= theta angle.

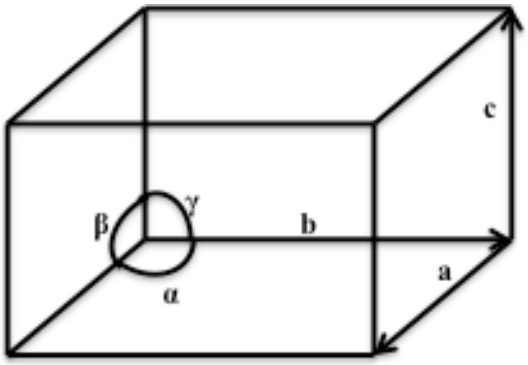

Figure 2.16 Example of unit cell parameters

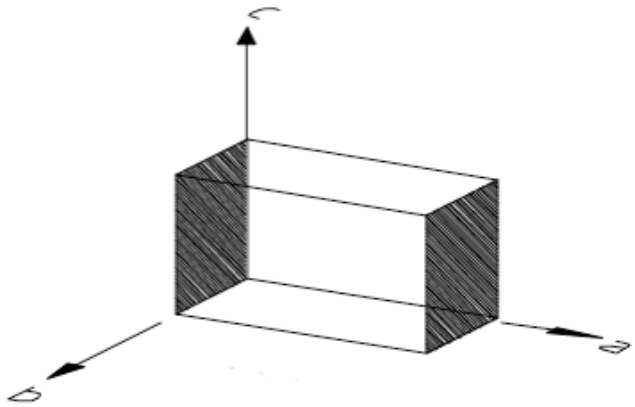

Figure 2.17 Example of (100) plane form

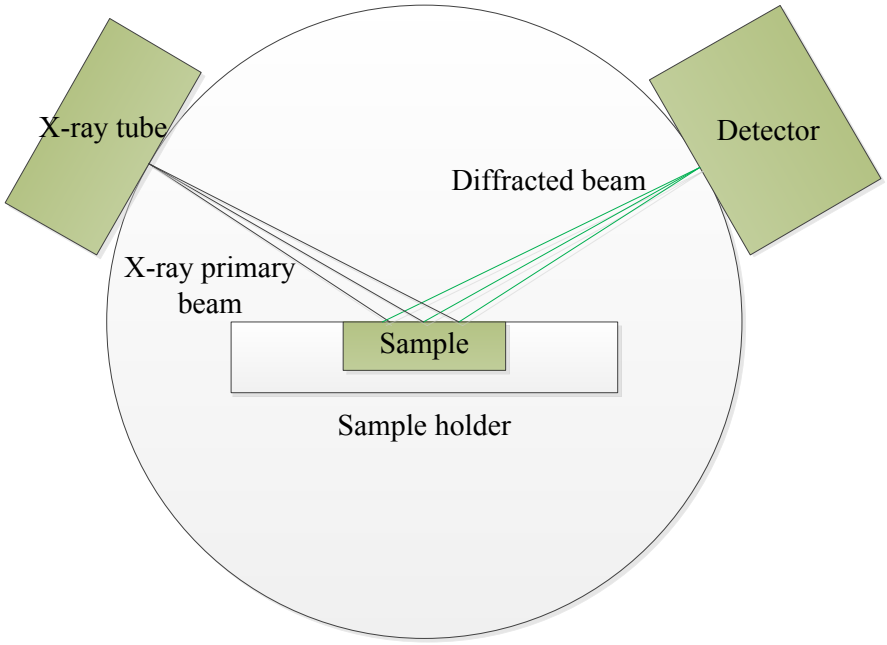

Figure 2.18 X-ray diffraction principles

XRD machine contains of three main parts, x-ray tube, sample holder and detector, this design called Bragg Brentano Theta: Theta goniometer, where the sample holder is stationary horizontal, but the x-ray tube and the detector move over a range of theta angles in a focusing circle, and distance between the x-ray tube and sample is the same as the distance between the sample and the detector. The x-ray tube contains of two main parts, cathode and anode, where cathode has the filaments and focusing cup, the common x-ray tubes contains dual metal filaments, which emit electrons by AC current applied to them, where are focused

to move in a small stream by focusing cup to the targeted anode, the anode is either sealed (old tube) or rotating, where the most common metal target is made of copper, and Kv applied the anode target to accelerate electron that give radiation in X-ray region. The reflected x-rays are collected to flat panel sensor.

2.5.2 Equipment

The equipment used for XRD was a X'Pert PRO, manufactured by PAN Analytical. The metal used to generate x-rays was Cu Kα (λ = 1.5418 Å), with a voltage of 40 kV and a current of 30 mA. This technique was used to determine the structure of the samples used as catalysts for methanol oxidation to formaldehyde, where every sample was analyzed when it was fresh and after being used for the oxidation reaction.

2.6 X-ray photoelectron spectroscopy (XPS)

X-ray photoelectron spectroscopy is a powerful tool for surface analysis. It analyzes the surface composition and the chemical state, as every element has a characteristic binding energy. It analyzes atoms on the surface layers within 1 micrometer. XPS is a surface sensitive technique and is also referred to as electron spectroscopy for chemical analysis (ESCA).

2.6.1 Theory

The XPS instrument is an ultra high vacuum system (UHV) (Figure 2.19), and contains an ultra high vacuum chamber where the sample is held. An x-ray source is fixed to the top of the sample with. The sample is placed on a sample holder and is then placed into the instrument in the sample introduction chamber. A low vacuum is then applied before it is moved to the ultra high vacuum chamber. The x-ray source contains of cathode part that emits electrons when heated, the electrons hit a metal target (anode) that normally has potential applied to it (5-20 Kv), which produce x-ray radiations, the anode is normally either Mg Kα at 1253.6 ev Al Kα at 1486.6 eV. However, other unwanted radiations are produced (satellites, Bremstahlung), which can be removed by monochromatizing x-ray radiations using quartz crystal. x-ray (Rowland circle). The x-ray photons from the source are absorbed by the surface atoms, either the top layer atoms or the lower layers atoms (causing signal noises, because the

emitted electron collides with another electron in the upper layers and loses some of its energy, and scattered photoelectron collides to surrounded electron that reduced its energy). Then the core electrons leave the atoms and travel to the detector where they are detected. This leaves an electron vacancy which lets another electron with higher energy occupy the vacancy and second photoelectron emitted as Auger electron, whereas fluorescence is fall of electron from higher energy level to fill vacancy and photon will be emitted instead of photoelectron.

Electrons pass through the concentric hemispherical analyzer (CHA) to the detector. The CHA contains magnetic and electrostatic lens that allow ejected electrons from the sample to pass through them to hemispherical part, where the hemispherical part contains of inner hemisphere and outer hemisphere, where ejected electrons pass through the two hemisphere which then are filtered as their velocity or energies, and electrons are directed to the detector that within selected energy range. This will then be detected according to their kinetic energy (KE). The result is given in binding energy as per the following relationship: $KE=h\nu-BE-Ø$, where KE is measured by the XPS spectrometer, $h\nu$ is the photon energy from x-rays which are controlled, Ø is the work function which can be found by calibrating the instrument. Using this, BE is calculated. As the photoelectron spectrum is plotted as electron intensity against binding energy, this is used also to show the change in the compound and the oxidation sate.

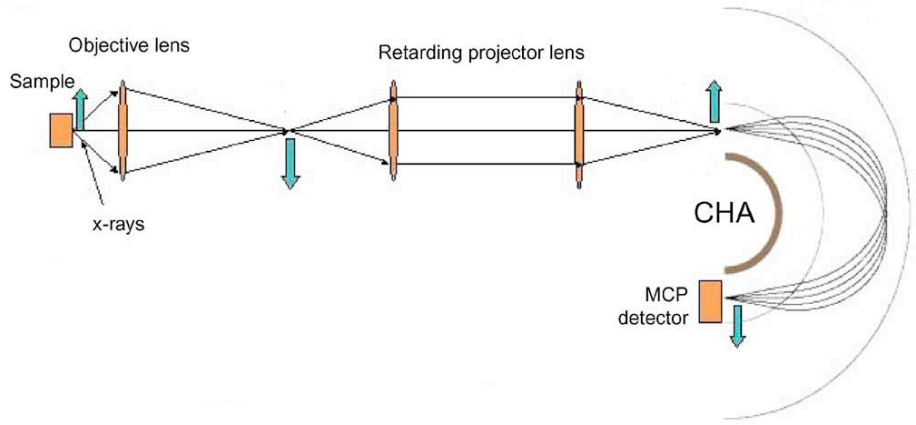

Figure 2.19 schematic XPS instrument (KRATOS) [15]

2.6.2 Equipment

The XPS instrument that was used in this study was the AXIS Ultra DLD, manufactured by KRATOS Analytical, (figure 2.20). It has more than one use in that it has a quantitative parallel imaging system, a snapshot spectroscopy and a charge neutralization system. It has a KRATOS patent with regard to the magnetic immersion lens, the spherical mirror and the concentric hemispherical analyzers. It gives high XPS resolution because of the refocusing lens and monochromator. It has the newly developed delay-line detector (DLD).

Figure 2.20 AXIS Ultra DLD by KRATOS Analytical

It offers a large pass of energy (160 eV) in a single sweep, and a 0.5 eV step. This shows all elements on the surface in the form of a survey scan. Another high resolution scan was applied to the samples. It was collected with a low passing energy of 40 eV, and sweeps from 5 to 10, with a 0.1 eV step.

2.7 BET surface area measurement

BET is an adsorption isotherm which was published by Brunauer, Emmett and Teller in 1938[16]. It measures the adsorption of a gas on a solid surface. The BET equation was published after the Langmuir isotherm. The Langmuir isotherm is simpler than the BET isotherm. It is used when the gas pressure is low and explains only a monolayer of gas on the surface of a solid[17]. On the other hand, the BET isotherm applies to a multilayer gas adsorption on the

surface of a solid[18]. It gives the total surface area depending on the gas vapour, adsorbed gas on the surface, and the surface sites of a solid.

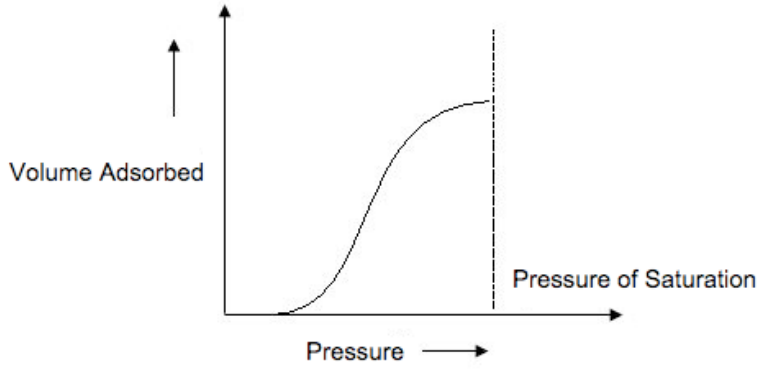

Figure 2.21 Langmuir monolayer adsorption isotherm[17]

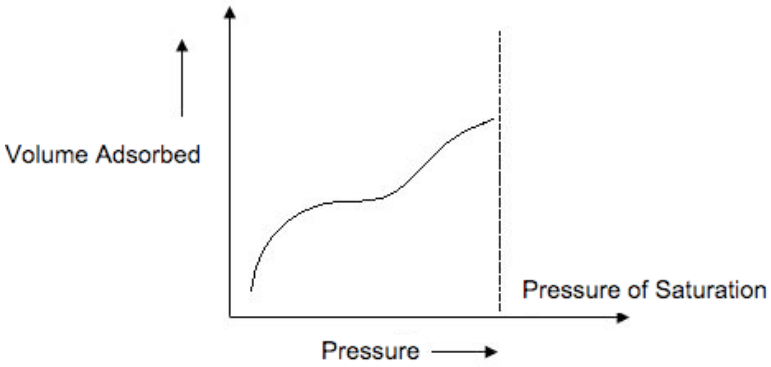

Figure 2.22 BET isotherm[18]

1.7.1 Theory

The BET isotherm is used when gas reaches a solid surface and is physically adsorbed on the surface to make a bond. This is caused by the van der Waals force and the energy released is known as the heat of adsorption. Further layers appear by condensation of the gas on the first layer, which depends on the heat of liquifaction. The adsorbed gas molecules are in equilibrium with the gas phase and with surface sites. The BET equation is as follows:

$$P/V(P_0–P) = (1/V_{mon}C)+(C-1/ V_{mon}C)*(P/P_0) \qquad \textbf{(Eq 2.1)}$$

Where C is:

$$C = e^{(\Delta Hads- \Delta Hlq)/RT} \qquad \textbf{(Eq 2.2)}$$

Where C is constant, ΔH_{ads} is the adsorption enthalpy, ΔH_{lq} is the gas liquifaction enthalpy, R is the gas constant and T is the temperature. From equation 2.2, P is

the equilibrium gas pressure, P_o is the saturated pressure, V is the volume adsorbed from the gas and V_{mon} is the volume of the monolayer coverage.

Normally, the BET isotherm is solved by a linear plot of $P/V(P_0–P)$ on the y-axis against (P/P_0) on the x-axis as shown in Figure 2.21, where the slope is $(C-1/V_{mon}C)$, and the y-intercept is $(1/V_{mon}C)$, and then the surface area is calculated by From these parameters the surface area for a given gram of solid can be calculated in meters square per gram as in Eq 2.3, 2.4, 2.5 and 2.6 below.

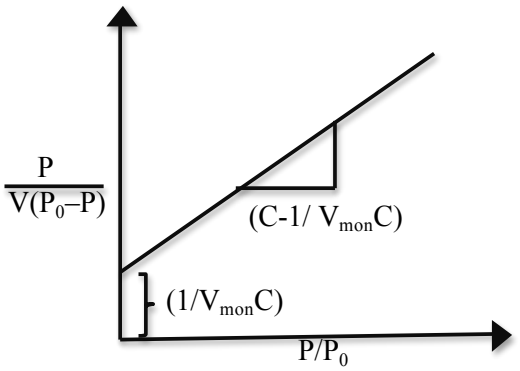

Figure 2.21 Graphical determination of BET

$$\mathbf{C = 1+ (slope\ value\ /\ y\text{-}intercept\ value)} \qquad \textbf{(Eq 2.3)}$$

$$\mathbf{V_{mon} = 1/\ (\ slope\ value + y\text{-}intercept\ value)} \qquad \textbf{(Eq 2.4)}$$

$$\mathbf{S_{BET,\ Total} = (V_{mon}\ N\ s)\ /\ V} \qquad \textbf{(Eq 2.5)}$$

$$\mathbf{S_{BET} = S_{BET,\ total}\ /\ a} \qquad \textbf{(Eq 2.6)}$$

Where S is the surface area, **(V)** is the adsorbed gas molar volume; **(N)** is the Avogadro's No, where **(a)** is the mass of the placed powder sample and **(s)** is the adsorption cross section for adsorbate, which is 16.2 A^2 for nitrogen.

2.7.2 Equipment

A Gemini 2360 Micromeritics was used to determine the surface area of all catalysts before being used for methanol oxidation, where nitrogen gas was used as the adsorbate, using the BET isotherm. In practice, a known weight of the

catalyst was placed in a sample glass tube. This was then heated to 120^{o}C with a vacuum to remove any water. It was then placed in a tube holder with another empty tube as a reference. The two tubes were dipped into liquid nitrogen, then the rest of the experiment was controlled by the computer. Five different pressure points were taken to plot the BET isotherm graph as in Figure 2.21. Then the surface area of the catalyst was calculated using the BET isotherm in ($m^2.g^{-1}$).

2.8 References

[1]. John, R. (2007). *Catalyst preparation: science and engineering*. CRC press: Boca Raton.
[2]. Bowker, M. (1998). *The basis and application of heterogeneous catalysis.* Oxford University Press Inc: New York.
[3]. Peter J, Miedziak, Qian He, Jennifer K. E, Stuart H. Taylor, David W. K, Brian T, Christopher J.K, Graham J. H. Catalysis Today.2011,163:47-54.
[4]. Hiden Isochema Limited.(2005). *CATLAB user manual*. Document number: HA-085-083. Hiden analytical. England.
[5]. Hiden Isochema Limited.(2005). *QIC-20 gas analysis system user manual*. Document number: HA-085-073. Hiden analytical. England.
[6]. Hiden Isochema Limited.(2005). *RC RGA analyzer operator's manual*. Document number: HA-085-073. Hiden analytical. England.
[7]. Hiden Isochema Limited.(2005). *QIC fast sampling capillary inlet user manual*. Document number: HA-085-027. England.
[8]. PFEIFFER vacuum (2005). *Turbomolecular drag pump*. Operation instructions: PM800504 BE/I (0308). PFEIFFER vacuum GmbH. Germany.
[9]. Walter Umarth. (2007). *Fundamentals of vacuum technology. Oerlikon leybold vacuum*. Cologne, Germany.
[10]. Karl Jousten. (2008). Handbook of Vacuum technology. Wiley –VCH: Germany.
[11]. Loader, J. (1970). *Basic laser spectroscopy*. Heyden, London.
[12]. Hammond, C. (2010). *The basics of crystallography and diffraction*. (3rd Ed) International union of crystallography/ Oxford university press, Oxford.
[13]. Barr, T.L. (1994). Modern ESCA. CRC press. Boca Raton, London.
[14]. KRATOS Analytical. AXIS Ultra DLD. Manchester, U.K. 21-07-2011 [Accessed 13 Jan 2012]. Available from:http://surface.kratos.com/Axis-Ultra-DLD/axisultradld.html
[15] F. Reniers, C. Tewell. (2005). New improvement in energy and spatial resolution in AES and XPS application. Journal of electron spectroscopy and related phenomena: 142, 1-25.
[16]. James I. D. (2005). Surface and ground water, weathering and soils. Elsevier: Oxford.
[17] K. S. Sing, Langmuir, 1987, 3, 2.
[18] S. Brunauer, L. S. Deming, W. E. Deming, and E. Teller, J. Am. Chem. Soc., 1940, 62, 1723.

3. The oxidation of methanol on transition metal oxides

3.1 Introduction:

This chapter concerns an evaluation of the efficacy of a range of simple oxides as methanol oxidation catalysts, because transition metal oxides especially can be good catalysts for this reaction. According to their properties oxides are often rich in reactive oxygen and electrons at their surface. Some metal oxide properties were presented in the first chapter (introduction). It was shown that they are important in heterogeneous catalysis in that their surfaces can bond with gaseous molecules and let them dissociate then react, providing a lower activation energy to reach the products. Metal oxides have a wide range of properties according to their surface and bulk structure. These oxides can be controlled to obtain the desired catalyst starting from the preparation method, temperature treatment, promotion, shaping and particle size. In this chapter oxides were chosen based on two points, relating to the fact that molybdenum oxide is a selective catalyst. The first point concerns the selectivity of other elements in the periodic table. These elements correspond to molybdenum in some properties, and are different in other properties. As an example, an oxide that differentiates from molybdenum oxide in this study is CoO, which has +2 oxidation states, whereas WO_3 corresponds to molybdenum oxide in terms of oxidation state (+6). The methodology in this study is based on the preparation method of all catalysts, combined with characterisation before their use as catalysts, and after the reaction, and with reactor measurements.

3.1.1 Fe_2O_3

Some properties of iron oxide catalyst were summarised in the first chapter. It is a poor catalyst for methanol oxidation to formaldehyde[1-6]. It burns methanol to carbon dioxide at any conversion. However, the catalyst is very active compared to other catalysts; it converts methanol at a temperature lower than 200 ^{o}C. Iron oxide is known in several forms according to its structures, oxidation states and other physical properties like magnetism. The form used is in this study is α-Fe_2O_3, which is a stable and active catalyst. Iron molybdate is an active and selective catalyst for methanol oxidation. Its activity comes from the iron part, as molybdenum is not a very active catalyst but is selective. Therefore, in this study iron oxide was used as standard reference catalyst for activity[1-6].

3.1.2 MoO_3

Molybdenum oxide was also considered in the first chapter. It has two oxides, as MoO_3 and MoO_2, where MoO_2 is less selective than molybdenum trioxide. Also the trioxide has two forms, which are α-MoO_3 and β-MoO_3. α-MoO_3 is an orthorhombic structure, whereas β-MoO_3 is a monoclinic structure. MoO_3 is a highly selective catalyst. It is 100% selective to formaldehyde at low conversion, however, it not an active catalyst compared to iron molybdate[1-6]. Again, we show results later for reference to the other oxidic materials.

3.1.3 V_2O_5

Vanadium has several oxides - VO, VO_2, V_2O_3 and V_2O_5. In the co-precipitation synthesis method often used, V_2O_5 is formed rather than the other oxidation states, and it is the most stable of vanadium oxides. Vanadium oxides are easily reduced, this redox property makes them very interesting catalysts for oxidation reactions, especially the highest oxidation oxides (V_2O_5). V_2O_5 is a selective catalyst for oxidation of n-butane and benzene. It is also used in supported catalysts for methanol oxidation to formaldehyde [7].

Vanadium based catalysts have been studied by many scientists. Tatibouet studied vanadium oxide, the target was to determine its selectivity and structures, as well as to compare it with molybdenum oxide catalysts. The results shows that both molybdenum oxide and vanadium oxide behave as redox sites. In terms of surface characterisation, a single crystal of V_2O_5 was used with (001) and (100) faces, where it was shown that formaldehyde formation depends on (001) face as the selective plane. The other (100) plane is more active but less selective to formaldehyde, compared with molybdenum oxide. The (100) face is also selective to formaldehyde at low conversion and low temperature, which confirms that the reaction route is sensitively affected by the catalyst structure. Using powdered V_2O_5 at 50% methanol conversion the main product is formaldehyde, whereas at higher conversion $HCOOCH_3$ is the main product. At total conversion, CO and CO_2 are the products[8].

Supported vanadium oxide catalyst reactivity was also reported by Kim and Wachs [9]. V2O5/Al_2O_3 contains at least 10% vanadia on alumina, as

methanol oxidation to formaldehyde increases with the number of vanadia on the surface of high surface area alumina, where vanadium on the surface appear as polymeric VO_4, monomers of VO_4 and nano V_2O_5 on the surface of alumina. Here the dehydrated $V2O5/Al_2O_3$ consisted of isolated VO_4 and polymeric VO_4, but the nano-form of V_2O_5 is in region of vanadia monolayer and less. The result shows that formation of formaldehyde increases with the increase of VO_4 coverage of the alumina, as alumina has acidic sites, which dehydrate methanol to dimethyl ether [9].

Another study of bulk vanadium oxide and supported vanadia by Laura et al.[4] reported that V_2O_5 is a selective catalyst producing 79% formaldehyde, 10.5% dimethyl ether and 10.5% as a mixture of methyl formate and dimethoxy methane; this was obtained at low conversion and a temperature of 300 ^oC, where the TOF value is 9.8 s^{-1}. They show in their study that V_2O_5 has Raman bands at 994, 702, 527, 404, 284, 146 cm^{-1}, and XRD analysis shows peaks at $2\theta = 14.9^o$, 18.0^o, 21.3^o, 23.5^o, 28.1^o. They showed that vanadium oxide is more active than molybdenum oxide - vanadium starts converting methanol at 300 ^oC, whereas molybdenum oxide is only active by 380 ^oC. The turnover frequency of vanadium oxide (9.8 s^{-1}) and molybdenum oxide (0.6 s^{-1}) clearly shows that vanadium has more active sites than molybdenum oxide using, but nonetheless molybdenum oxide is nearly 100% selective to formaldehyde [10].

One of the most important issues that needs to be resolved is the volatilisation of molybdenum during methanol oxidation, which leads to the degradation of iron molybdate catalysts, as molybdenum is the selective part of the catalyst. Nevertheless, vanadium is also volatile in the same conditions as molybdenum. There was a study done by Mariano et al. to prepare a more stable iron molybdate to reduce the operational cost. They prepared Fe_3O_4 that accommodated vanadium and molybdenum in its structure, as Fe_3O_4 has Fe^{3+} tetrahedron and Fe^{2+} octahedron, where the octahedron sites involve vacancies. Therefore, the general formula is $Fe_{2.50(1-z/3)}\ V_{0.20(1-z/3)}\ Mo_{0.30(1-z/3)}\ \square_z\ O_4$, where z is the vacancy number, ($\square$) is the cation vacancies , which varies according to the preparation method. For a sample being calcined at 80 ^oC, it has a formula of $Fe_{2.40}V_{0.19}Mo_{0.29}\ \square_{0.12}\ O_4$. The result shows that metals are allowed to change

their oxidation state within this structure and can be easily reduced and re-oxidised at the same ratio. In other words, there will be no missing molybdenum or vanadium from the total composition like $Fe_2(MoO_4)_3$ when changed to $FeMoO_4$, catalyst more stable than the iron molybdate catalyst. The catalyst is also active (86% conversion) and selective to formaldehyde (86%) by 450 ^oC[11].

In this study, V^{5+} and V^{4+} will be investigated to determine their behaviour for methanol oxidation. Both of the samples were in powder form; V_2O_5 was a fresh sample prepared in the lab using the co-precipitation method, but VO_2 was a commercially obtained sample.

3.1.4 MnO_x

Manganese oxides are scientifically good catalysts for oxidation processes, and one of those oxidation reactions is CO oxidation to CO_2, as CO is a highly toxic gas for humans. The catalyst is nano-sized palladium on manganese dioxide, where this catalyst oxidises CO at low temperature (40 ^oC,10% conversion). A study reported by Salker et al. shows that Pd/MnO_2 catalyst is a highly active catalyst, where MnO_2 is also an active catalyst (10% CO conversion at 80 ^oC), but less than the Pd doped MnO_2 catalyst [10]. Moreover, manganese is also supported on silver catalyst, which shows high activity for carbon monoxide oxidation. $Mn_{0.90}Ag_{0.10}O_2$ is the most active catalyst of the manganese/silver catalysts; it converts 10% of CO at 55 ^oC to carbon dioxide [13].

The structure of MnO_2 consists of octahedral MnO_6 units. Two types of MnO_2 hollow structures were studied by Xiaobo et al., - γ-MnO_2 and β-MnO_2. Figure 3.1 shows XRD patterns of γ-MnO_2, β-MnO_2 and Mn_2O_3. MnO_2 can be reduced, especially in an oxidation reaction like cinnamyl alcohol, where Mn (IV) was reduced to Mn_2O_3. Also, the result shows further possible reduction to Mn_3O_4 from both MnO_2 and Mn_2O_3, and Mn_2O_3 can be reduced to MnO [14]. α-Mn_2O_3 is not pure. A fresh sample was calcined at a temperature below 550 ^oC. By 400 ^oC it seems to be a mixture of Mn_2O_3, Mn_3O_4 and Mn_5O_8, as in figure 3.2 where (a) is the as-synthesized sample, (b) the sample calcined at 400 °C, showing peaks for tetragonal Mn_3O_4 and monoclinic Mn_5O_8, and (c) is for sample calcined at 700 ^oC, which is pure cubic α-Mn_2O_3. [15].

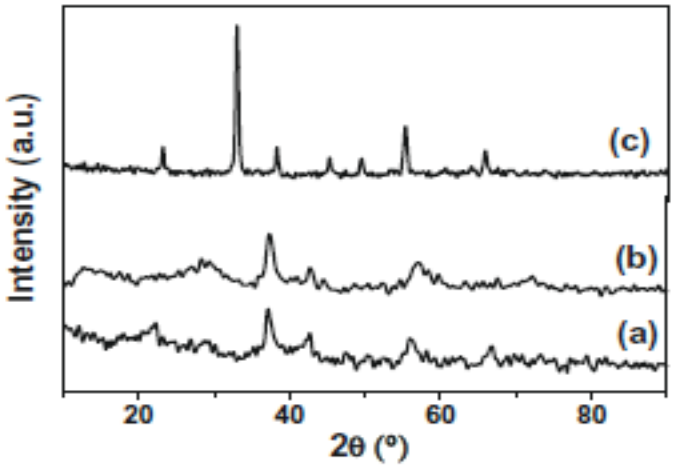

Figure 3.1 XRD patterns of (c) Mn_2O_3, (b) β-MnO_2, (a) γ-MnO_2 [12]

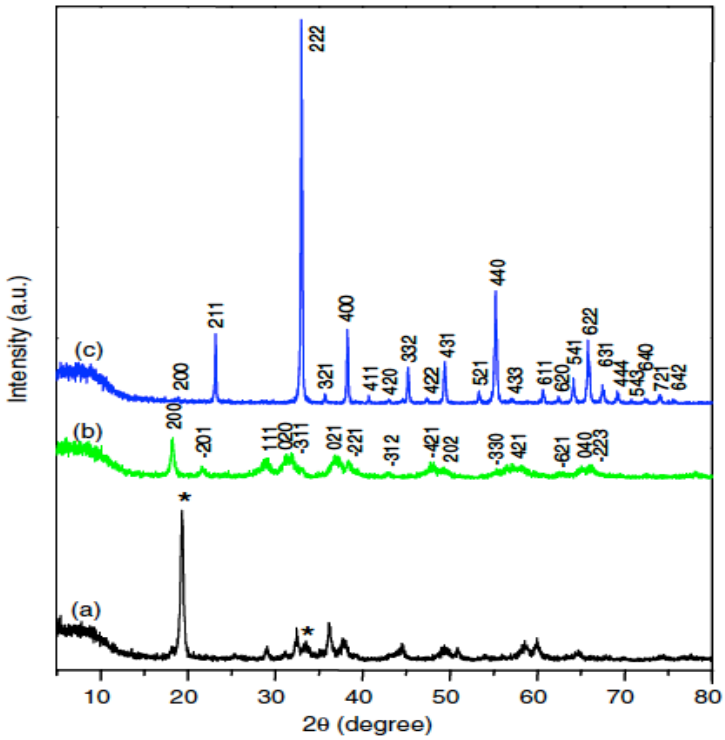

Figure 3.2 XRD patterns of Mn_2O_3

Manganese oxide was used as methanol oxidation catalyst to formaldehyde. The catalyst for methanol oxidation is Pd doped $LaMnO_3$ catalyst. Chia-Liang et al. reported that $LaMn_{0.93}$ $Pd_{0.07}$ O_3 is 65% selective to formaldehyde, and the rest is CO_2 by 350 ^oC, where it converts 70% of methanol to these products. Moreover, the catalyst starts to be active by 140 ^oC, when the

main product was CO_2 as sequence of full methanol oxidation and the methanol conversion was less than 10%, but at higher temperature, the oxidation reaction turned to partial oxidation and the main product was formaldehyde [10]. Furthermore, another study carried out by Chia-Liang reported the catalytic behaviour when Pd was replaced by other metals such as Rh, Pt and even pure $LaMnO_3$. The physical properties of these catalysts are interesting as the pure $LaMnO_3$ has only 6.3 m^2/g of surface area, whereas the rest have higher surface area, such as LaMnPd (14.1 m^2/g), LaMnPt (14.5 m^2/g) and LaMnRh (11.1 m^2/g). The study also showed that the highest selectivity to formaldehyde is 90% and ordered as follows: LaMn < LaMnPt < LaMnRh < LaMnPt. The highest conversion was 70%, reached using LaMnPt catalyst [16].

One of the other uses of catalysts containing manganese is methanol synthesis, where the catalyst is $Cu/ZnO/Al_2O_3$ and uses manganese as a promoter. Because manganese has the ability to change its oxidation state from 4+ to 3+, Cu changed to Cu^+ and to Cu^{2+}, which enhances the catalyst activity by increasing Cu dispersion and the number of active sites. This results in a 10% increase of methanol yield by manganese doping [12]. Manganese catalysts were used for pollutants removing that are results in organic industrial processes, which removed by conversion to CO_2. Reactant either can be carried by air, or just a gas exhaust containing low oxygen, a high concentration of water, and may also carry a low concentration of carbon monoxide. Where the catalyst is bimetallic PdO with a mixture of Mn^{3+} and Mn^{4+}, the result shows that the catalyst is still active even with a poor oxygen feed, but is less active than the first feed, which contains air. The catalyst has the ability to share its lattice oxygen and form Pd^o instead of PdO, and MnO_2/ Mn_2O_3 may change to Mn_3O_4 [19].

In this study, both Mn^{III} and Mn^{IV} were tested as catalysts for methanol oxidation.

3.1.5 CoO

Cobalt has two types of oxides according to its oxidation state. The first Co^{2+} appears as CoO, but with 1/3 as Co^{3+} in Co_3O_4. Both of the oxides are well characterised, where Co^{III} can be easily reduced to Co^{II}. Co^{II} can be oxidised to

Co^{III} in the presence of oxygen, which makes cobalt oxide such a good catalyst in oxidation reactions because of its ability to change within its oxidation state cycles of Co^{III}/Co^{II}. CoO is rock salt oxide, where Co^{2+} is in the octahedral holes, but Co_3O_4 is a spinel type oxide with tetrahedral Co^{2+} and octahedral Co^{3+}, where CoO is high spin because of its d^7 configuration, whereas Co_3O_4 is low spin of d^6. This means it is weakly magnetic and both oxides are face centred cubic (fcc) with oxygen in close packed structures. The CoO surface shows has (100) facets, and has well ordered bulk structure. It also has stoichiometric surface because of balance charge and non-polar planes. It is a close packed structure (fcc). Co_3O_4 has two facets, (110) and (111), as it is a truncated octahedron, where (110) planes forms in two types of structures (A) and (B). Type A has tetrahedral and octahedral Co sites, whereas type B has only half filled octahedral sites, as in figure 3.3 below[20].

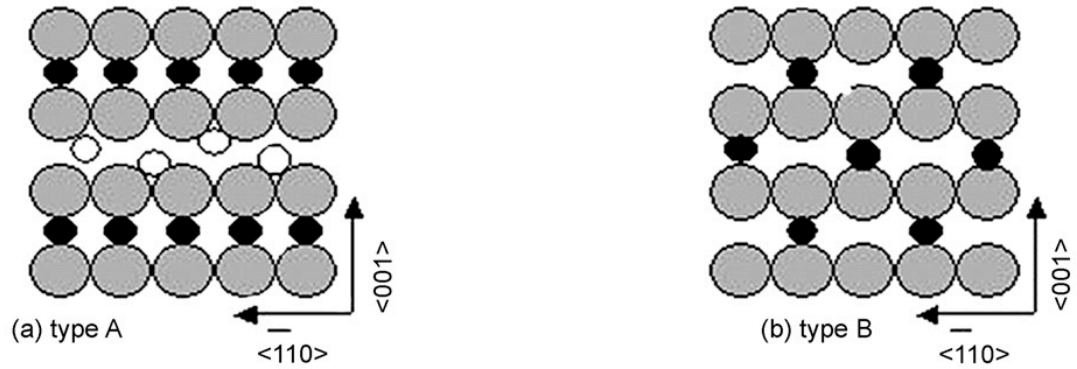

Figure 3.3 Co_3O_4 layers for (110) planes [20]

Co_3O_4 (110) forms a CoO layer when heated, which makes it a good catalyst for oxidation and reduction process, because of its ability to donate and accept oxygen, and change its structure in between. The other structure of Co_3O_4 is (111) hexagonal, poorer in surface hydroxylation than other forms of cobalt oxide, in appearance of oxygen and water, and is recorded by O1s Peak using XPS that has higher binding energy [20].

Zafeiratos and his co-researcher studied cobalt oxides behaviour during methanol oxidation. Two oxides were tested; CoO and Co_3O_4. CoO oxide was obtained by oxidising metallic Co in oxygen at 520K, which resulted in a few layers of CoO on Co surface. The result shows that methanol oxidised to

formaldehyde on CoO-like catalysts (containing metallic Co, and CoO) and that both catalysts were active to convert methanol, where the favourite product using pure Co_3O_4 is carbon dioxide,. However, Co_3O_4 changes to be a mix of CoO/Co_3O_4, which was recorded to be the active phase for formaldehyde, depending on the ratio of CoO and Co_3O_4 in the complex. Formaldehyde is formed in the surface of cobalt when the methoxy group covers the surface in a low flow of oxygen MR=2, where extra oxygen may bond with the surface and forms a formate group on the surface that decomposes as CO_2, illustrated in equation 3.1 and 3.2. Also the formation of formaldehyde requires nucleophilic surface sites, whereas the formation of CO_2 requires electrophilic oxygen [21].

$CH_3OH + ½\ O_2$ à $CH_2O + H_2O$ Eq 3.1

$CH_3OH + 1.5\ O_2$ à $CO_2 + 2H_2O$ Eq 3.2

3.1.6 Cr_2O_3

Chromium oxide is an important catalyst in heterogeneous catalysis. The most usual oxidation states for chromium are Cr (III) and Cr (VI), where Cr (VI) is not a stable catalyst for reaction it loses oxygen, and converts to Cr (III).

Chromium oxide, Cr_2O_3, is the stable oxide for catalytic reactions, which has several structures. The first structure is the α-phase with R3c spacing group, and lattice parameters of a = 4.958 A^o , b = 13.594 A^o. It is a rhombohedron of six molecule of α-Cr_2O_3 as a close-packed hexagonal structure[16]. Another structure reported is the spinel Cr (111) tetragonal, , as well as spinel cubic γ-phase in thin film. A crystallography study of chromium oxide shows that there are three faces present at the surface, Cr_2O_3 (110), Cr_2O_3 (100) and Cr_3O_4 (111)[23].

Two molybdenum containing chromium catalysts were studied by Ivanov et al., which are $Cr_2(MoO_4)_3$ and modified $NaCr(MoO_4)_2$. The results show that $Cr(MoO_4)_3$ is iso-structural of $Fe_2(MoO_4)_3$, and even has the same mechanism, with a similar activity and selectivity to formaldehyde. Its activity can reach up to 95% by 320 ^oC and formaldehyde selectivity of 90%. However, the addition of sodium on chromium-molybdenum catalysts lead to a slightly different result;

0.10% of Na on Cr-Mo catalyst made by a co-precipitation method, makes it more selective to formaldehyde (96.2% at 350 ^{o}C), but less active (82.4% at 350 ^{o}C). Further addition of sodium (0.25%) drops the catalyst activity down to 67.4%, whereas 0.50% of Na added to Cr-Mo catalyst leads to a more selective catalyst than the earlier catalyst (0, 0.10 and 0.25%) to formaldehyde up to 97% selectivity, but only 50.1% of methanol converted by 350 ^{o}C to formaldehyde, and other products like DME (less than 1%) and CO (approx. 2%), where there [24].

CrO_3 supported on different metal oxides was studied, since CrO_3/SiO_2 is good catalyst for ethylene polymerisation and CrO_3/Al_2O_3 is selective catalyst for ether hydrogenation and dehydrogenation of hydrocarbons. This makes it interesting for researchers to study them in an oxidation reaction, according to their activity. The Raman technique was reliable for this study, as Raman is able to determine the metal oxide and the support and their interactions together. This shows that the chromium unit is CrO_4 in a tetrahedral unit with two terminal oxygen, C=O, which is good sign for oxidation reaction in that it makes the catalyst more active and selective to products like formaldehyde. Wachs et al. studied methanol partial oxidation on CrO_3, supported in several oxides such as TiO_2, ZrO_2, Nb_2O_5, Al_2O_5, with 1% loading of CrO_3. The table below shows the results of all catalysts tested, where yield for a product is the sum of selectivity of that product, and the total conversion of methanol to all carbon products.

Support *	**Yield %**				
	HCHO	**$HCOOCH_3$**	**$(CH_3O)_2CH_2$**	**CH_3OCH_3**	**$CO+CO_2$**
ZrO_2	54.1	34.4	0	0	11.5
TiO_2	68.7	20.4	0	2.6	8.3
SiO_2	60.5	11.5	1.5	0.8	25.7
Nb_2O_5	50.5	0	4.2	42.6	2.7
Al_2O_3	0.4	0	0	99.0	0.6

Table 3.1 methanol oxidation yielded on 1% CrO_3 on Supports *

However, using Nb_2O_5 and Al_2O_3 supports, the product is affected by the support acidity in which the main product is DME in table 3.1. The best support was titanium oxide in terms of formaldehyde yield and low combustion to either CO or CO_2[25]. In another study, more chromium was loaded; 1%, 2% and 3% of chromium were loaded on SiO_2. For 1% CrO_3/ SiO_2 the yields were the same as in table 3.1. Secondly, 2% CrO_3/ SiO_2 yields 71% formaldehyde (FA), 9% $HCOOCH_3$ (MF), 1% $(CH_3O)_2CH_2$ (DMM), 1% CH_3OCH_3 (DME) and 18% $CO+CO_2$ (CO_x). Finally, 3% CrO_3/ SiO_2 yields 76% FA, 6% MF, 2% DMM, 1% DME and 15% CO_x[20]. Moreover, the result of 1% CrO_3/ SiO_2 was compared with 1% MoO_3/SiO_2 that yields only 45% FA, 28% MF, 19% DMM, 8% CO_x, where was no DME yield using this catalyst, which makes Cr/Si more selective than Mo/Si catalyst[26].

3.1.7 WO_3

The most interesting form of tungsten is (6+) oxidation state oxide. However, there are oxides in different oxidation states being reported in published papers, e.g. WO_2 and WO. However, in this chapter WO_3 was tested to determine its selectivity for each product.

In terms of structure, WO_3 consists of distorted WO_6 units in octahedral structure; Yu showed that the reduction of tungsten (VI) lead to form WO_2 in temperatures higher than 725 ^oC, or in the presence of a redox agents like methanol. WO_2 has rutile monoclinic structure, but other WO_x oxides were observed, where x is ($2 \leq X \leq 3$). Results obtained using the XPS technique shows that a series of changes occurred from WO_3 via $WO_{2.77}$ then $WO_{2.3}$ to WO_2[27].

Tungsten was supported on many common supports with high surface area like titania and alumina. Ostromecki et al. studied tungsten oxide supported on alumina, and their results show that tungsten is formed as a two dimensional structure. This became more distorted and polymerised with an increase of W loading, where XANES results present two kinds of bonds as mono-oxo tungsten (W=O) and di-oxo tungsten (O=W=O). Moreover, tungsten was found to appear as tetrahedral coordination in low coverage (0.33 monolayer), but at higher coverage it is a mixture of tetrahedral and octahedral coordination[28].

In another study tungsten was loaded on titania, where the catalysts contain different tungsten density (12 to 69 monolayers) to determine its effect in catalyst activity. Raman bands were obtained for all catalysts and show that the W=O band at 1017 cm^{-1} increased with W density rather than forming W-O-W species, which lead to strong Brønsted acid sites and more activity, as catalysts containing 1.7 W atom/nm^2 or less show very low activity for propene formation. However, catalysts containing higher coverage of tungsten are more active as they contain stronger Brønsted acid sites[29].

Tungsten oxides catalysts were studied for methanol oxidation, as it is iso-structural of molybdate catalysts, but the reaction pathway is different compared to molybdate catalysts, where molybdate oxides are selective to formaldehyde, and tungsten forms mainly dimethyl ether (DME). However, molybdenum catalysts still face issues in terms of stability when molybdenum evaporates from its oxides during methanol oxidation, causing catalyst deactivation.

Many researchers have studied other systems containing other elements in the molybdate system. For instance, Fe-W-Mo, by co-preciptation method, different concentration of tungsten oxides were added to molybdate system, $[Fe_2(MoO_4)O_3.MoO_3.\ x(WO_3)]$, where x= 0, 1.9, 8 and 15.9 wt%. The result by x-ray diffraction shows that tungsten atoms could be replaced with molybdenum atoms and form $Fe_2(Mo_xW_{1-x}O_4)_3$ composition, where Fe^{3+} is surrounded by both Mo^{6+} and W^{6+}. Furthermore, the results of a methanol oxidation study confirm that any addition of tungsten leads to increased selectivity of formaldehyde, starting from pure iron molybdate up 15.9 wt% of W added to the system, as in table 3.2 below:

WO_3	**Conversion (%)**				**Selectivity to**
(wt.%)	**CH_2O**	**CO**	**DME**	**Total**	**CH_2O (%)**
0.0	90.2	3.5	1.2	95	95
1.9	92.7	2.8	0.9	96.5	96.2
3.6	93.4	2.3	1.3	97	96.3

4.9	93.4	2.3	1.3	97	96.3
8.0	87.6	2	1.4	91	96.3
15.9	87	1.6	1.4	90	96.6

Table 3.2 methanol oxidation on WO_3 /$Fe_2(MoO_4)_3$ at 350 ^oC[30]

Tungsten oxide increased the selectivity of formaldehyde production. However, when W was loaded above 5 (wt.%), catalyst activity drops, whereas formaldehyde selectivity continued increasing [30].

3.1.8 ReO_3

Rhenium has a wide range of common oxidation states; 3+, 4+, 5+, 6+ and 7+. However, the oxidation state of 7+, is not stable at temperatures higher than 220 ^oC (Re_2O_7, 220 ^oC melting point), whereas the reaction of methanol oxidation often requires temperatures of up to 500 ^oC, so 6+ rhenium oxide (ReO_3) was chosen as a catalyst for methanol oxidation. In general, Re is an important metal for petroleum catalysis. For example, Re-Pt catalyst is used in a naphtha refinery to convert compounds from low to high octane, to be used as fuel like gasoline for car engines. Re does have other applications in catalysis, such as electro-oxidation of methanol and hydrogen. However, Re oxidised in the presence of oxygen and at temperatures higher than 500 ^oC, completely to (6+) oxidation state, as reported by Okal et al. [31].

Sanliang Ling and others studied the reactivity of ReO_3, supported by WO_3, where they used (9x9x9) crystal of perfect cubic ReO_3 with lattice constant of 3.748 ^oA. Methanol adsorption was studied on the surface of (001) ReO_3 and (001) ReO_3/WO_3 as in figure 3.4, which shows the simulations of ReO_3 and ReO_3/WO_3. The first is more active for both hydrogen and methanol adsorption on its surface, but figure 3.5 illustrates methanol adsorption on the Re_{5c} site and dissociates on the surface.

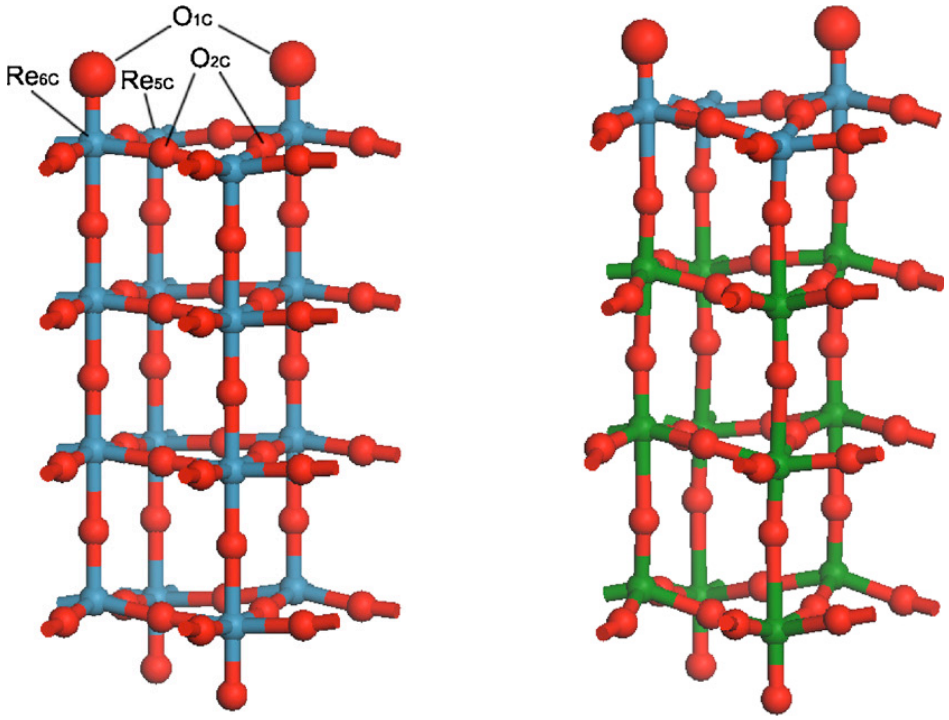

(a) **(b)**

Red=oxygen, green= tungsten and blue= Rhenium

Figure 3.4 slide show of (a) (001) ReO_3 (b) (001) ReO_3/WO_3[32]

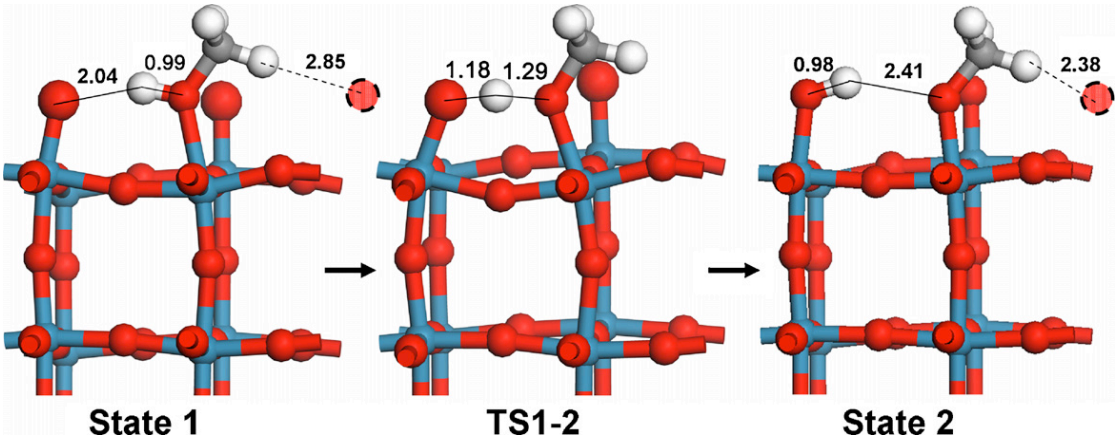

Figure 3.5 methanol adsorption on the surface of ReO_3[32]

This bonds with O_{1c} making methoxy group and hydroxyl on the surface, where the adsorption energy is -95.3 kJ/mol, and the dissociation energy is -85.3 KJ/mol. However, that energy increases on the surface of ReO_3/WO_3 to -83.7 KJ/mol for adsorption energy, and -44.3 KJ/mol for dissociation energy. Then methoxy reacts with the lattice oxygen making dioxymethylene (–H2COO), and then further reacts with either neighbour methoxy or methanol, and decomposes

as (DMM) [32]. Two papers showed that both ReO_3 and ReO_3/WO_3 oxides are selective to dimethoxymethane. In the two papers, also Re oxide was supported on TiO_2, and the resulted catalyst was tested which showed that the main products are DMM and a small amount of formaldehyde, dimethyl ether at low conversion, and CO_x at high temperature [33][34].

3.1.9 Nb_2O_5

Niobium oxide, and catalysts containing niobium, have important applications as effective catalysts for many reactions, for either oxidation or dehydrogenation and even hydrating reactions. It is an active catalyst for carbon monoxide hydrogenation and pollutant treatments. The surface study of niobium oxide on supports shows that NbO_x can be formed in three types on a support. NbO_4 at low coverage of niobium on the support, but with intermediate higher niobium coverage. NbO_5 can identified using Raman and XANES as in figure 3.6 below, and NbO_6 units were found at high surface coverage of niobium on a support [29].

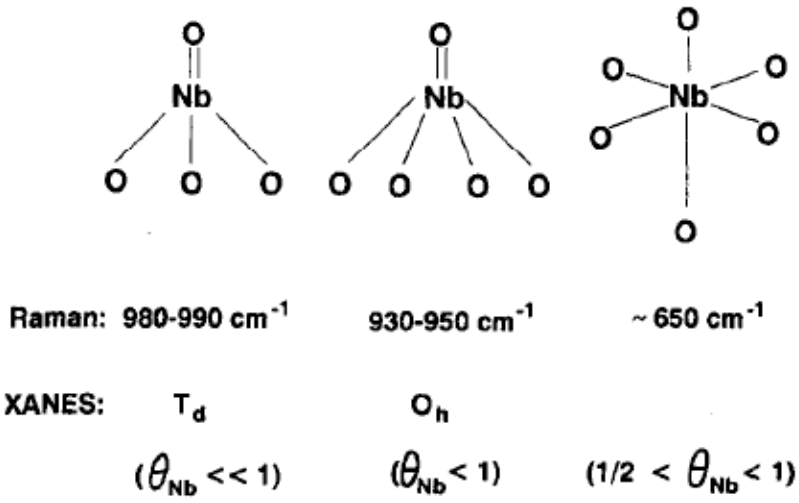

Figure 3.6 niobium species by Raman and XANES [34]

Wachs et al. have studied niobium oxide acidity and basicity during methanol oxidation, which confirm that niobium oxide behaviour can be affected by the support. From table 3.3 below, niobium behaves as acid sites by producing dimethyl ether (95%). However, on silicon oxide support, niobium catalyst is redox, which produces formaldehyde, methylformate and dimethoxymethane due

to Nb-O-Si bond, and the Raman result of Nb_2O_5/SiO_2 show that NbO_4 is formed on the surface [34].

Catalyst	Redox %	Acid %	CO_x
20% Nb_2O_5/Al_2O_3	0	100	0
7% Nb_2O_5/TiO_2	2.5	96.5	1
5% Nb_2O_5/ZrO_2	0	98	2
2% Nb_2O_5/SiO_2	87.2	5.2	7.6

Table 3.3 Methanol oxidation on supported niobium oxides [34]

Niobium oxide was used as support for a number of phases for methanol oxidation. Table 3.4 shows the selectivity of each catalyst supported on niobium oxide, where the most selective catalyst is vanadia on niobium oxide and has more redox properties than the supported molybdenum oxide. This is due to V-O-Nb bond that is easily reduced compared to the other catalysts in the table below. The other catalyst that is selective to formaldehyde, like CrO_3/niobia, MoO_3/niobia and surface rhenia, confirm that niobium can be modified to be a selective catalyst for formaldehyde by increasing its redox properties, rather than having acidic properties, which the responsibility of dimethyl ether formation using bulk niobium oxide[29].

Catalyst	Selectivity %			
	HCHO	CH_3OCH_3	$(CH_3O)_2CH_2$	CO_x
Nb_2O_5	5	95	-	-
1% P_2O_5/ Nb_2O_5	-	100	-	-
1% SO_4^{2-}/ Nb_2O_5	-	100	-	-
1% CrO_3/ Nb_2O_5	45.3	46.9	4.5	1.0
1% WO_3/ Nb_2O_5	-	98.3	-	1.7
1% Re_2O_7/ Nb_2O_5	30.4	58.3	5.5	5.8
1% MoO_3/ Nb_2O_5	21.8	69.2	7.5	1.5
1% V_2O_5/ Nb_2O_5	61.4	35.2	-	3.4

Table 3.4 Methanol oxidation on catalysts on niobium oxide support [34]

3.1.10 Ta_2O_5

Tantalum oxide has important applications in heterogeneous catalysis. Its importance is in its redox properties like the other elements in same group of the periodic table, i.e. vanadium and niobium. Tantalum pentoxide has two structure phases, orthorhombic and hexagonal. The orthorhombic (β-Ta_2O_5) structure has lattice parameters of a = 0.6198 nm, b = 4.029 nm and c = 0.3888 nm, which only occurs in temperatures above 600 ^oC[36], while the hexagonal (α-Ta_2O_5) has lattice constants of a= 6.17 A^o and c/a=1.9[36]. Both oxides have a terminal Ta=O, which makes them selective catalyst in oxidation catalysis. There are a number of papers which have studied preparing tantalum oxide in nano-sized structures, like thin films.

Tantalum oxide has acidic properties similar to niobium oxide. This acidic property is important in hydrocarbon reactions, like hydration of ethene to ethanol using ether hydrated niobium oxide or tantalum oxides. However, the acidic property changes using support like SiO_2, which is catalytically active for Beckmann rearrangement of cyclohexanoneoxime to caprolactam up to 97.5% selectivity. Moreover, in the case of methanol oxidation, niobium is selective to dimethyl ether (95%), a similar result to tantalum oxide, as both have strong acidic properties [37]. Tantalum oxide has been chosen in this chapter to have logical study from one lab of wide range of single oxides to compare with MoO_3, using the same range of techniques.

3.2 Results

Here I will illustrate the results for the 10 single oxides we have studied. All catalysts were characterised using Raman, BET, XRD, XPS, temperature programmed desorption (TPD) and XPS and tested using pulsed temperature programmed reaction.

3.2.1 Fe_2O_3 catalyst

Iron oxide has high surface area compared with other catalysts in this study; it has 8 m^2/g. Figure 3.6 below is the Raman bands for iron oxide were observed as 820,604,487,400,240 and 219cm^{-1}. This result was compared

with literature that confirmed as α-Fe_2O_3 (hematite). However, iron oxide catalyst was not changed after being used for methanol oxidation [38]. Iron oxide bulk was studied using XRD as in figure 3.7. The result shows that iron oxide is the hematite structure, though a small band at 2θ=45° appears after methanol oxidation, and is related to the formation of a small amount of either magnetite or maghemite, or can be a mixture of them, because both have similar XRD peak references from literature. Iron oxide catalyst shared its oxygen leaving a reduction in some of iron species to make Fe_3O_4 [39]. TPD result shows iron oxide as a combustor catalyst for methanol oxidation, figure 3.8. The only carbon product peak is for carbon dioxide, with a main peak at 300°C. Moreover, the reaction profile (fig 3.9) also confirms that methanol was converted to carbon dioxide at any conversion point and even at temperatures lower than 200 °C. However, from figure 3.9, iron oxide is a very active catalyst compared to molybdenum oxide catalyst, it converts methanol at temperatures lower than 200 °C.

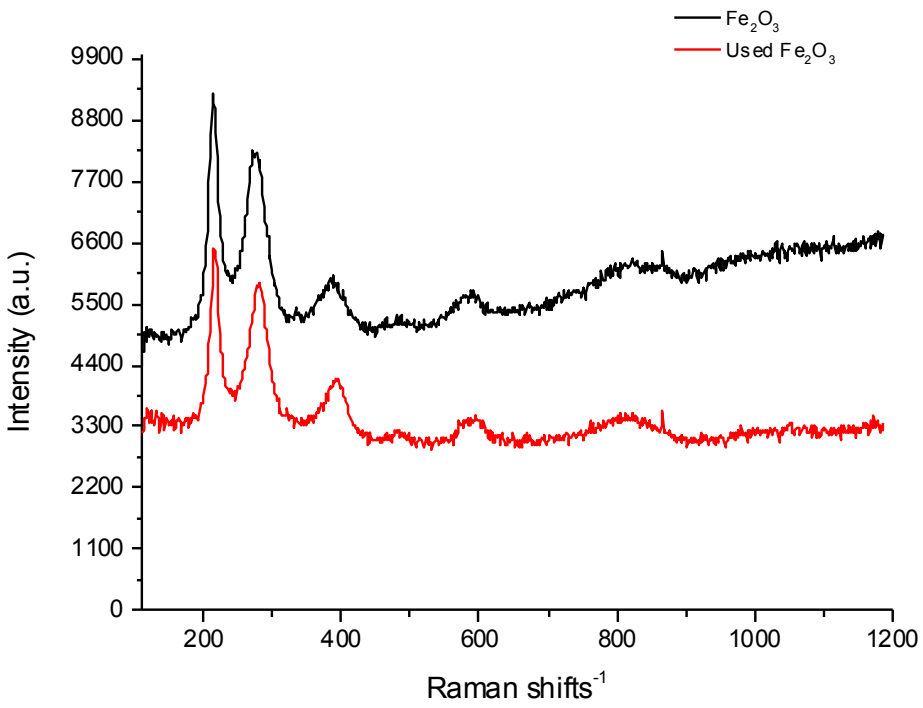

Figure 3.6 Raman spectra of iron oxide catalyst

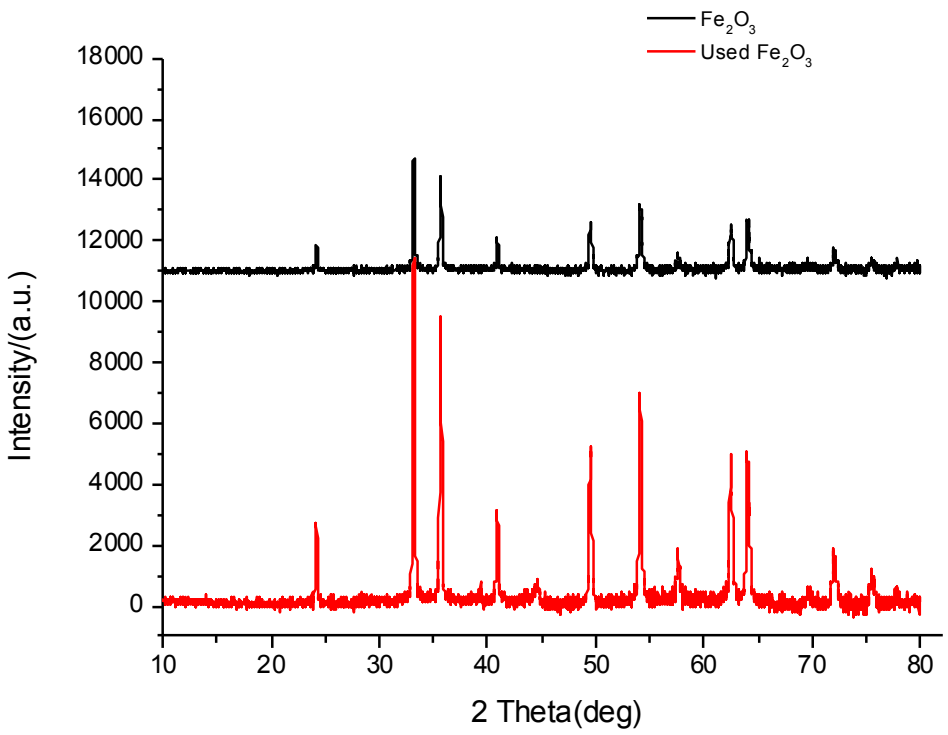

Figure 3.7 XRD spectra of iron oxide catalyst

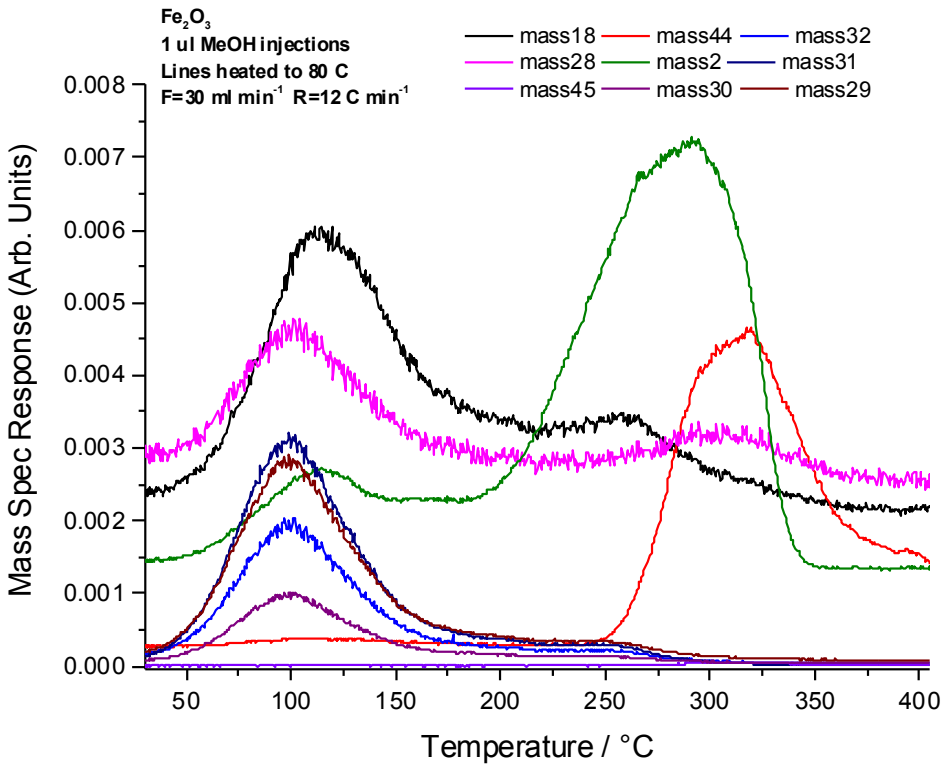

Figure 3.8 TPD result for iron oxide catalyst

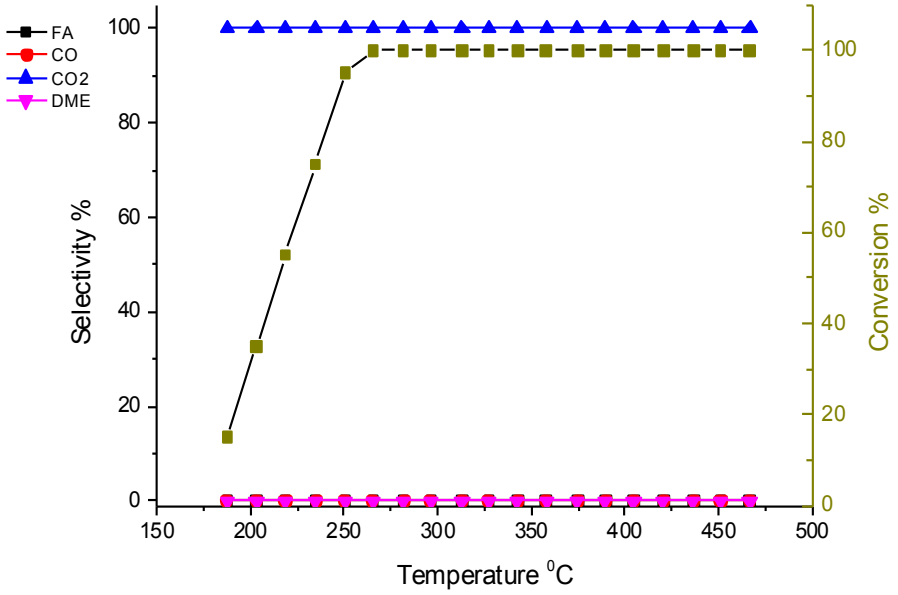

Figure 3.9 Reaction profile result of iron oxide catalyst

3.2.2 MoO_3 catalyst

Molybdenum is very different from iron oxide. Molybdenum oxide catalyst is very selective for formaldehyde, being 95% formaldehyde at 20% conversion, the selectivity decreasingat higher temperatures, and CO selectivity increased. However, molybdenum oxide is not a very active catalyst, and the maximum conversion was only 86% by 500 ^{o}C. There was no sign of carbon dioxide production that comes from full oxidation of methanol as in figure 3.10. Furthermore, TPD results in figure 3.11 show that formaldehyde formation is the only preferred pathway of oxidative dehydration of methanol (desorption peak of mass 30 by 212 ^{o}C) in the absence of oxygen, but the peak was weak due to weak adsorption of methanol on the low surface area of molybdenum oxide catalyst. The surface area of molybdenum oxide is only 1 $m^2.g^{-1}$ using BET surface area measurement. Characterisation of MoO_3 using XRD in figure 3.12 tells us that MoO_3 is (010) plane molybdenum oxide[40], with lattice parameters of a = 3.963 A^{o}, b = 13.855 A^{o} and c =3.696 A^{o}. figure 3.12 (XRD) and figure 3.13 (Raman) showed that the catalyst has not changed when used as catalyst for methanol oxidation

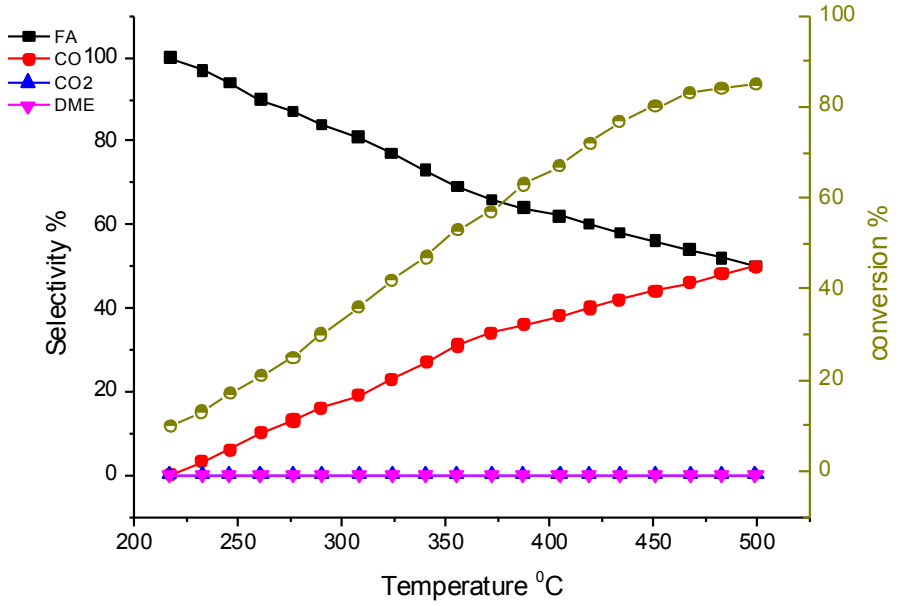

Figure 3.10 Reaction Profile result for MoO_3 catalyst

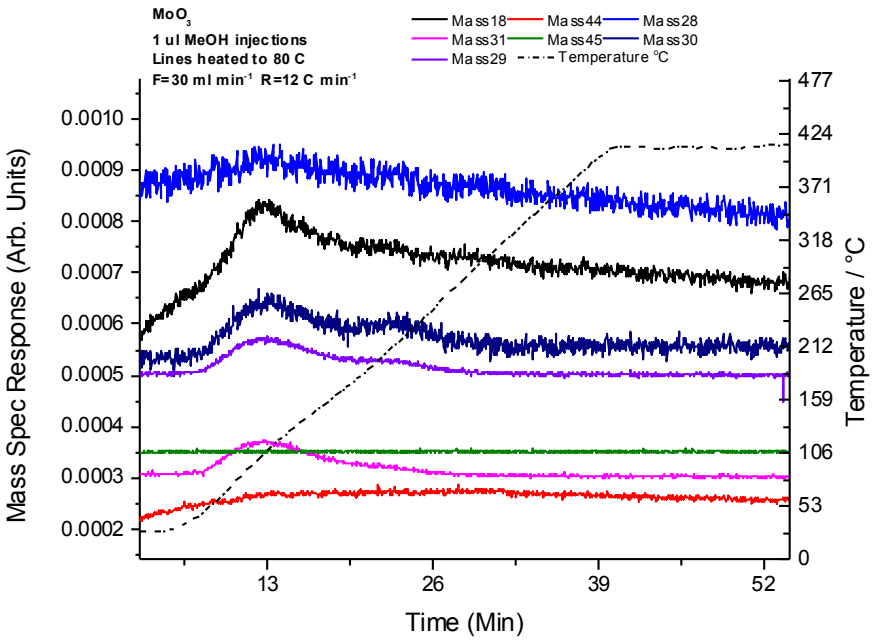

Figure 3.11 TPD result of molybdenum oxide catalyst

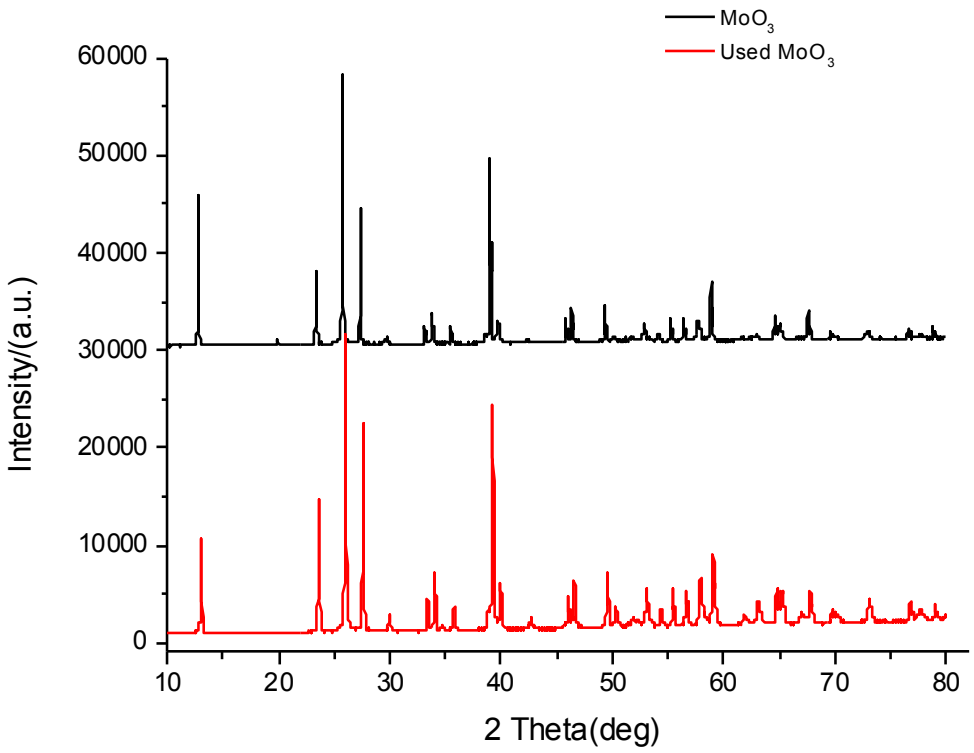

Figure 3.12 XRD result of molybdenum oxide catalyst

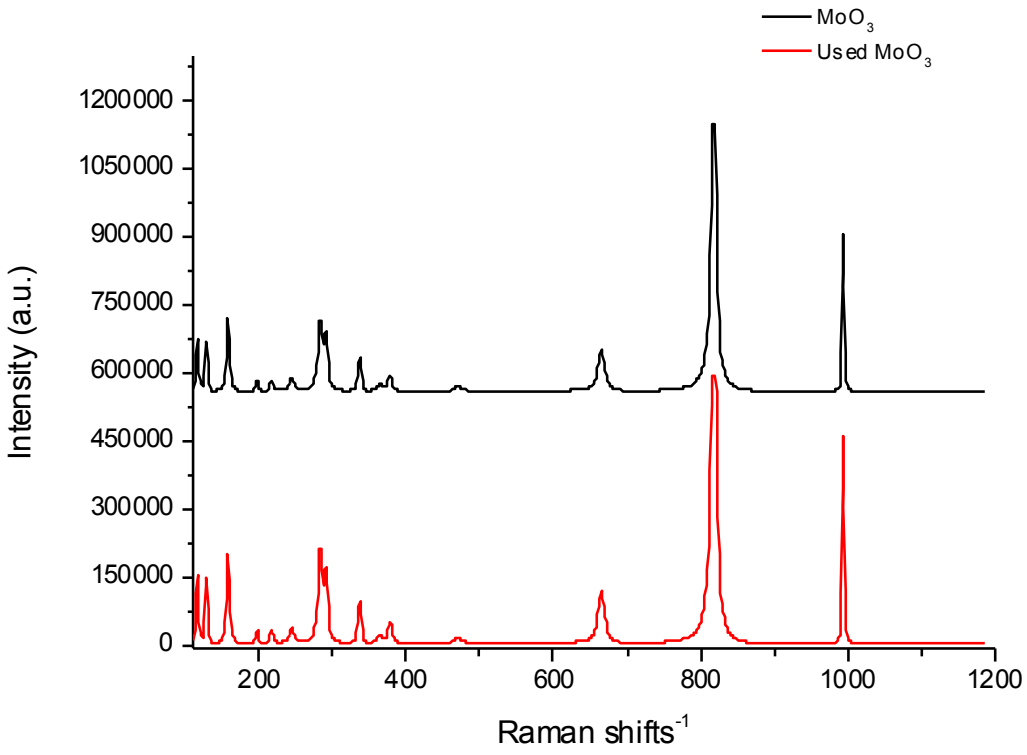

Figure 3.13 Raman result of MoO_3 catalyst

3.2.3 VO_x catalyst

The vanadium catalysts used have two oxidation states; V_2O_5 and VO_2. Both catalysts were tested, however the Raman bands of both catalysts are similar because VO_2 is a mixture of V^{5+} (V_2O_5) and V^{3+} (V_2O_3). As in figure 2.14 and 2.15, the peaks were repeated in both figures, which are 139, 190, 285, 410, 490, 510 and 995 cm^{-1}. With expiation of VO_2 has a weaker peak compared to V_2O_5, and is weaker than V_2O_5 in terms of absorbing laser. But overall V^{5+} segregates on the surface of VO_2, confirmed by XPS result in figure 3.16, which shows the same peak at the same binding energy. In addition, the surfaces of both catalysts do not show any change after being used for methanol oxidation according to the Raman result, where VO_2 shows more intense and sharper peaks closer to V_2O_5 Raman. In comparison of the two catalysts, V_2O_5 has surface area of 2 m^2/g, whereas VO_2 has 4 m^2/g surface area. Even the colour of samples are different. Vanadium pentoxide is brown, and vanadium dioxide is dark blue. Raman XPS results were compared to the published results [41], [42].

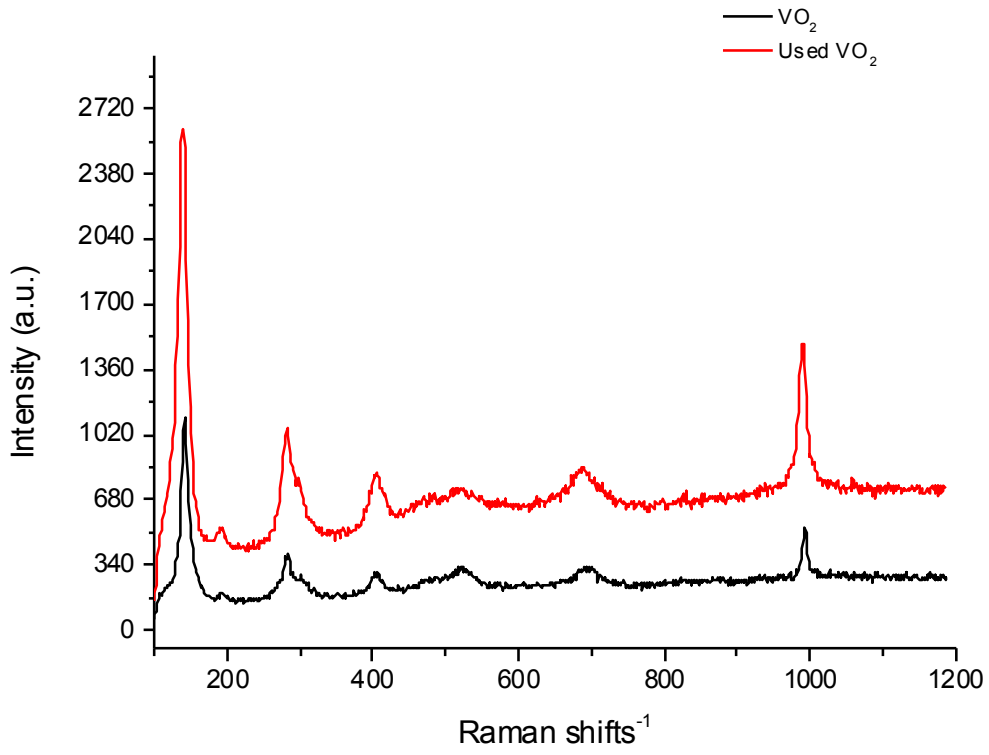

Figure 3.14 Raman result of VO_2

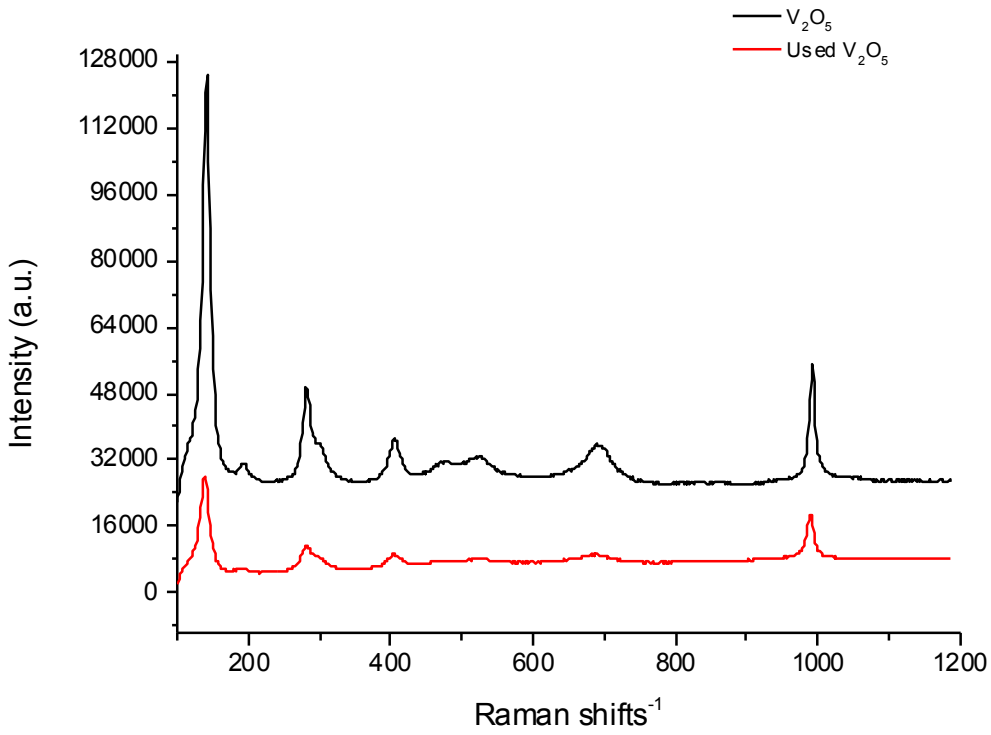

Figure 3.15 Raman result of V_2O_5

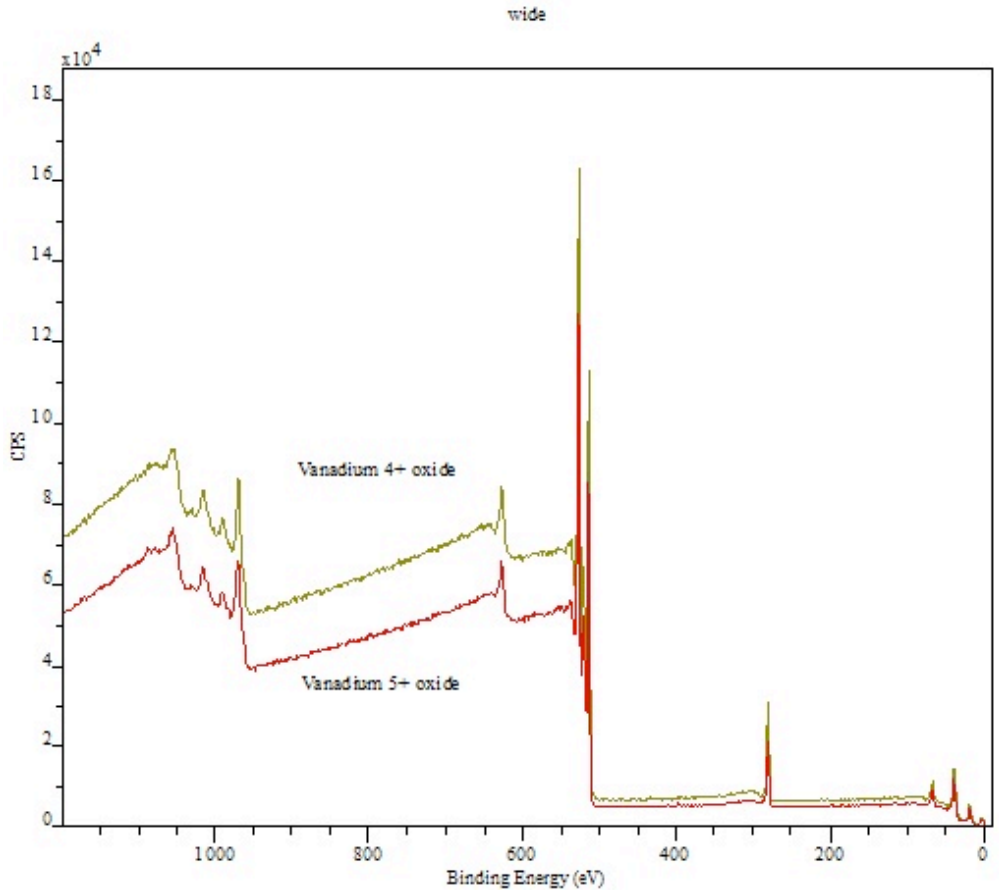

Figure 3.16 XPS spectra of VO_2 and V_2O_5

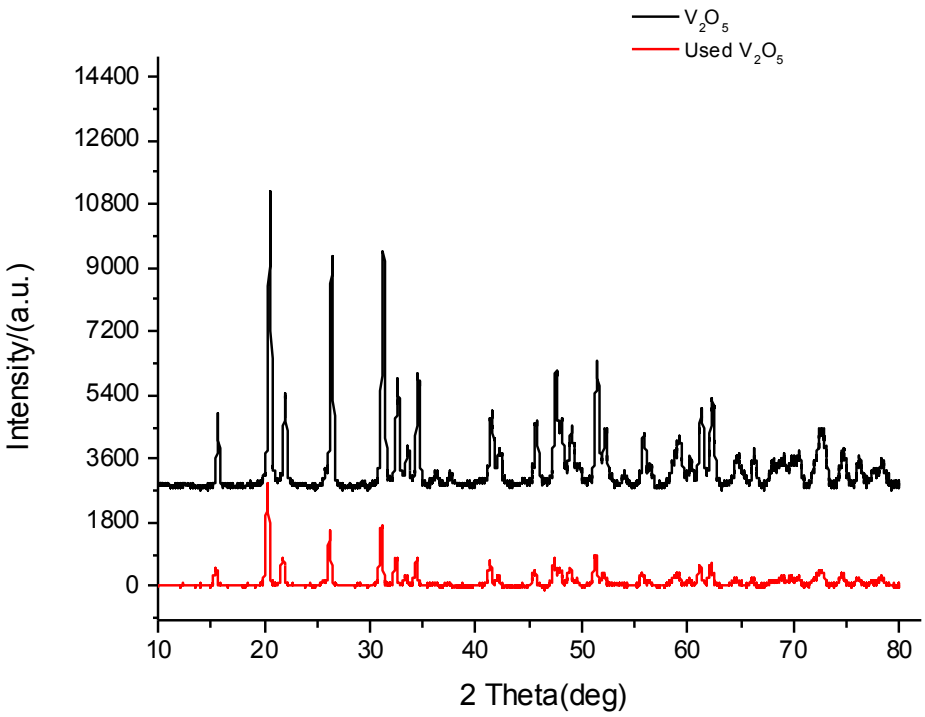

Figure 3.17 XRD spectra of V_2O_5 catalyst

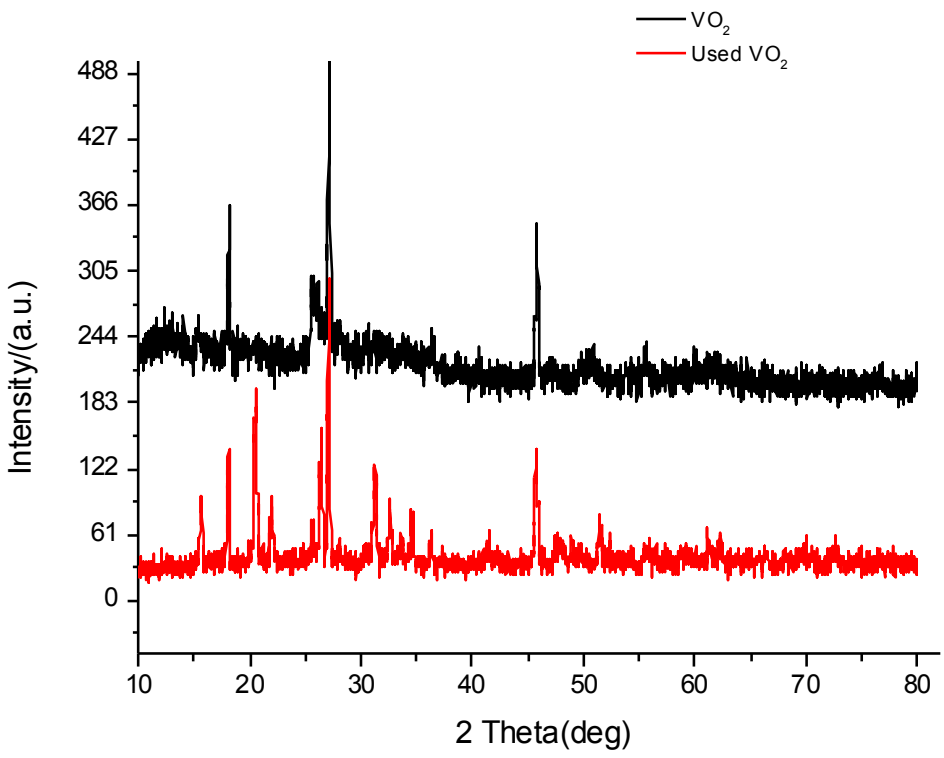

Figure 3.18 XRD spectra of VO_2

XRD results show the bulk composition of oxidation states according to the literature, where figure 3.17 is XRD spectra of pure V_2O_5. This does not change after methanol oxidation catalysis, but figure 3.18 is XRD spectra of VO_2 (also called V_2O_4). The result shows that VO_2 bulk is V_2O_3 (26, 28 and 46 deg). After being used for methanol oxidation, the oxide undergoes a large change. More peaks appear that relate to V_2O_5 and less for V_2O_3. This confirms that the oxide is oxidised to the high vanadium oxidation state (V^{5+}). Before use the colour of VO_2 was dark blue. However, the colour changed to brown/bluish, similar to vanadium pentoxide which is a brown coloured powder[43][44].

Furthermore, the two oxides were tested using the cat-lab micro-reactor. From figure 3.19 vanadium pentoxide is the active catalyst for methanol oxidation. It converts 10% of methanol at a temperature of 138 ^oC, compared to molybdenum oxide catalyst that converts methanol by 220 ^oC. Vanadium catalyst also converts 100% of methanol by 290 ^oC, whereas molybdenum catalyst converts only 85% of methanol by 500 ^oC.

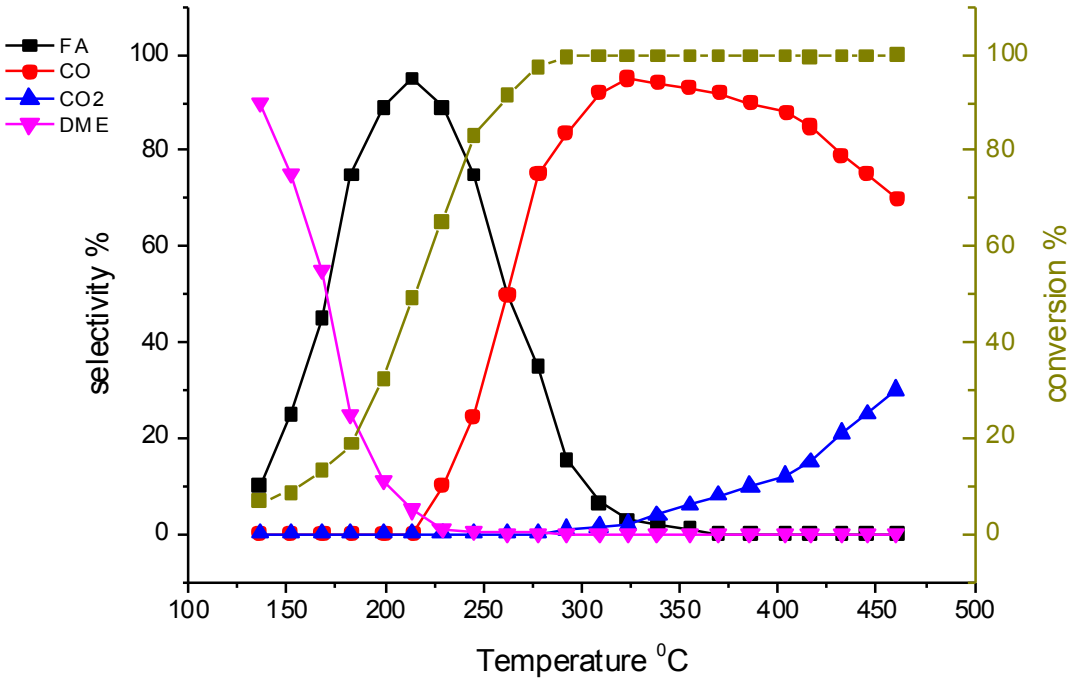

Figure 3.19 Reaction profile result of V_2O_5

It is selective to formaldehyde, where it produces 90% formaldehyde by methanol conversion of 30%. However, at low conversion, the main product is

dimethyl ether that is normally formed by reaction of two methanol molecules at low temperature (170 ^{o}C and lower). This decreased at higher temperature, and formaldehyde production increased. Above 220 ^{o}C formaldehyde decreases and CO increases, making vanadium oxideless selective than molybdenum oxide at high conversion. Some CO2 is seen at the highest temperatures. Overall the maximum formaldehyde yield of vanadium pentoxide is 60% by 220 ^{o}C.

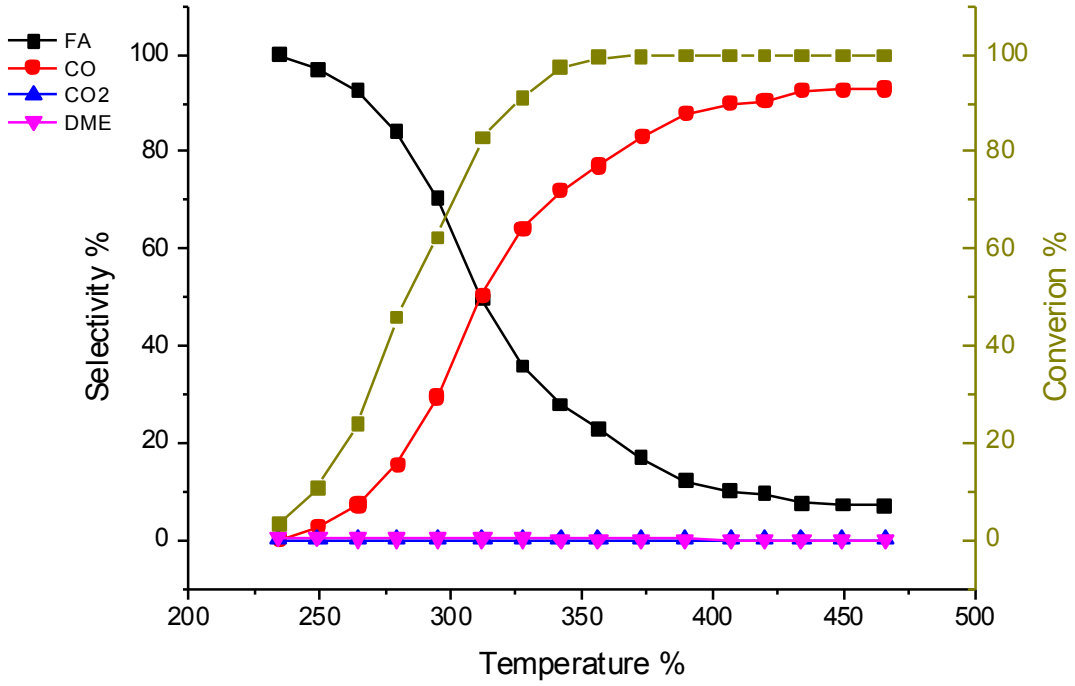

Figure 3.20 Reaction profile result of VO_2 catalyst

In comparison, vanadium dioxide (figure 3.20) is less active than vanadium pentoxide; it converts 7% of methanol by 215 ^{o}C, whereas vanadium pentoxide converts 10% of methanol by 180 ^{o}C. Also, vanadium pentoxide converts 100% of methanol at 290 ^{o}C, whereas for vanadium dioxide it only occurs at 360 ^{o}C. Nevertheless, it is more selective than vanadium pentoxide to formaldehyde; it yields 40% formaldehyde. That is higher compared to 60% as the highest yield with vanadium pentoxide, and formaldehyde kept being produced at high temperatures up to 470 ^{o}C. In the case of vanadium dioxide, where vanadium pentoxide formaldehyde totally disappeared by 325 ^{o}C. In addition, CO_2 was produced by vanadium pentoxide, which makes it more combustive than vanadium dioxide, which did not produce CO_2. The TPD results (figure 3.21 and

3.22) show that both catalysts are selective to formaldehyde and CO, where the two are broadly similar and support the formaldehyde and CO seen in the reaction profiles (3.19 and 3.20).

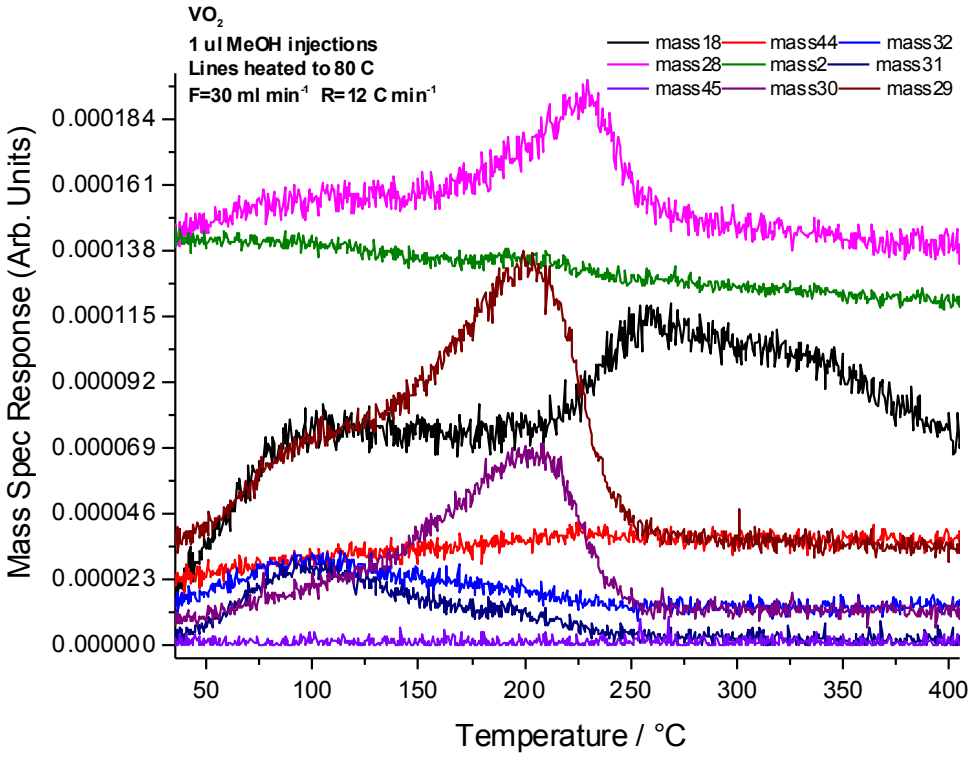

Figure 3.21 TPD result of VO_2 catalyst

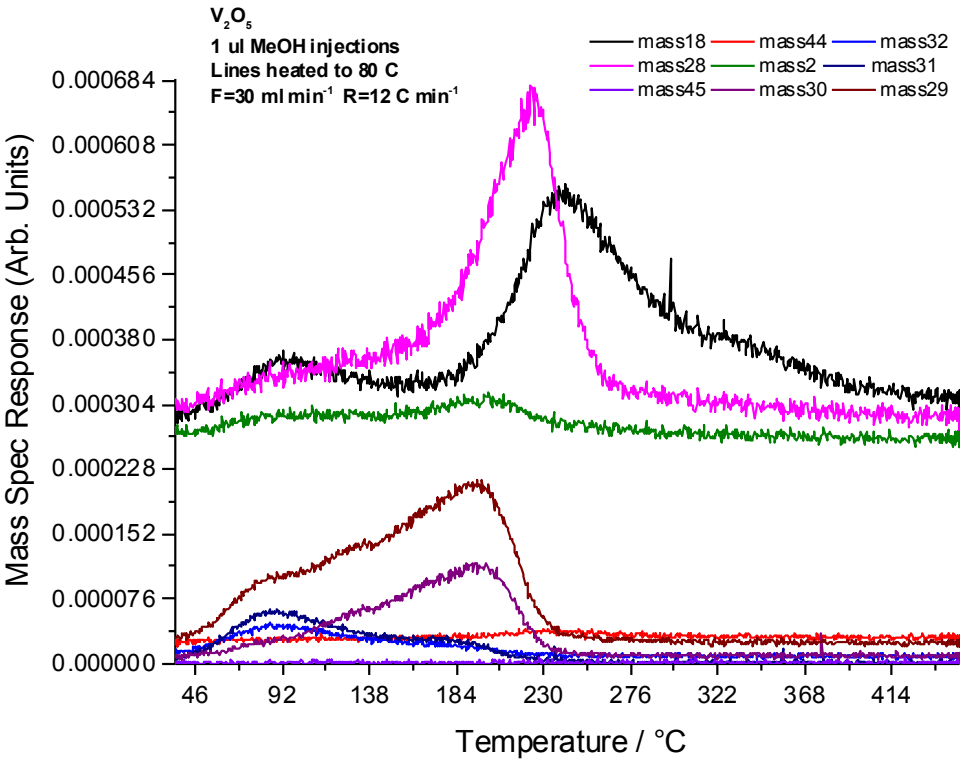

Figure 3.22 TPD result of V_2O_5 catalyst

3.2.4 MnO_x

Two manganese catalysts were studied, MnO_2 and Mn_2O_3. MnO_2 has surface area of 4 m^2/g, where Mn_2O_3 has 3 m^2/g. Figure 3.23 shows the Raman result of Mn_2O_3. Compared to the published papers Mn_2O_3 (380 cm^{-1}) has major change in its structure. Before being used as catalyst that has Raman shifts of 382 cm^{-1}, which is Mn^{3+} oxide, where the change after catalysing methanol oxidation, the catalyst changed to be spinel Mn_3O_4 (665 cm^{-1}), which is a mixture of Mn^{2+} and Mn^{3+}. In other words, Mn_2O_3 reduced to a lower oxidation state. The Raman spectra in figure 3.24 indicate the presence of γ-MnO_2 with hexagonal structure, with peaks at 630, 380, 305 and 290 cm^{-1}. However, the used MnO_2 has changed in its structure from γ-MnO_2, recognised to be mixture of γ-MnO_2 and β-MnO_2. This has a peak of 665 cm^{-1}, compared to the literature [45][46], where the gamma peak by 630 cm^{-1} is not clear as separate peak and can be contributed with 665 cm^{-1}. Furthermore, XRD spectra also confirmed that the phase for used MnO_2 is β-MnO_2 and γ-MnO_2 as in figure 3.25. This has peaks of 29, 38, 41, 43, 46, 57, 59 and 74° [47]. Moreover, figure 3.26 show XRD spectra of Mn_2O_3, as 24, 34, 45, 54, 55, 62, 63, 64, 65, 66, 67, and 74°. The result did not show any change in the bulk of Mn_2O_3 after being used for methanol oxidation.

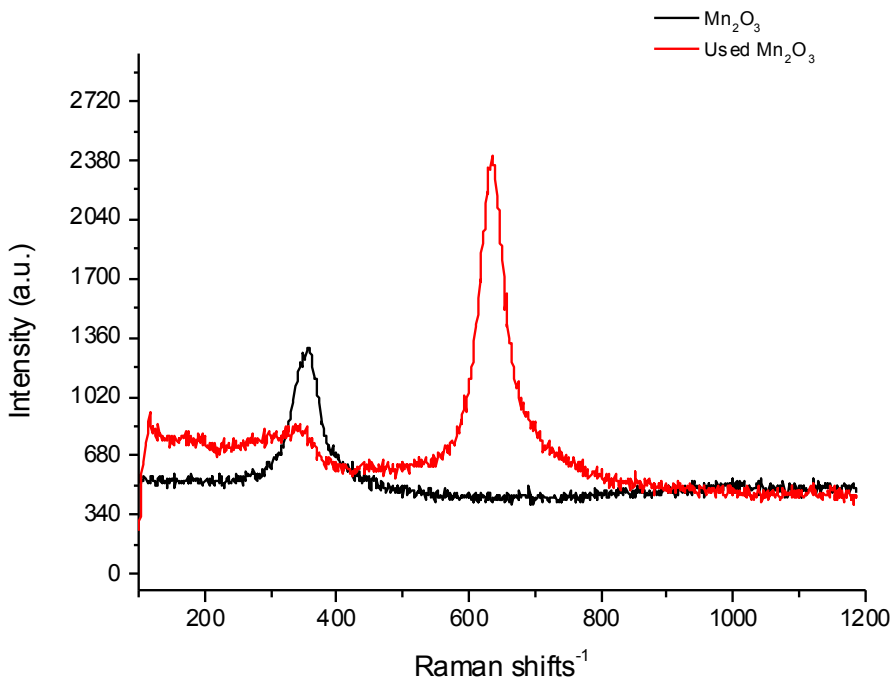

Figure 3.23 Raman result of Mn_2O_3 catalyst

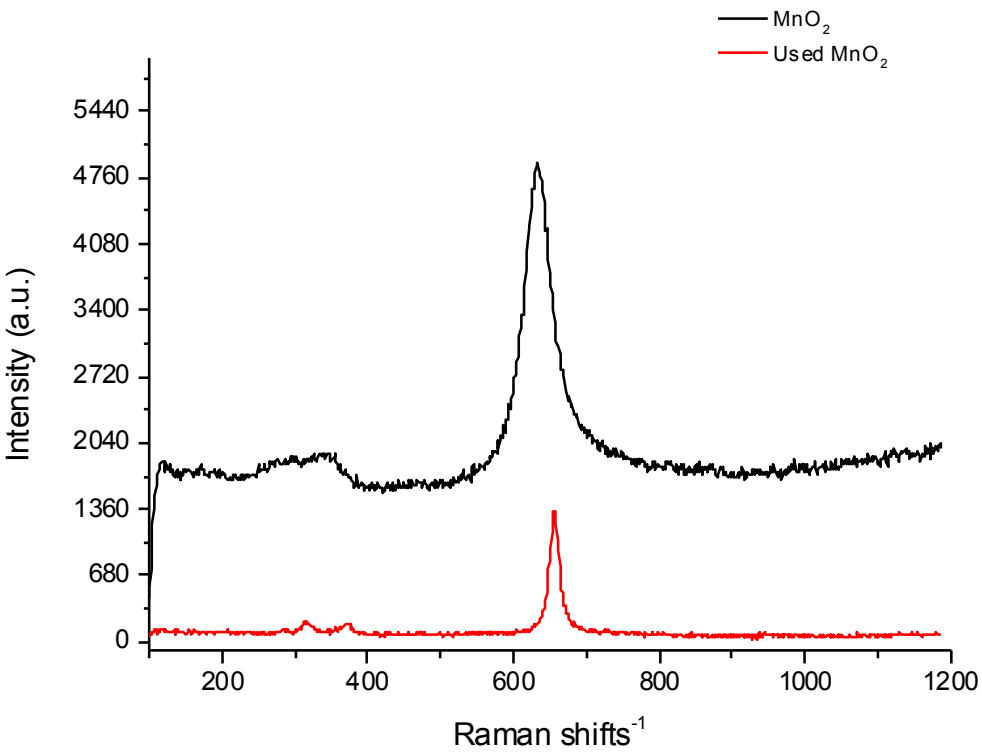

Figure 3.24 Raman result of MnO_2

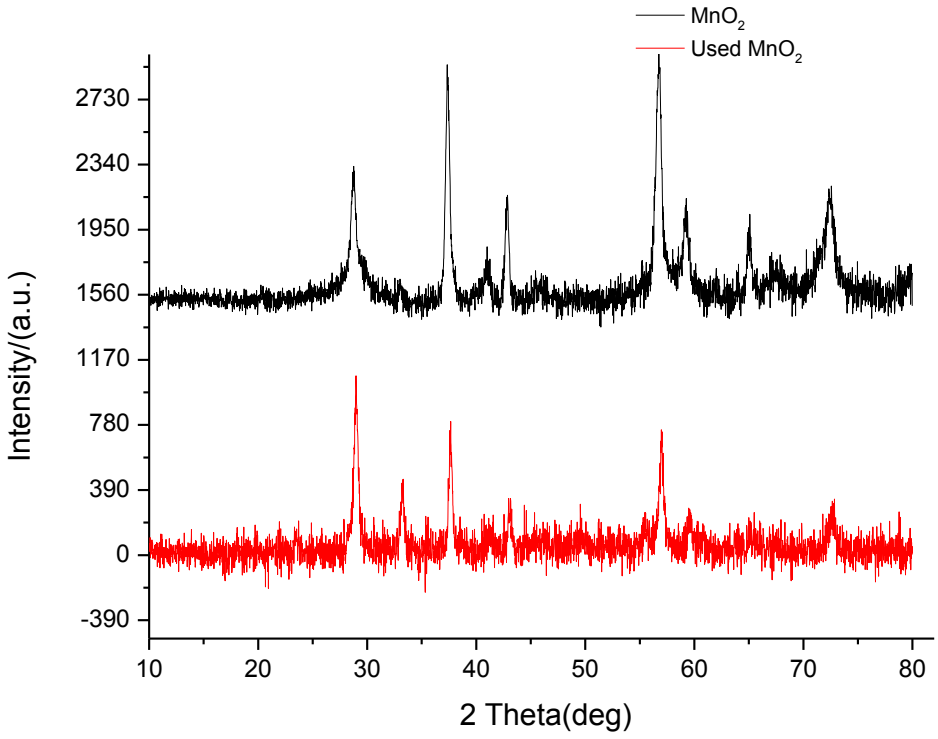

Figure 3.25 XRD spectra of MnO_2 catalyst

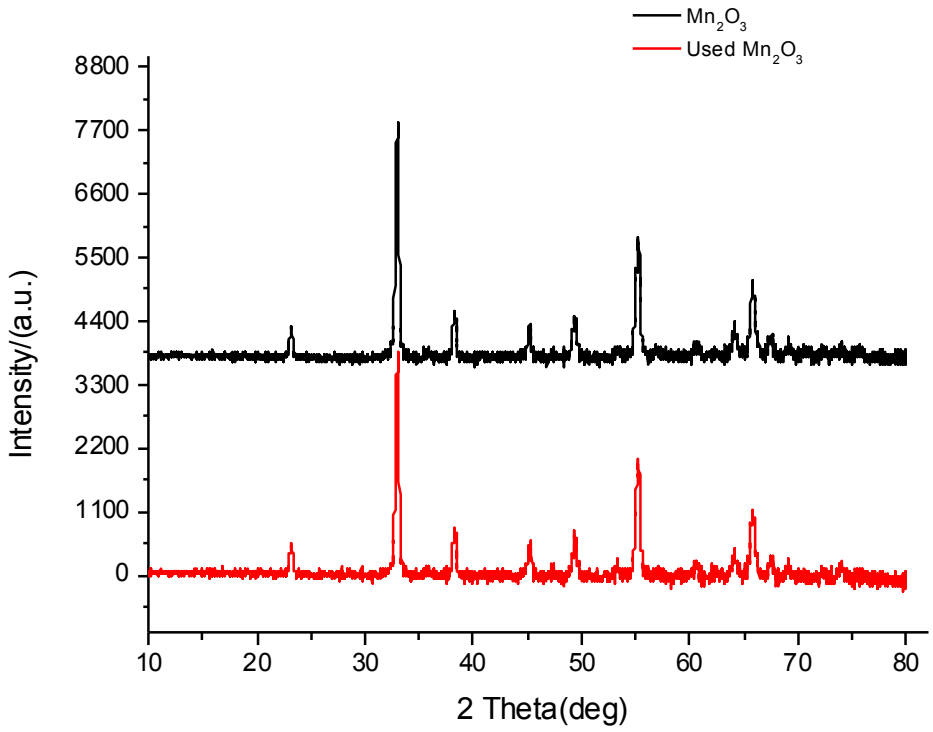

Figure 3.26 XRD result of Mn_2O_3 catalyst

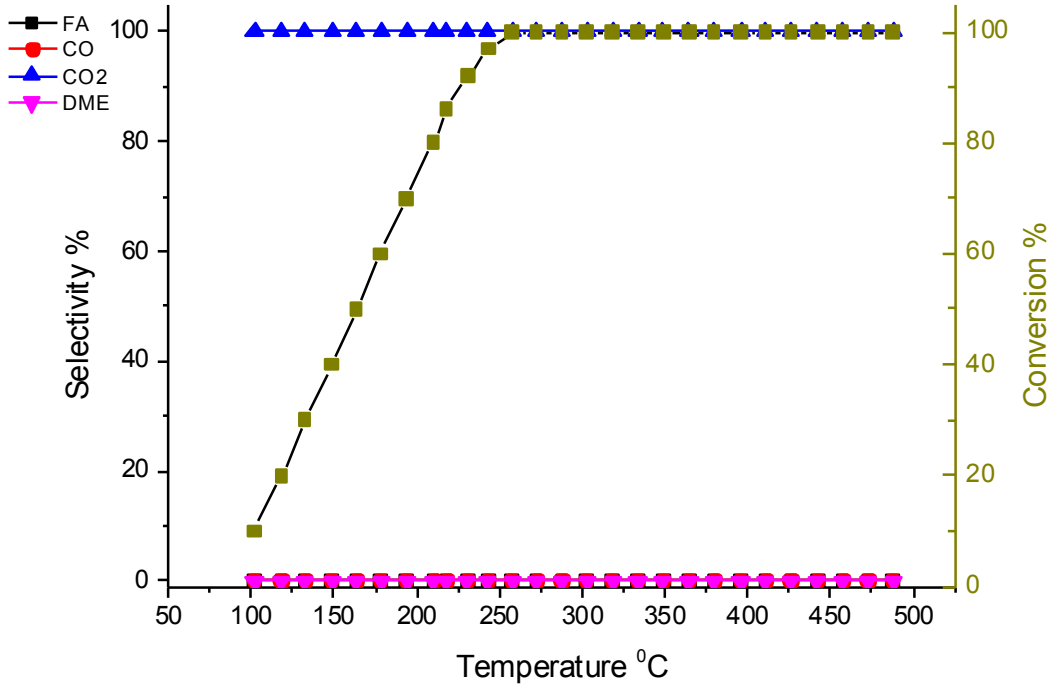

Figure 3.27 Reaction profile result of Mn_2O_3 catalyst

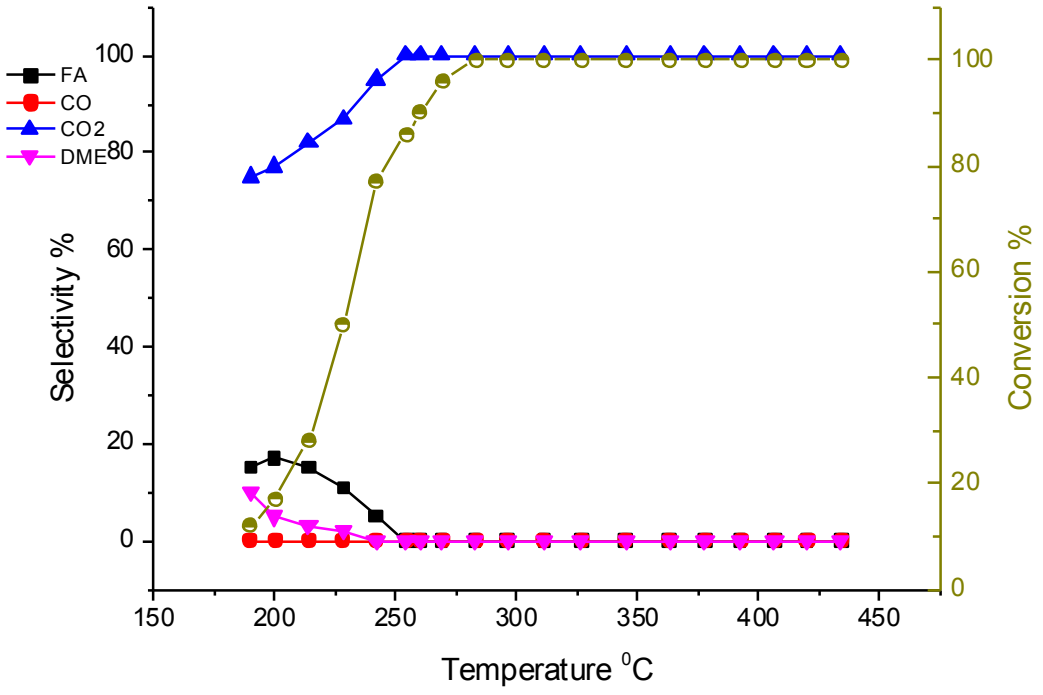

Figure 3.28 Reaction profile result of MnO_2 catalyst

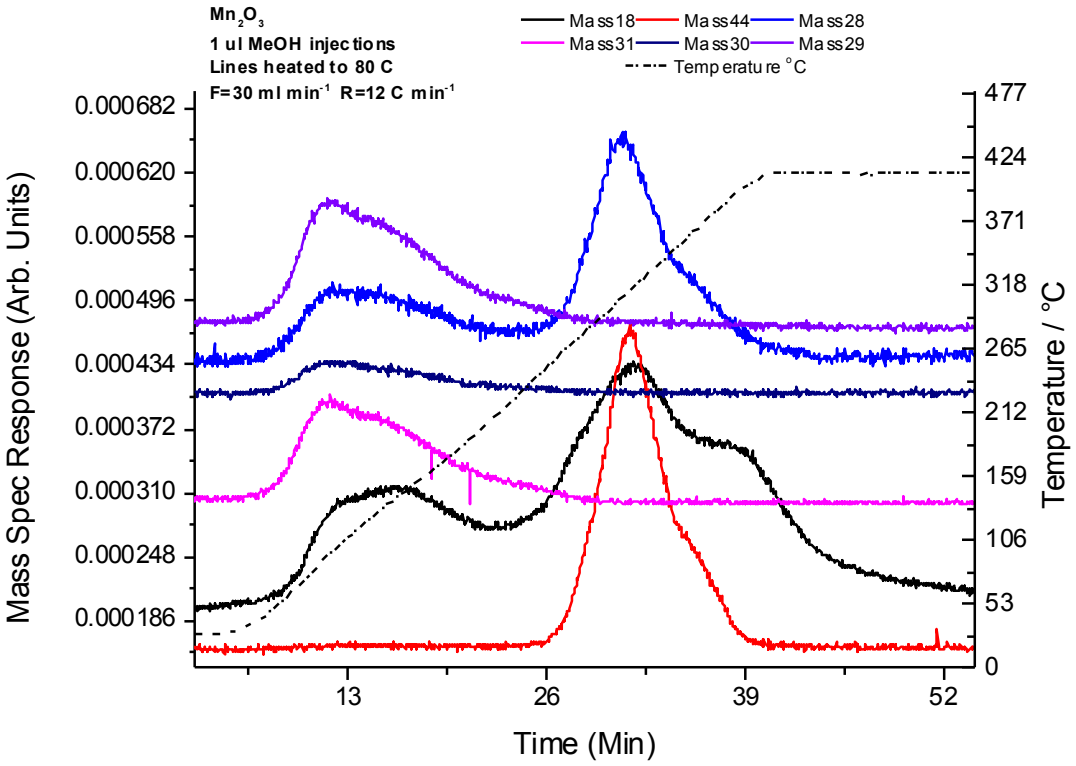

Figure 3.29 TPD result of Mn_2O_3 catalyst

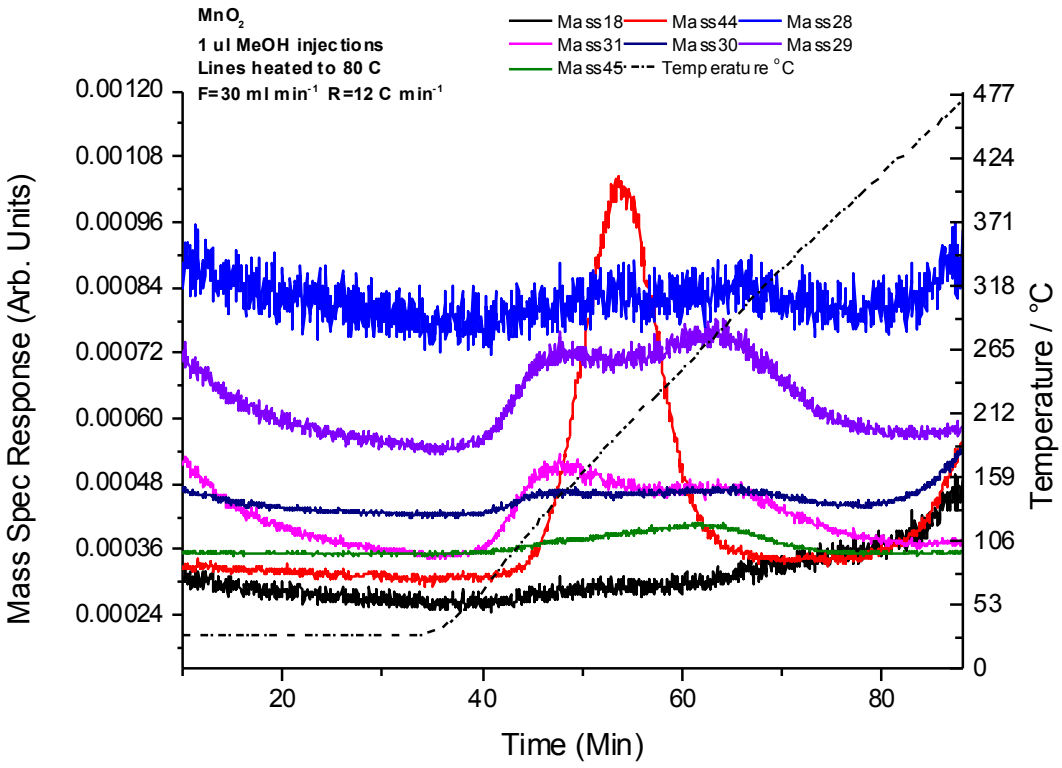

Figure 3.30 TPD result of MnO_2 catalyst

However, both MnO_2 and Mn_2O_3 catalysts are combustors for methanol oxidation. Where Mn_2O_3 (figure 3.27) converts methanol to carbon dioxide at any conversion, like the iron oxide catalyst, MnO_2 in figure 3.28 produces a small amount of formaldehyde and dimethyl ether at low conversion. However, when the conversion of methanol increases, formaldehyde and dimethyl ether totally disappear, Moreover, TPD results also confirms that both catalysts are selective to CO_2 in figures 2.29 (Mn_2O_3) and 2.30 (MnO_2), but Mn^{4+} oxide has desorption peak for dimethyl ether, whereas Mn^{3+} has only desorption peak for carbon dioxide even in absence of oxygen.

3.2.5 Cr_2O_3

The chromium oxide catalyst has a surface area of 2 m^2/g. Cr_2O_3 has Raman shifts of 294, 395, 564 and 602 cm^{-1}. As in figure 3.31, the catalyst was not changed to any other phase, or different oxidation state, after being used as a catalyst for methanol oxidation [48]. Figures 3.32 shows the activity and during methanol oxidation and 3.33 is the TPD in He after dosing methanol at ambient temperature. Chromium (III) oxide is selective to CO at low conversion, and CO_2 increases to 100% at high conversion. In TPD, chromium oxide catalyst preferred

to produce CO_2 and a small amount of CO, which overall means that chromium oxide catalyst is a methanol combustor, similar to the iron oxide catalyst.

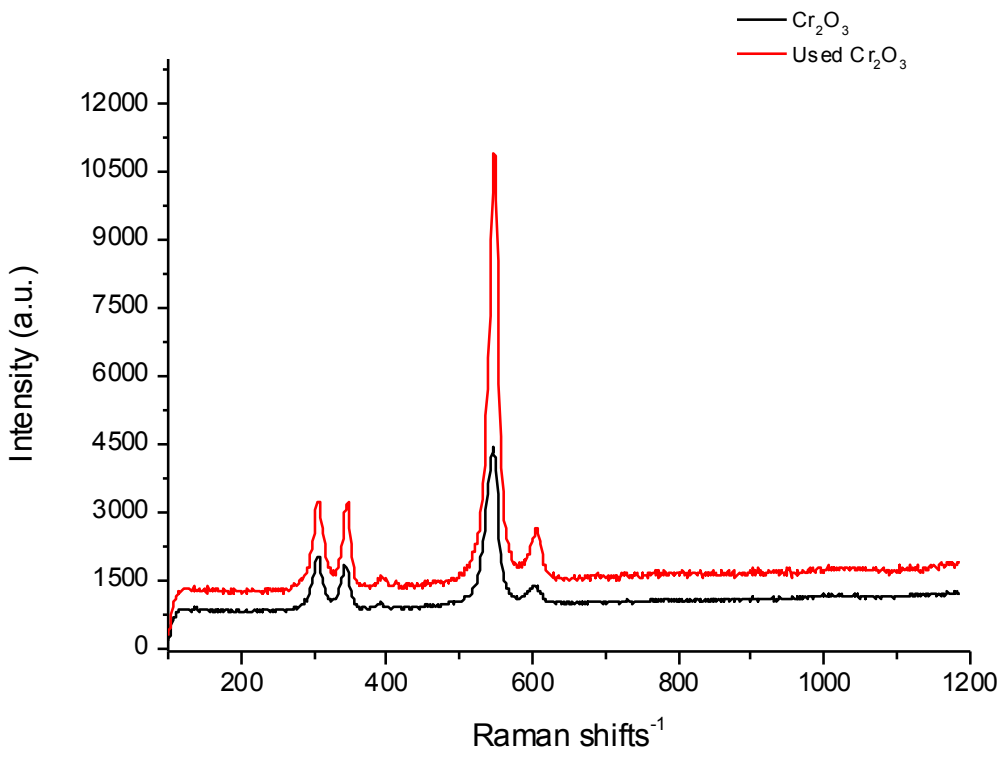

Figure 3.31 Raman result of Cr_2O_3 catalyst

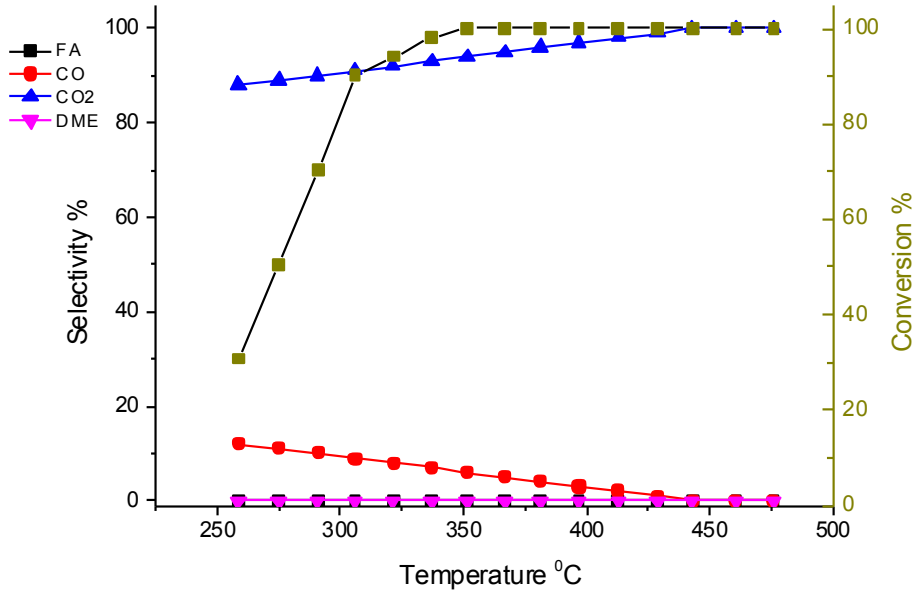

Figure 3.32 Reaction profile result of Cr_2O_3 catalyst

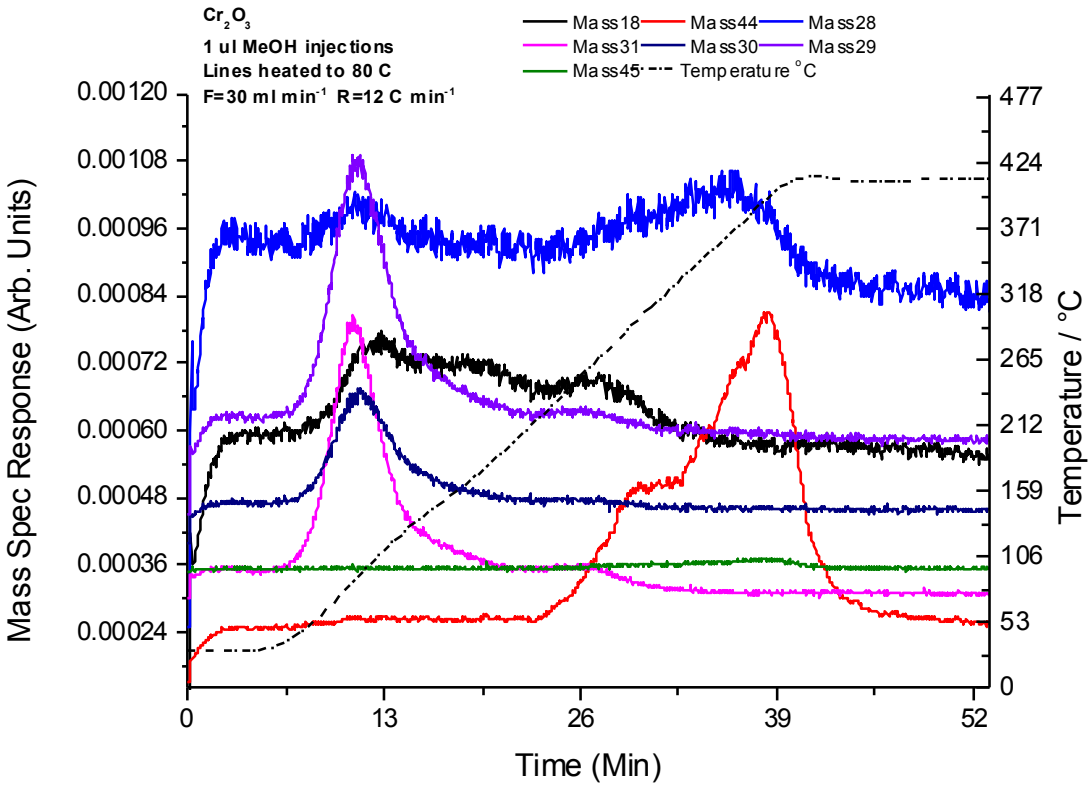

Figure 3.33 TPD result of Cr_2O_3 catalyst

3.2.6 Nb_2O_5

Niobium oxide has a surface area of 2 m^2/g. It was studied using the Raman technique in figure 3.34, and shows little change in the oxide structure after being used for methanol oxidation. Where the fresh niobium oxide Raman show Nb^{5+}, with tetrahedral NbO_4 units (sharper band at 830 cm^{-1}), compared to the literature [44]. Moreover, XRD results in figure 3.35, Nb_2O_5 is a mixture of hexagonal monoclinic structures with recognised peaks by 22.7° and 28.6°[49][50].

Figure 3.36 shows that the niobium oxide catalyst, is not a very active catalyst, the maximum methanol conversion was 85% by 530 °C. However, the catalyst is good in terms of selectivity to formaldehyde, where it showed similar results to vanadium oxides. It yields 35% formaldehyde by a temperature of 460 °C. This is even better than vanadium oxide as there is less combustion of methanol at higher temperature and formaldehyde was produced up to a temperature of 530 ^{0}C, being gradually replaced by CO at these high temperatures. The catalyst has more acidic properties than molybdenum oxide

and vanadium oxide catalysts. The proof of its high acidity is the formation of dimethyl ether at low temperature, and selectivity starting from 100% at ~5% methanol conversion. dimethyl ether selectivity decreased with the increase of conversion, becoming very low above 400 C . What is special of niobium oxide catalyst is that the catalyst kept producing dimethyl ether at high temperatures up to 530 ^{o}C with yield of 7%. This means the catalyst is Lewis acid site and has redox properties, as it yields 40% formaldehyde by 415 ^{o}C. This result was confirmed by the TPD result in figure 3.37. The TPD shows the preferred reaction pathways, with formaldehyde at approximately 420 ^{0}C, whereas dimethyl ether is at 320 ^{0}C.

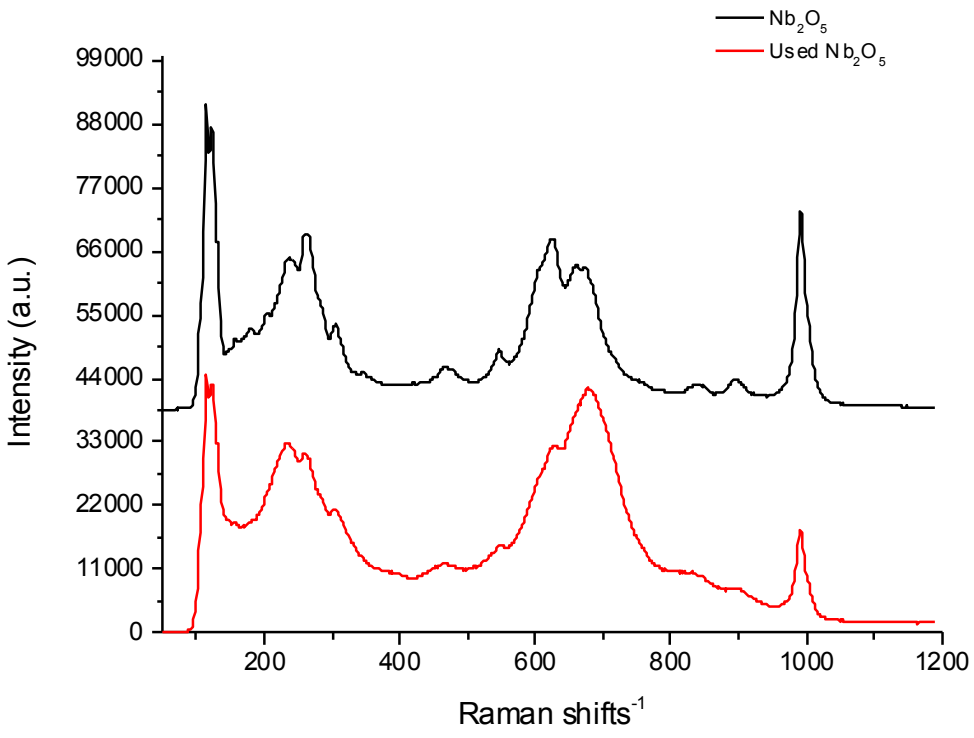

Figure 3.34 Raman result Nb_2O_5 catalyst

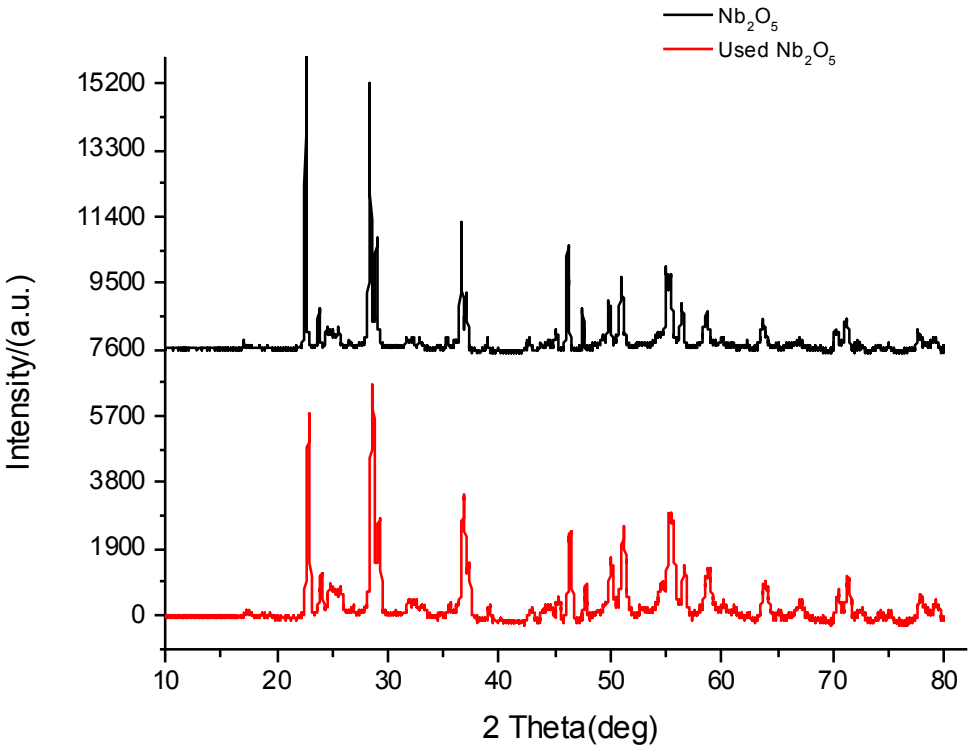

Figure 3.35 XRD spectra of Nb_2O_5 catalyst

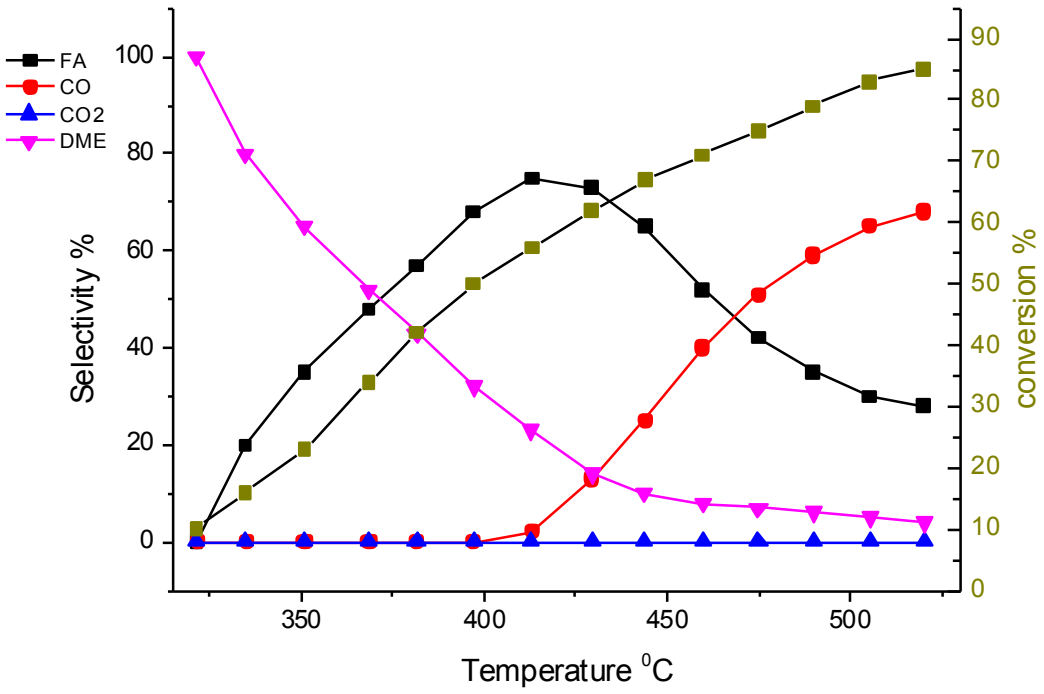

Figure 3.36 Reaction profile result of Nb_2O_5 catalyst

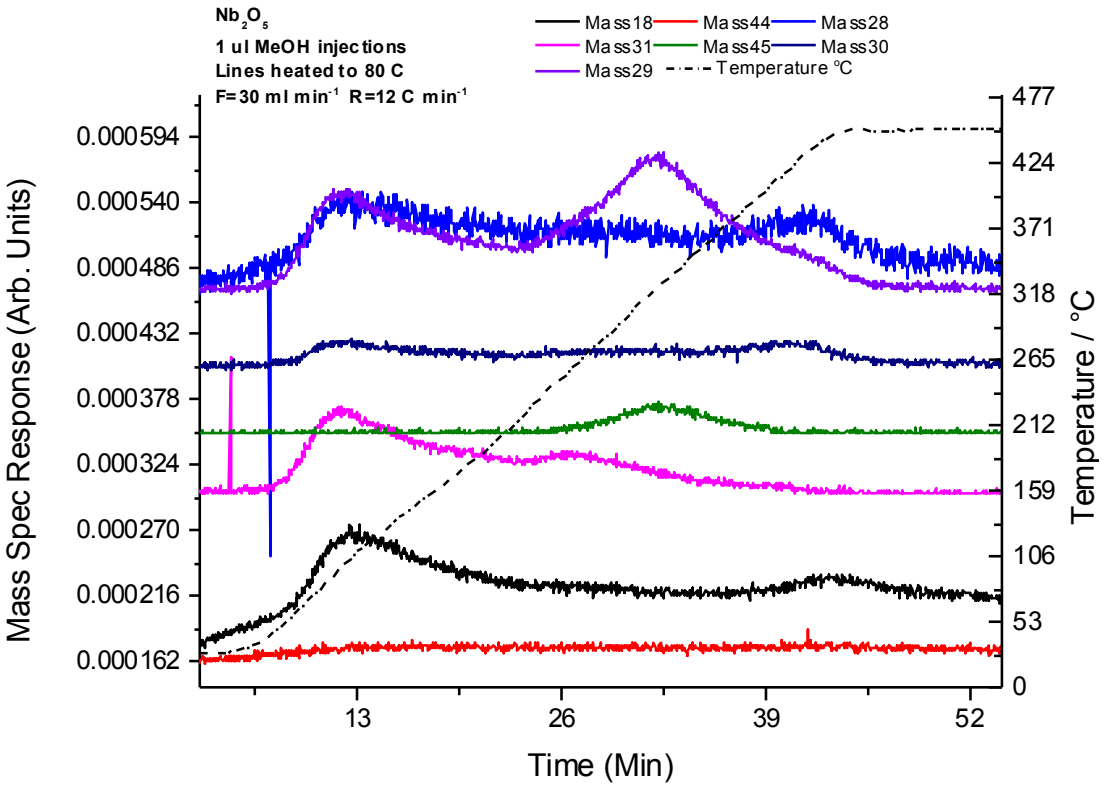

Figure 3.37 TPD result of Nb_2O_5 catalyst

3.2.7 Ta_2O_5

The tantalum oxide sample has 4 m^2/g surface area, and has Raman bands at 200, 280, 330, 521, 639, 719 and 850 cm^{-1} that do not change after use as shown in figure 3.38[51]. Moreover, the XRD spectra in figure 3.39 confirms that tantalum oxide catalyst did not have a notable change in its structure, where the spectra compared to literature is related to the β-Ta_2O_5 phase [52][53].

Tantalum oxide catalyst has a close result to niobium oxide catalyst in terms of catalytic behaviour as in figure 3.40 for methanol oxidation, which has redox and acid sites. In other words, it produces formaldehyde and dimethyl ether, but it produces more formaldehyde (40% selectivity, 10% conversion) than niobium oxide at low conversion, and less dimethyl ether (60% selectivity, 10% conversion). The niobium oxide catalyst produces 100% dimethyl ether at low conversion (10% conversion). Moreover, the maximum formaldehyde yield was

42% by 400 ^{o}C on tantalum oxide catalyst, which is a higher yield compared to 65% using niobium oxide catalyst. The tantalum oxide catalyst is more active than niobium oxide, as it converts 100% of methanol, whereas niobium oxide catalyst has 85% of methanol conversion as the highest conversion. Nevertheless, after 400 ^{o}C the production of both dimethyl ether and formaldehyde decreased at high temperature, with carbon monoxide being the main product at a temperature of 450 ^{o}C.

TPD result confirms that tantalum oxide catalyst is more selective to formaldehyde than niobium oxide, as shown in figure 3.41.

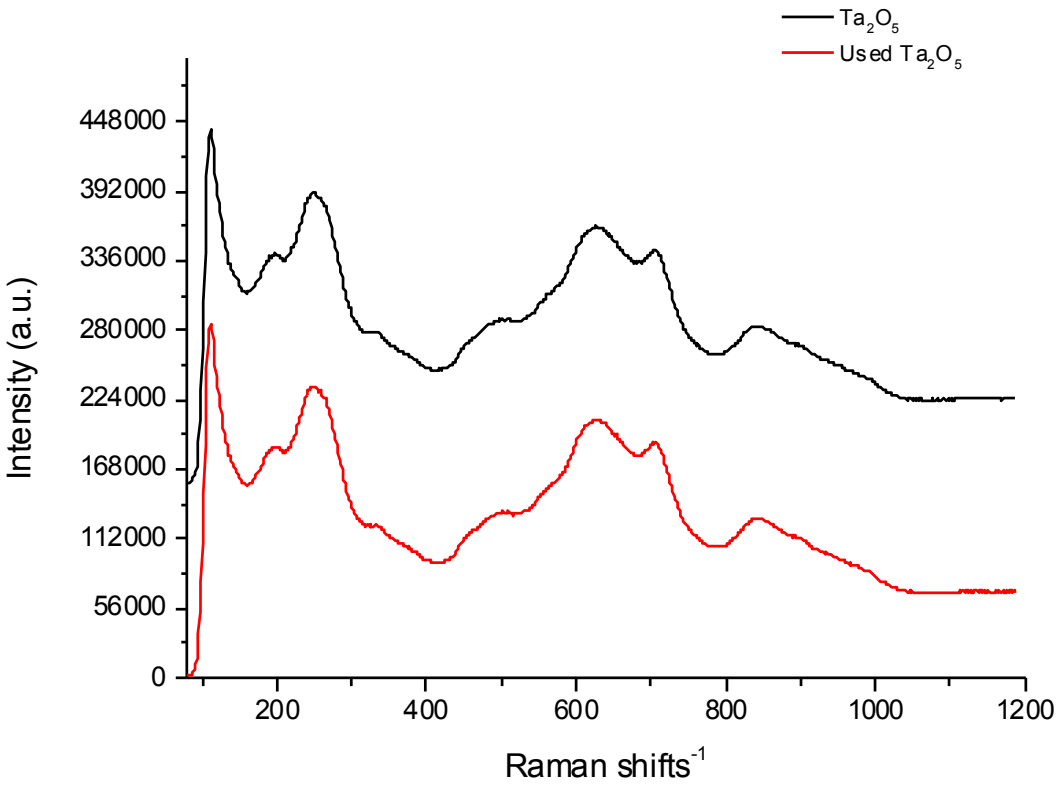

Figure 3.38 Raman result of tantalum oxide catalyst

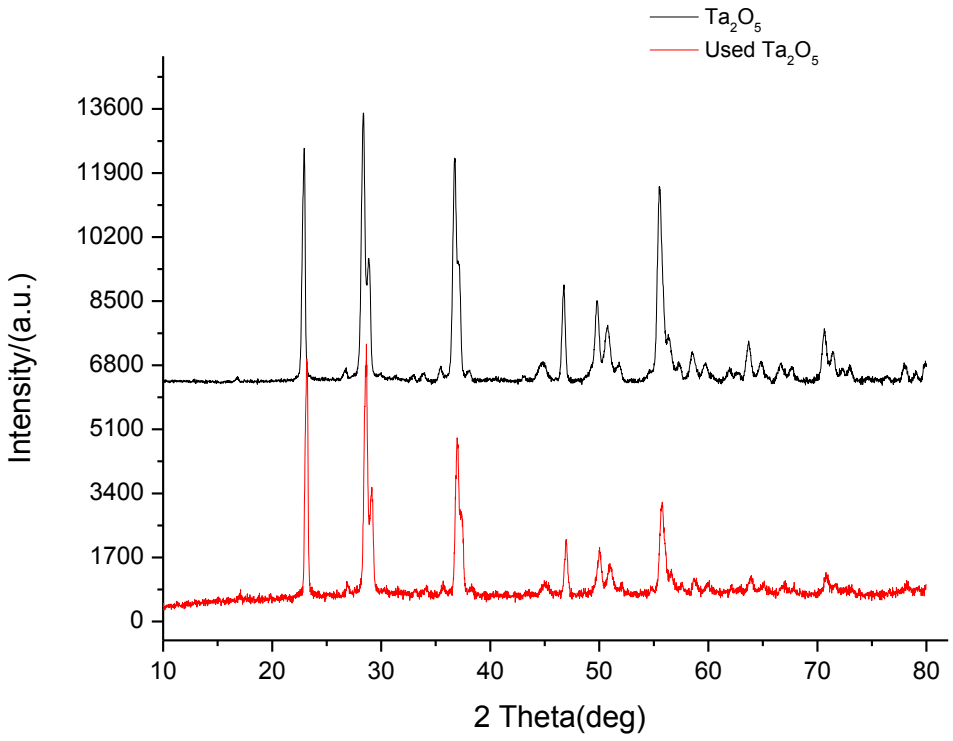

Figure 3.39 XRD spectra of Ta_2O_5

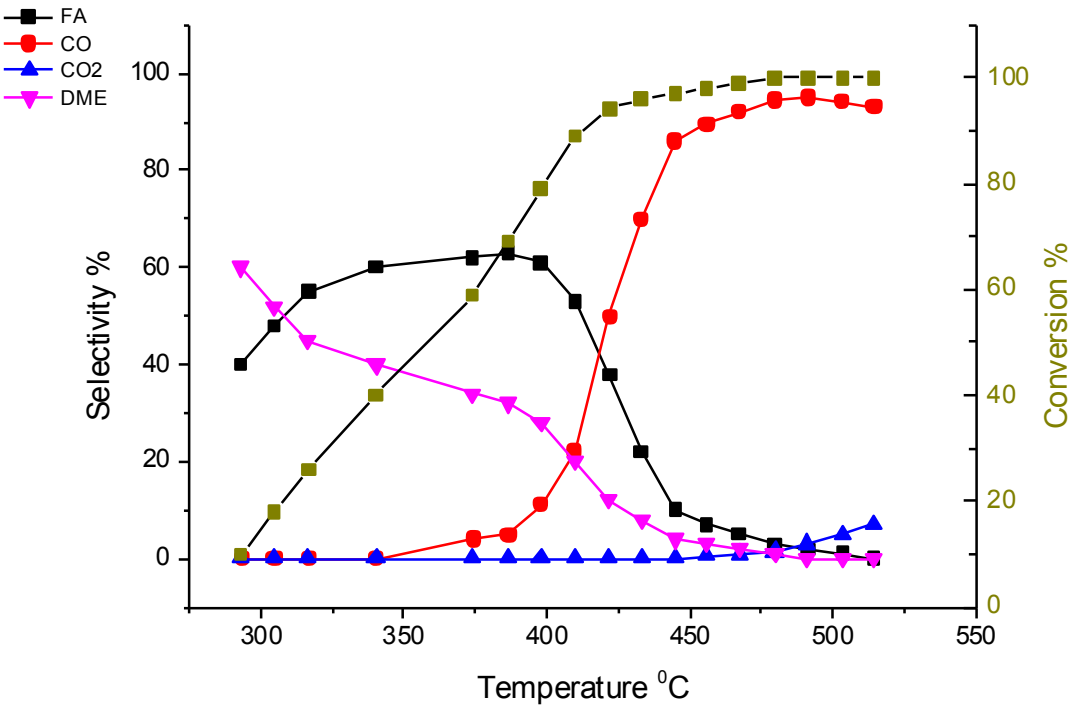

Figure 3.40 Reaction profile result of tantalum oxide catalyst

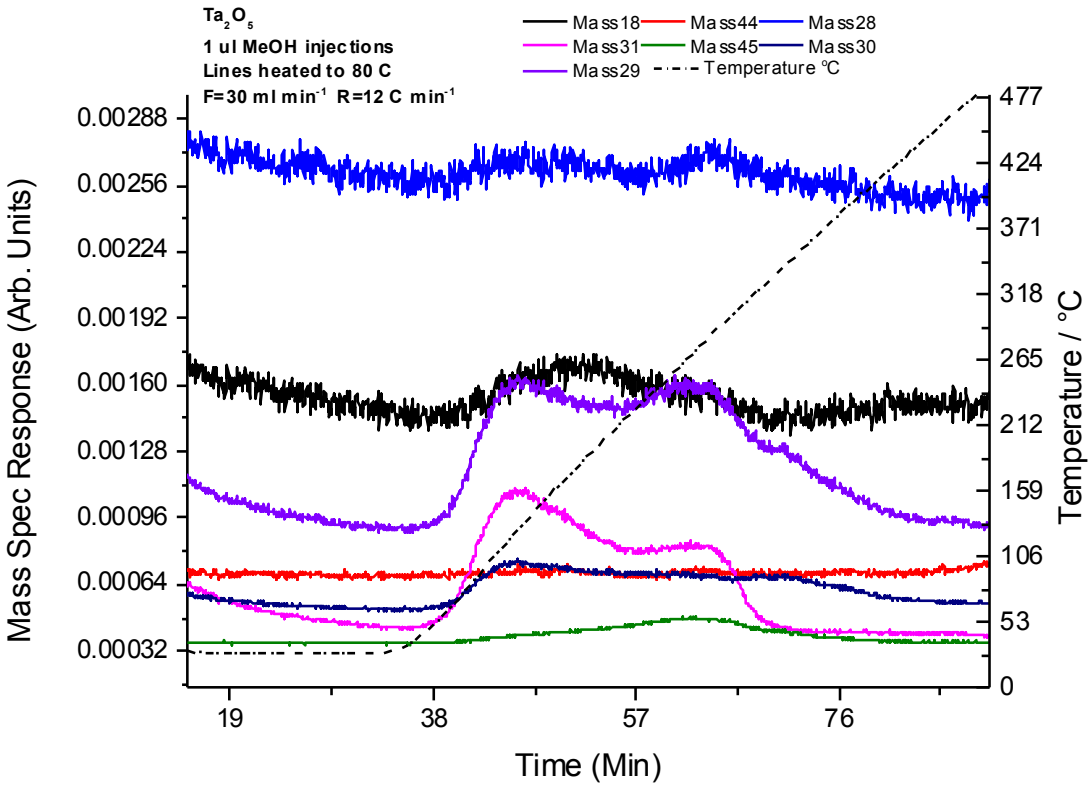

Figure 3.41 TPD result of Ta_2O_5 catalyst

3.2.8 WO_3

Tungsten oxide has surface area of 4 m^2/g. It has two common phases - monoclinic and orthorhombic, but the Raman result (figure 3.42) shows that the phase of the catalyst here is monoclinic with bands at 275, 320, 718 and 800 cm^{-1}. In literature[54] the bands are 273, 323, 716 and 508 cm^{-1}. Also the XRD result in figure 3.43 is that of pure monoclinic WO3 catalyst, as it has peaks by 42° and 29° [54]. The catalyst did not change between the fresh and the used samples. The result compared to literature with peaks of 2θ= 23° (002), 29° (211), 33° (112), 33° (110), 36° (202), 42° (110), 44° (222) and 46° (004)[55][56]).

The sample is more selective than molybdenum oxide (figure 3.44), where the only product was formaldehyde at any conversion, even at temperatures up to 420 °C. Here molybdenum oxide catalyst has CO production increased by an increase of temperature, however both molybdenum oxide and tungsten oxide have poor activity, where the maximum methanol conversion was 55% by 420 °C. Moreover, TPD in figure 3.45 also confirms that tungsten oxide

catalyst is only selective to formaldehyde, and one desorbed peak of formaldehyde.

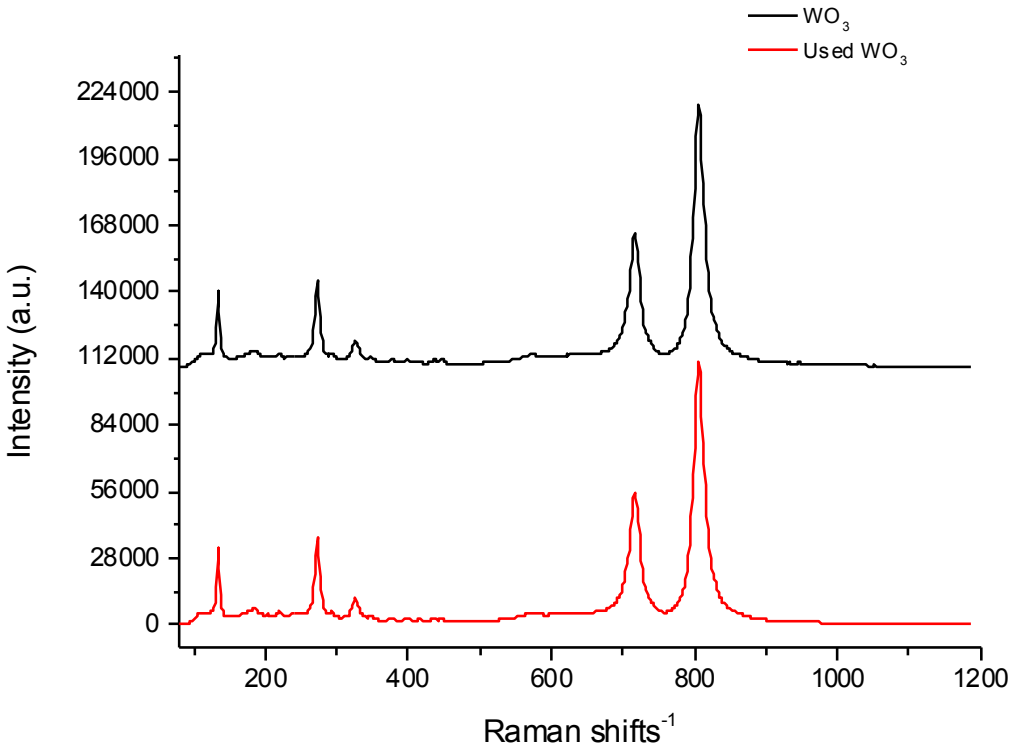

Figure 3.42 Raman result of tungsten oxide catalyst

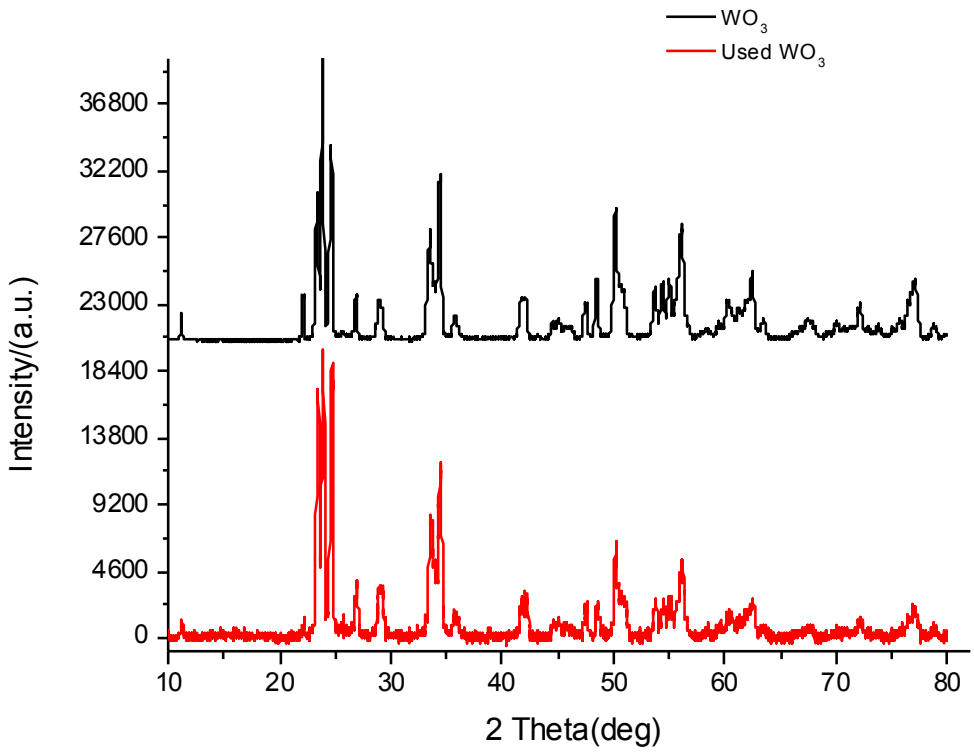

Figure 3.43 XRD result of tungsten oxide catalyst

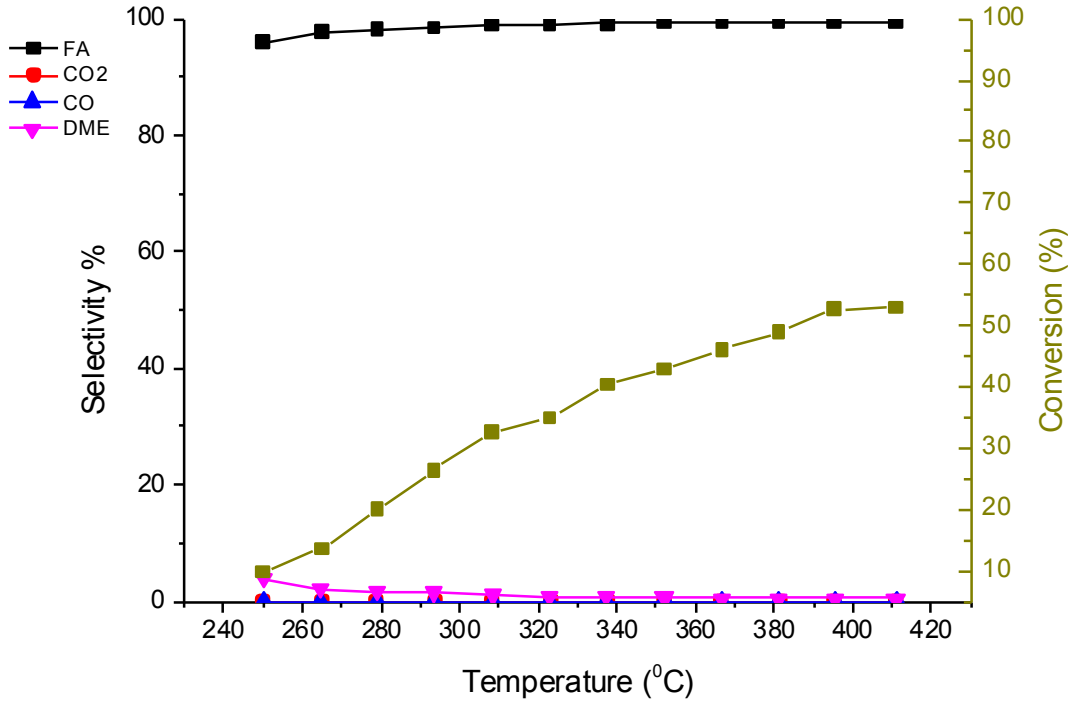

Figure 3.44 Reaction profile result of tungsten oxide catalyst

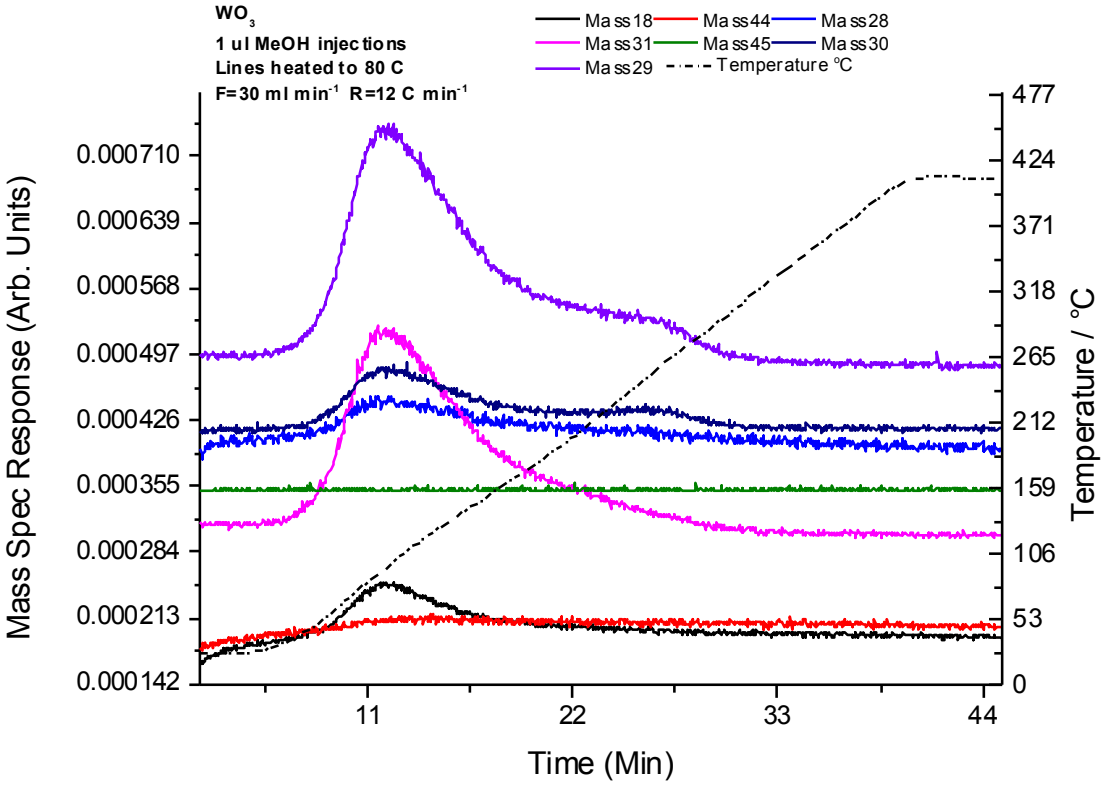

Figure 3.45 TPD result of tungsten oxide catalyst

3.2.9 ReO_3

Rhenium oxide has surface area of 5 m^2/g. The Raman results for rhenium oxide in figure 3.46 do not show any change in the catalyst surface before and after reaction. Here a Raman shift of 883 cm^{-1} is related to the Re=O stretch (literature= 880 cm^{-1}). The band at 909 is assigned to octahedral ReO_3, as is also shown by the XRD in figure 3.47 (XRD spectra). The peaks compared to the literature were (110) 16.8°, (121) 25.7°, (200) 30.7°, (211) 33.8°, (240) 41.1°, (161) 47.1° and (170) is 51.4° [57][58], it is body centre cubic structure.

Figure 3.48, shows the acidic nature of the catalyst as significant amounts of dimethyl ether are produced. Nevertheless, more than half of the methanol was converted to formaldehyde and kept increasing up to 430 °C. After 430 °C, the selectivity of dimethyl ether and formaldehyde decreased and the selectivity of CO increased. Moreover, the TPD result (figure 3.49) shows that ReO_3 is selective to formaldehyde and dimethyl ether, whereas CO was not formed in the absence of oxygen.

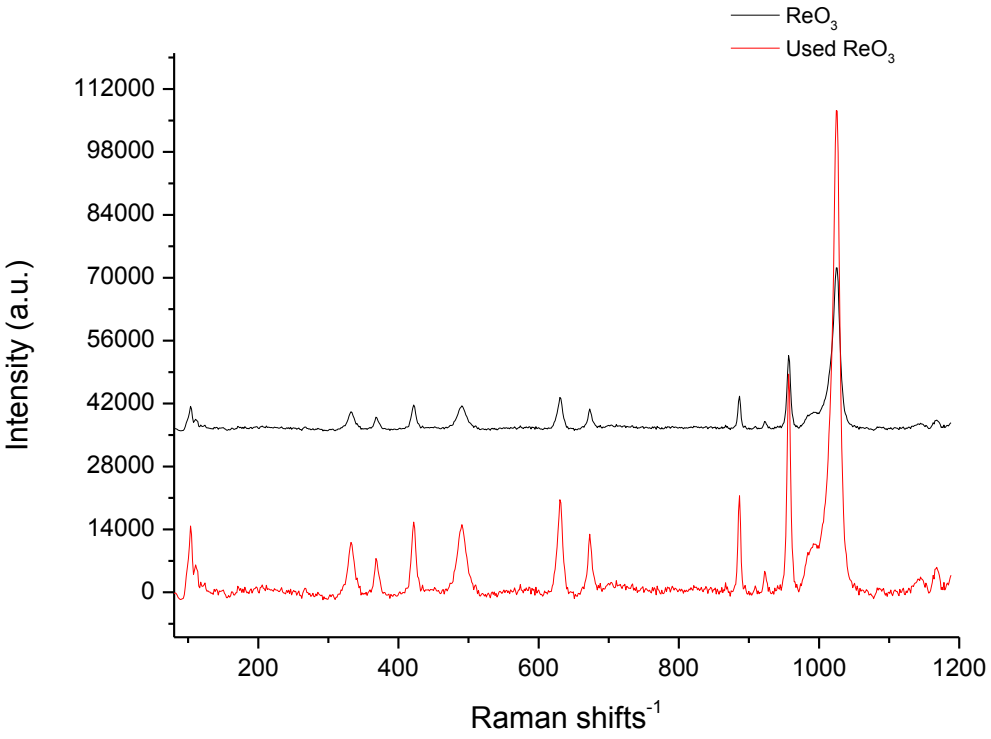

Figure 3.46 Raman result of ReO_3 catalyst

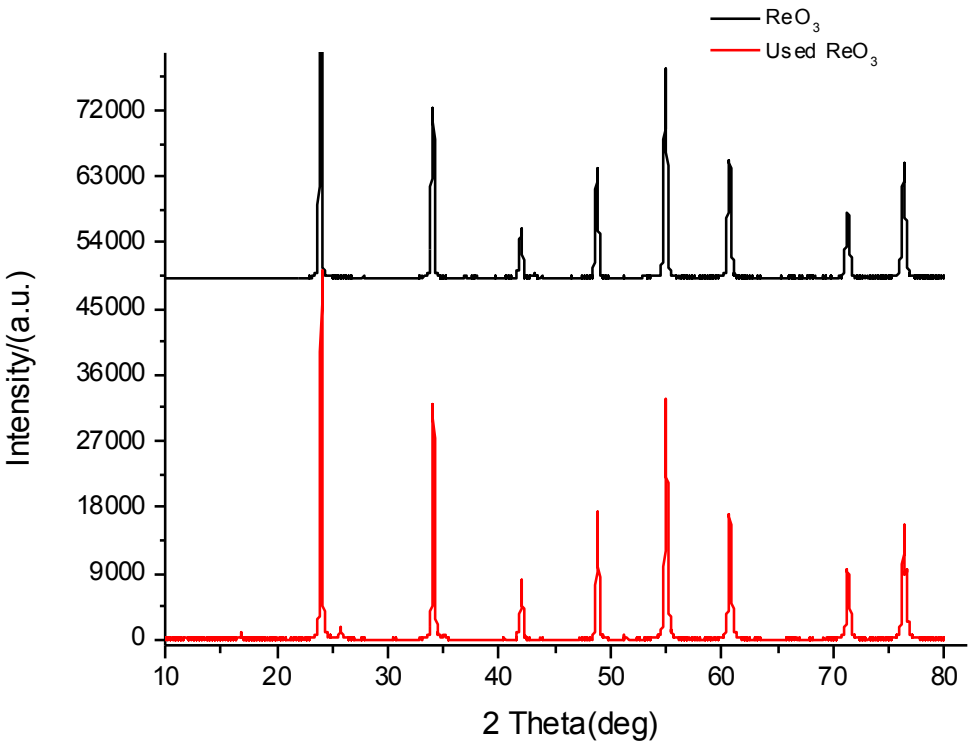

Figure 3.47 XRD spectra of ReO_3

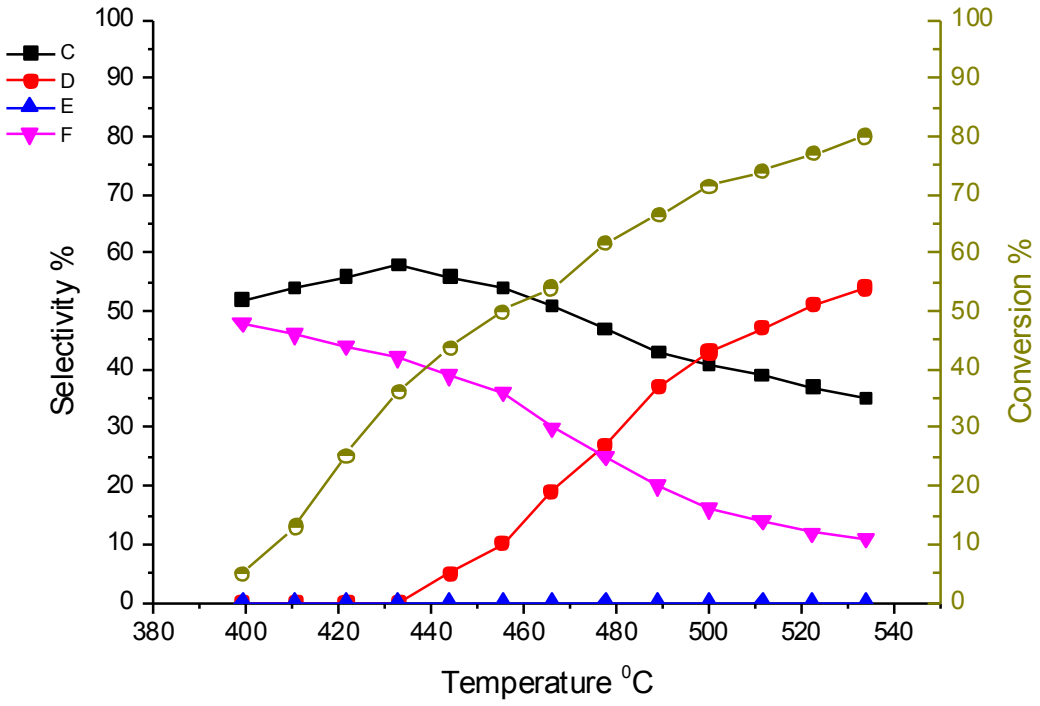

Figure 3.48 Reaction profile result of ReO_3 (c-formaldehyde, d-CO, e-CO_2 and f-Dimethyl ether)

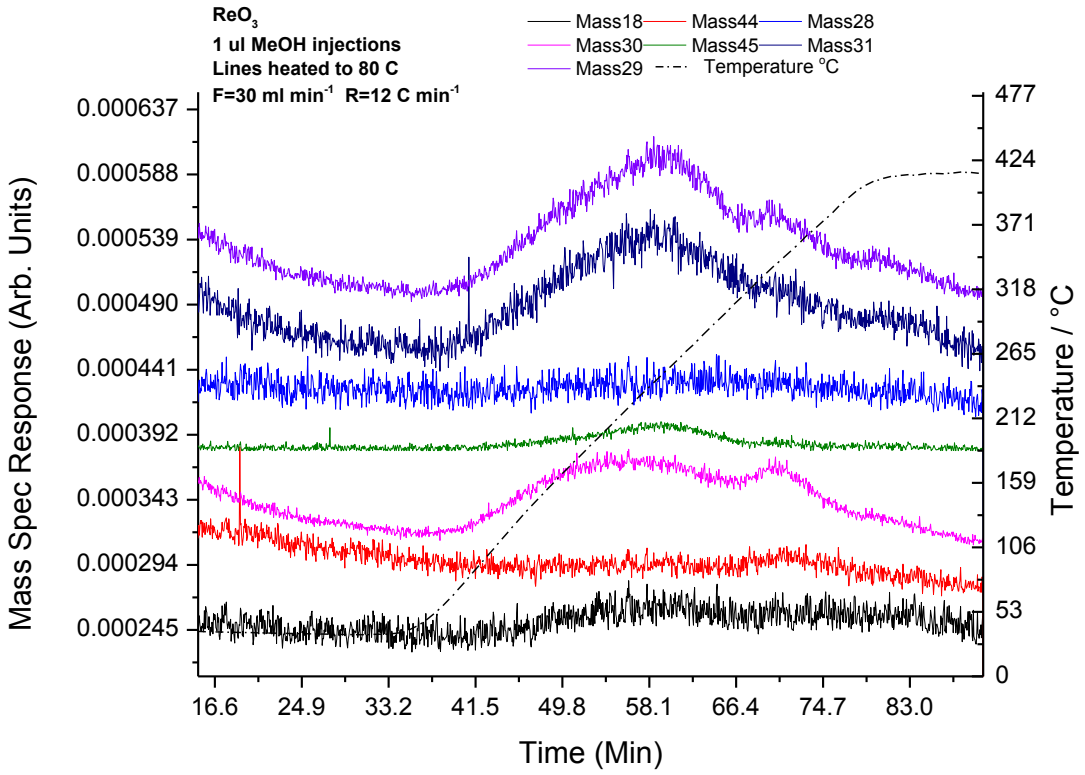

Figure 3.49 TPD result of ReO_3 catalyst

3.2.10 CoO

Cobalt oxide catalyst has a surface area of 4 m^2/g. The catalyst is not pure Co^{2+}, but it contains Co^{+2} and Co^{+3} as a mix of face-centered cubic CoO and spinel Co_3O_4[59]. The Raman shifts of FCC CoO are at 455 and 675 cm^{-1}, whereas the spinel Co_3O_4 has bands at 482, 519, 621 and 690 cm^{-1}. However, in figure 3.50 the Raman result shows the catalyst has not changed its structure after reaction. The catalyst acts as methanol combustor (figure 3.51), however, the catalyst is more active than the iron oxide catalyst. It starts to convert methanol by a temperature of 150 ^oC, whereas for iron oxide it is 180 ^oC. Nevertheless, V_2O_5 is still the most active catalyst used in this study since converts methanol by 140 ^oC. Moreover, the TPD result in figure 3.52 shows only CO_2 as a reaction product, in agreement with the reaction findings.

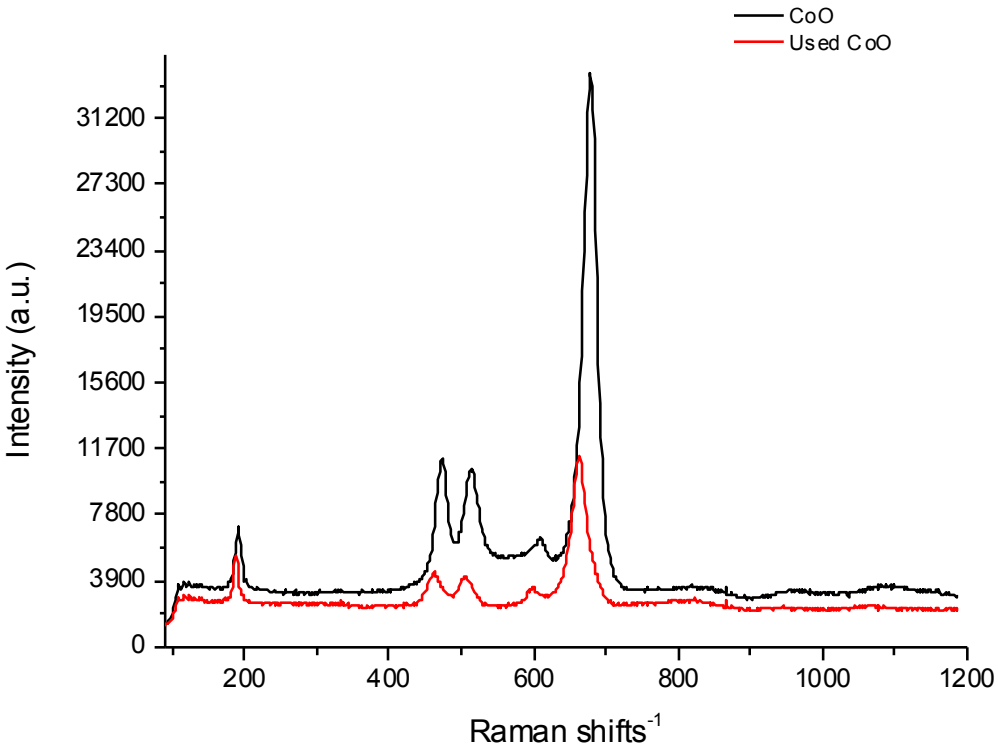

Figure 3.50 Raman result of CoO catalyst

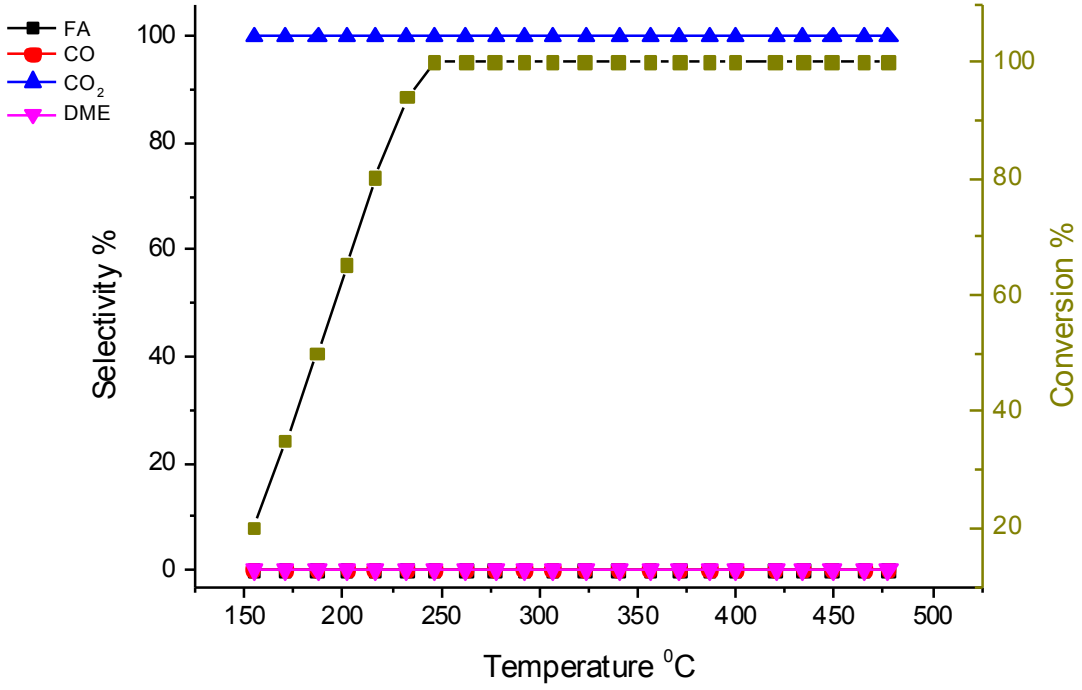

Figure 3.51 Reaction profile result of CoO catalyst

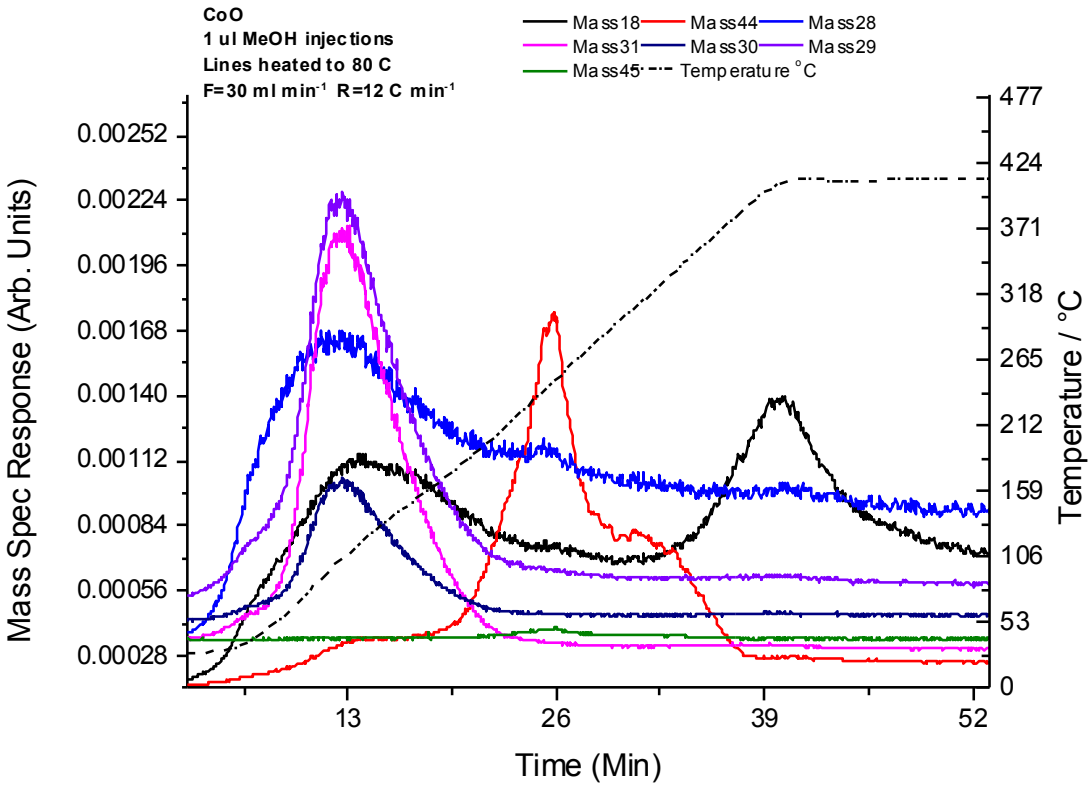

Figure 3.52 TPD result of CoO catalyst

3.3 Discussion

We can establish some rules of thumb from the previous result of all the catalysts used in this study. The main factors dictating methanol oxidation selectivity are the metal oxidation state and its acidic properties. Even the catalytic activity is affected by oxidation state. In what follows the catalysts studied in this chapter are divided into three groups according to their catalytic behaviour for methanol oxidation as combustion catalysts, partly selective catalysts and selective catalysts, table below summarises the catalytic activity and formaldehyde selectivity of catalysts in result section, the table below shows how oxidation state is affected in methanol oxidation reaction, where the low oxidation state catalysts burn methanol to carbon dioxide, but 5+ oxidation state catalysts are partly selective to formaldehyde, whereas 6+ oxidation state catalyst are more selective to formaldehyde.

Catalyst	The highest selectivity		Full conversion	
	FAS (%)	Con (%)	Tem (^{o}C)	FAS (%)
CoO	0	100	250	0

Mn_2O_3	0	100	250	0
Cr_2O_3	0	100	345	0
Fe_2O_3	0	100	240	0
MnO_2	18	15	275	0
VO_2	100	5	350	55
V_2O_5	96	50	300	12
Nb_2O_5	75	55	*550@85%	30
Ta_2O_5	60	65	475	5
MoO_3	100	10	*500@85%	45
WO_3	100	55	*420@55%	100
ReO_3	60	35	*535@80%	35

Table 3.3 Summary of catalysts activity and formaldehyde selectivity. (Tem: temperature, Con: methanol conversion, and FAS: Formaldehyde selectivity, (*) is an exception for some catalysts did not converted 100% methanol).

3.3.1 Combustion catalysts

Combustion catalysts are oxide metals in low oxidation state (2+,3+,4+). These catalysts burn methanol at any conversion point. In this chapter these catalysts are cobalt oxide (CoO, 2+), chromium oxide (Cr_2O_3, 3+), iron oxide (Fe_2O_3, 3+), manganese oxide (Mn_2O_3, 3+) and manganese dioxide (MnO_2). However, VO_2 is one of the productive catalysts, where it is V_2O_5 segregated on the surface as proofed using XPS in result section, and V_2O_3 in the bulk, which catalytically behaves as V_2O_5, or 5+ metal oxide catalyst, as stated in the results section. These catalysts are very active usually converting methanol at temperatures lower than 200 ^oC.

The mechanism of methanol oxidation on a surface of a combustive catalyst is explained by first methanol being adsorbed in its surface. This kind of catalyst has bridging metal oxygen bonds, and the metal hosts methanol by bonding with oxygen atom in the hydroxyl part of methanol molecule. This produces chemisorbed methanol (M-OCH_3) and the missed hydrogen bonds to the next neighbouring oxygen in the oxide catalyst lattice[1-6]. Then another hydrogen of adsorbed methanol leaves to another neighbouring lattice oxygen to form another hydroxyl group bonded to the surface. This also forms (M-OCH_2) after leaving the hydrogen. Next, it either decompose to gaseous formaldehyde or interacts by another available neighbouring oxygen. In the case of these combustive catalysts, it reacts with another lattice oxygen to form formate group (M-OCOH), which either decomposes as formic acid or carbon dioxide with hydrogen[1-6]. However, the two hydroxyl groups react and form water gas with

lattice oxygen vacancy formation, which would be then taken from the gas oxygen as shown in the equations below:

CH_3OH + Surface M →M-OCH_3^------H^+ (Eq 3.1)

M-OCH_3^------H^+ + lattice O-$M_{(1)}$ → M-OCH_3^- + H-O-$M_{(1)}$ (Eq 3.2)

M-OCH_3^- + lattice O-$M_{(2)}$ → M-OCH_2 + H-O-$M_{(2)}$ (Eq 3.3)

M-OCH_2 + O-$M_{(3)}$ → M-OCOH + H-O-$M_{(3)}$ (Eq 3.4)

M-OCOH → CO_2 + ½ H_2 + M^+ (Eq 3.5)

½ H_2 + H-O-$M_{(1)}$ → H_2 + O-M (Eq 3.6)

H-O-$M_{(2)}$ + H-O-$M_{(3)}$ → H_2O + M^+ + O-M (Eq 3.7)

2 M^++ gaseous O_2 → 2 O-M (Eq 3.8)

Beginning from the adsorption of methanol to form adsorbed methoxy, then adsorbed formate, then decomposition to carbon dioxide, shown with in-situ Raman [60]. In this study, an in-situ Raman was not used, but TPD gave similar result, where carbon dioxide desorbed first, followed by water peak as the last product. However, there is a factor which makes these catalysts selective to carbon dioxide. One notable factor is in the catalyst structure, where these kind of catalysts participate their bridging oxygen into the adsorption and dissociation steps, by making bridging methoxy[61]. This makes the catalyst unstable and quickly causes another bridging oxygen to react to form adsorbed formate[1-6], which then desorbs as CO_2.

3.3.2 Partly selective catalysts

The meaning of partly selective catalysts comes from their catalytic behaviours. These are selective at low conversion to products, are not combustive (CO, CO_2), and start to give CO and CO_2 with increased heat and methanol conversion, but still at some point produce products. In this chapter they are Ta_2O_5, Nb_2O_5, VO_2, V_2O_5, these catalysts have terminal oxygen, and have an oxidation state of 5+. Moreover, they are less active than the combustion catalysts. In mechanism, methanol is adsorbed at the catalyst surface and bonds to terminal oxygen from the methanol hydroxyl group (M-OCH_3, where M= Ta, Nb and V). Then adsorbed methanol reacts with neighbouring lattice oxygen to form methoxy (M-OCH_3) and hydroxyl groups are bonded to the surface.

Formaldehyde then desorbs, but at higher temperature, some methoxy groups further react to carbon monoxide by adsorbed gaseous oxygen . Then the hydroxyl groups recombine to water and leave the surface reduced, where the missing oxygen is taken up from the gas phase.

The difference between 5+ oxide catalysts, and oxides with a lower oxidation state, is in their surface structures. 5+ oxide catalysts have more terminal M=O, where methanol is chemisorbed on this kind of terminal bond, (the surface is less perturbed than in the case of bridging oxygen involvement), as a consequence, methoxy will stay longer compared to the combustor catalysts. That is confirmed in the results section, where all catalysts are active and selective to formaldehyde at temperatures higher than 250 ^{o}C. The combustive catalysts convert methanol at temperatures lower than 200 ^{o}C.

$M\text{-}OCH_2 \rightarrow CO + H_2$ **(Eq 3.9)**

Dehydrogenation of methanol to CO is most notable for 5+ oxide catalysts. Here all catalysts start as selective catalysts to either formaldehyde or dimethyl ether at low temperature. The selectivity to these products decreases with an increase of temperature[61-69], while CO production increases. At even higher temperature V_2O_5 further oxidises CO to CO_2. Dimethyl ether is a dehydration reaction of methanol at low temperature, where two methanol molecules are adsorbed on the surface. As a result, interaction between two adsorbed molecules leads to abstraction of water and the formation of dimethyl ether as shown below (e.q. 3.10 and 3.11). However, the formation of dimethyl ether decreases with an increase of temperature, probably because of dimishing surface concentration of adsorbed methanol.

$2CH_3OH + 2M\ (surface\ metal) \rightarrow 2M\text{----}HOCH_3$ **(Eq 3.10)**

$2M\text{----}HOCH_3 \rightarrow 2M + CH_3OCH_{3(gas)} + H_2O_{(gas)}$ **(Eq 3.11)**

However, dimethyl ether formation is clear even at high temperatures on catalysts like Ta_2O_5 and Nb_2O_5. Here the two catalysts have strong acid

properties and the catalyst surface acts as an electron pair acceptor, or Lewis acid type[65].

3.3.3 Selective Catalysts

Selective catalysts in this study are catalysts converting methanol efficiently to formaldehyde. However, at high temperatures there is notable formation of carbon monoxide as result of methoxy group oxidation. In general they are selective to either dimethyl ether or formaldehyde. Rhenium oxide catalyst has acidic properties compared to molybdenum oxide and tungsten oxide. Here it is more selective to dimethyl ether than formaldehyde. However, molybdenum oxide is selective to formaldehyde but the increase of temperature methoxy oxidises to CO. Tungsten oxide is near 100% selective to formaldehyde at any conversion point, even at the highest temperature (500 ^{o}C).

However, terminal methoxy groups on the surface are more reactive than the bridging methoxy in lower oxidation state catalyst (lower than 6+), it converts to formaldehyde if the surface has redox sites or acid sites for dimethyl ether formation, where the surface of 6+ oxidation state catalyst has more terminal oxygen than lower oxidation state catalyst, and this terminal oxygen is responsible for terminal methoxy that converted to formaldehyde. Likewise, molybdenum oxide and tungsten oxide catalysts are selective to formaldehyde, whereas ReO_3 catalyst acts as Lewis acid surface that eliminates water and dimethyl ether. Nevertheless, these oxides are not very active at temperatures up 500 ^{o}C, more heat required to reach the methanol conversion comparing to 5+, 4+, 3+, 2+ oxides catalysts were tested above, where tungsten is found to be 100% selective to formaldehyde at 420 ^{o}C with 55% methanol conversion.

3.4 Conclusion

The oxidation state of an oxide catalyst is the main factor in the oxidation reaction of methanol. Where the low oxidation state (4+ and lower) of the catalyst results in less terminal oxygen, this is important in keeping the surface of these catalysts more stable, which leads to CO_2 formation. Moreover, even the stability of the surface leads to keeping the methoxy group more relaxed than being oxidised to CO. This gives more time for methoxy to convert to

formaldehyde. However, 6+ oxidation are the most selective to dimethyl ether and formaldehyde, whereas, 5+ catalysts have more selectivity to CO than 6+ catalyst. The formation of dimethyl ether is determined by Lewis acid properties of the used catalyst. However, the more selective catalysts to formaldehyde have lower activity in converting methanol. Here the tungsten oxide catalyst is the most selective to formaldehyde.

3.5 References

[1] Kiennemann, A., Soares, A. P. V., Portela, M. F.(2004) *Methanol selective oxidation to formaldehyde over iron-molybdate catalysts*. Taylor & Francis. 47, 125-174.

[2] Bowker, M., Holroyd, R., House, M., Bracey, R., Bamroongowndee, C., Carley A. and Shannon M. (2008). *The Selective Oxidation of Methanol on Iron Molybdate Catalysts*. Springer science, 48, 158-165.

[3] Michael Bowker, Albert F. Carley, Matthew House. (2008). *Contrasting the Behaviour of MoO3 and MoO2 for the Oxidation of Methanol*. Catal Lett. 120, 34–39.

[4] House, M.P., Shannon, M.D. and Bowker, M.(2008). *Surface Segregation in Iron Molybdate Catalysts*. Springer science,122, 210-213.

[5] Bowker, M., Holroyd, R., Elliott, A., Morrall, P., Alouche, A., Entwistle, C. and Toerncrona, A.(2002). *The selective oxidation of methanol to formaldehyde on iron molybdate catalysts and on component oxides*. Plenum Publishing Corporation,83, 3-4.

[6] Bowker, M., Carley, A. and House, M.(2007). *Selective oxidation of methanol on iron molybdate catalysts and the effects of surface reduction*. Journal of catalysis, 252, 88-96.

[7] Alan S. T., Gail R. W., Esther S. T. (2007). *Vanadium: chemistry, biochemistry, pharmacology and practical applications*. CRC Press: USA.

[8] J. M. Tatibouet. (1997). *Methanol oxidation as a catalytic surface probe*. Applied catalysis A: 148, 213-252.

[9]Taejin Kim, Israel Wachs. (2008). *CH_3OH oxidation over well-defined supported V_2O_5/Al_2O_3 catalysts: influence of vanadium oxide loading and surface vanadium- oxygen functionalities*. Journal of catalysis: 255, 197-205.

[10] Laura E. B., Jih-Mirn J., Laura C., Andrew M. H., Israel E. Wachs. (2003). *Quantitative determination of the number of surface active sites and the turnover frequency for methanol oxidation over bulk metal vanadates*. Catalysis today: 78, 257-268.

[11]Mariano M., Robert H., Staffan H., Arne A. (2011). *Oxidation of methanol to formaldehyde on cation vacant Fe-V-Mo oxide*. Applied catalysis A: 408, 63-72.

[12]A. V. Salker, R. K. KunKalekar. (2009). *Palladium doped manganese dioxide catalyst for low temperature carbon monoxide oxidation*. Catalysis communication: 10, 1776-1780.

[13] A. V. Salker, R. K. KunKalekar. (2010). *Low temperature carbon monoxide oxidation over nanosized silver doped manganese dioxide catalysts*. Catalysis communication: 12, 193-196.

[14] Xiaobo Fu, Jiyun Feng, Huan Wang, Ka Ming Ng. (2009). *Manganese oxide hollow structure with different phases: synthesis, characterization and catalytic application*. Catalysis communication: 10, 1844-1848.
[15] Ren T., Yong Yuan Z., Hu W., Zou X. (2008). *Single crystal manganese oxide hexagonal plates with regulated mesoporous structures*. Microporous and mesoporous materials: 112, 467-473.
[16] C. Li, B. Jiang, W. Fanchiang, Y. Lin. (2011). *The effect of Pd content in $LaMnO_3$ for methanol partial oxidation*. Catalysis communications: 16, 165-169.
[17] Chia-liang Li, Yu-chuan Lin. (2011). *Methanol partial oxidation over palladium, platinum and rhodium integrated $LaMnO_3$ perovskites*. Applied catalysis B: Environmental: 107, 284-293.
[18] H. Y. Chen, T. Lin, K.L. Tan, T. Li. (1998). *Comparative studies of manganese-doped copper-based catalysts: the promoter effect of Mn on methanol synthesis*. Applied surface science: 126, 323-331.
[19]V.A. de la Pena O'Shea, M.C. Alvarez-Galvan, J.L.G. Fierro, P.L. Arias. (2005). *Influence of feed composition on the activity of Mn and $PdMn/Al_2O_3$ catalyst for combustion of formaldehyde/methanol*. Applied catalysis B: Environment: 57, 191-199.
[20]S. C. Petitto, E. M. Marsh, G. A. Carson, M. A. Langell. (2008). *Cobalt oxide surface chemistry: the interaction of $CoO(100)$, $Co_3O_4(110)$ and $Co_3O_4(111)$ with oxygen and water*. Journal of molecular catalysis: 281, 49-58.
[21]S. Zafeiratos, T. Dintzer, D. Teschner, R. Blume, M. Havecker, A. Knop-Gericke, R. Schlogl. (2010). *Methanol oxidation over model cobalt catalysts: infulnce of the cobalt oxidation state on the reactivity*. Journal of catalysis: 269, 309-317.
[22]L. Li, Z.H. Zhu, S.B. Wang, X.D. Yao, Z.F. Yan. (2009). *Chromium oxide catalysts for CO_x free hydrogen generation via catalytic ammonia decomposition*. Journal of molecular catalysis A: Chemical: 304, 71-76.
[23]W.A.A Priyantha, G. D. Waddill. (2005). *Structure of chromium oxide ultrathin films on Ag(111)*. Surface science: 578, 149-161.
[18]K. IVanov, S. Krustev, P. Litcheva. (1998). *Oxidation of methanol on sodium modified chromium – molybdenum catalysts*. Journal of alloys and compounds: 279, 132-135.
[24]Du Soung Kim, Israel E. Wachs. (1993). *Surface chemistry of supported chromium oxide catalysts*. Journal of catalysis: 142, 166-171.
[25]J. M. Jehng, H. Hu, X. Gao, I. E. Wachs. (1996). *The dynamic states of silica-supported metal oxide catalysts during methanol oxidation*. Catalysis today: 28, 335-350.
[26]O. Yu. Khyzhum. (2000). *XPS, XES and XAS studies of the electronic structure of tungsten oxides*. Journal of alloys and Compounds: 305, 1-6.
[27]M. M. Ostromecki, L. J. Burcham, I. E. Wachs. (1998). *The influence of metal oxide additives on the molecular structures of surface tungsten oxide species on alumina II. In situ conditions.* Journal of molecular catalysis A: chemical: 132, 59-71.
[28]T. Onfroy, V. Lebarbier, G. Clet, M. Houalla. (2010). *Quantitative relationship between the nature of surface species and the catalytic activity of tungsten oxides supported in crystallized titania*. Journal of molecular catalysis A: chemical: 318, 1-7.
[29]K. Ivanov, I Mitov, S. Krustev. (2000). *Selectivity oxidation of methanol on Fe-Mo-W catalysts*. Journal of alloys and compounds: 309, 57-60.
[30]J. Okal, W. Tylus, L. Kepinski. (2004) *XPS study of oxidation of rhenium*

metal on Υ-Al_2O_3 support. Journal of catalysis: 225, 498-509.
[31]S. Ling, D. Mei, M. Gutowski. (2011). *Reactivity of hydrogen and methanol on (001) surface of WO_3, ReO_3, WO_3/ReO_3 and ReO_3/WO_3*. Catalysis today:165, 41-48.
[32]O. Nikonova, M. Capron, G. Fang, J. Faye, A. Mamede, L. Jalowiecki-Duhamel, F. Dumeignil, G. Seisenbaeva. (2011). *Novel approach to rhenium oxide Catalysts for selective oxidation of methanol to DMM*. Catalysis today: 279, 310-318.
[33]X. Secordel, E. Berrir, M. Capron, S. Gristol, J. Paul, M. Fournier, E. Payen. (2010). *TiO_2-support rhenium oxide catalysts for methanol oxidation, effect of support texture on the structure and reactivity evidenced by operando Raman study*. Catalysis today: 155, 177-183.
[34] I.E. Wachs, J.M. Jehng, G. Deo, H. Hu, N. Arora. (1996). *Redox properties of niobium oxide catalysts*. Catalysis today: 28, 199-205.
[35] P. Chang, H. Liu. (1995). *Structure of tantalum pentoxide thin films formed by reactive sputtering of Ta metal*. Thin solid films: 258, 56-63.
[36] J. Harvey, H. Wilman. (1961). *The Crystallization of thin amorphous tantalum oxide films heated in air or vacuo, and the structure of crystalline oxide*. Acta Oryst:14, 1278.
[37] T. Ushikubo. (2000).*Recent topics of research and development of catalysis by niobium and tantlum oxides.* Catalysis today:57, 331-338.
[38]Y. Li, J. Church, A. Woodhead.(2012). *Infrared and Raman spectroscopic studies on iron oxide magnetic nano-particles and their surface modifications*. Journal of magnetism and magnetic materials: 324, 1543-1550.
[39]G. Schimanke, M. Marin. (2000). *In situ XRD study of the phase transition of nanocrystalline maghemite (γ-Fe_2O_3) to hematite (α-Fe_2O_3)*. Solid state ionics: 136-137, 1235-1240.
[40]P. Delporte, F. Meunier, C. Pham-Huu, P. Vennnegutes, M. Ledoux, J. Guille. (1995). *Physical characterization of molybdenum oxycarbide catalyst; TEM, XRD and XPS*. Catalysis today: 23, 251-267.
[41]S. Lee, H. Cheong, M. Seong, P. Liu, C. Tracy, A. Mascarenhas, R. Pitts, S. Deb. (2003). *Raman spectroscopic studies of amorphous vanadium oxide thin films*. Solid state ionics: 165, 111-116.
[42]E. Cazzanelli, G. Mariotto, S. Passerini, W. Smyrl, A. Gorenstein. (1999). *Raman and XPS characterization of vanadium oxide thin films deposited by reactive RF sputtering*. Solar energy materials & solar cells: 56, 249-258.
[43]M. Occhiuzzi, D. Cordischi, R. Dragone. (2005). *Reactivity of some vanadium oxides: An EPR and XRD study*. Journal of solid state chemistry: 178, 1551-1558.
[44]B. Barbero, L. Cadus, L. Hilaire. (2003). *XPS studies for vanadium pentoxide along the catalytic bed: oxidative dehydrogenation of propane*. Applied catalysis A: General: 246, 237-242.
[45]M. Ferrandon, J. Carno, S. Jaras, E. Bjornbom. (1999). *Total oxidation catalysts based on manganese or copper oxides and platinum or palladium I: Characterization*. Applied catalysis A: General: 180,141-151.
[46]C. Julien, M. Massot, R. Baddour-Hadjean, S. Franger, S. Bach, J. Pereira-Ramos. (2003). *Raman spectra of birnessite manganese dioxid*e. Solid state ionics: 159, 345-356.
[47]F. Lima, M. Calegaro, E. Ticianelli. (2007). *Electrocatalytic activity of manganese oxides prepared by thermal decomposition for oxygen reduction*. Electrochimia Acta: 52, 3732-3738.

[48]D. Stanoi, G. Socol, C. Grigorescu, F. Guinneton, O. Monnereau, L. Tortet, T. Zhang, I.N. Mihailescu. (2005). *Chromium oxides thin films prepared and coated in situ with gold by pulsed laser deposition*. Materials science and engineering B: 118, 74-78.
[49]A.A. Moconnell, J.S. Anderson, C.N. Rao. (1976). *Raman spectra of niobium oxides*. Spectrochimica Acta: 32A, 1067-1076.
[50]T. Onfroy, O. Manoilova, S. Bukallah, D. Hercules, G. Clet, M. Houalla. (2007). *Surface structure and catalytic performance of niobium oxides supported on titania*. Applied catalysis A: General: 316, 184-190.
[51]M. Paulis, M. Martin, D.B. Soria, A. Diaz, J.A. Odriozola, M. Montes. (1999). *Preparation and characterization of niobium oxide for the catalytic aldol condensation of acetone*. Applied catalysis A: General: 180, 411-420.
[52]P.S. Dobal, R.S. Katiyar, Y. Jiang, R. Guo, A.S. Bhalla. (2001). *Structural modification in titania-doped, tantalum pentoxide crystals: a Raman scattering study*. International Journal of inorganic materials: 3, 135-142.
[53]Y. X. Leng, J. Y. Chen, P. Yang, H. Sun, J. Wang, N. Huang. (2006). *The biocompatibility, of tantalum and tantalum oxide films synthesized by pulse metal vacuum arc source deposition*. Nuclear instruments and methods in physics research B: 242, 30-32.
[54] L. Zhou, Q. Ren, X. Zhou, J. Tang, Z. Chen, C. Yu. (2008).*Comprehensive understanding on the formation of highly ordered mesoporous tungsten oxides by X-ray diffraction and Raman spectroscopy*. Microporous and Mesoporous Materials: 109, 248–257.
[55] A. K. Chawla, S. Singhal, H. O. Gupta, R. Chandra. (2008). *Effect of sputtering gas on structural and optical properties of nanocrystalline tungsten oxide films*. Thin Solid Films: 517, 1042–1046.
[56] S. Yamamoto, K. Takano, A. Inouye, M. Yoshikawa. (2007). *Effects of composition and structure on gasochromic coloration of tungsten oxide films investigated with XRD and RBS*. Nuclear Instruments and methods in physics research B: 262, 29–32.
[57] X. Secordel, E. Berrier, M. Capron, S. Cristol, Jean-Franc¸Ois Paul, M. Fournier, E. Payen. (2010). *TiO2-supported rhenium oxide catalysts for methanol oxidation: Effect of support texture on the structure and reactivity evidenced by an operando Raman study*. Catalysis today: 155, 177–183.
[58] J. P. Bravo-Vasquez, R. H. Hill. (2008). *Solid-state photochemistry of dirhenium carboxylates and the deposition of rhenium oxide thin films*. Journal of photochemistry and photobiology A: chemistry: 196,1–9.
[59] C. Tang, C. Wang, S. Chien. (2008). *Characterization of cobalt oxides studied by FT-IR, Raman, TPR and TG MS*. Thermochimica Acta: 473, 68–73.
[60] C. Wang, R. J. Willeyy. (2001).*Mechanistic Aspects of Methanol Partial Oxidation over Supported Iron Oxide Aerogels*. Journal of Catalysis: 202, 211–219.
[61] Z. Wu, M. Li, D. R. Mullins, S. H. Overbury. (2012). *Probing the Surface Sites of CeO2 Nanocrystals with Well-Defined Surface Planes via Methanol Adsorption and Desorption*. ACS Catal. 2, 2224-2234.
[62]J.R.B. Gomes, J.A.N.F. Gomes, F. Illas. (1999). *Methoxy radical reaction to formaldehyde on clean and hydroxy radical-covered copper (111) surfaces: a density functional theory study*. Surface Science: 443,165–176.
[63] J.P. Camplin, E.M. McCash. (1996). *A RAIRS study of methoxy and ethoxy on oxidised Cu(100)*. Surface science: 360, 229-241.

[64] L.E. Briand, A. M. Hirt, I. E. Wachs. (2001). *Quantitative Determination of the Number of Surface Active Sites and the Turnover Frequencies for Methanol Oxidation over Metal Oxide Catalysts: Application to Bulk Metal Molybdates and Pure Metal Oxide Catalysts*. Journal of Catalysis: 202, 268–278.
[65] W. Wang, A. Buchholz, A. Arnold, M. Xu, M. Hunger. (2003).*Effect of surface methoxy groups on the 27Al quadrupole parameters of framework aluminum atoms in calcined zeolite H–Y*. Chemical Physics Letters: 370, 88–93
[66] S.L. Silva, T.M. Pham, A.A. Patel, S. Haq, F.M. Leibsle. (2000).*STM and FTIR studies of methoxy and acetate on Cu(110) surfaces resulting from reactions with methyl acetate and preadsorbed oxygen*. Surface Science: 452, 79–94.
[67] D.A. Duncan, W. Unterberger, D. Kreikemeyer-Lorenzo, D. Woodruff. (2012). *Does methanol produce a stable methoxy species on Ru(0001) at low temperatures?*. Surface Science: 606, 1298–1302.
[68] L. E. Briand, J Jehng, L. Cornaglia, A. M. Hirt, I. E. Wachs. (2003). *Quantitative determination of the number of surface active sites and the turnover frequency for methanol oxidation over bulk metal vanadates*. Catalysis Today: 78, 257–268.
[69] Xiang Wang, Israel. E. Wachs. (2004). *Designing the activity/selectivity of surface acidic, basic and redox active sites in the supported K2O–V2O5/Al2O3 catalytic system*. Catalysis Today: 96, 211–222.

4. The selective oxidation of methanol on chosen complex oxides.

4.1. Introduction

The previous chapter (Chapter 3) was about single oxides, but this chapter concerns the structure and reactivity of mixed cationic oxides. The most interesting single oxides catalysts were selected for use in mixed oxides together with some alternative materials which have been used for selective oxidation catalysis like bismuth molybdate and iron antimony oxide catalysts. In this chapter, methanol was not the only reactant targeted to be oxidized: ethanol and propanol were also oxidized using iron molybdate, which is the commercial catalyst for methanol oxidation. Thus, this study focuses on changing either the iron or the molybdenum component to determine any change in its catalytic behavior.

4.1.1 Catalysts

Most of the studied materials were introduced earlier in Chapter One and Chapter Three, and the rest, that were not introduced, will be reviewed in this part of Chapter Four.. Iron vanadate has been studied by many scientists. Israel Wachs et al. have studied bulk $FeVO_4$ and V_2O_5 supported by α-Fe_2O_3. The first noted point is surface area improvement, iron vanadate $FeVO_4$ has only 4 m^2 g^{-1} of surface area whereas 4% V_2O_5/α-Fe_2O_3 has a surface area of 24 $m^2.g^{-1}$. Both catalysts are covered by vanadium on their surfaces. However, the bulk iron vanadate has more VO_x units, as $O=VO_3$ unit in its surface, whereas the surface of supported V/Fe catalyst has more bridging V-O-V and V-O-Fe. However, iron with a monolayer of vanadium catalyst behaves similarly to the bulk iron vanadate catalyst in terms of reacting with methanol. Both catalysts react with methanol via vanadium, and iron is less effective to bond with methanol; bulk iron vanadate is 83% selective to formaldehyde and 17% selective to DMM, whereas the supported V/Fe catalyst is 78% selective to formaldehyde, 7% selective to DME and 15 % selective to DMM. Thus, both catalysts are selective to formaldehyde, but the supported vanadium/ iron catalyst has more acidic sites[1].

iron and vanadium were mixed with another metal; in a series of $Fe_{1-x}Al_xVO_4$ materials, where the bulk Fe VO_4 is in the triclinic phase. However, this structure changed after methanol oxidation to spinel type structure, which was caused by a reduction in oxidation state from Fe (III) to Fe (II), and from V (IV) to V (III). However, the new composition that was formed is $Fe_{1.5}V_{1.5}O_4$. The unstable structure was improved by the addition of Al, which gives more stability than the pure iron vanadate. The catalyst was compared with iron molybdate catalyst and bulk iron vanadate catalyst, and the result showed that bulk iron vanadate ($FeVO_4$) is 90% selective to formaldehyde with 95% conversion, whereas the addition of Al in iron vanadate increases the activity and makes no change in selectivity to any products, where the best ratio is $(0 \leq X \leq 1)$[2].

Iron antimonite catalysts are the selective catalyst for partial oxidation reactions. This is the selective catalyst for oxidation of propene to acrolein, and ammoxidation of propane to acrylonitrile, where the activation temperature is 500 ^oC. In propene oxidation, $FeSbO_4$ catalysts were tested in terms of activity and selectivity. The literature reviewed showed that selectivity was controlled by surface oxygen, whereas activity is controlled by bulk oxygen within 1.6 to 2.6 layers. However, as with many studies of catalysts, the ratios were modified to improve selectivity to acrolein. Bowker et al. suggest that the rich skin of Sb is increasing the selectivity. However, by 420 ^oC the skin was reduced to metal, which drops the activity. Furthermore, the reason behind increasing the antimony ratio to more than the stoichiometric ratio is to form more Sb=O on the surface, and that terminal oxygen is responsible for acrolein selectivity. A study carried by E. Steen et al. showed that stoichiometry $FeSbO_4$ was reduced after propene oxidation to show new phases of Sb2O3, Fe_2O_3 and Fe_3O_4, that led to the catalyst deactivation that was in the result, whereby at a temperature between 250 to 350 ^oC the products were acrolein and CO_2, and at a temperature between 500 to 600 ^oC, the catalyst produces only CO_2 as result of that reduction. Thus the increase of Sb ratio is to avoid that catalyst deactivation, where the right ratio is Sb/Fe=1.5, which is the active phase with high selectivity to acrolein beside the same activity as in stoichiometry ratio catalyst[3].

Moreover, propene is ammoxidized to acrylonitrile; the antimony catalyst was $FeSb_2O_4$, which had an additive of a promoter, tellurium (Te). The presence of tellurium increases the selectivity toward acrylonitrile. However, the activity was not much changed with doping of Te. However in the ratio and formula $Fe_{30}Sb_{60}Te_2O_x$ the activity was higher with this ratio. Nevertheless, the preparation method was considered to be a factor in the catalytic activity, where co-precipitation, impregnation and reaction of solid oxides have similar result of activity, which confirms that the preparation method does not change in this catalyst activity[4].

Bismuth molybdate catalysts have also been used for propene oxidation and ammoxidation, and their use has been extended to other alkenes. However, there are three phases of bismuth molybdate catalysts, which are α-$Bi_2Mo_2O_9$, β-$Bi_2Mo_3O_{12}$ and γ-Bi_2MoO_6. The three catalysts were prepared within co-precipitation method and studied for butane oxidation. However, thermal study showed that α-$Bi_2Mo_2O_9$ is unstable when calcined to 420 ^oC and above, when it converts to both β-$Bi_2Mo_3O_{12}$ and γ-Bi_2MoO_6. Therefore it is not efficient for this reaction, which required a temperature of 420 ^oC as the reaction conditions. However, β-$Bi_2Mo_3O_{12}$ is less active and selective to 1,3 butadiene than γ-Bi_2MoO_6, because γ-Bi_2MoO_6 has a higher oxygen mobility than β-$Bi_2Mo_3O_{12}$, where γ-Bi_2MoO_6 catalyst is 82.2% selectivity to 1,3 butadiene with n-butene conversion of 81.8%, while β-$Bi_2Mo_3O_{12}$ catalyst produces 73.2% 1,3 butadiene with conversion of 37.2% by 420 ^oC for 12h[5].

4.1.2 Alcohols oxidation

Alcohol in general reacts through the hydroxyl group in its structure, ethanol can be oxised in a similar way to methanol producing acetaldehyde, but can also be dehydrated to ethylene. n-propanol has also a similar case to ethanol as it converts to propanal, propene, and /or propane. iso-propanol is like n-propanol and can be converted to aldehyde, ketones and alkane, where the products are acetone and propene. Also n-butanol is possible to be converted to aldehyde and ketone. [6].

Furthermore, ethanol oxidation was studied over various supported catalysts. Pt/Al_2O_3 is the selective catalyst to acetic acid due to its highly acidic sites. However, Pt/ZrO_2 catalyst oxidized ethanol to acetaldehyde, whereas, Pt/ CeO_2 is also a selective catalyst to acetaldehyde, then the catalyst became selective CO_2 and methane. However, the reason behind this is that Pt/CeO_2 has a higher exchange capacity of oxygen that leads to lowering the concentration of ethoxy species, which will be converted later to acetaldehyde, whereas Pt/CeO_2 or higher exchange capacity of oxygen favored an intermediate as acetate bonded to the surface, which will decomposes as methane and CO_2. A third support was studied is $Ce_{0.50}Zr_{0.50}O_2$, where $Pt/ Ce_{0.50}Zr_{0.50}O_2$ catalyst has similar result to Pt/CeO_2 catalyst and is not selective to acetaldehyde as Pt/ZrO_2 catalyst, because again it has higher exchange capacity of oxygen than in the case of Pt/ZrO_2 catalyst[7].

iso-propanol oxidized to acetone on a clean surface of nickel catalyst foil using microbach reactor. However, iso-propanol was converted to acetone, carbon monoxide, carbon dioxide, water and hydrogen, where the selectivity to acetone is 79%. Yet, in reaction conditions of 700 K constant temperature, partial pressure of oxygen is 30 torr and initial pressure of alcohol is 30 torr. With the same initial alcohol pressure, and changing oxygen partial pressure to reach 30 torr, the yield of acetone increased up to 91%, whereas in oxygen partial pressure of 15 torr, acetone yield was only 76%. That is strong proof of oxygen pressure dependency and that affected the reaction, but even a temperature above 700K increases the CO_2 production[8]. However, the oxidation of propanol in a complete oxidation is proposed with another application. Where iso-propanol is a volatile organic compound, that pollutant has to be converted before blowing in air, it is fully oxidized to water and CO_2. Gold catalysts with four different supports were studied in this reaction. While the target is to burn 2-propanol with less heat and cost, so, the catalyst with higher activity is more interesting for full oxidation reactions. These catalysts are 1.6% Au/CeO_2, 1.6% Au/Al_2O_3, 1.4% Au/TiO_2 and 1.7% Au/Fe_2O_3, where the activity for these catalysts as 1.6% Au/CeO_2> 1.7% Au/Fe_2O_3 >1.6% Au/Al_2O_3 > 1.4% Au/TiO_2. However, the products were not only the desired CO_2, there were products like acetone and propene. However, they were intermediates before being burned to CO_2 by heat.

In the catalytic activity, 1.6% Au/CeO_2 was the most interesting because it converts iso-propanol to acetone by 100 ^oC[9].

Furthermore, n-propanol was studied in a very important application in fuel cells; it is a hydrogen energy source on 7% Ni/Y_2O_3-ZrO_2 catalyst by oxidative steam reforming, which can be more interesting than the current biomass reactions that are ethanol and methanol, because n-propanol and n-butanol have more density of energy. However, when 773k 100% of n-propanol was converted to H_2 and CO, there are detected amounts of methane and carbon dioxide, but the catalyst was improved by changing ratio of Y_2O_3 to the support, where the first has 2% wt/wt of Y_2O_3 to 41% ZrO_2, the next has 19% Y_2O_3 and the result is more selectivity to H_2[10].

4.2. Results

The oxides used were analyzed and tested in the same way as the single oxides in the previous chapter (Chapter 3). This part of Chapter 4 will illustrate the catalytic behavior of each catalyst and the characterization, to determine any change that occurred during methanol oxidation.

4.2.1. $FeVO_4$ catalysts

$FeVO_4$ catalysts have a surface area of 5 $m^2 g^{-1}$, even for the catalysts that contains addition of vanadium (2V:1Fe) ratio and (3V:1Fe) ratio. Figure 4.1 illustrates the catalytic performance of iron vanadate; the catalyst is selective (95%) to formaldehyde at low methanol conversion (70% and lower). the catalyst is active as it converts 100% of methanol by temperature of 250 ^oC, but the maximum yield of form, aldehyde is only ~ 50%. from the TPD is shown in figure 4.2, showing formaldehyde and large amounts of carbon monoxide, also there is production of small amounts of carbon dioxide.

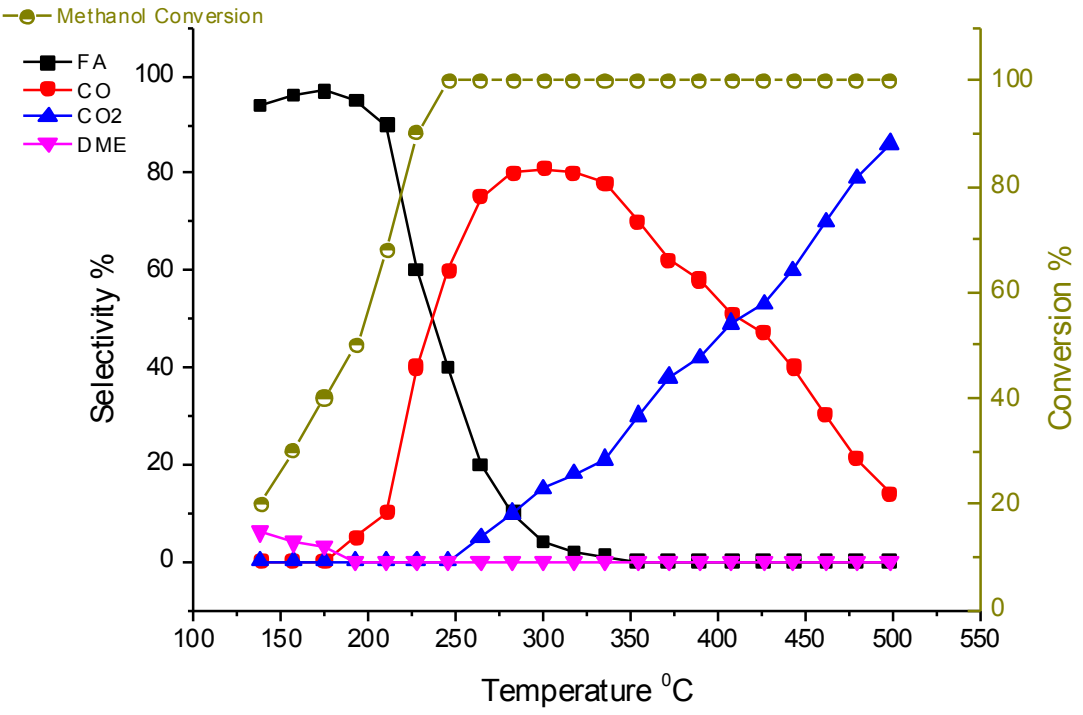

Figure 4.1 Reaction profile result of $FeVO_4$ catalyst

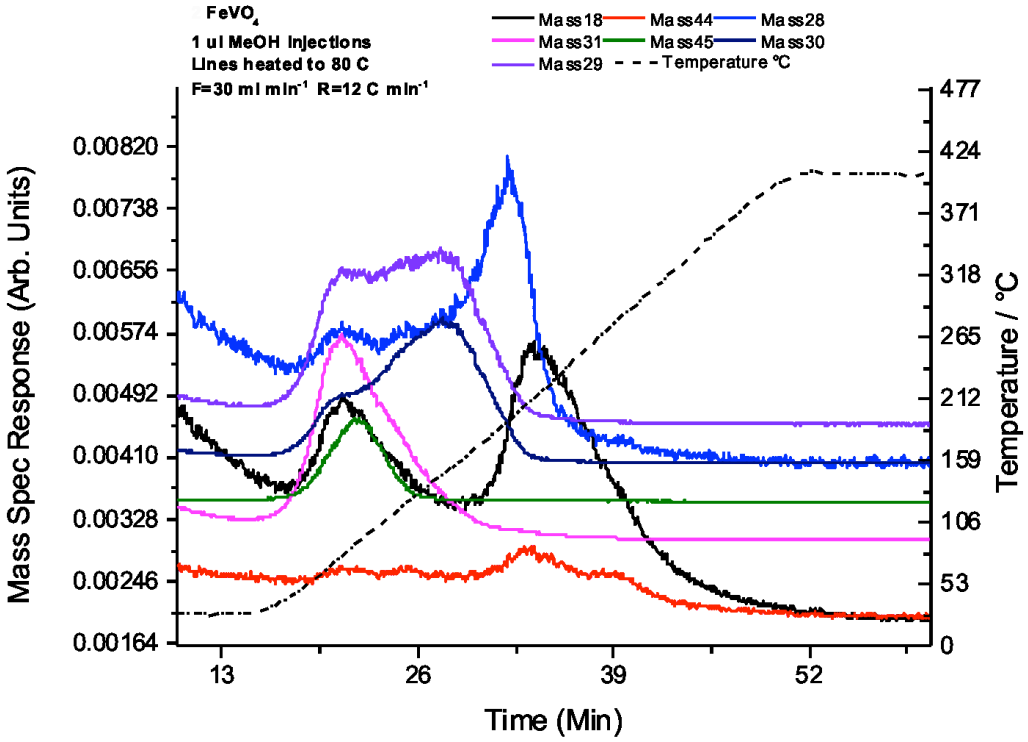

Figure 4.2 TPD result of $FeVO_4$ catalyst

In figure 4.3, the 2V:1Fe ratio catalyst data is shown, and 3V:1Fe in figure 4.4. From figure 4.3, 2 ratio iron vanadate is 100% selective at low methanol conversion and low temperature, where the most interesting point is at 200 ^{o}C, when the catalyst yields 100% formaldehyde, which means that the catalyst is so active by 200 ^{o}C and converts 100% of methanol to only formaldehyde. However, above 200 ^{o}C, carbon monoxide was produced and the selectivity to it increased with increasing temperature, which is the result of further oxidation of methoxy to CO and to CO_2 at even higher temperatyures, However, the greater addition of vanadium to iron vanadium in ratio as 3V to 1Fe, lead to more vanadium oxide behavior. In Chapter 3, vanadium oxide is the selective catalyst to both formaldehyde and carbon monoxide at high temperatures. Figure 4.4, shows that the catalyst has decreased selectivity compared to 2:1. figures 4.5 and 4.6 show the TPD of these two catalysts, ratio 2 (figure 4.5) and ratio 3 in figure 4.6. Both of the catalysts produce formaldehyde and carbon monoxide even without oxygen gas, though the peak of CO in 3 ratio catalyst appeared at 175 ^{o}C, whereas in 2 ratio it appeared at a higher temperature (212 ^{o}C). In other words, the more preferred product would desorb first, and the lower heat in 3 ratio catalyst for CO peak means that CO production is the preferred pathway of methanol oxidation rather than in the case of using 2 ratio iron vanadate.

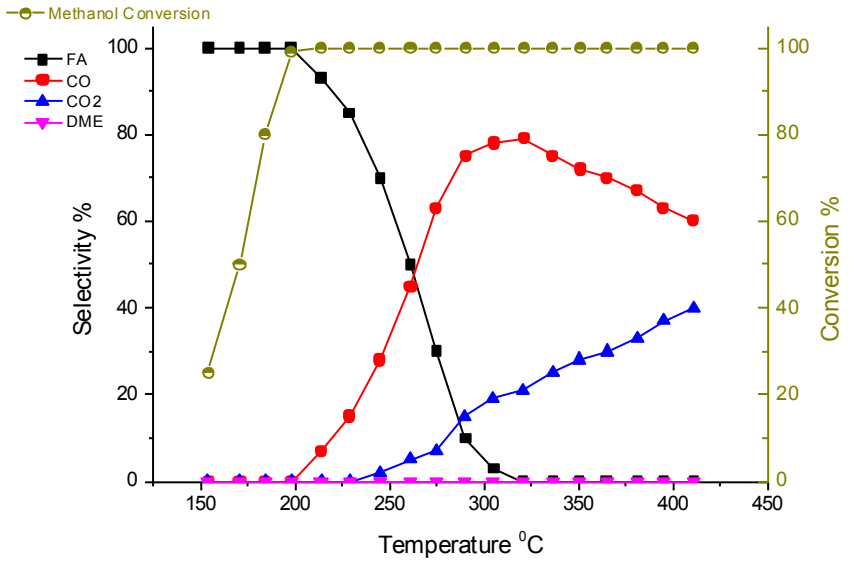

Figure 4.3 Reaction profile result of (ratio-2V)$FeVO_4$ catalyst

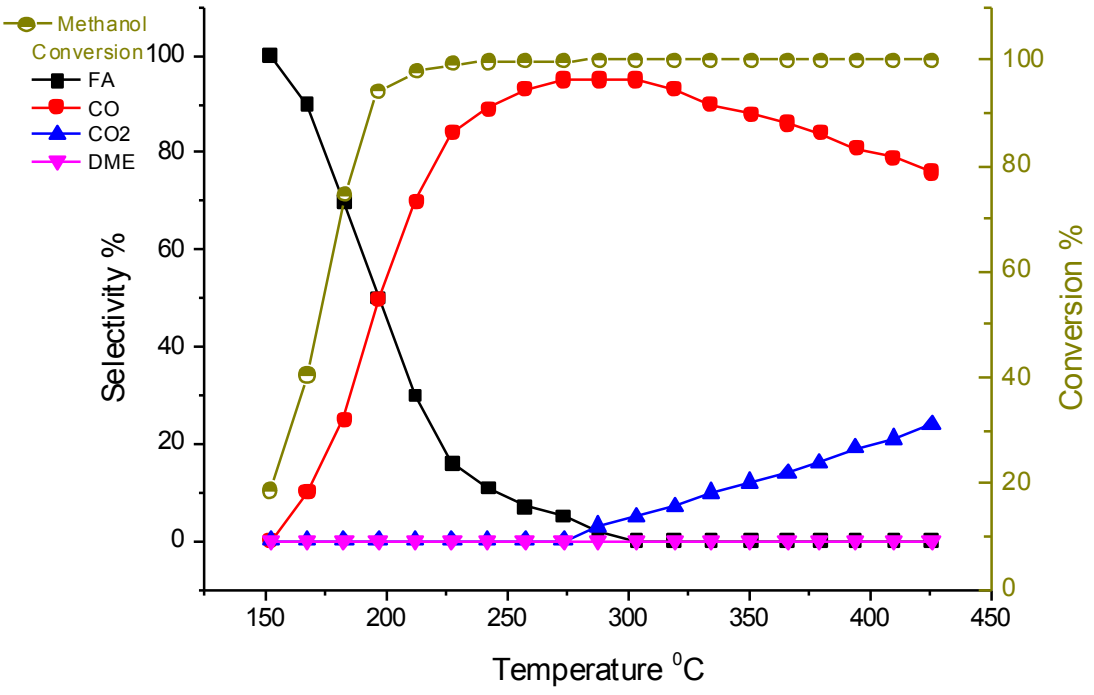

Figure 4.4 Reaction profile result of (ratio-3V) iron vanadate catalyst

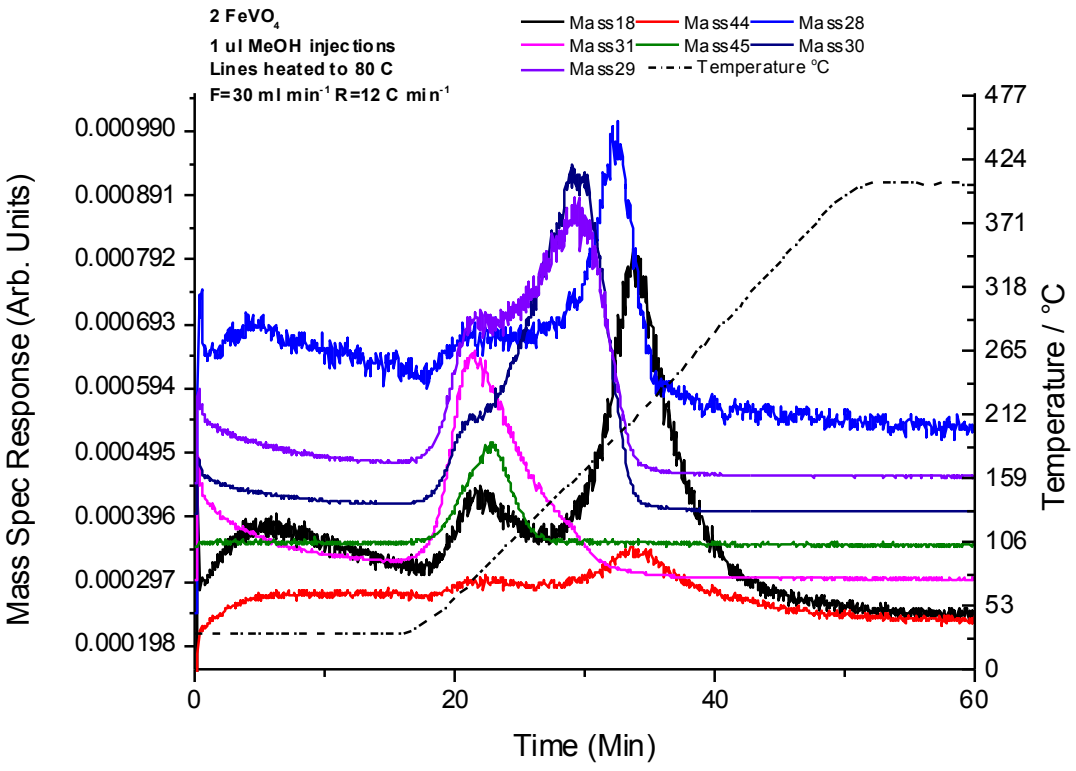

Figure 4.5 TPD result of iron vanadate catalyst (ratio-2V)

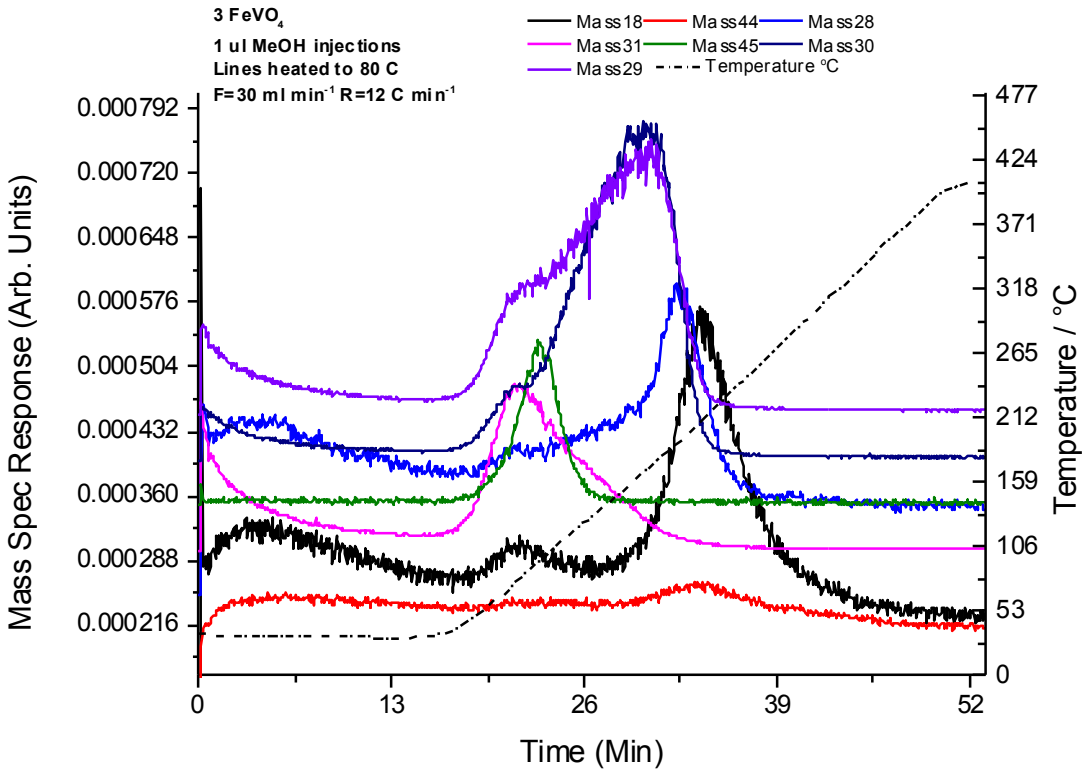

Figure 4.6 TPD result of iron vanadate catalyst (ratio-3V)

Pure $FeVO_4$ has Raman band of 971, 936, 910, 900, 850, 835, 773, 738, 664, 634, 370 and 325 cm^{-1} as in figure 4.7 and was also was compared to the literature [1]. However, the catalyst has changed when used as a methanol oxidation catalyst, where new peaks appeared as 210 and 405 cm^{-1} that related to Fe_2O_3. Also, 275, 289, 460, 530 and 995 cm^{-1} are related to V_2O_5, which in other words means that $FeVO_4$ was reduced to form iron oxide and vanadium pentoxide instead of the pure iron vanadate, where the change is due to loss of lattice oxygen during methanol oxidation, which should be fed by gas oxygen and reoxidize the catalyst. However, the catalyst is not stable in the case when it is not able rexodize its surface by the gaseous oxygen instead of changing its structure.

Figure 4.8, shows the result for the 2:1 ratio iron vanadate that has 280, 300, 405, 479, 525 700 and 995 cm^{-1}.These are related to vanadium pentoxide plus the Raman shifts of $FeVO_4$ but smaller in intensity. However, the peaks of

pure iron vanadate get lower in intensity with more addition of vanadium, as shown in figure 4.9, which is the result of ratio 3:1 iron vanadate, where the intensity of stoichiometric iron vanadate is lowering compared with the result in figure 4.7, and vanadium oxide peaks are clearer with more addition of vanadium. This means the greater addition of vanadium is formed as vanadium pentoxide covering the surface of bulk $FeVO_4$, and the behavior the catalyst is affected by the addition of vanadium as shown earlier. However, even the pure iron vanadate, vanadium is segregated on the surface with full vanadium atoms in the first layer, where iron atoms are in the second layer and more in the deeper layer to the bulk as reported in literature [10], and that is a similar case to iron molybdate catalyst, where molybdenum segregates on the surface of iron molybdate.

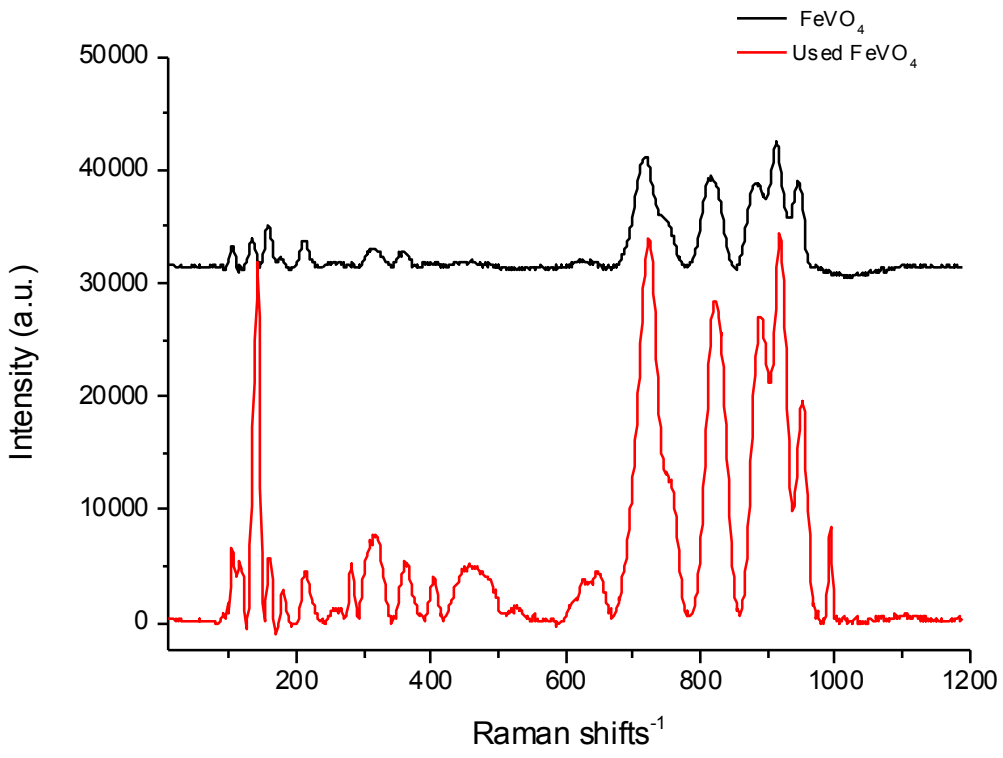

Figure 4.7 Raman result of stoichiometric $FeVO_4$ catalyst

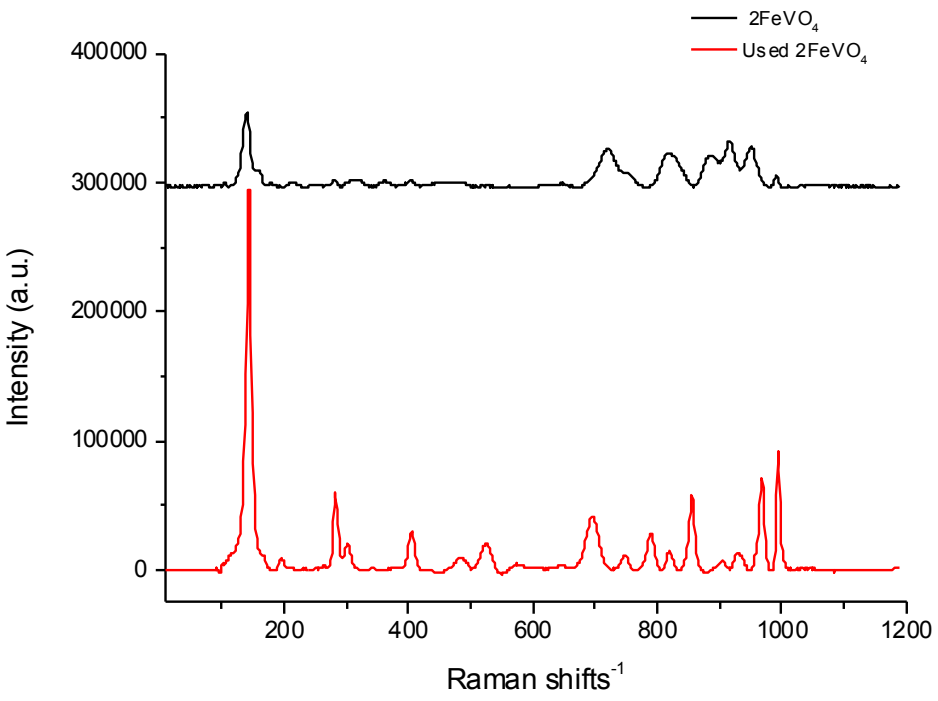

Figure 4.8 Raman result of ratio 2 $FeVO_4$ catalyst

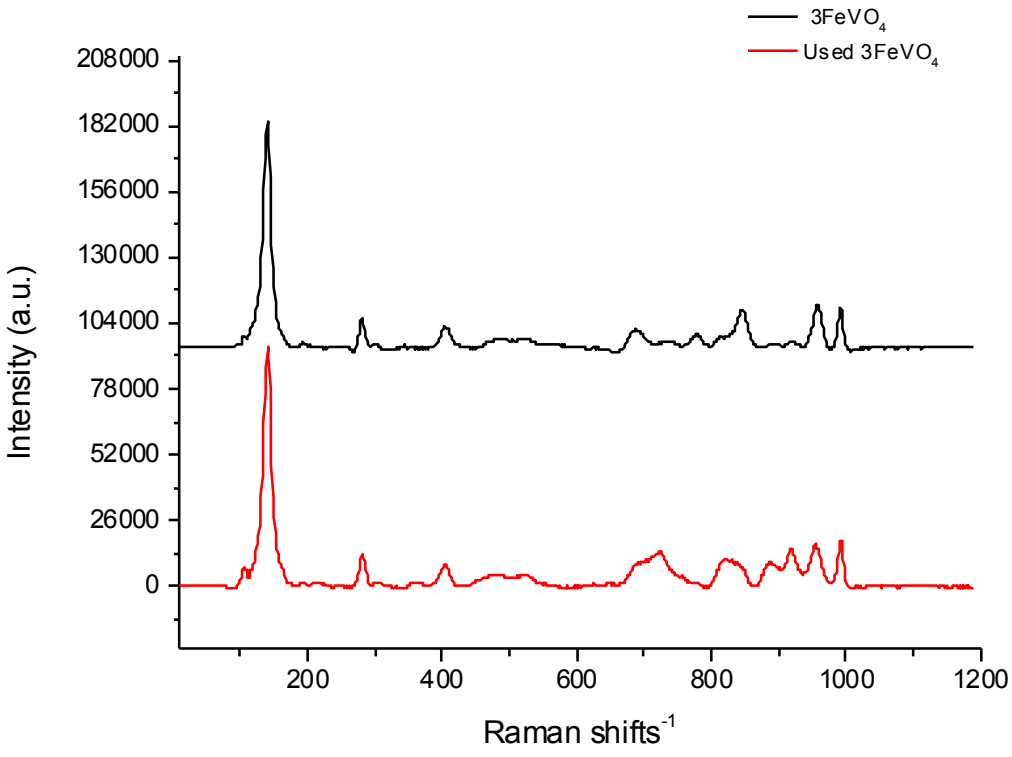

Figure 4.9 Raman result for ratio 3- $FeVO_4$ catalyst

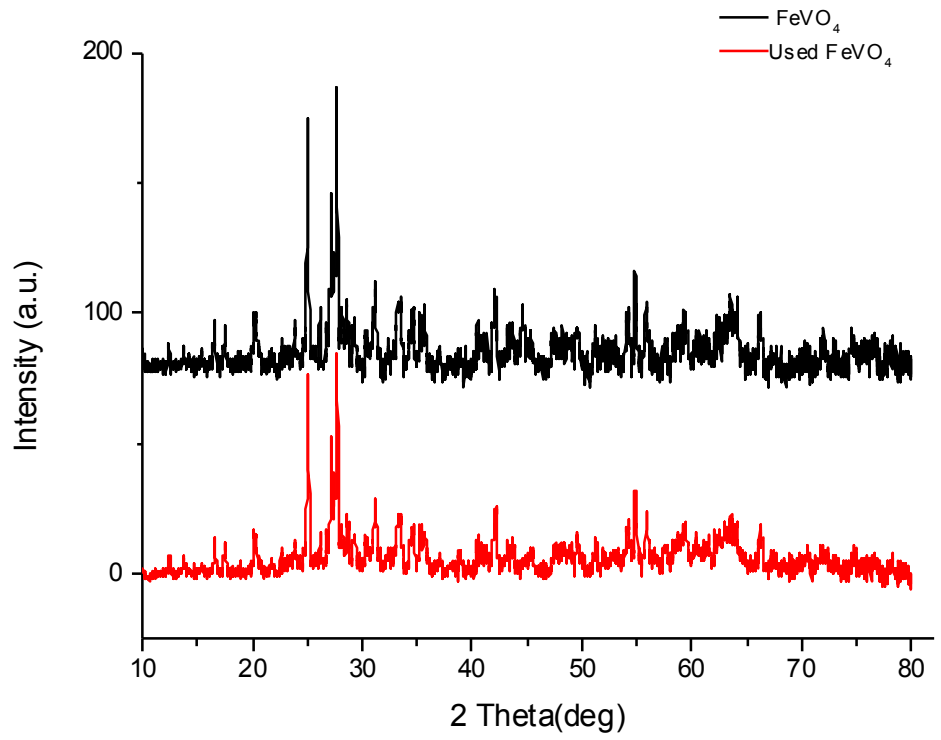

Figure 4.10 XRD result of stoichiometric $FeVO_4$ catalyst

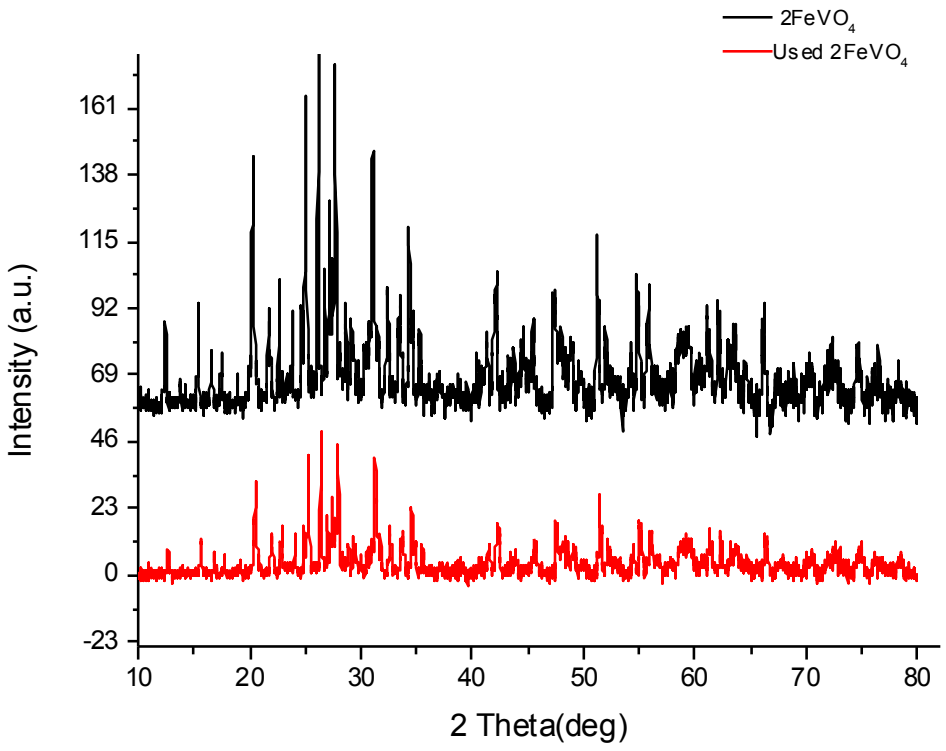

Figure 4.11 XRD result of ratio 2 $FeVO_4$ catalyst

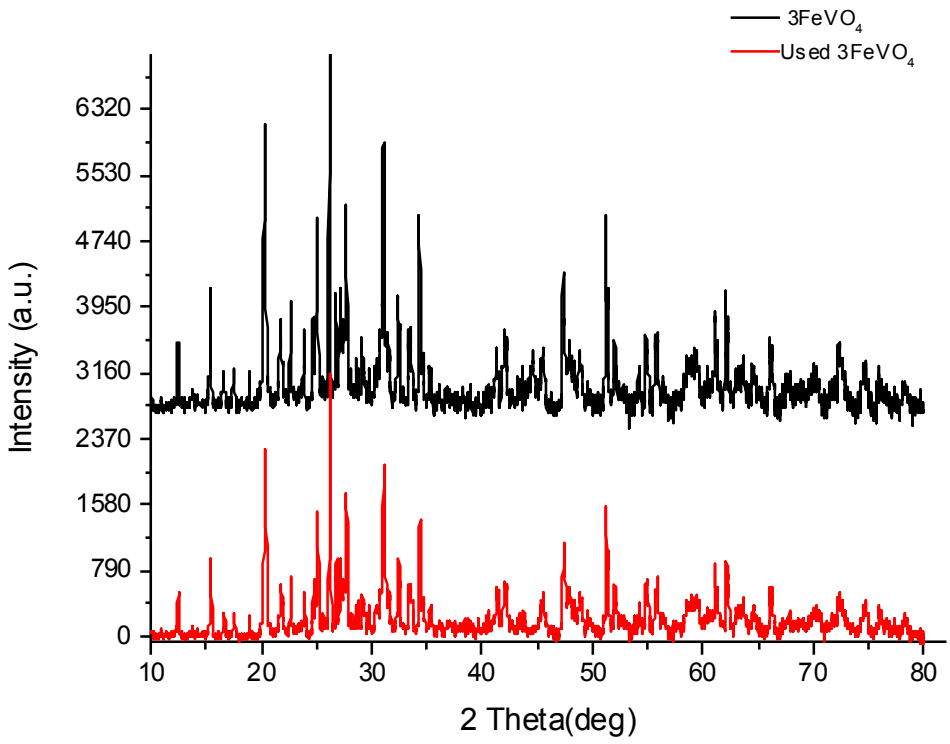

Figure 4.12 XRD result of ratio 3 $FeVO_4$ catalyst

Moreover, the XRD result in figure 4.10 shows that three spectra are related to triclinic $FeVO_4$, which are 25.04°, 27.16° and 27.66° as compared to the literature [11]. Figure 4.12, which is XRD result for ratio 3 iron vanadate, shows a very close result to ratio 2 iron vanadate in figure 4.11, their close result confirms that V_2O_5 is formed on the surface of iron vanadate. Moreover, XPS is a surface analysis technique, where in the case of more vanadium addition can be either segregated on the surface or mixed up into the bulk structure. However, the results below in figures 4.13, 4.14 and 4.15 show that vanadium segregates on the surface, where figure 4.13, which is XPS spectra of stoichiometry iron vanadate, has V 2P 3/2 peak area of 8363.24, and that area is 12931.78 for ratio 2V:1Fe catalyst (figure 4.14) and 16559.87 for ratio 3V:1Fe catalyst (figure 4.15). However, the segregated vanadium oxide behaves like molybdenum oxide iron molybdate catalyst, where in figure 4.15 the peak area was bigger than in figure 4.16 which is XPS result of used ratio 3V:1Fe iron vanadate catalyst, In other words, vanadium oxide evaporates from the surface during methanol oxidation and the surface loses vanadium, which leads to deactivation in a long time of use.

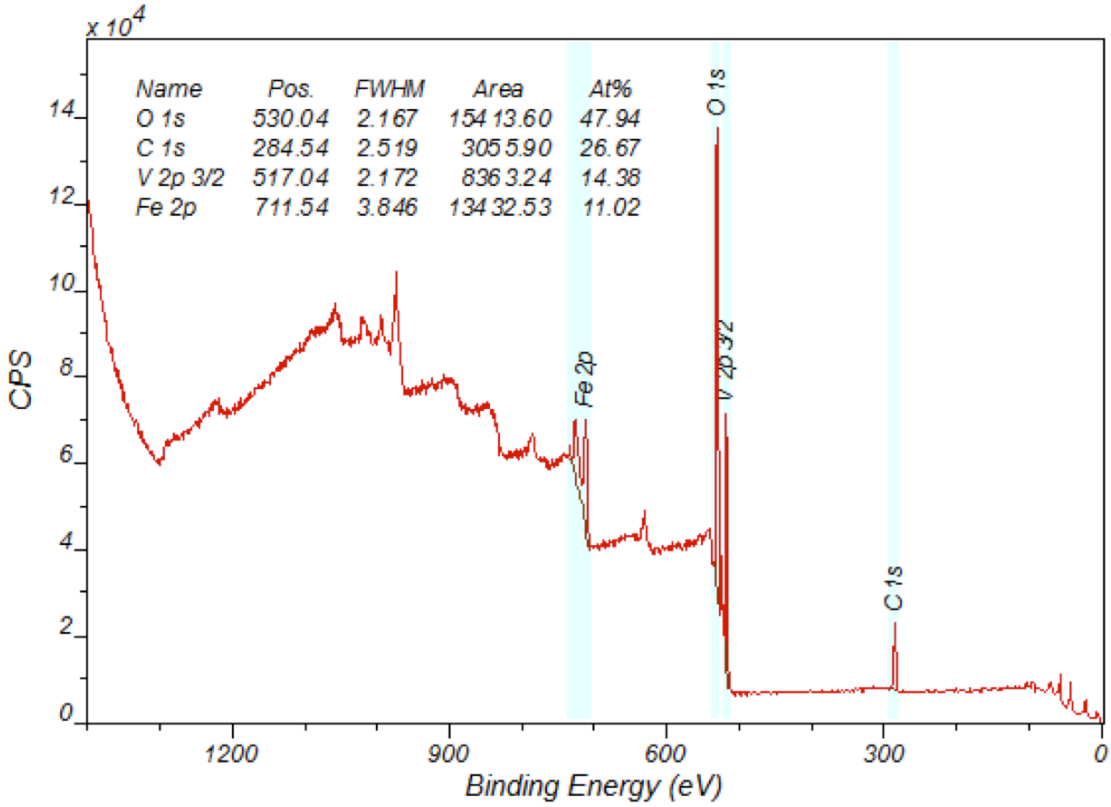

Figure 4.13 XPS spectra of pure iron vanadate catalyst

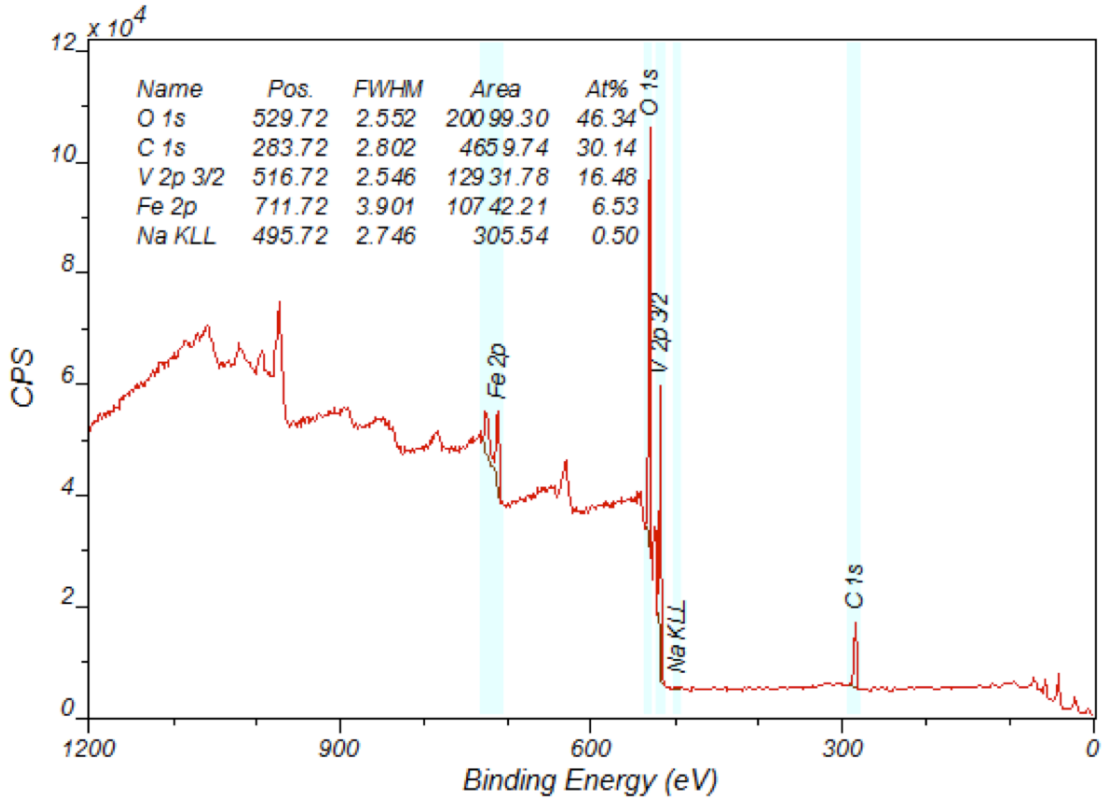

Figure 4.14 XPS spectra of ratio 2V:1Fe iron vanadate catalyst

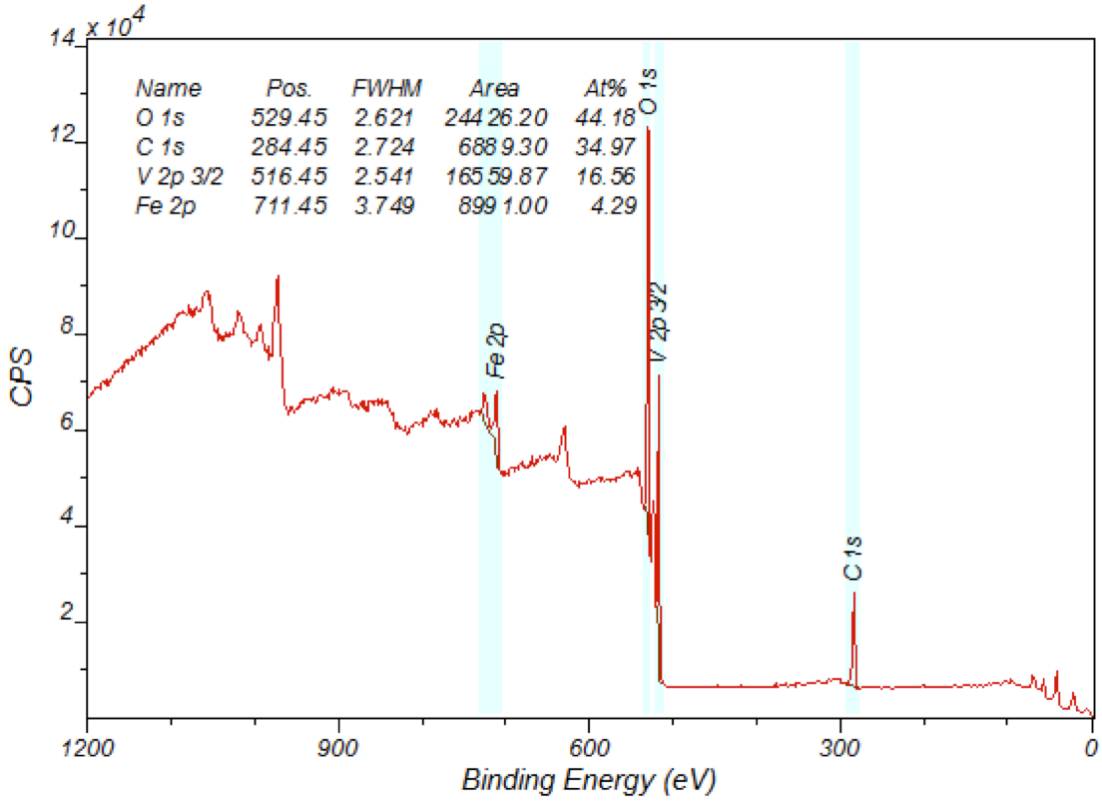

Figure 4.15 XPS spectra of ratio 3V:1Fe iron vanadate catalyst

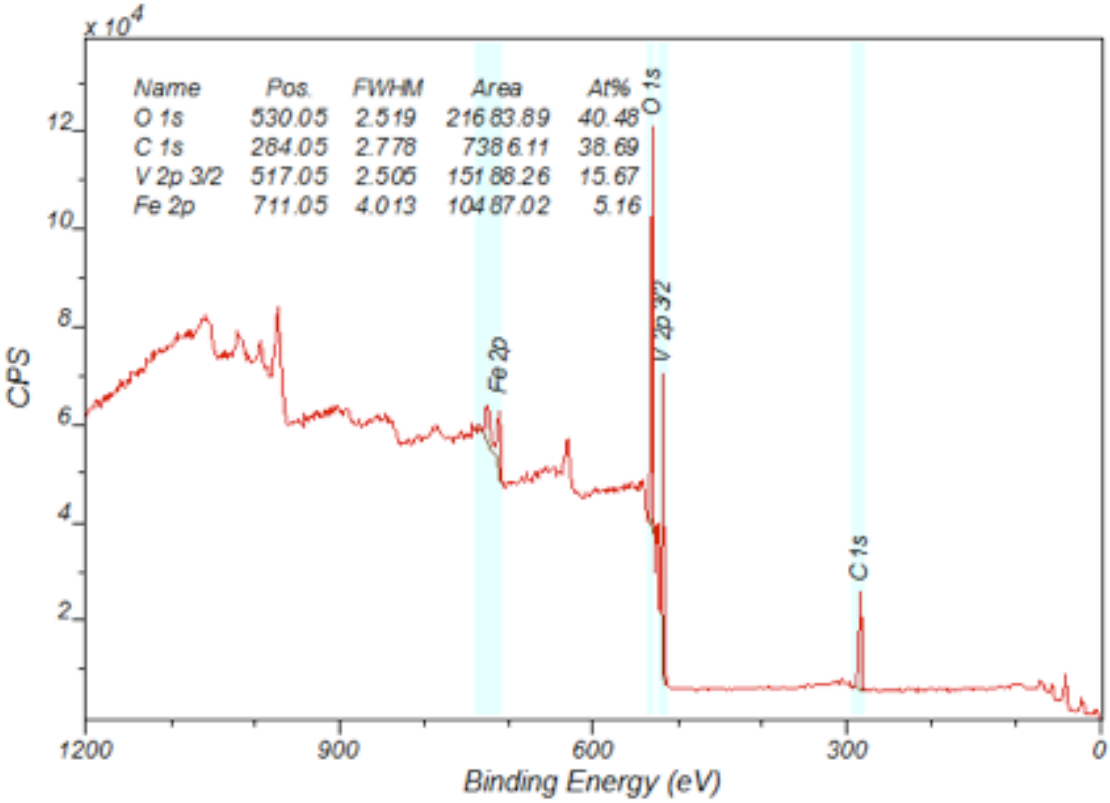

Figure 4.16 XPS spectra of used ratio 3V:1Fe iron vanadate catalyst

4.2.2. $Fe_2(WO_4)_3$ catalysts

Iron tungstate has a surface area of 13 m^2/g. However, another ratio of iron tungstate was tested, with the ratio is W/Fe = 2.2, which will be called 2.2 $Fe_2(WO_4)_3$, and which has a surface area of 6 m^2/g. The two catalysts have been studied as shown below: figure 4.17 (stoichiometric catalyst) and figure 3.18 (ratio 2.2 iron tungstate catalyst) show Raman results for both catalysts, where the Raman shift by 989 cm^{-1} is associated to Fe-O-W bond. The two catalysts have sharp bands by 720 and 800 cm^{-1} that is the same as the pure tungsten oxide, and relate to the WO_6 unit. Figure 4.17 shows the Raman result of stoichiometric iron tungstate for the fresh and used samples, and the catalyst does not show any change after being used for methanol oxidation. However, figure 4.18 shows that there is WO3 in the catalyst as Raman shifts at 320 and 1010 cm^{-1} is associated to tungsten oxide, which is a similar result to iron molybdate catalyst with ratio 2.2. Moreover, XRD spectra of both catalysts show that the two catalysts have different bulk structures. Figure 4.19 is the pure iron tungstate and figure 4.20 is (W/Fe=2.2) iron tungstate. However, the pure iron tungstate has two small peaks by 24^o and 36^o related to Fe_2O_3 being formed as compared to literature [12], and even appears not clear in the ratio W/Fe=2.2 iron tungstate spectra, where it has more peaks that are related to WO_3 in 27^o 23.5^o[13]. However, these peaks lowered in intensity after methanol oxidation that was due to volatilization of tungsten oxide, which is similar behavior to molybdenum oxide in iron molybdate catalyst.

XPS spectra show the composition of these catalyst surfaces. figure 4.21 is for iron tungstate with W (4d) ratio is 11.80%, whereas the peak area in ratio 2.2 iron tungstate is 12.49%, which clearly shows that any addition of tungsten will be segregated on the surface of stoichiometry iron tungstate, because iron ratio in the stoichiometric catalyst is 9.68 %, and 2.2 catalyst is only 8.49, and iron amount is the same in both catalyst when prepared. Moreover, even the bulk tungsten segregated on the surface, as in figure 4.23, which is XPS spectra of used stoichiometric iron tungstate with W (4d) peak area of 12.22% whereas the fresh catalyst is 11.80, because of the reaction temperature that is 500 ^oC in case of methanol oxidation.

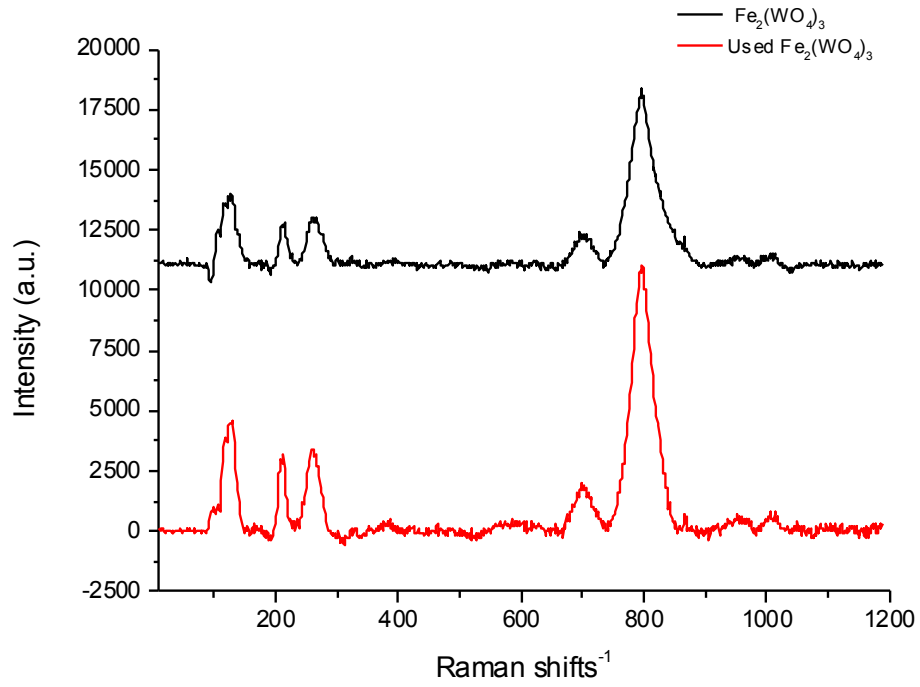

Figure 4.17 Raman result of stoichiometric iron tungstate catalyst

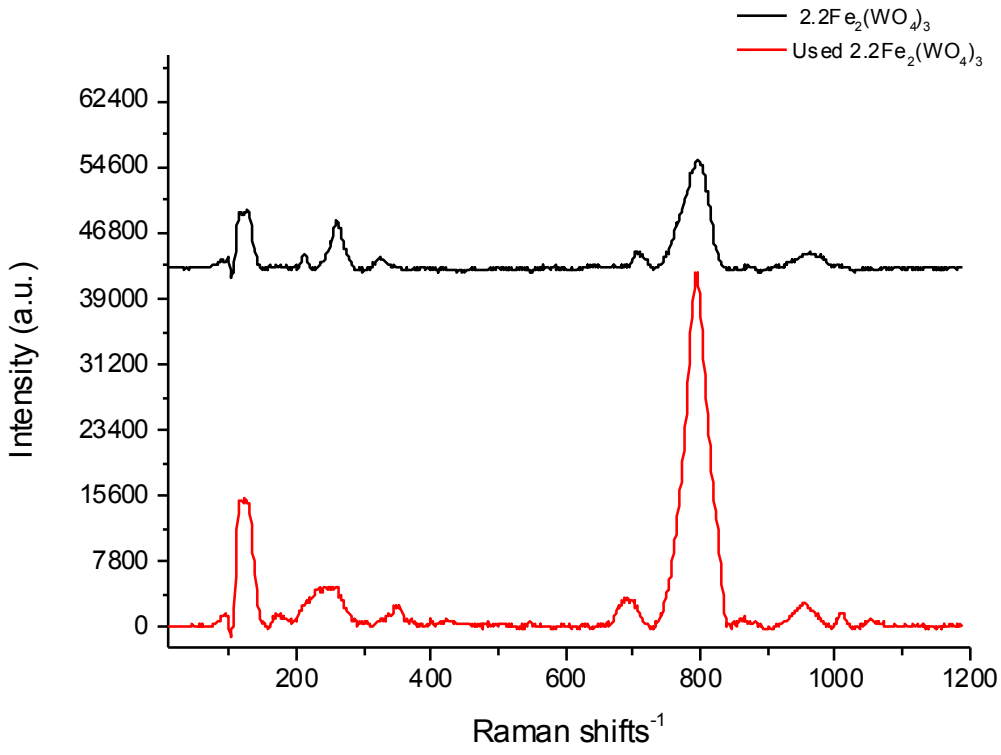

Figure 4.18 Raman result of ratio 2.2 iron tungstate catalyst

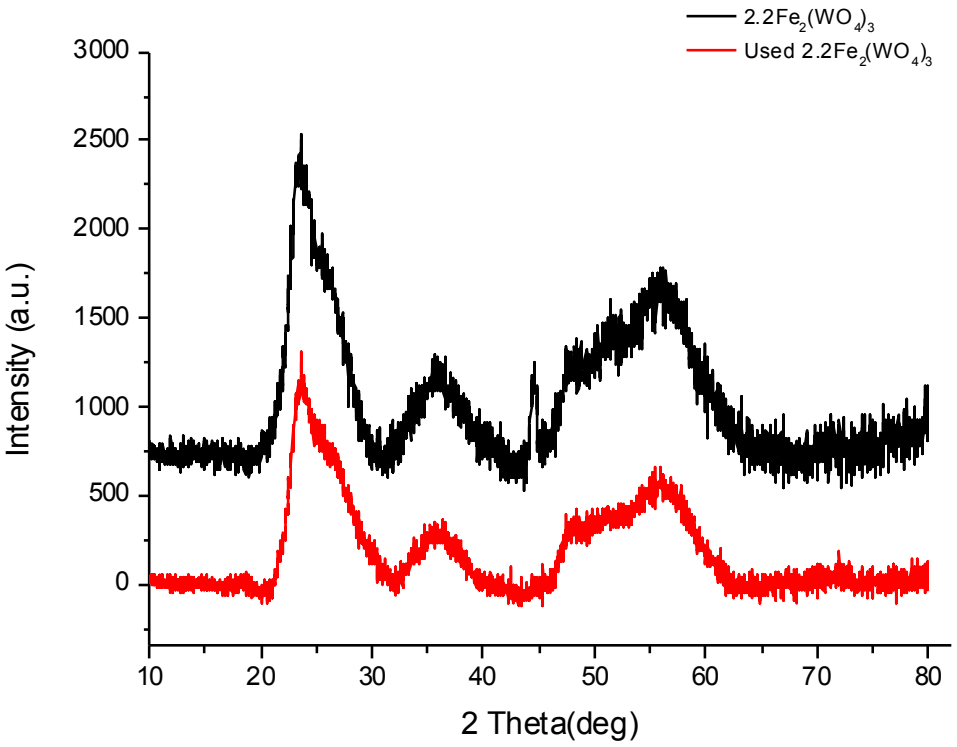

Figure 4.19 XRD result 2.2 $Fe_2(WO_4)_3$ catalyst

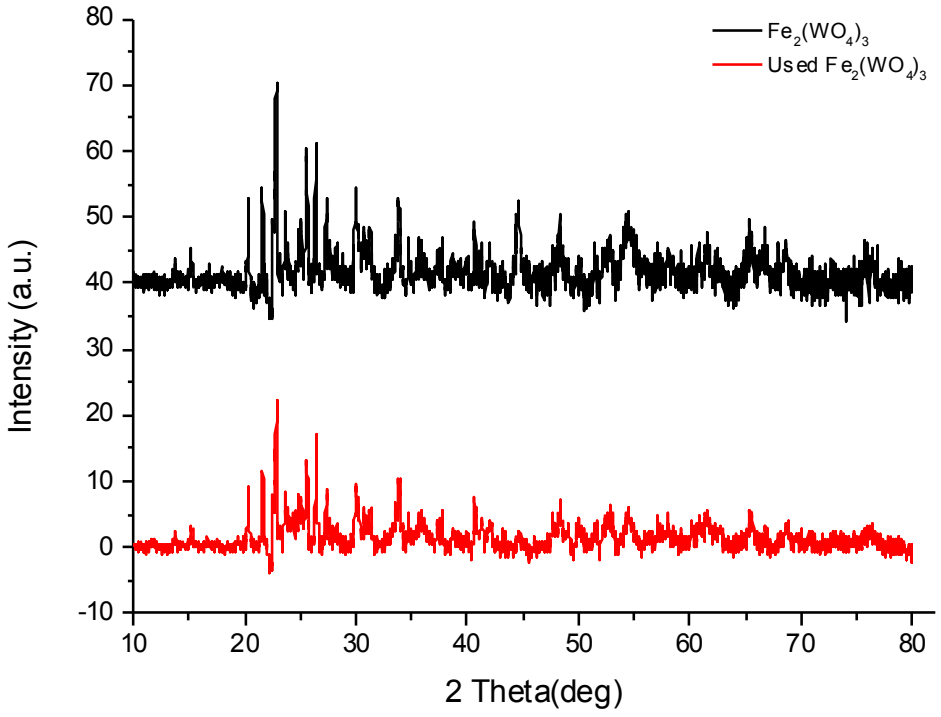

Figure 4.20 XRD result 1.5 $Fe_2(WO_4)_3$ catalyst

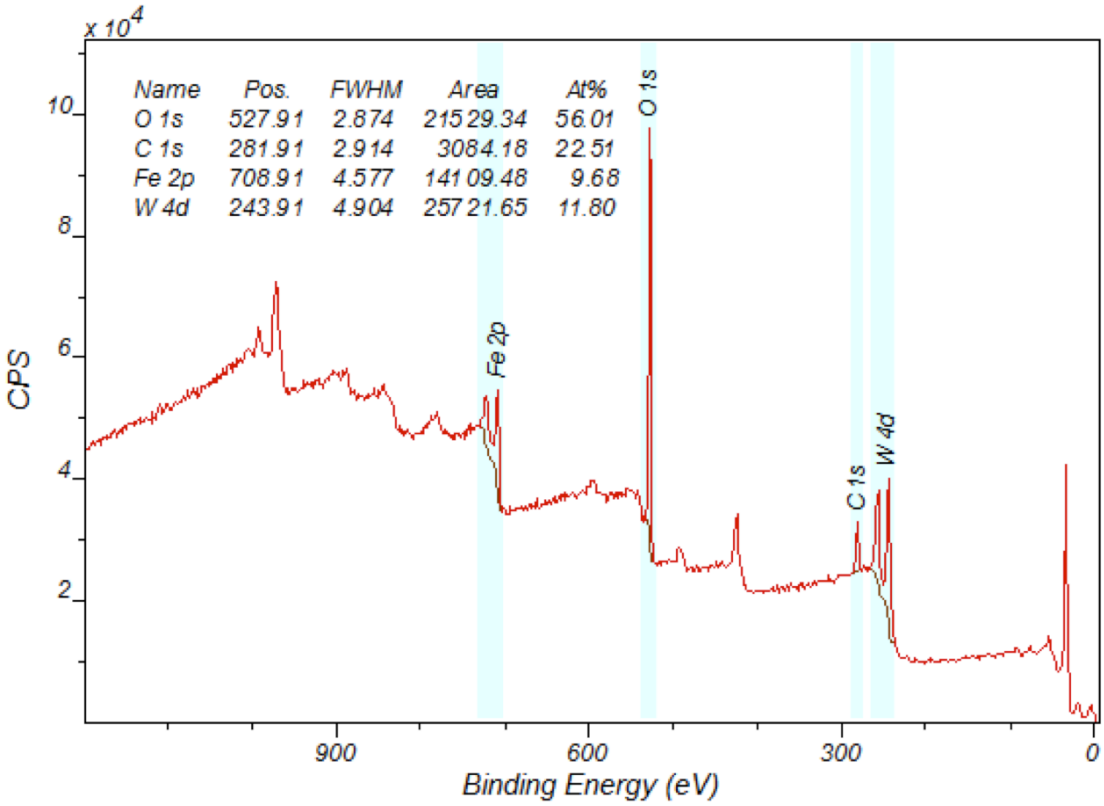

Figure 4.21 XPS spectra for pure iron tungstate catalyst

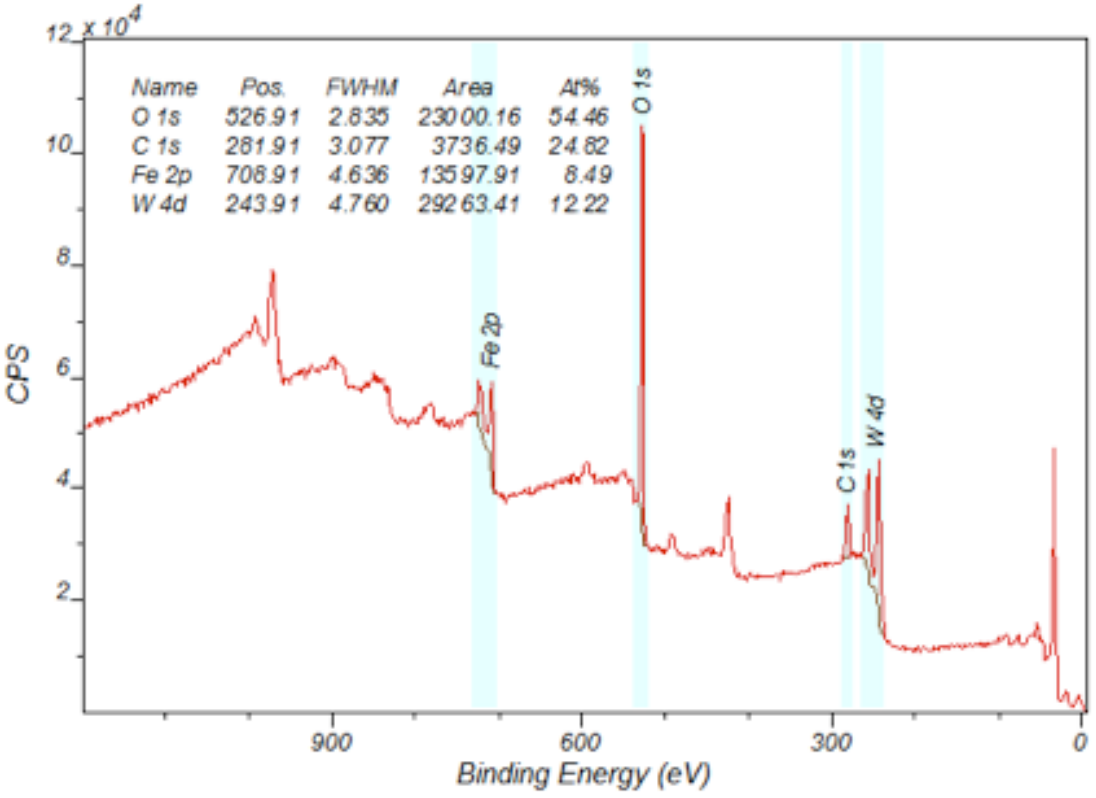

Figure 4.22 XPS spectra for used iron tungstate catalyst

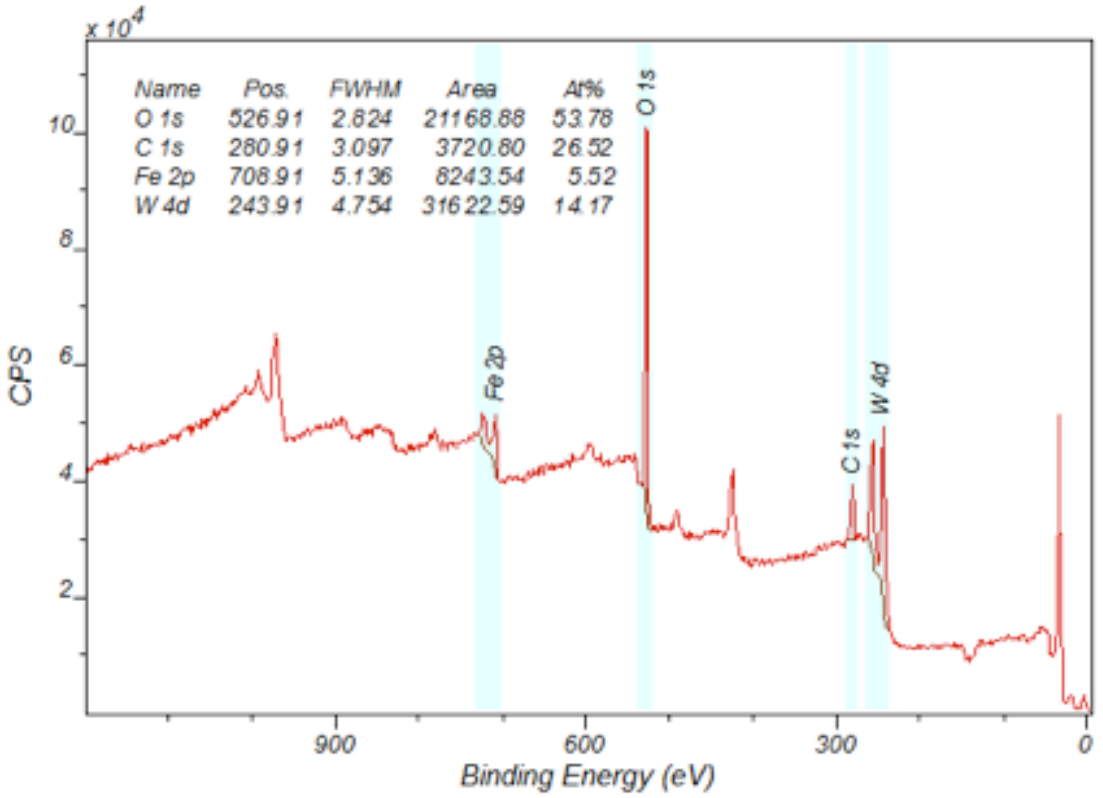

Figure 4.23 XPS spectra of W/Fe=2.2 iron tungstate catalyst

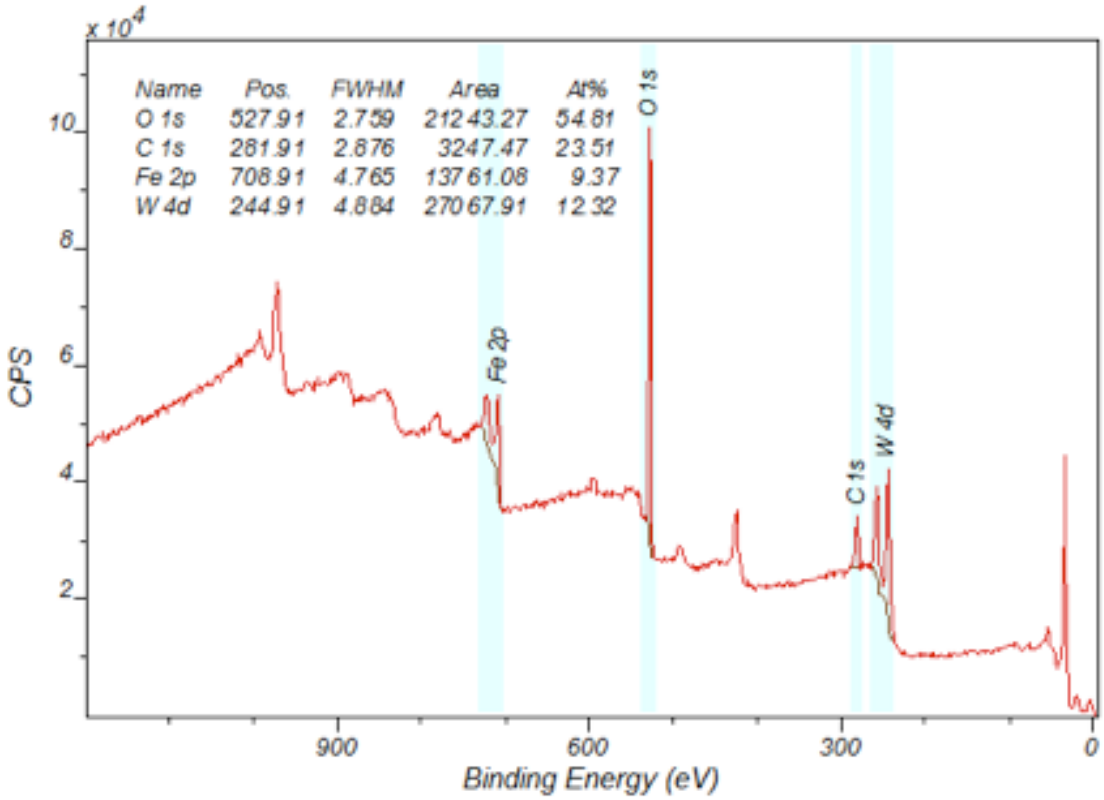

Figure 4.24 XPS spectra of used W/Fe=2.2 iron tungstate catalyst

Iron tungstate catalysts (W/Fe= 1.5, 2.2) are selective catalysts to formaldehyde, and the single tungsten oxide is the most selective catalyst for formaldehyde (100% selectivity) in this study (Chapter 3) and even more selective than molybdenum oxide to formaldehyde. Though, the tungsten has poor activity and does not fully convert methanol to formaldehyde (maximum conversion is 53% by 420 ^{o}C),. In figure 4.25 the stoichiometric iron tungstate is 100% selective to formaldehyde by 200 ^{o}C and above,. However, the methanol conversion is low and the maximum conversion is 83% by 288 ^{o}C, but the production of combustive products as CO and CO_2 occurs at high temperature. The increase of tungsten ratio leads to less activity, as in figure 4.26. However, both stoichiometric and 2.2 iron tungsten are selective catalysts to formaldehyde in the presence of oxygen, but without oxygen as in the result of TPD for both catalyst figures (4.27, 4.28), which show that there are peaks of dimethyl ether (mass 45) and formaldehyde (mass 30). However, dimethyl ether is being produced at a low temperature in TPR that has flow of oxygen with methanol in the gas system, and as it is a very small amount at very low conversion which disappeared when the catalyst start to be active, that means dimethyl ether is not a main product in presence of oxygen but it is a main product in the absence of oxygen.

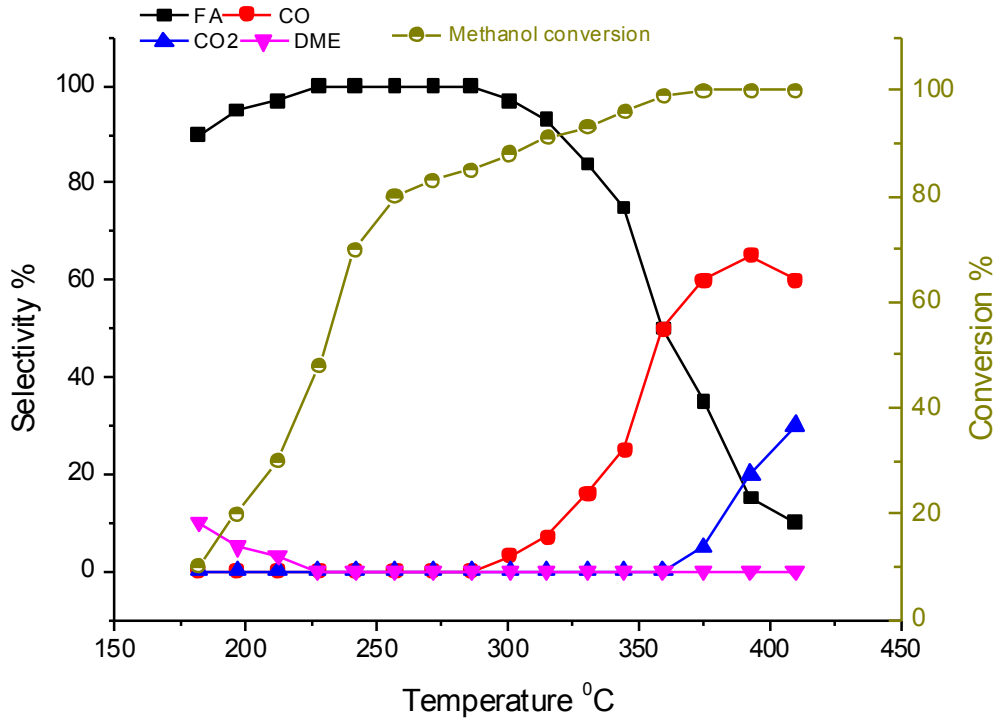

Figure 4.25 Reaction profile result of $Fe_2(WO_4)_3$ catalyst

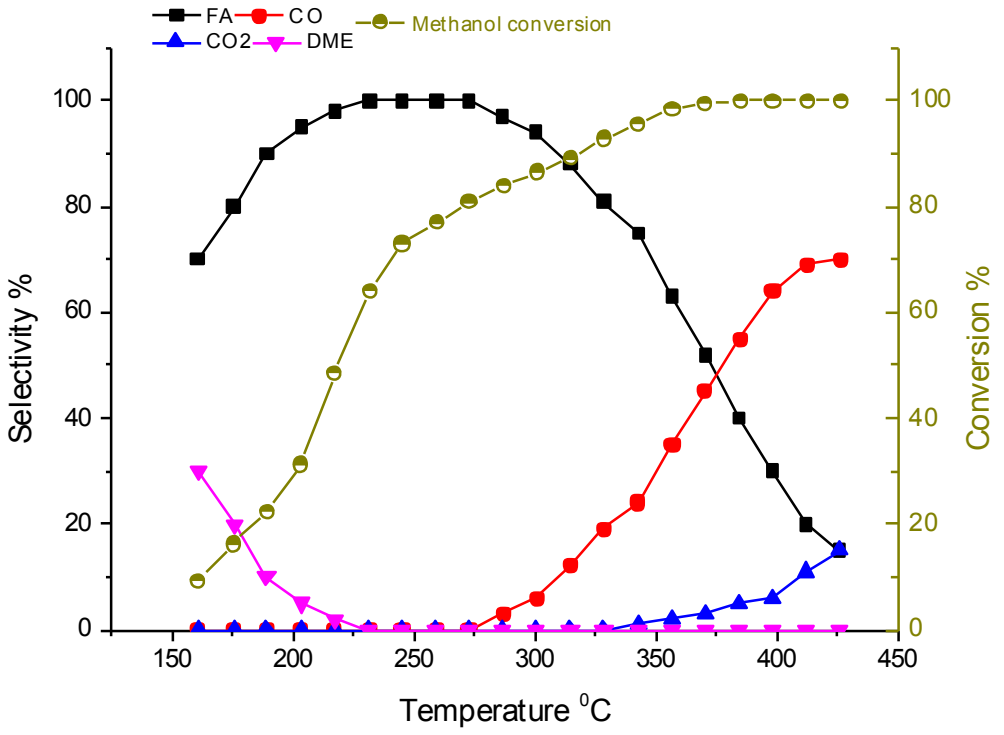

Figure 4.26 Reaction profile result of 2.2 $Fe_2(WO_4)_3$ catalyst

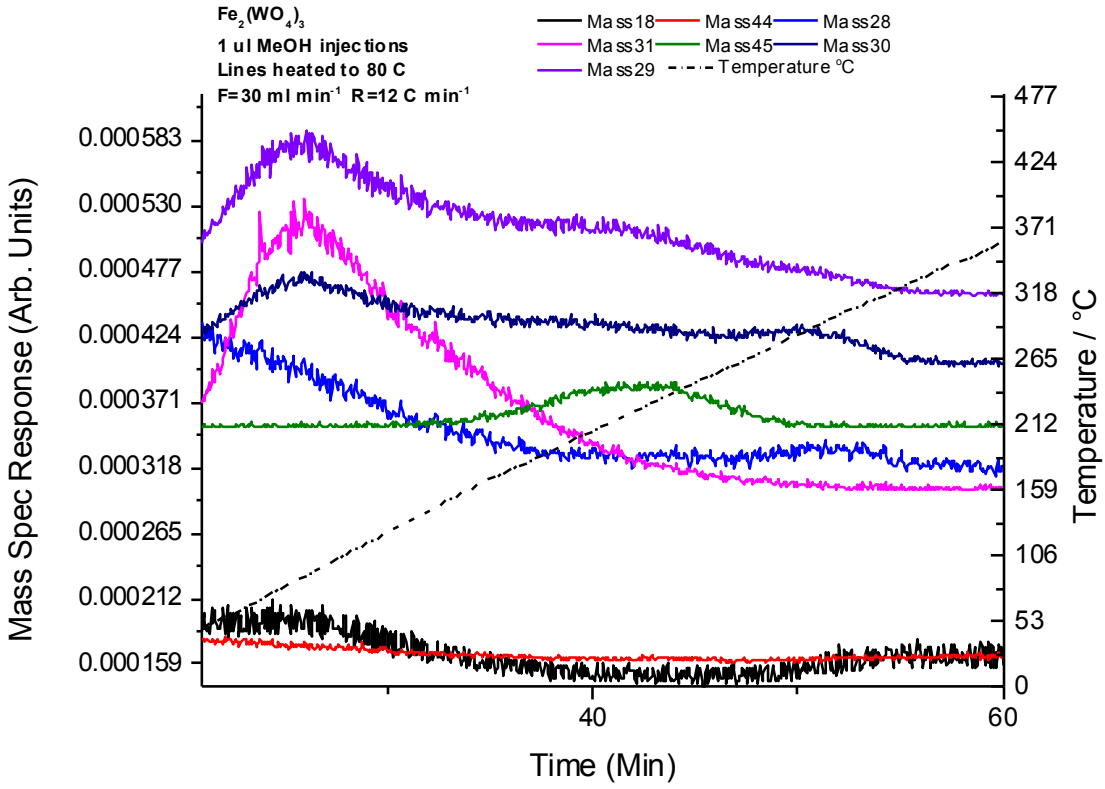

Figure 4.27 TPD result of pure iron tungstate catalyst

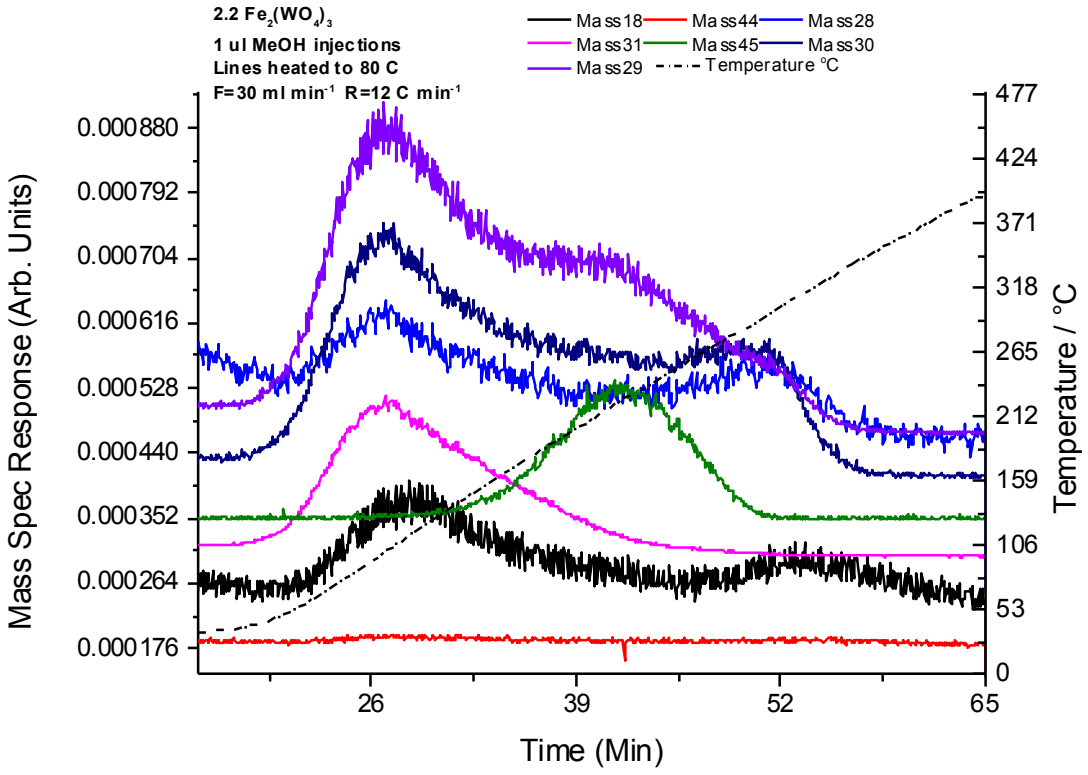

Figure 4.28 TPD result of W/Fe=2.2 iron tungstate catalyst

4.2.3. $FeNbO_4$ catalyst

Iron niobium oxide catalyst has a surface area of 10 m^2/g, which is quite a large surface area compared to the rest of the catalysts were used in this study. However, the single oxide of niobium does not have that large surface area, (2 m^2/g, Nb_2O_5), and so the complex oxide with iron increases the catalyst's surface area. Moreover, the catalyst is active by 180 ^oC, and converts all methanol by 290 ^oC, nevertheless, the catalyst is selective to formaldehyde at low conversion. However, the catalyst started to convert methanol with high conversion, formaldehyde production decreased and CO increased up 90%, as in figure 4.29. Also figure 4.30 shows that there is mainly dimethyl ether production at low temperature but large yields of CO and CO2The formaldehyde production is very low in TPD mode.

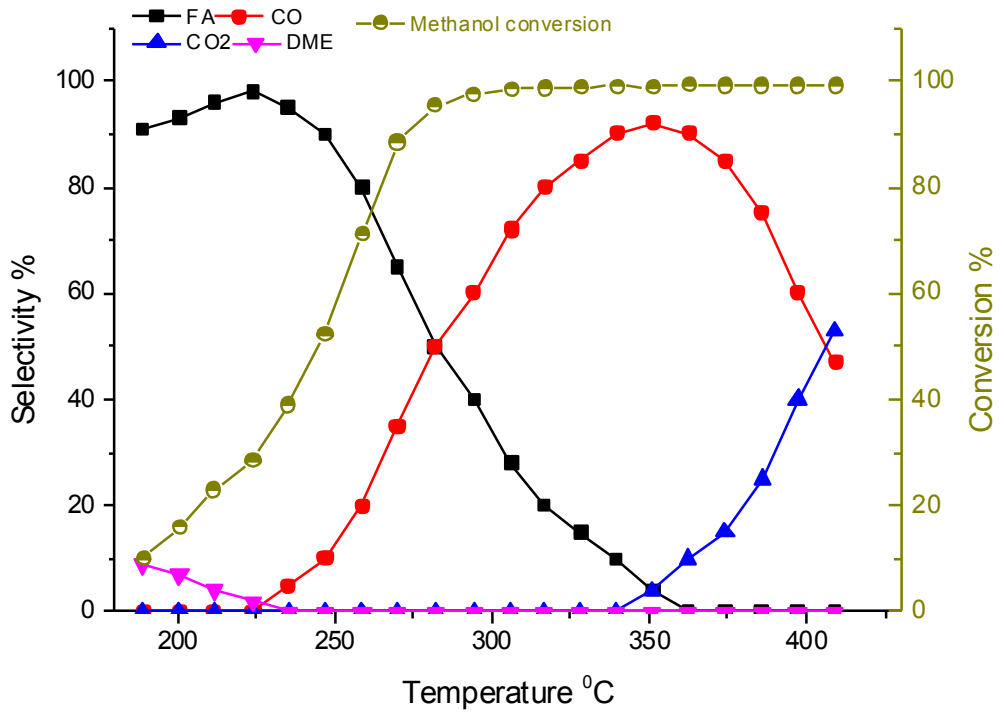

Figure 4.29 Reaction profile result of $FeNbO_4$ catalyst

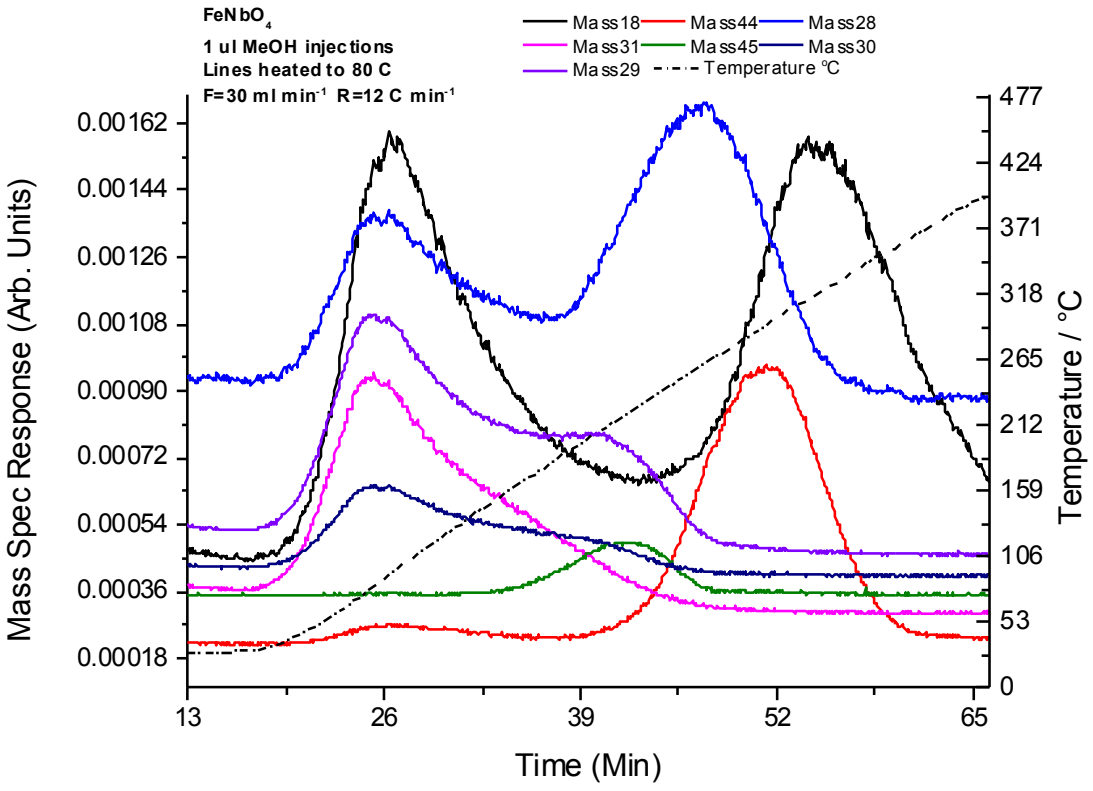

Figure 4.30 TPD result $FeNbO_4$ catalyst

4.2.4. $FeSbO_4$ catalyst

Iron antimonate has a surface area of 4 m^2/g. However, the catalyst was not very selective to formaldehyde. Figure 4.31 shows the TPR result using $FeSbO_4$ catalyst, where there is a low yield of formaldehyde the major products being CO and CO2, implying this is a combustion catalyst. Figure 3.32 is the TPD result for which shows that the catalyst is mainly selective to carbon monoxide and carbon dioxide. However, there are small peaks that are related to dimethyl ether and formaldehyde: formaldehyde was seen in TPR result even at low production, whereas dimethyl ether was not seen in TPR in presence of oxygen.

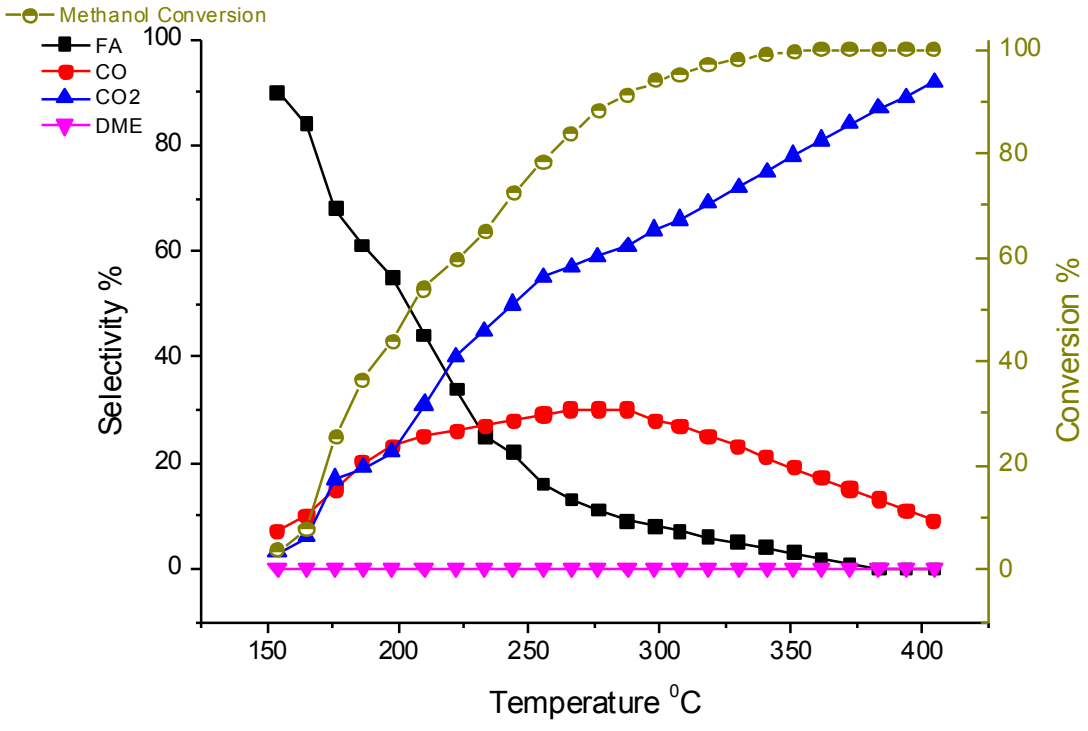

Figure 4.31 Reaction profile result of $FeSbO_4$ catalyst.

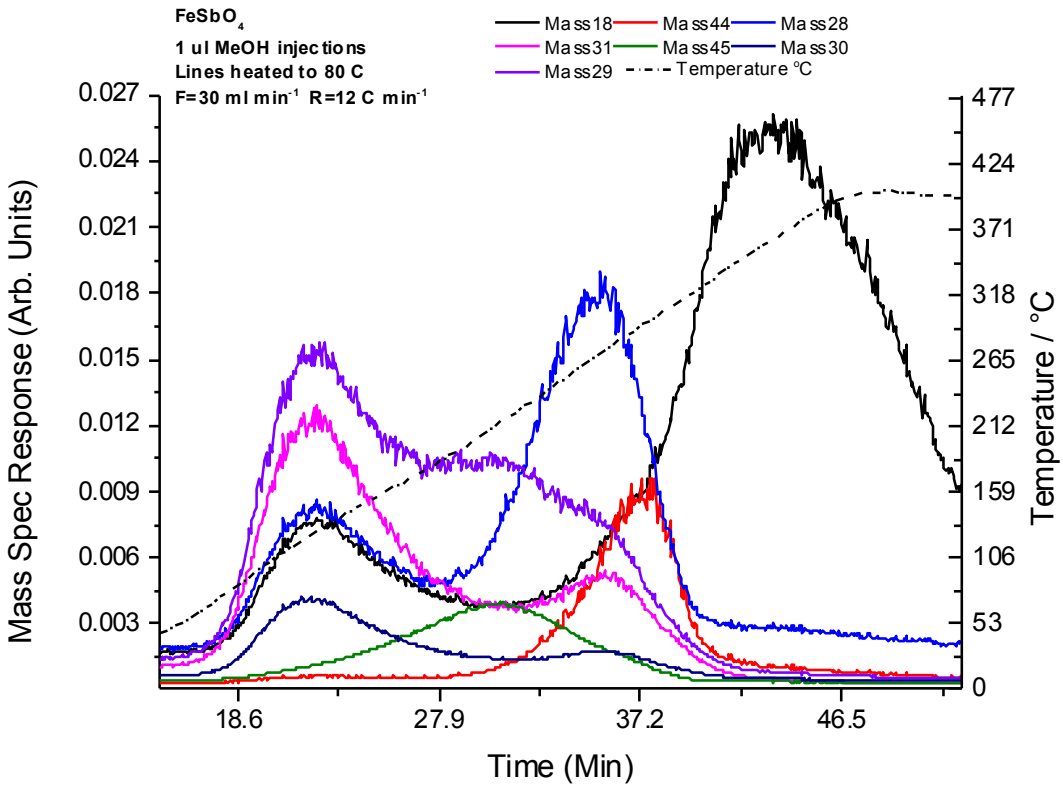

Figure 4.32 TPD result of $FeSbO_4$ catalyst.

4.2.5. $CuMoO_4$ catalysts

Copper molybdate [14], catalysts were used. This divided into three types according to the ratio of molybdenum access in the catalyst structure, as pure stoichiometric $CuMoO_4$ (MO/Cu=1) with surface of 6 $m^2.g^{-1}$, ratio 1.5 =Mo/Cu, $CuMoO_4$ catalyst with surface area of 5 $m^2.g^{-1}$ and ratio 2Mo:1Cu (Mo/Cu=2) copper molybdate catalyst with surface of 4 $m^2.g^{-1}$. The catalytic behavior of the three catalysts is shown in figure 4.33 for stoichiometric $CuMoO_4$, figure 4.34 for ratio 1.5Mo:1Cu $CuMoO_4$ catalyst, and figure 4.35 for 2Mo:1Cu ratio copper molybdate catalyst. The stoichiometric copper molybdate started to be active by 180 ^oC. However, the catalyst is 100% selective to formaldehyde only at low conversion (maximum 10%), then formaldehyde selectivity decreased with increase of carbon monoxide selectivity. Methanol conversion increased up to 100% by 325 ^oC, and by this point, formaldehyde selectivity is 80% (yield = 80%) and the rest is carbon monoxide.. Some CO2 is seen at high temperature. With increased Mo the activity appears to increase a little, and formaldehyde continues to be the major product, at least up to ~ 350 °C. From these data this catalyst appears to perform well for the selective oxidation of fomaldehyde.

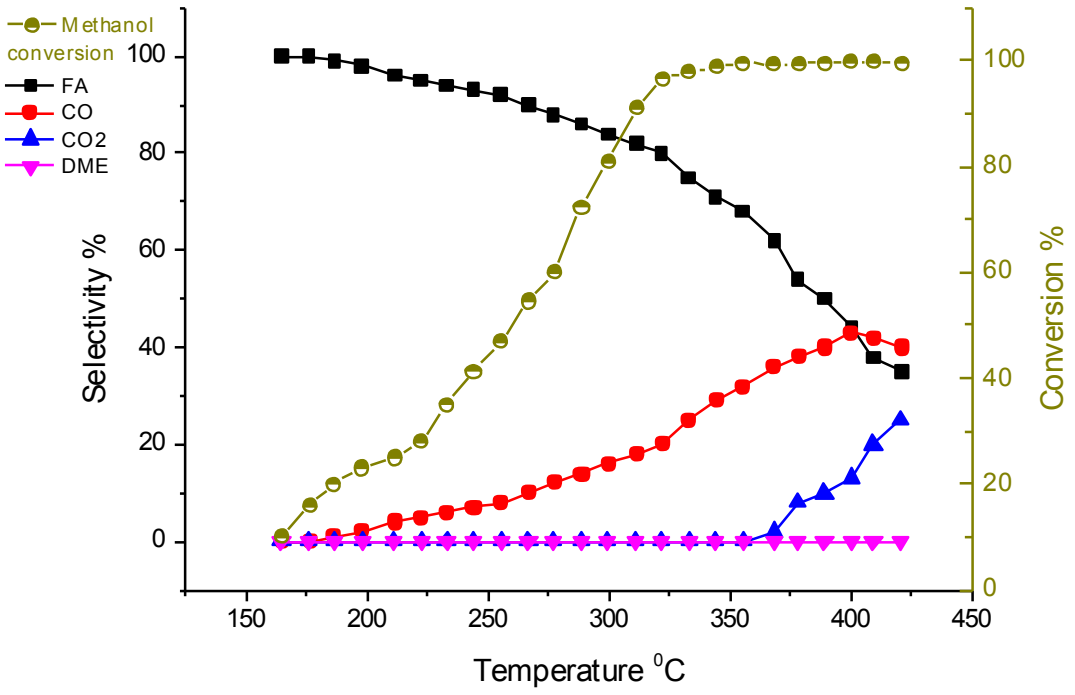

figure 4.33 Reaction profile result of pure copper molybdate catalyst .

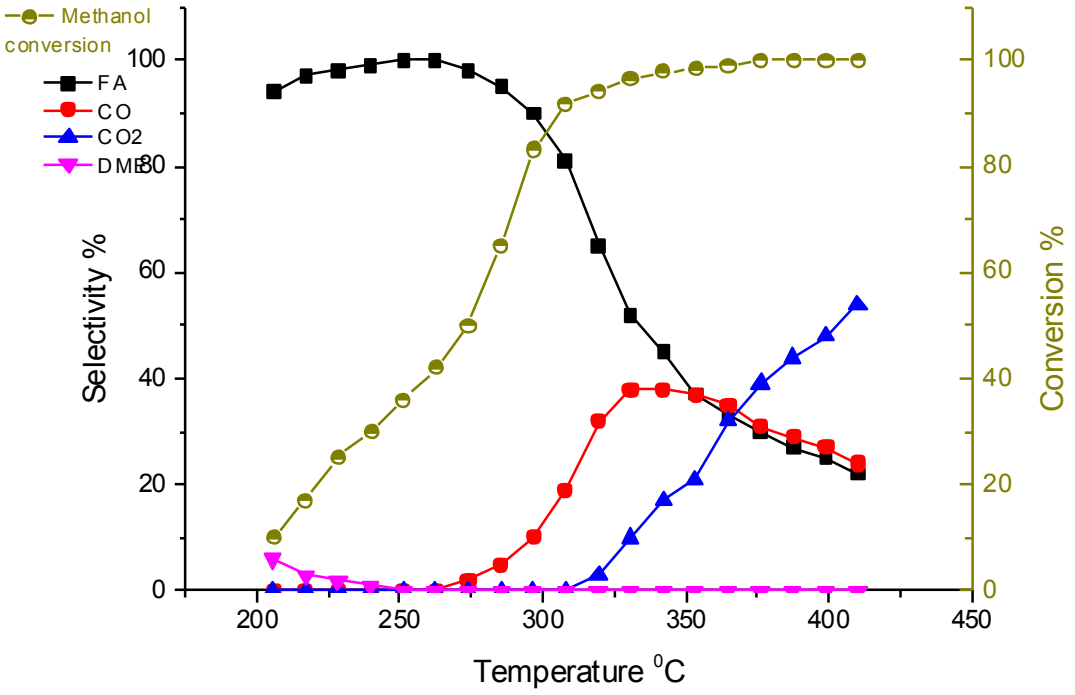

Figure 4.34 Reaction profile result of (Mo/Cu=1.5) $CuMoO_4$ catalyst.

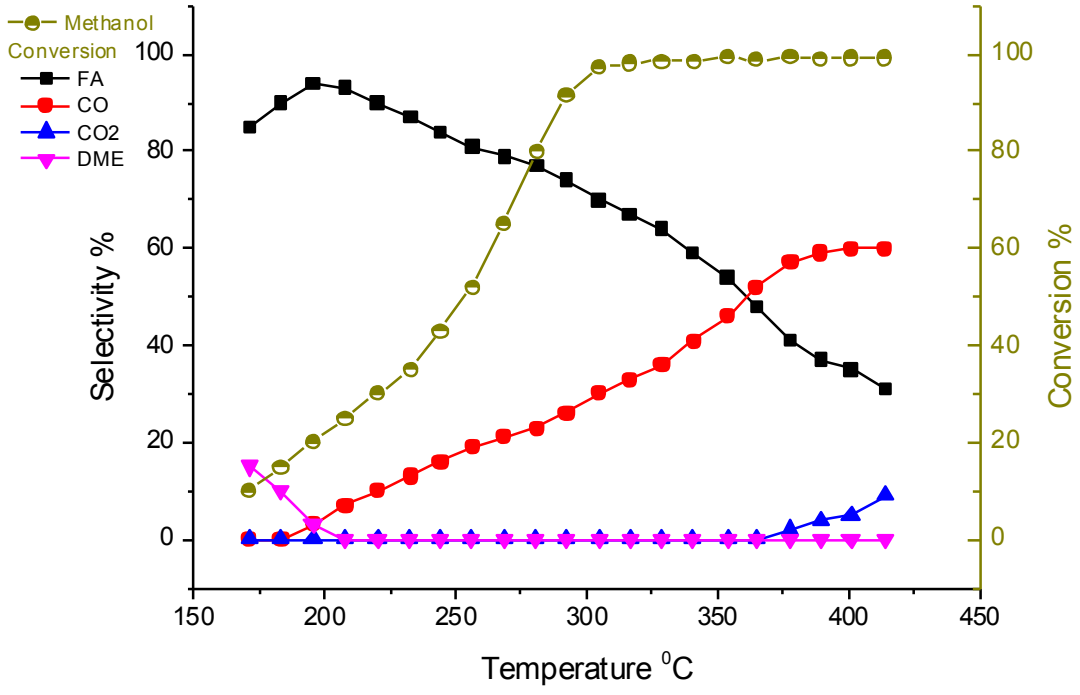

Figure 4.35 Reaction profile result of (Mo/Cu=2) $CuMoO_4$ catalyst.

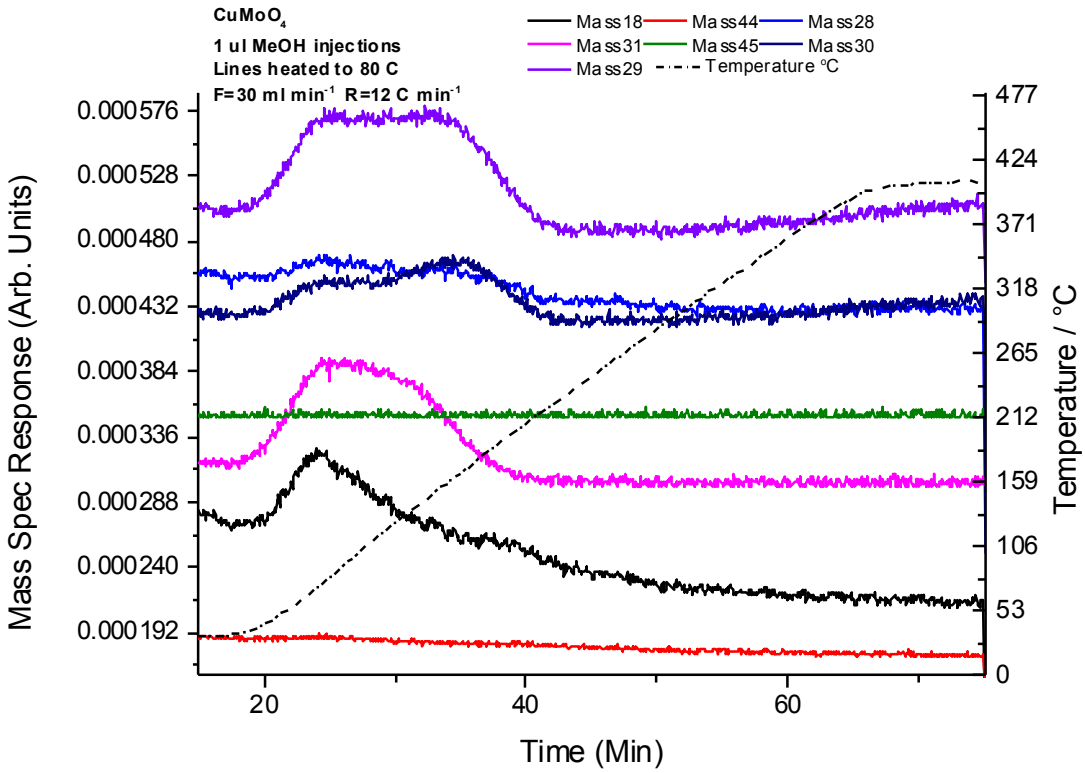

Figure 4.36 TPD of pure $CuMoO_4$ catalyst.

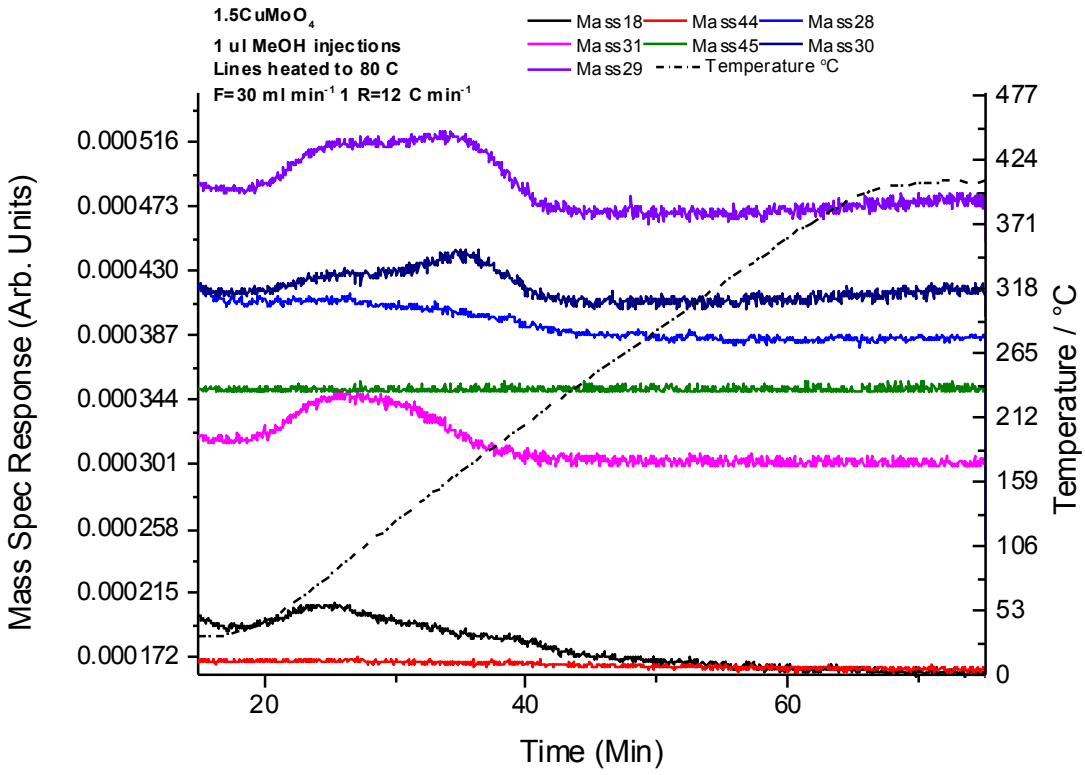

Figure 4.37 TPD result of (Mo/Cu=1.5) $CuMoO_4$ catalyst.

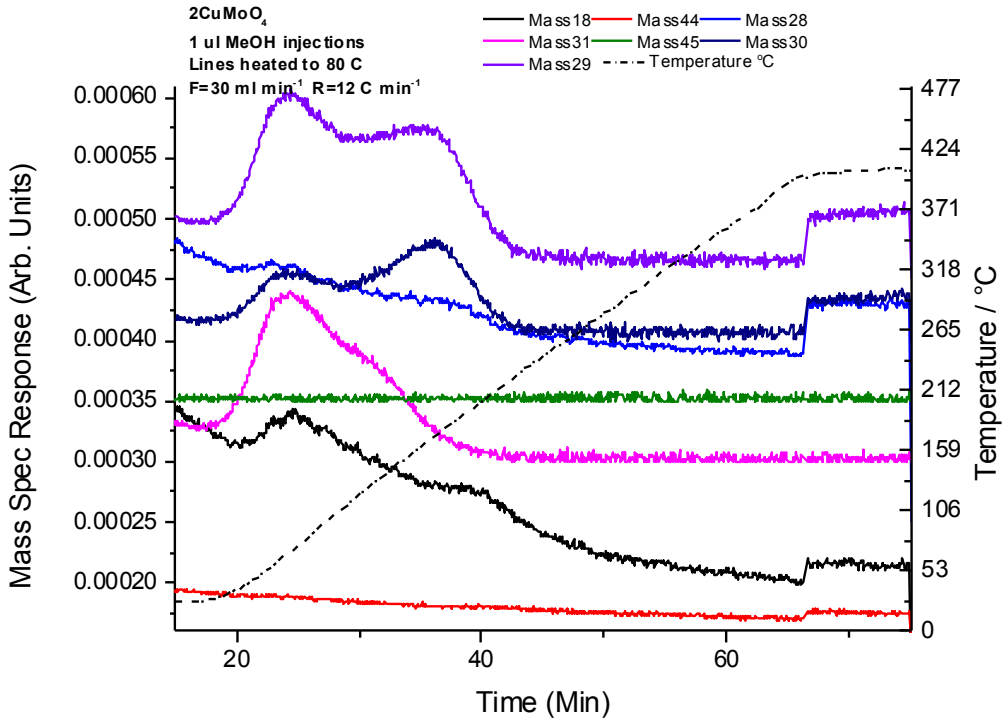

Figure 4.38 TPD result of (Mo/Cu=2) $CuMoO_4$ catalyst.

Figure 4.36-4.38 are TPD results of three copper molybdate catalysts. In all three cases, there is only one peak associated to mass 30 (formaldehdye), which confirms that the three catalysts are selective to formaldehdye. CO and CO2 were not seen in TPD result, confirming the good performance of these materials. XRD result obtained for the three catalysts show no change in bulk when the catalysts were run for methanol oxidation, showing that the catalysts are stable.

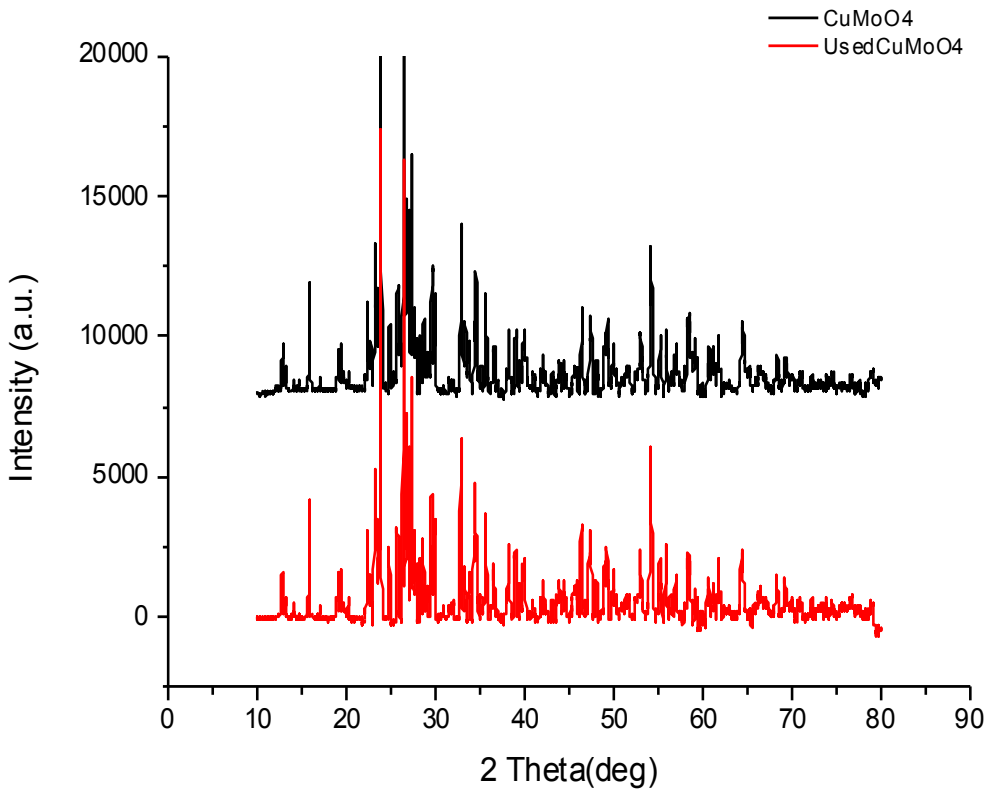

Figure 4.39 XRD spectra of stoichiometric $CuMoO_4$ catalyst

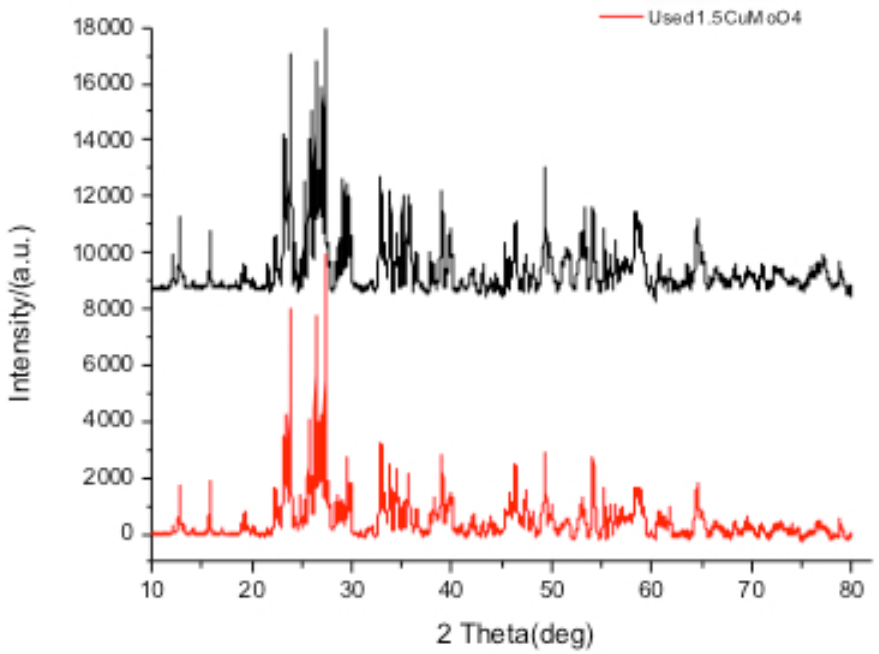

Figure 4.40 XRD spectra of (Mo/Cu=1.5) $CuMoO_4$ catalyst

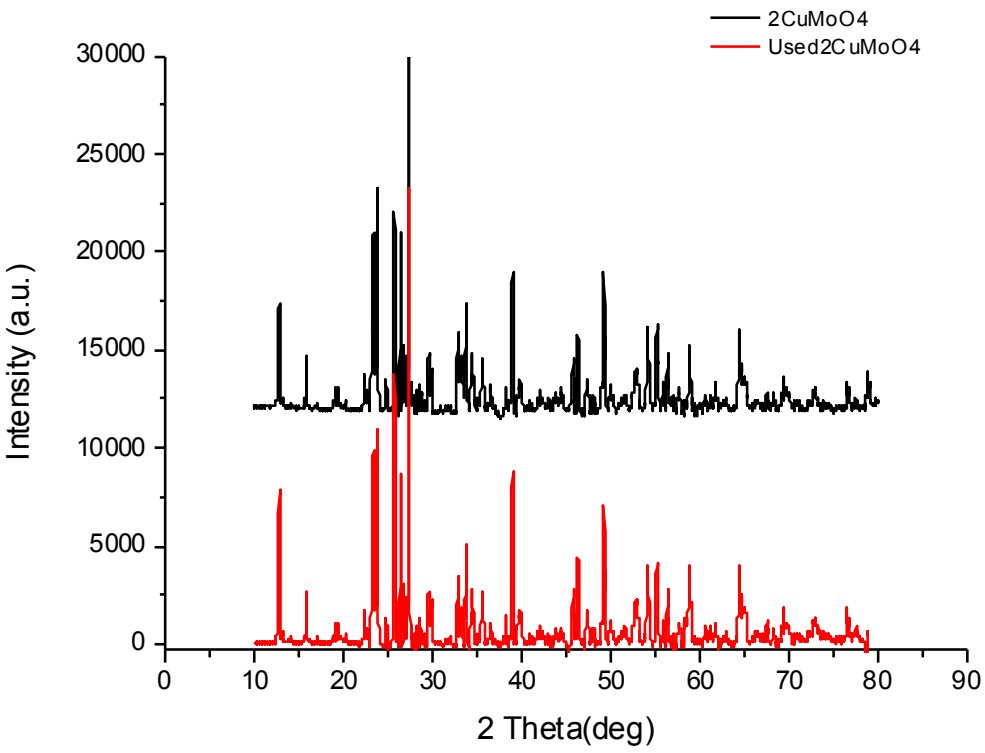

Figure 4.41 XRD spectra of (Mo/Cu=2) $CuMoO_4$ catalyst

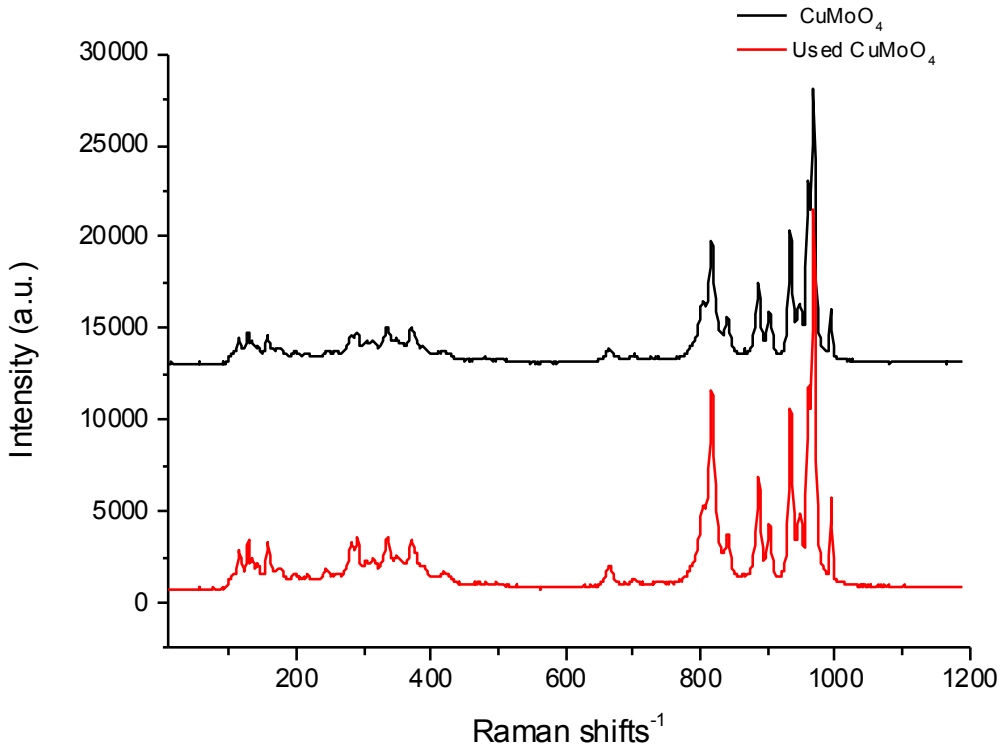

Figure 4.42 Raman result of stoichiometric copper molybdate catalyst

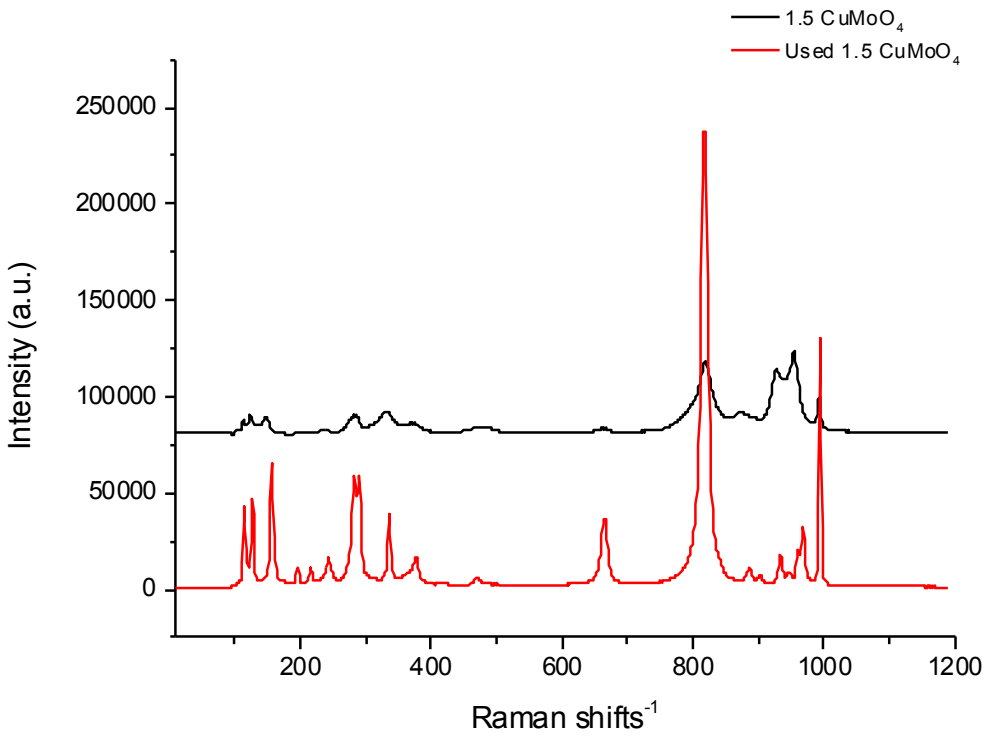

Figure 4.43 Raman result of (Mo/Cu=1.5) $CuMoO_4$ catalyst

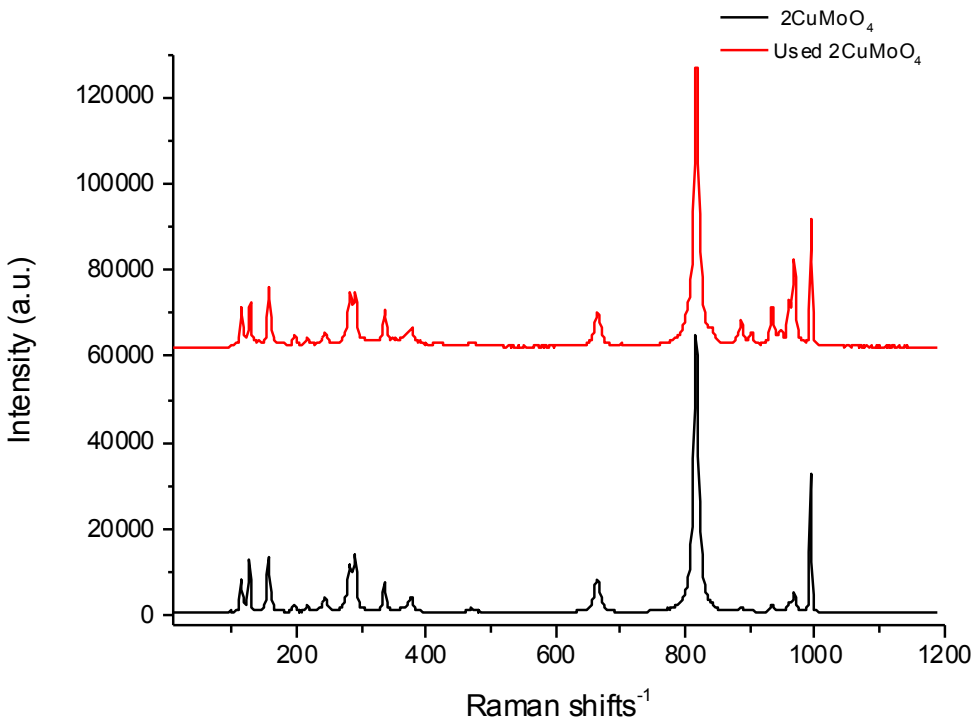

Figure 4.44 Raman result of (Mo/Cu=2) $CuMoO_4$ catalyst

Raman result tells more about surface layers. Figure 4.42, figure 4.43 and figure 4.44 show that there are missed peaks with molybdenum higher ratio than 1Mo:1Cu. However, 990 and 820 bands have appeared for the high Mo loading, due to the increasing presence of MoO3 in the catalysts. catalysts, which was not seen in figure 4.42 that is the pure copper molybdate catalyst. In other words, the more addition of molybdenum above the stoichiometry ratio will cover the surface, and does not have a big affect in bulk, as seen from the XRD result. Moreover, the three catalysts are stable as seen in the XRD result and the Raman result, where there was no change in the three catalysts' structures when analyzed after methanol oxidation experiments, which shows that the three catalysts are stable.

4.2.6. $MnMoO_4$ catalysts

Manganese molybdate [15] was prepared in three ratios, the stoichiometry (Mo/Mn=1) ratio, 1.5 Mo: 1 Mn, and 2 Mo : 1 Mn manganese molybdate. The three catalysts have different surface areas: the stoichiometry manganese molybdate has 5 $m^2.g^{-1}$, 1.5Mo: 1Mn manganese molybdate catalyst has 4 $m^2.g^{-1}$,

and 2Mo : 1Mn manganese molybdate has a surface area of 3 $m^2.g^{-1}$. Molybdenum oxide itself has a low surface area ($1m^2.g^{-1}$), so it might indeed be expected that the greater addition of molybdenum ratio would lead to a lowering in surface area. However, all three catalysts are active, as in figure 4.45-47, which are the TPR results of the three catalysts. The 1.5Mo:Mn is more active, and started converting methanol by just 110 ^oC, while stoichiometric and 2Mo:Mn manganese molybdate catalysts converted methanol by 180 ^oC. However, in terms of complete conversion of methanol, stoichiometric manganese molybdate is the least active, where methanol fully converted by approx. 370 ^oC, while 1.5 Mo : 1Mn manganese molybdate is the most active of the three ratio catalysts, as it converted 100% methanol by approx. 273 ^oC. This makes it even more active than iron molybdate.

The selectivity toward formaldehyde using the three catalysts is very good, especially at moderate conversion, with, for instance, the 2Mo:Mn catalyst yielding 75% formaldehyde; the other main product being CO, with little sign of complete combustion. Similarly in TPD, all three catalysts performed very well, showing almost exclusively formaldehyde as a product in TPD (figures 4.48-50)

Raman in figure 4.51 is for stoichiometry manganese molybdate catalyst, figure 4.52 is for ratio 1.5 manganese molybdate catalyst, and figure 4.53 is for ratio 2 manganese molybdate catalyst. However, the peak by 820 cm^{-1} shows the molybdena ratio by its intensity, whereas in the pure catalyst result (figure 4.51) the peak is as it should be in the stoichiometry catalyst As Mo increases in the catalyst , so there is an increase in the MoO3 phase, evident by the increase in the peaksd at 990 and 820.. There appears to be little change after reaction in all cases. The XRD in figure 4.54, for stoichiometric catalyst, shows a change in its bulk structure, where peaks at 23^o, 33^o and 54^o are of much increased intensity in the used sample, which is for manganese oxide, and peaks by 26.5^o and 39^o are smaller in used line compared to the fresh catalyst line in the figure, which are related to molybdena. This means the bulk is losing some molybdenum after methanol oxidation, and Mn_2O_3 is formed instead. However in figure 4.55 (ratio 1.5, $MnMoO_4$) and in figure 4.56 (ratio 2, $MnMoO_4$) there was no change like that in the stoichiometry catalyst, where the bulk structures of these catalysts

(ratio 1.5 and ratio 2 catalysts) are more stable than the pure stoichiometry catalyst[15].

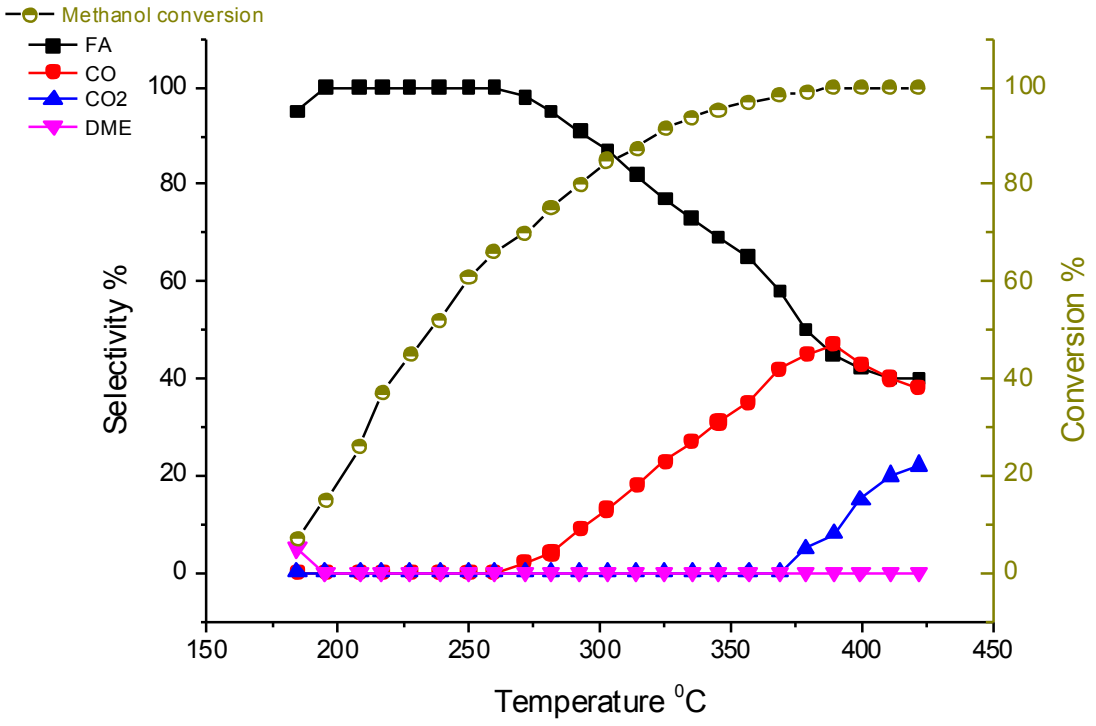

Figure 4.45 Reaction profile of stoichiometric manganese molybdate catalyst

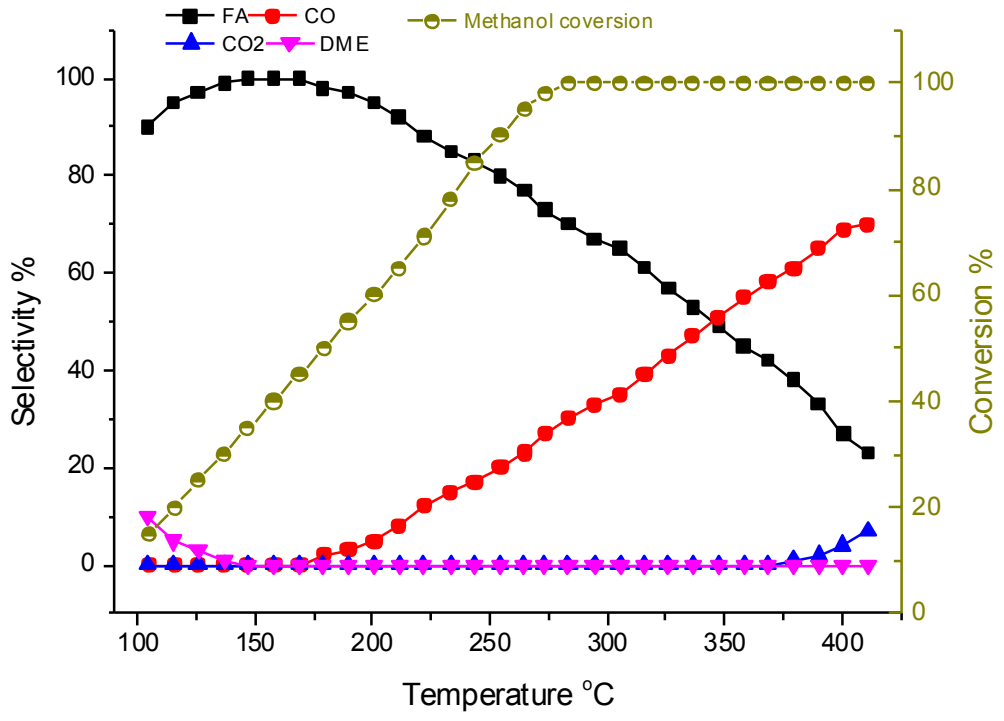

Figure 4.46 Reaction profile of (Mo/Mn=1.5) manganese molybdate catalyst

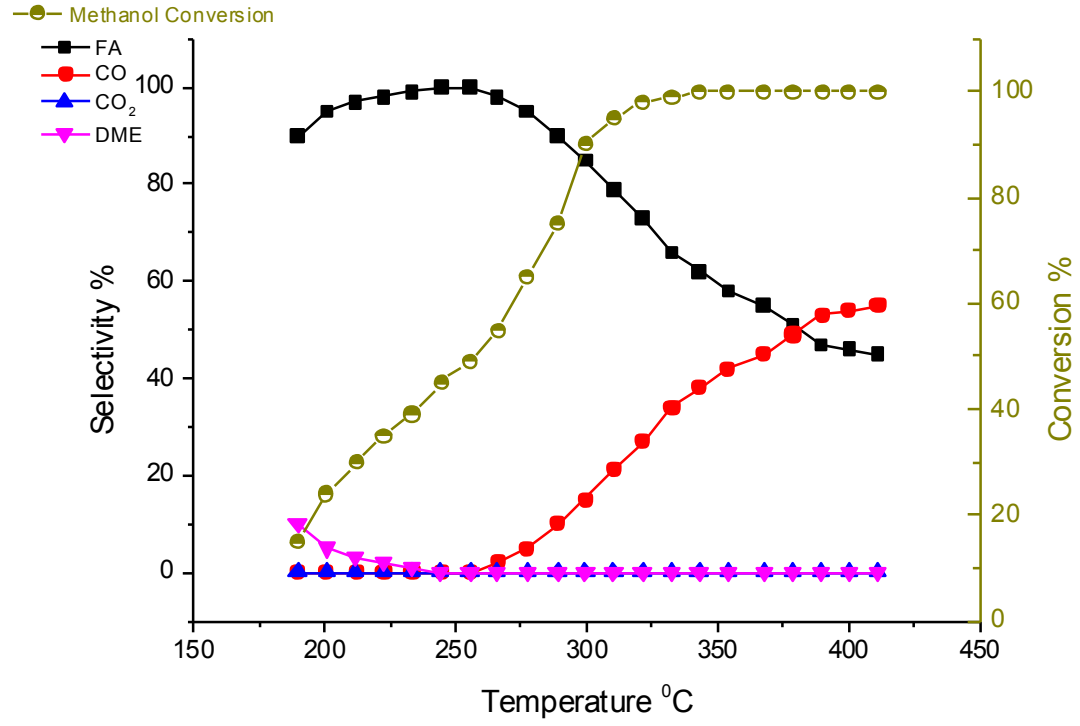

Figure 4.47 Reaction profile result of (Mo/Mn=2) manganese molybdate catalyst

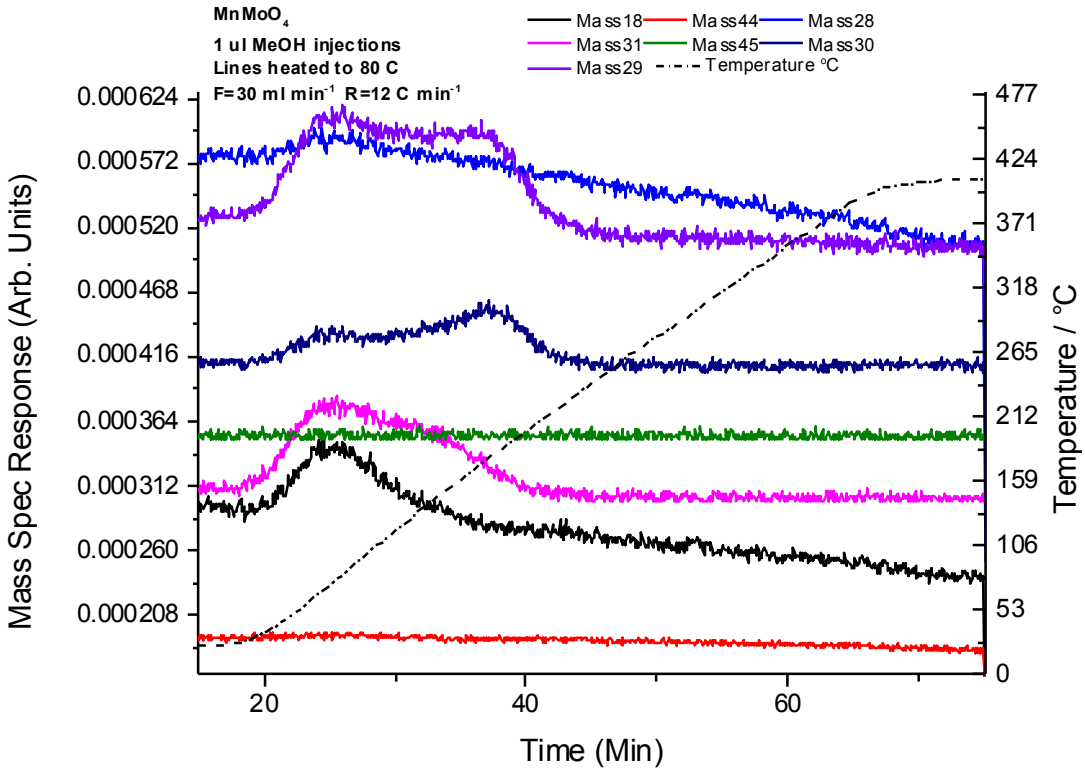

Figure 4.48 TPD result of stoichimetry manganese molybdate catalyst

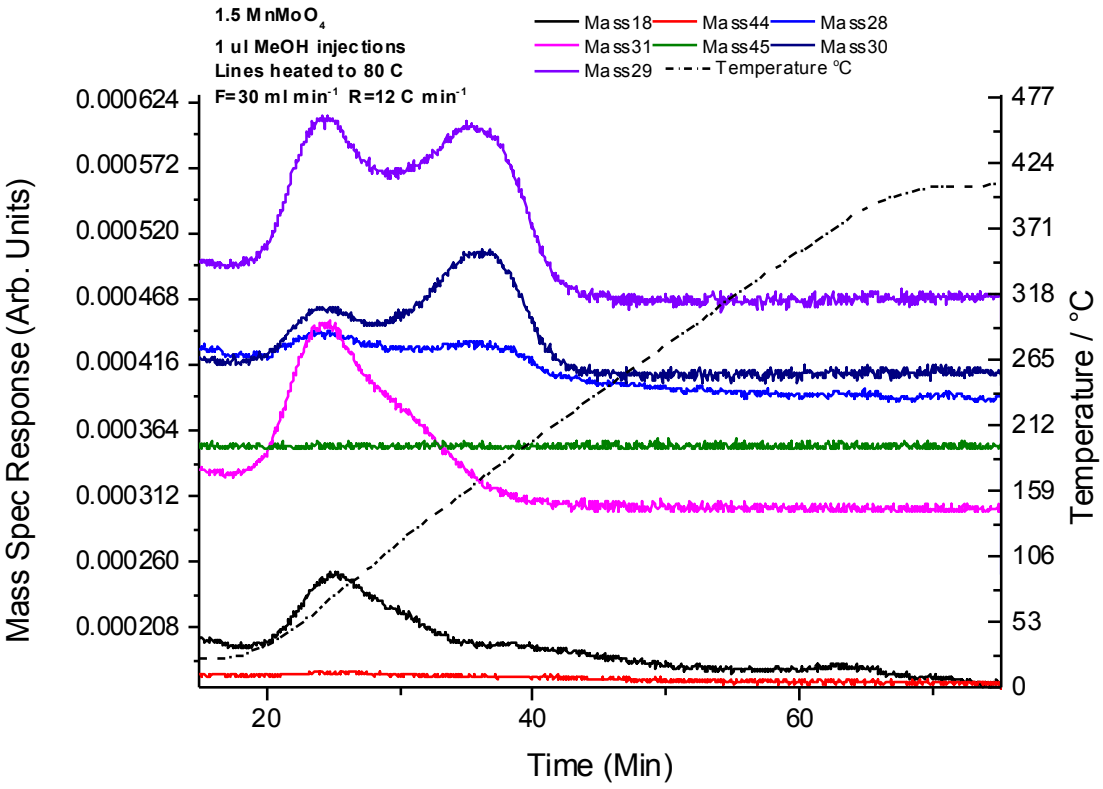

Figure 4.49 TPD result of (Mo/Mn=1.5) manganese molybdate catalyst

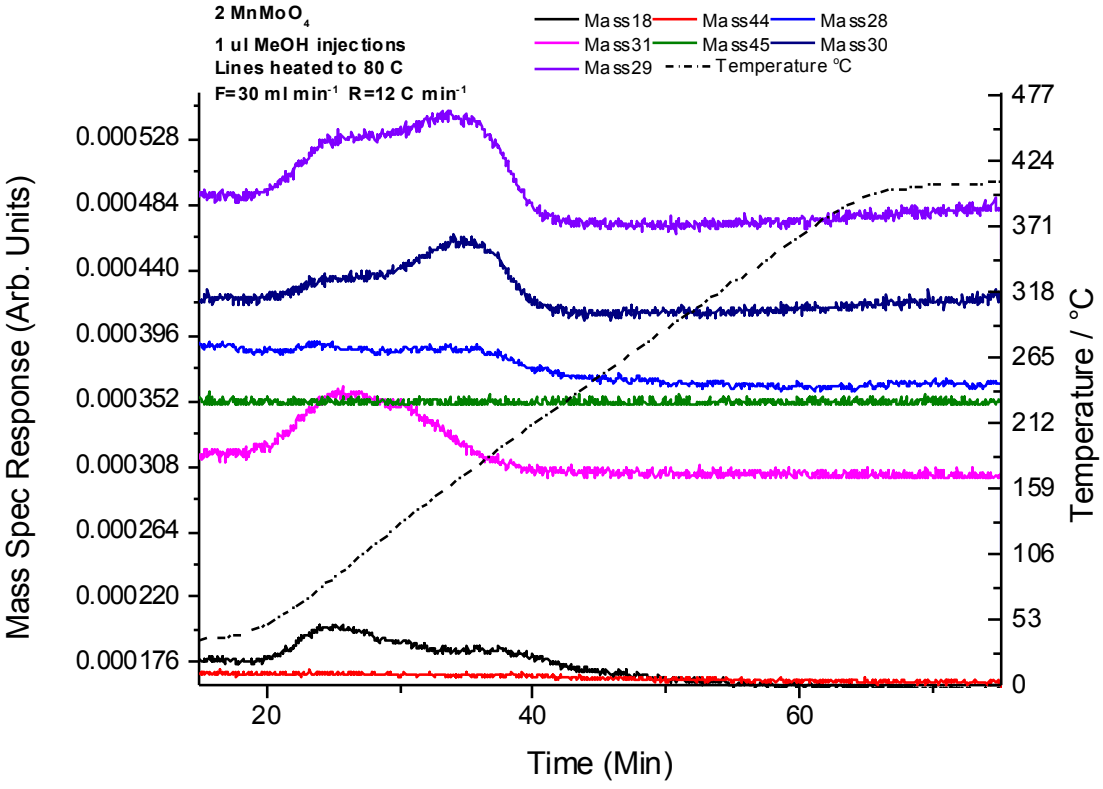

Figure 4.50 TPD result of (Mo/Mn=2) manganese molybdate catalyst

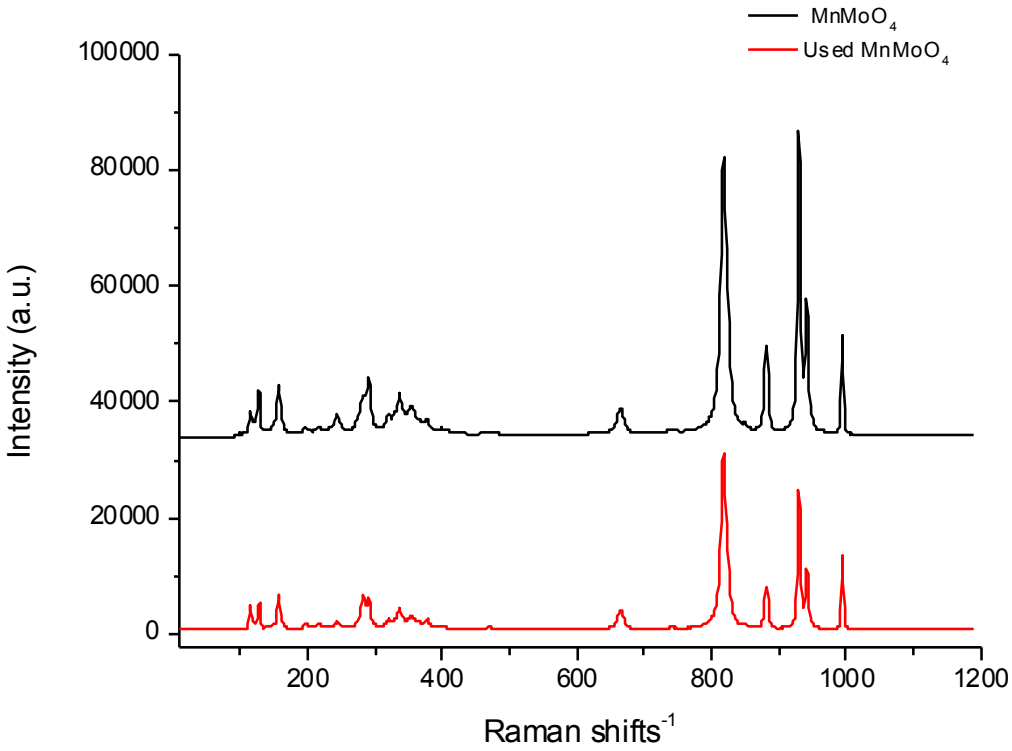

Figure 4.51 Raman result of stoichmetry manganese molybdate catalyst

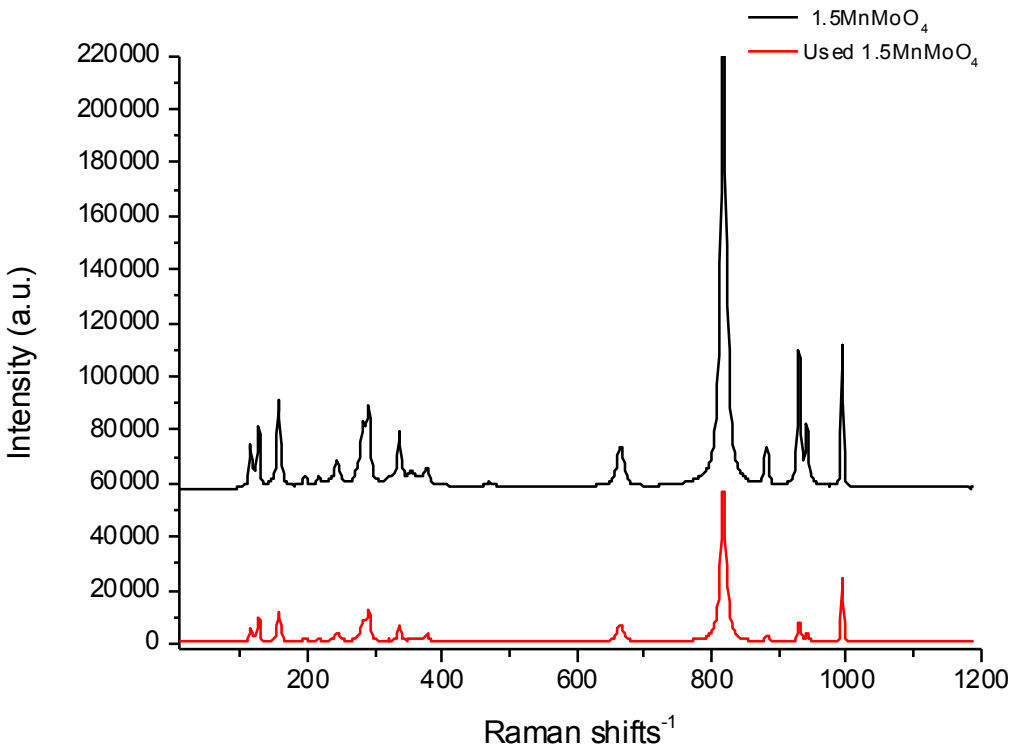

Figure 4.52 Raman result of (Mo/Mn=1.5) manganese molybdate catalyst

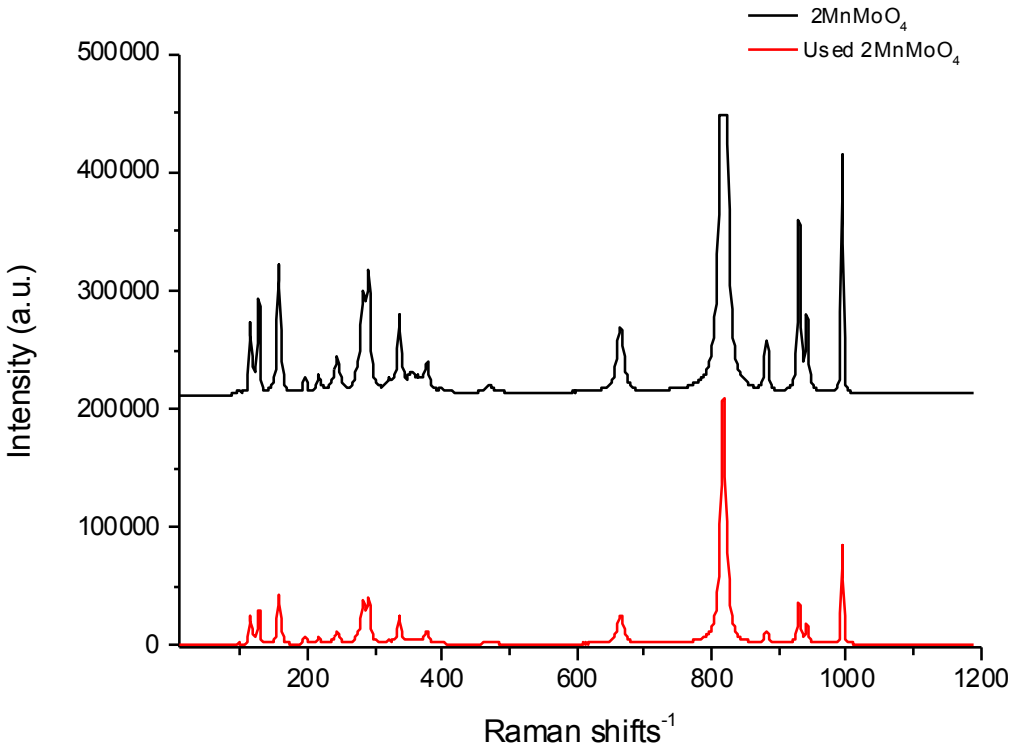

Figure 4.53 Raman result of (Mo/Mn=2) manganese molybdate catalyst

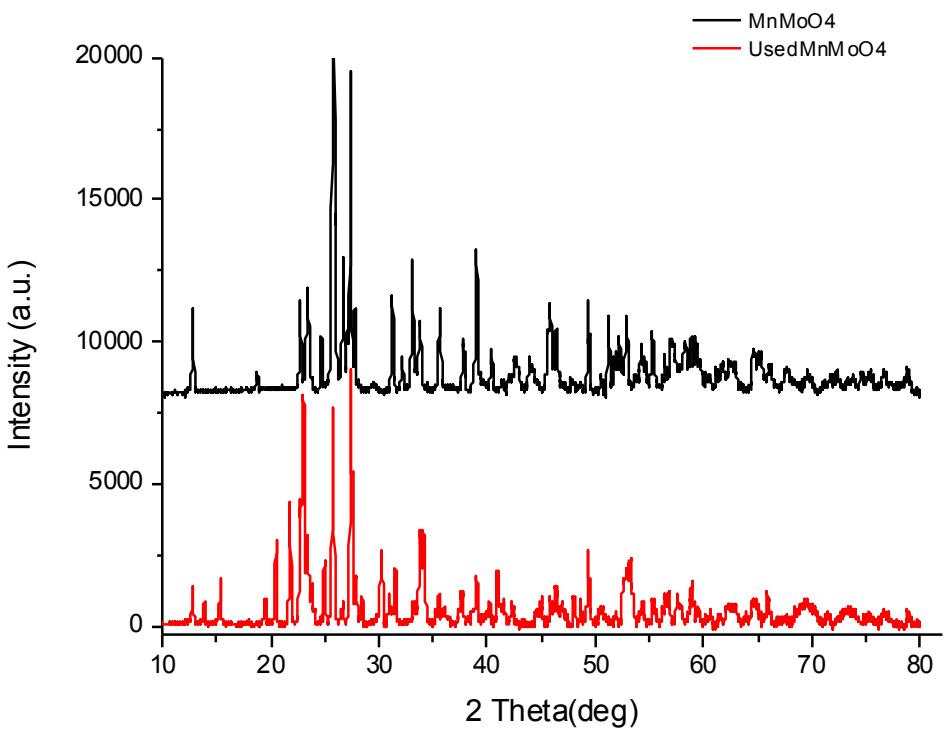

Figure 4.54 XRD spectra of stoichiometric manganese molybdate catalyst

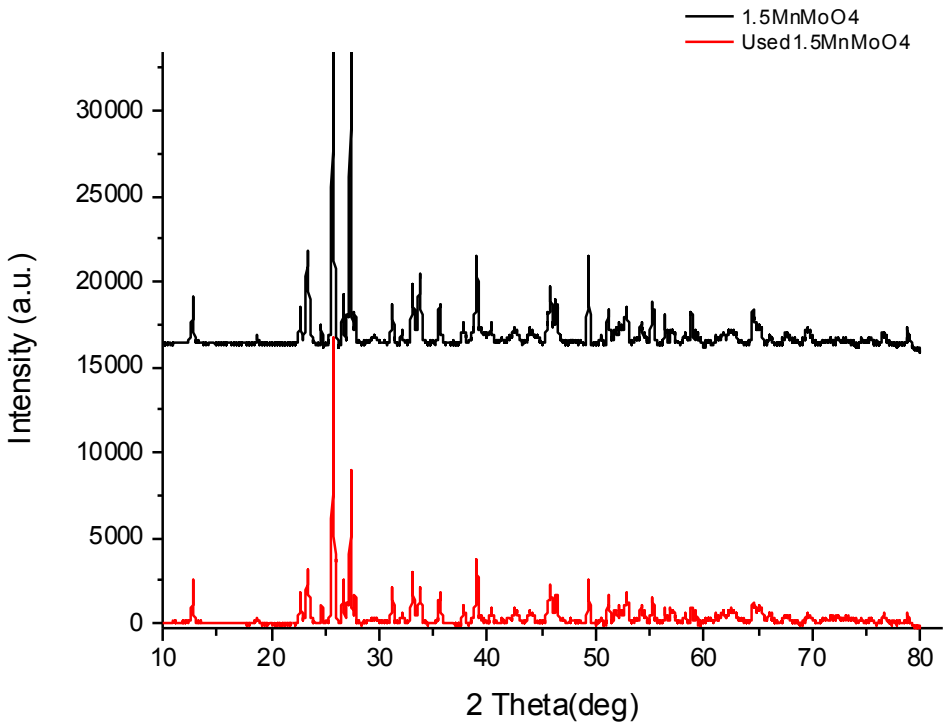

Figure 4.55 XRD spectra of (Mo/Mn=1.5) manganese molybdate

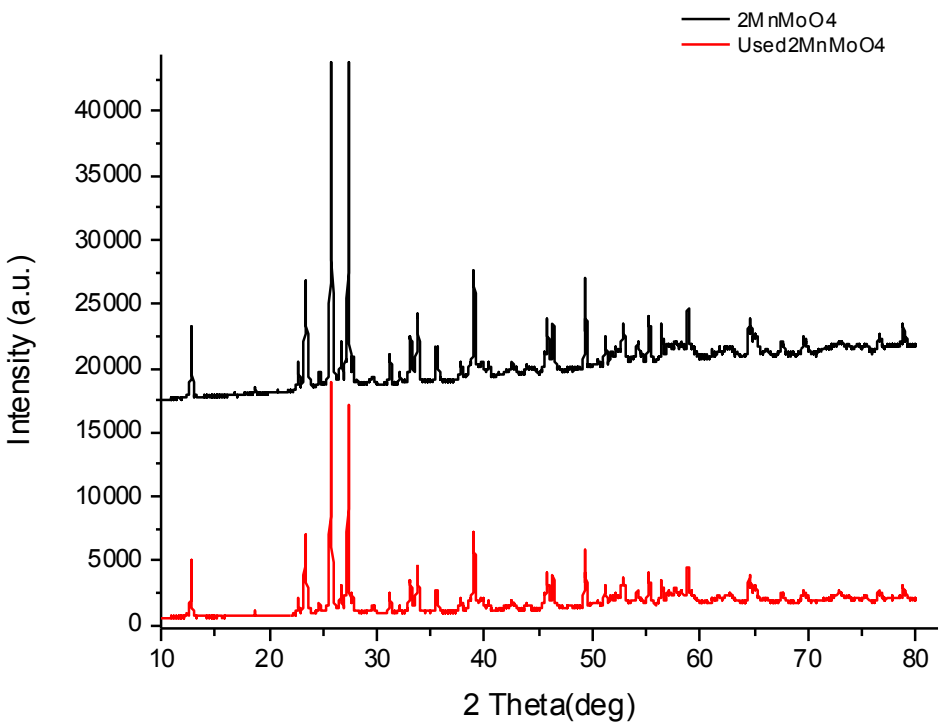

Figure 4.56 XRD spectra (Mo/Mn=2) manganese molybdate catalyst

4.2.7. $Bi_2Mo_2O_9$ catalyst

Bismuth molybdate catalyst has a surface area of 2 m^2 g^{-1}. The catalyst produced up has poor selectivity (fig. 4.57) and appears to be mainly a combustion catalyst Furthermore, the TPD result in figure 4.58 shows that although it produces formaldehyde at a relatively low temperature, carbon dioxide, is also a major product, Carbon dioxide formed at low temperature (260 ^oC). then CO formed at higher temperature than carbon dioxide, where selectivity of formaldehyde decreased with increase of the reaction temperature .

Figure 4.59 is Raman result of bismuth molybdate, where it shows that the catalyst does not have any significant spectral change after use [16].

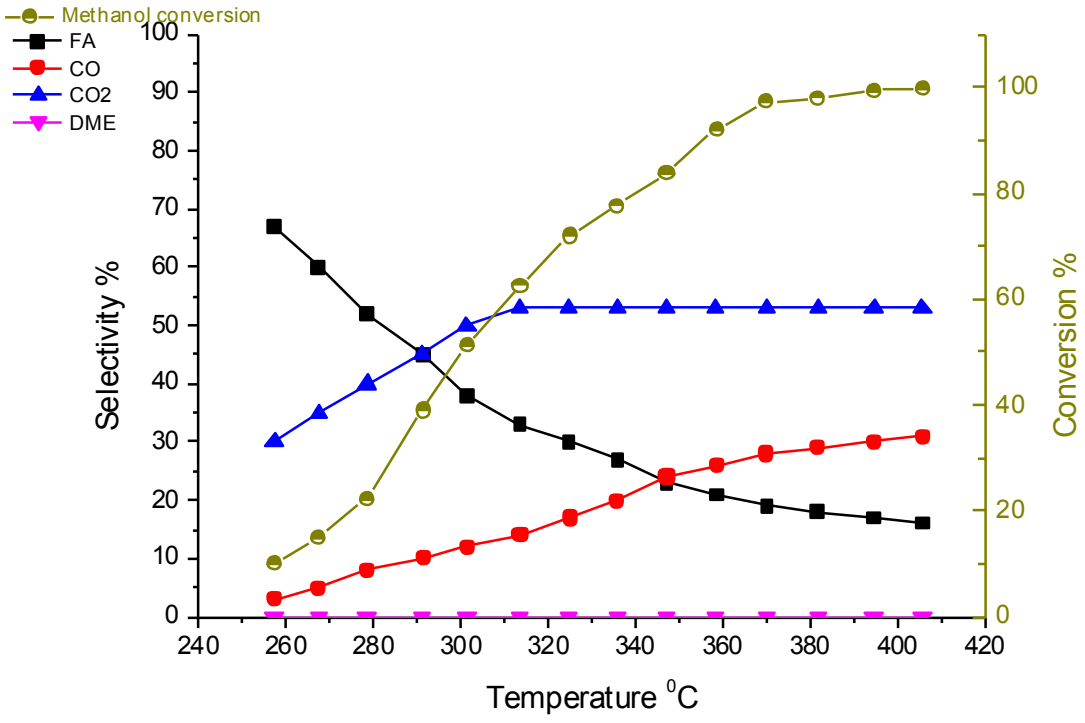

Figure 4.57 reaction profile result of bismuth molybdate catalyst

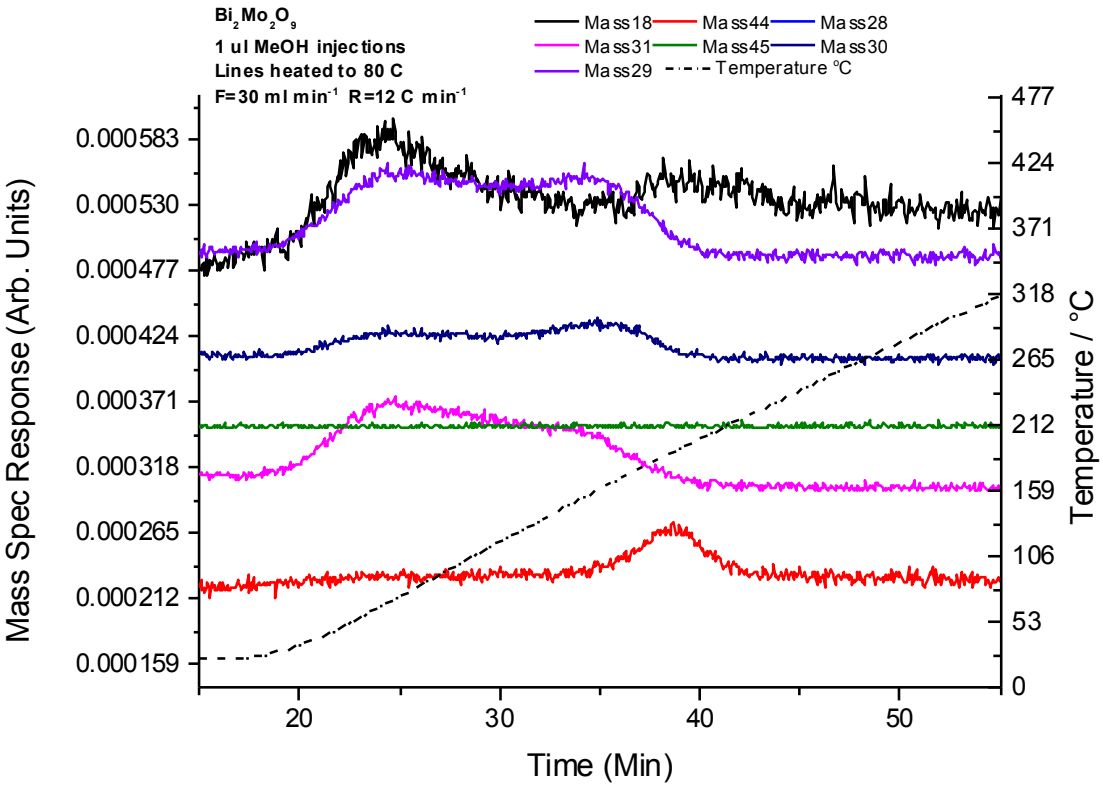

Figure 4.58 TPD result of bismuth molybdate catalyst

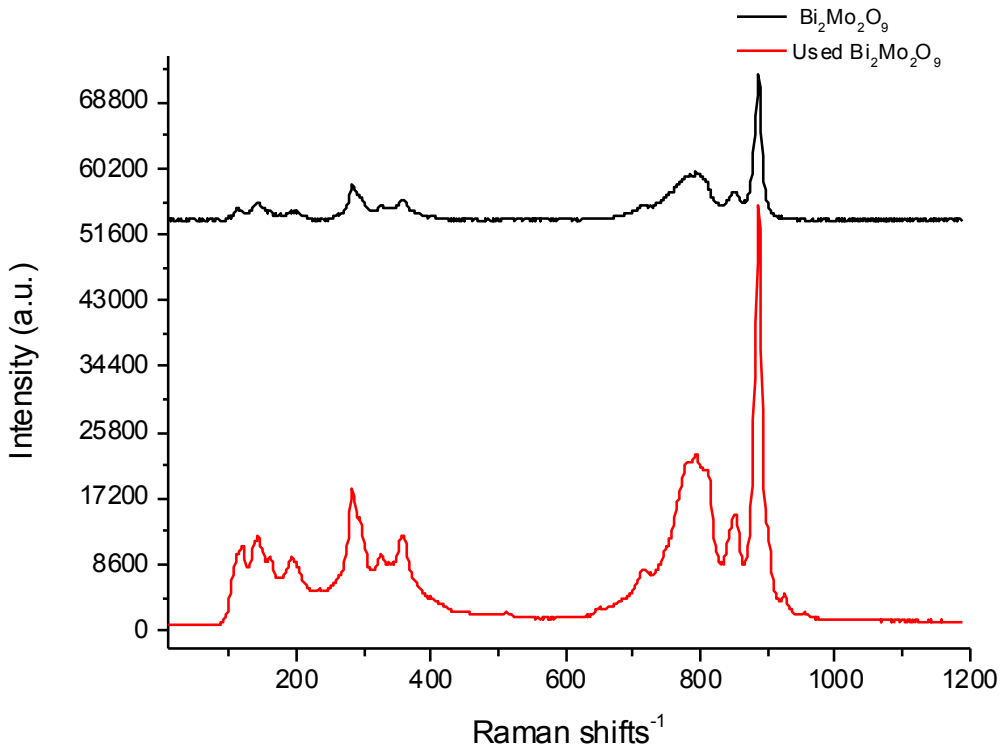

Figure 4.59 Raman result of bismuth molybdate catalyst

4.2.8. $Fe_2 (MoO_4)_3$ catalyst for ethanol and propanol and methanol.

Iron molybdate was introduced in Chapter one, It is the current commercial catalyst for methanol oxidation to formaldehyde, and this catalyst has a surface area of 5 m^2 g^{-1}, where it has excess molybdena (2.2 Mo to 1Fe), whereas the stoichiometry of $Fe_2(MoO_4)_3$ is 1.5 Mo to 1Fe. The catalyst yielded 96% formaldehyde as in figure 4.60, and showed high activity. However, 2.2 iron molybdate was also applied as catalyst for more complex alcohol oxidation to determine if is selective to the aldehyde as for methanol.

Figure 4.61 shows the temperature-programmed oxidation of ethanol on 2.2 iron molybdate. As in the figure, ethanol was converted at a temperature lower than in the methanol case, where the catalyst converted 10% of ethanol by 100 ^oC. By 120 ^oC, 20% of ethanol was converted to mainly to 65% ethylene and 35% acetaldehyde. Then at higher temperature and increased ethanol conversion, ethylene selectivity decreased, while acetaldehyde increased. Furthermore, the maximum yield of ethylene was 60% by 215 ^oC, and the maximum yield of acetaldehyde was 85% by 240 ^oC, then both ethylene and acetaldehyde decreased while CO selectivity increased, while CO2 was thye dominant product at the highest temperature[7].

Nonetheless, n-propanol has a different result in figure 4.62, where the catalyst is active by less than 100 ^oC, and 10% of n-propanol was converted to 100% propane. Moreover, the maximum yield of propane was 80% by 200 ^oC. However, propane selectivity decreased with increase of conversion and heat, while carbon monoxide increased up 200 ^oC. CO_2, dominates at the highest temperature, with some propene in between[9].

iso-propanol was oxidized on 2.2 iron molybdate catalyst as in figure 4.63. The catalytic reaction started at low temperature as with n-propanol and ethanol. The first product was acetone, at 5% conversion 100% was acetone. Acetone selectivity decreased gradually from temperature range of 100 ^oC to 275 ^oC, while propylene increased, whereas propane was produced between 300 ^oC and 400 ^oC with maximum selectivity of 5%. Nonetheless, CO formed in temperatures from 175 ^oC. CO_2 was formed at low temperatures and kept increasing with the increase of until it dominates at high temperature[10].

The TPD result in figures 4.64, 4.65 and 4.66, for ethanol, n-propanol and iso-propanol respectively, draws a map of favorite reaction pathways. Ethanol has two peaks that are related to acetaldehyde, which desorbed first, then another desorbed peak is for ethylene. However, a more complex alcohol like n-propanol has peaks associated to propane (figure 4.65, 4.66), then the second favorite is propene. However, the case of iso-propanol is slightly different from n-propanol. The first peaks are related to acetone, the second peaks are associated to propene, and the third peaks are for propane. Overall, the selectivity to aldehyde is decreased with more complex alcohols than methanol, and the selectivity toward alkene is increased. The figures below for the TPR and TPD results show that alkene products increased. In ethanol, the ethylene product was a small amount compared to acetaldehyde production, whereas in 1-propanol and 2-propanol, both had a larger production of propene. Overall, 2.2 iron molybdate was a good catalyst for alcohol oxidation to the respective aldehyde or ketone, though dehydration to the corresponding alkene competes at high conversion.

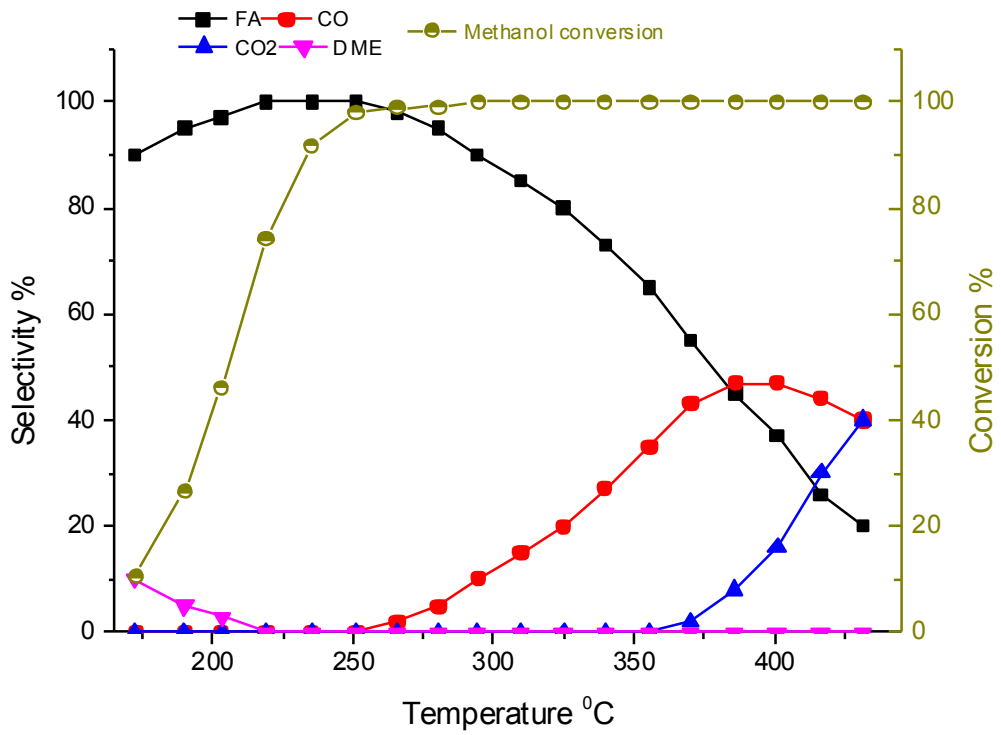

Figure 4.60 Reaction profile of Methanol oxidation on 2.2 iron molybdate catalyst

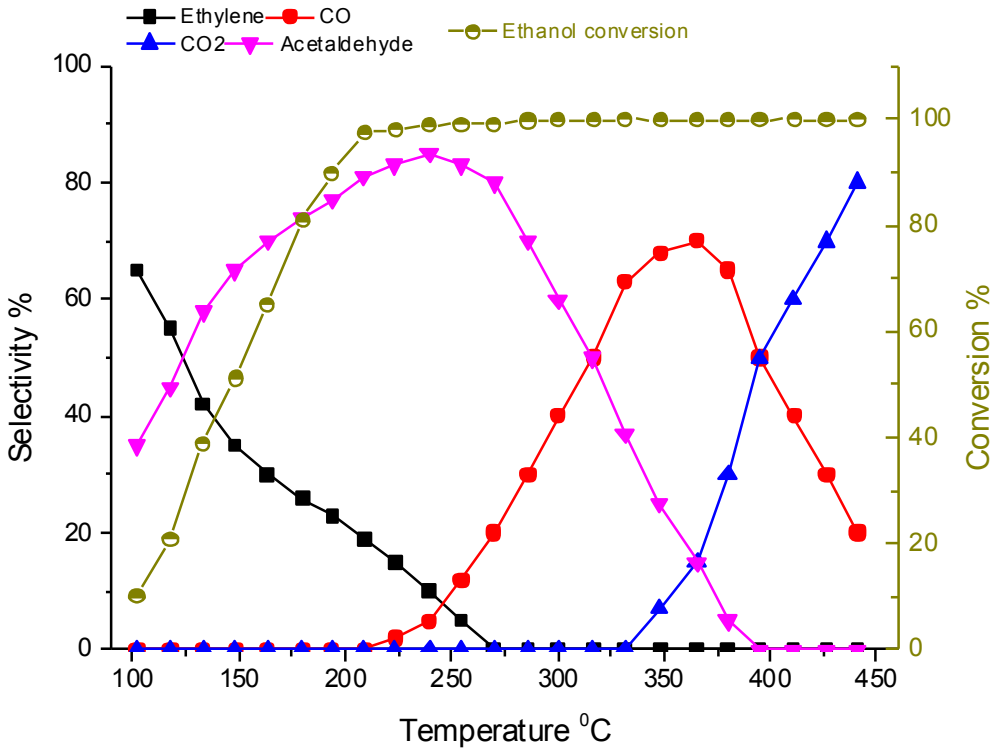

Figure 4.61 Reaction profile of Ethanol oxidation on 2.2 iron molybdate catalyst

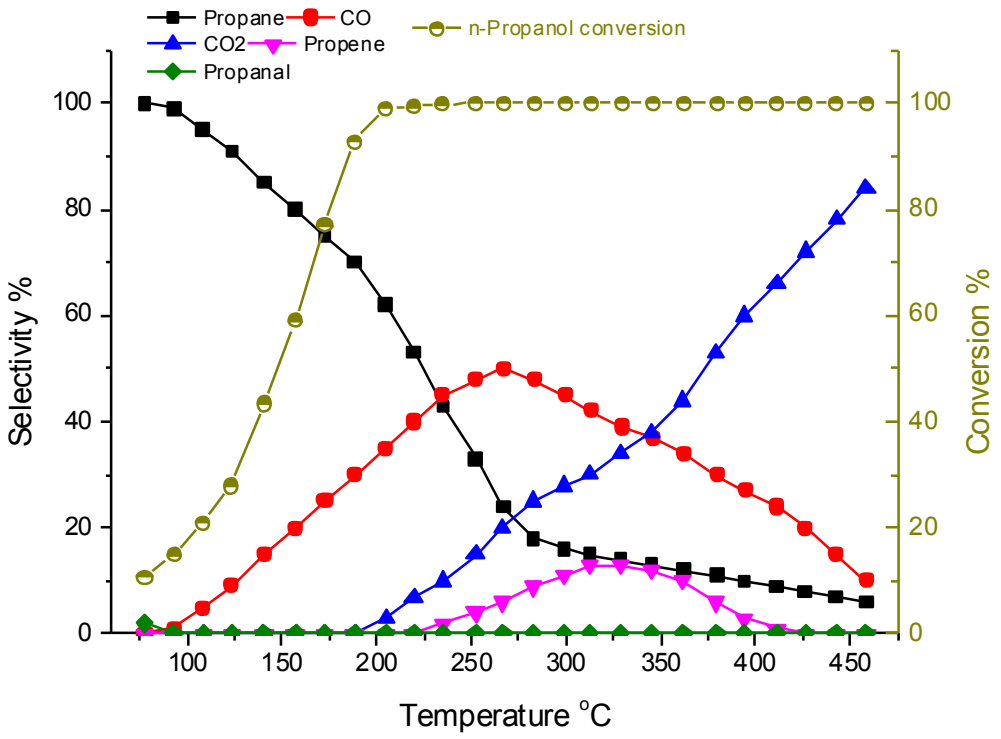

Figure 4.62 Reaction profile of n-Propanol oxidation on 2.2 Iron molybdate catalyst

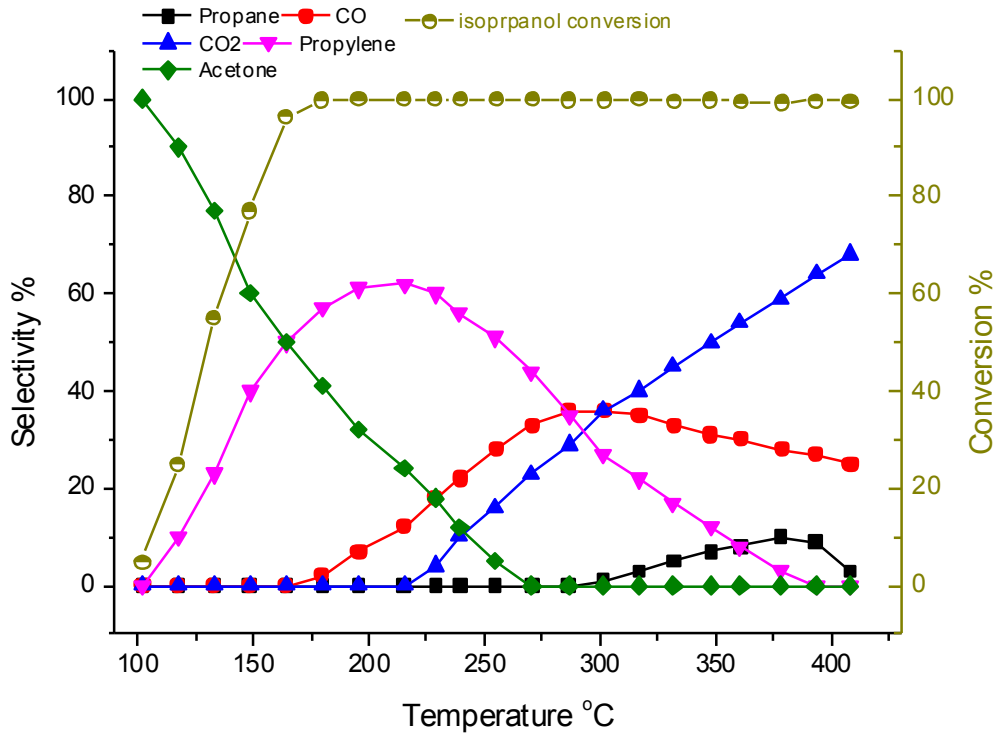

Figure 4.63 Reaction profile of iso-Propanol oxidation on 2.2 iron molybdate catalyst

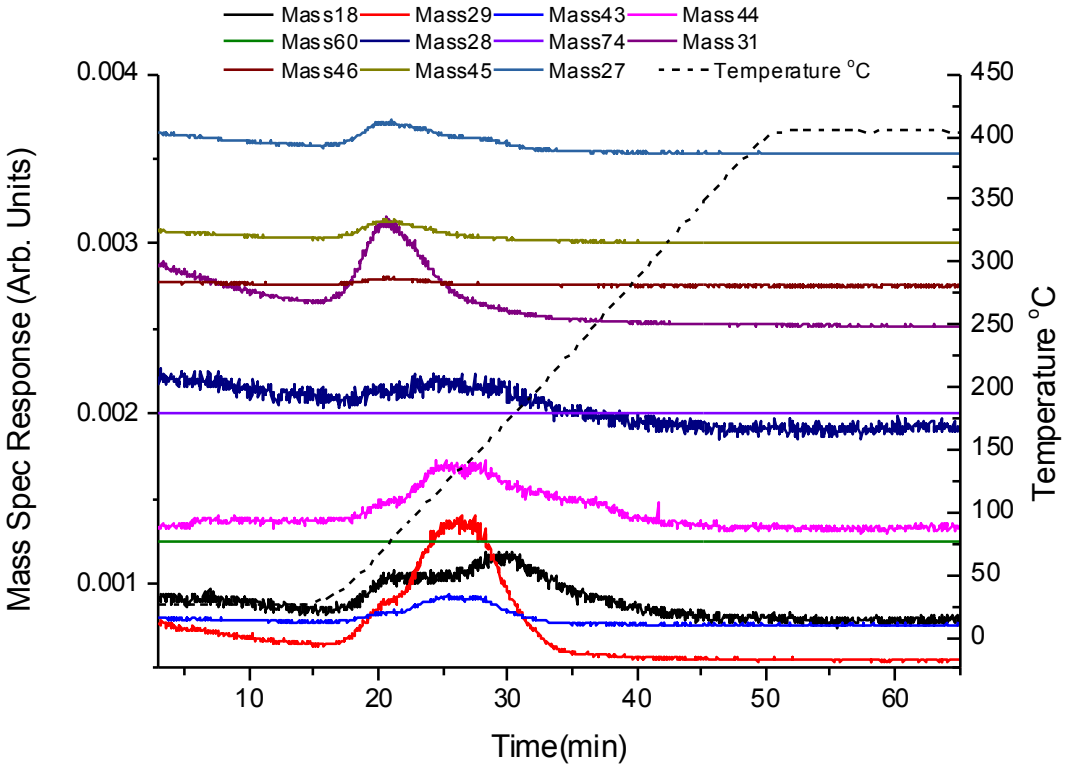

Figure 4.64 TPD result of ethanol oxidation 2.2 iron molybdate catalyst

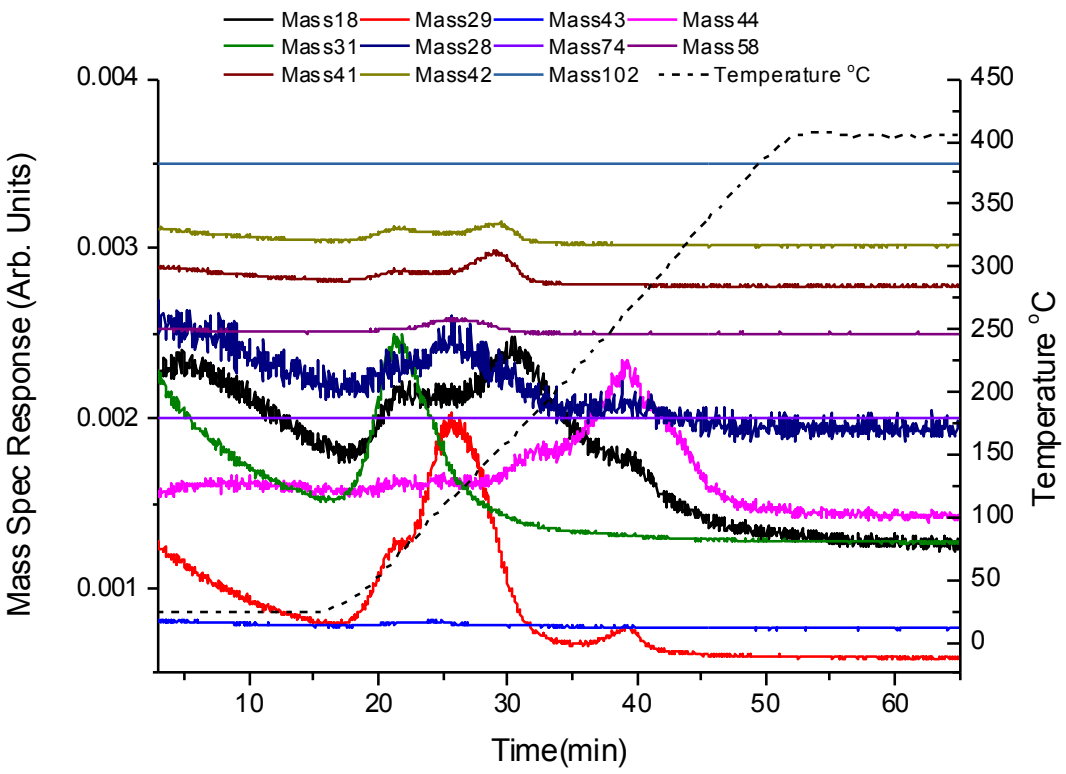

Figure 4.65 TPD result of n-Propanol oxidation on 2.2 iron molybdate catalyst

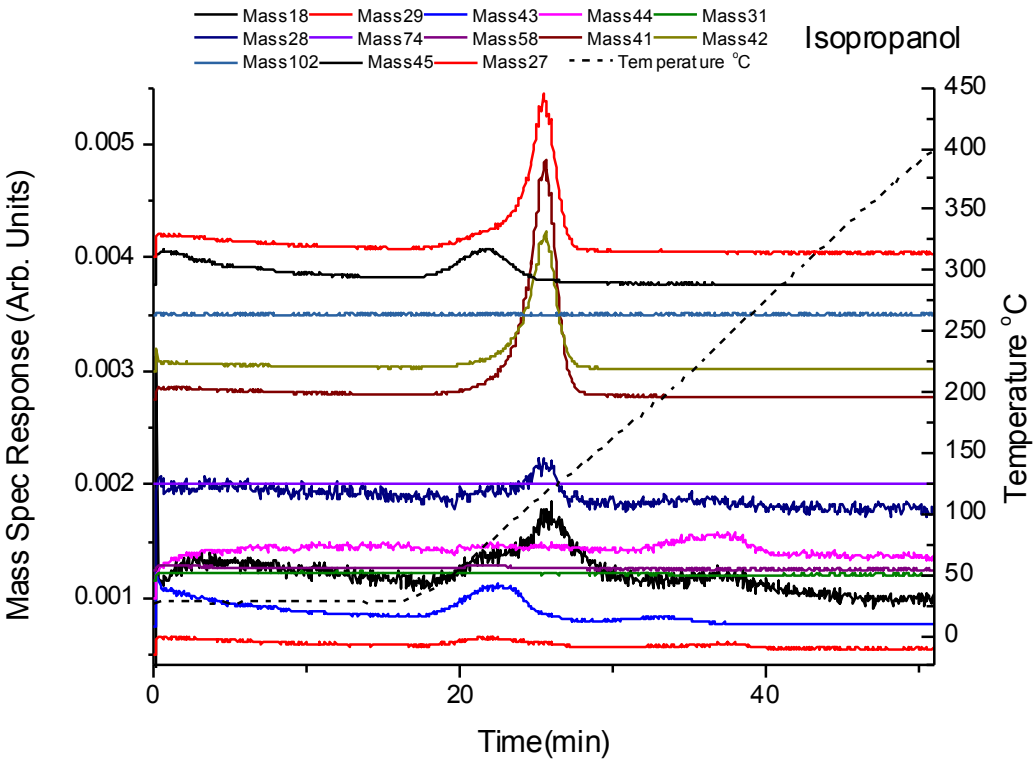

Figure 4.66 TPD result of iso-Propanol oxidation on 2.2 iron molybdate catalyst

4.3 Discussion

Catalyst	The highest FA selectivity			100% Activity	
	FA S. %	T ^{o}C.	Con.	T. ^{o}C	FA S. %
$FeVO_4$	100	116	28	205	43
2 $FeVO_4$	100	200	100	200	100
3 $FeVO_4$	100	150	10	200	100
$Fe_2(WO_4)_3$	100	250	80	350	75
2.2 $Fe_2(WO_4)_3$	100	270	80	375	70
$FeNbO_4$	100	225	40	260	40
$FeSbO_4$	92	150	6	350	3
$CuMoO_4$	100	175	18	320	80
1.5 $CuMoO_4$	100	262	43	370	50
2 $CuMoO_4$	97	190	20	300	70
$MnMoO_4$	100	255	60	375	60
1.5 $MnMoO_4$	100	255	48	325	70
2 $MnMoO_4$	100	258	50	320	72
$Bi_2Mo_2O_9$	65	240	10	360	20

Table 4.1 methanol oxidation selectivity to formaldehyde on complex oxide catalysts (FA= formaldehyde, S.= selectivity, Con. = methanol conversion and T= temperature)

4.3.1 Kinetics of alcohol oxidation

Alcohol oxidation is coordinated by the hydroxyl group (-OH) in its structure, whereas in methanol the hydroxyl is bonded to only one carbon (CH_3OH). However the rest bonded to that carbon are 3 hydrogen (-H), so, when molecule hits the surface fast with enough energy, oxygen of hydroxyl will bond to the metal that has a terminal oxygen, and the hydrogen in the hydroxyl group will bond to the surface oxygen as in eq 4.2.1. This will move the surface to an intermediate situation, another metal oxygen interact to dehydrogenate, the methyl group as in eq 4.2.2, then it leaves the surface as formaldehyde (eq 4.2.3). The surface reorders itself by eliminating water from the two hydroxyl groups that are bonded to the two metal (eq 4.2.4). Finally, the surface takes the missed lattice oxygen from the gas in re-oxidation step (eq 4.2.5)[17-22].

Formaldehyde not only the product obtained. Side reactions may occur using 2.2 iron molybdate catalyst that is selective to formaldehyde, but CO is being produced when methoxy has not interacted by its carbon hydrogen with neighbor oxygen on another metal (eq 4.2.6), then methoxy is affected by heat to decompose as CO and hydrogen. dimethyl ether is formed by reaction of two

methoxy molecules as the dehydration reaction that occurs at low temperature between adsorption intermediates (Eq 4.2.7). Even CO_2 can be formed by bonded methoxy reacting with bridging oxygen to convert to bonded formate that later decomposes as CO_2 (Eq 4.2.8). Also CO_2 is the result of full oxidation of methoxy and CO by affect of heat[17-22].

$$\mathbf{H_3C\text{-}OH + O{=}M_{(1)}\ (lattice\ oxygen) + heat \rightarrow H_3C\text{-}O\text{-}M\text{-}OH} \quad \text{(Eq 4.2.1)}$$

$$\mathbf{HO\text{-}M\text{-}OCH_3 + O{=}M_{(2)} \rightarrow H_2C^{+}O\text{-}M\text{-}OH + M\text{-}OH} \quad \text{(Eq 4.2.2)}$$

$$\mathbf{H_2C^{+}O\text{-}M\text{-}OH \rightarrow H_2C{=}O_{(g)} + M\text{-}OH} \quad \text{(Eq 4.2.3)}$$

$$\mathbf{2M\text{-}OH \rightarrow H_2O_{(g)} + O{=}M + M^{+}} \quad \text{(Eq 4.2.4)}$$

$$\mathbf{\tfrac{1}{2}\ O_2 + M^{+} \rightarrow O{=}M} \quad \text{(Eq 4.2.5)}$$

$$\mathbf{HO\text{-}M\text{-}OCH_3 \rightarrow CO + O{=}M + 2H_2} \quad \text{(Eq 4.2.6)}$$

$$\mathbf{HO\text{-}M\text{-}OCH_3 + M\text{-}O\text{-}M \rightarrow O\text{-}CH_2O\text{-}M\text{-}OH + 2M^{+}} \quad \text{(Eq 4.2.7)}$$

$$\mathbf{HO\text{-}M\text{-}OCH_3 + HO\text{-}M\text{-}OCH_3 \rightarrow H_3C\text{-}O\text{-}CH_3 + H_2O + M^{+} + O{=}M} \quad \text{(Eq 4.2.8)}$$

Still, when more complex alcohols are used, the situation is changed as new products are formed, such as alkenes and the selectivity toward aldehydes decreased with the decrease of hydrogen number that bonded to the hydroxyl carbon. When the ethanol molecule hits the surface and is adsorbed, then the ethoxy is formed, as in equation 4.2.9, and then ethoxy reacts with neighbor terminal oxygen to subtract hydrogen from the carbon bonded to the surface by hydroxyl oxygen, as in equation 4.2.10. This carbon has a positive charge that makes it unstable, and it desorbs as acetaldehyde (eq 4.2.11). Then the same steps are repeated as in the methanol case, where the water molecule desorbs (eq 4.2.12). The missing oxygen will be replaced from the gaseous oxygen as the final re-oxidation step (eq 4.2.13).

The new product is alkene, which has a lower selectivity than aldehyde in ethanol oxidation. Where acetaldehyde is formed after ethoxy shared hydrogen from the other carbon next to the hydroxyl carbon (**CH_3**-CH_2O-surface) with neighbor oxygen in the surface, this then leads to be in positive charge (eq 4.2.14), and to move from that positive intermediates compound (**$C^{+}H_2CH_2$**-O-surface**)** desorbs as ethylene ($CH_2{=}CH_2$) as in equation 4.2.15, It is simply a dehydration reaction at acid sites for which the C-O bond in the alcohol breaks. Later the same steps

for surface re-oxidation by eliminating water, and using gaseous oxygen to replace the missing oxygen. Carbon dioxide are two combustive products the same as in the methanol case, which are results of partial oxidation in CO, then followed by full oxidation to CO_2 that increases with increased temperature.

$$\mathbf{CH_3CH_2OH + O{=}M \rightarrow CH_3CH_2O\text{-}M\text{-}OH} \quad \text{(Eq 4.2.9)}$$

$$\mathbf{CH_3CH_2O\text{-}M\text{-}OH + O{=}M \rightarrow CH_3C^{+}H\text{-}O\text{-}M\text{-}OH + M\text{--}OH} \quad \text{(Eq 4.2.10)}$$

$$\mathbf{CH_3C^{+}H\text{-}O\text{-}M\text{-}OH \rightarrow CH_3CHO + M\text{-}OH} \quad \text{(Eq 4.2.11)}$$

$$\mathbf{2M\text{-}OH \rightarrow H_2O + O{=}M + M^{+}} \quad \text{(Eq 4.2.12)}$$

$$\mathbf{1/2\ O_2 + M^{+} \rightarrow O{=}M} \quad \text{(Eq 4.2.13)}$$

$$\mathbf{CH_3CH_2O\text{-}M\text{-}OH + O{=}M \rightarrow C^{+}H_2CH_2\text{-}O\text{-}M\text{-}OH + M\text{--}OH} \quad \text{(Eq 4.2.14)}$$

$$\mathbf{C^{+}H_2CH_2\text{-}O\text{-}M\text{-}OH \rightarrow H_2C{=}CH_2 + O\text{-}M\text{-}OH} \quad \text{(Eq 4.2.15)}$$

$$\mathbf{O^{-}\text{-}M\text{-}OH + HO\text{-}M \rightarrow H_2O + O{=}M + M^{+}} \quad \text{(Eq 4.2.16)}$$

Propanol oxidation is more complex than ethanol, in which a new product was recorded, that is alkane, in addition to alkene and aldehyde, n-propanol hits the surface to bond with surface metal via hydrogen bond to the terminal oxygen that was double bonded to surface metal, making a hydroxyl group (eq 4.2.17). Then n-propoxy interacts with neighbor oxygen that subtracts hydrogen from the carbon that is in link with hydroxyl or the oxygen that bonded to the surface as in equation 4.2.18. The extracted hydrogen causes a positive charge on the carbon as stated earlier, which then converts to propanal (eq 4.2.19), while the two hydroxyl groups that bonded to the surface form water and leave the surface (eq 4.2.20), and the removed oxygen will be taken from the gas phase (eq 4.2.21) as the final re-oxidation step.

$$\mathbf{CH_3CH_2CH_2OH + O{=}M + heat \rightarrow CH_3CH_2CH_2O\text{-}M\text{-}OH} \quad \text{(Eq 4.2.17)}$$

$$\mathbf{CH_3CH_2CH_2O\text{-}M\text{-}OH + O{=}M \rightarrow}$$

$$\mathbf{CH_3CH_2C^{+}HO\text{-}M\text{-}OH + HO\text{-}M} \quad \text{(Eq 4.2.18)}$$

$$\mathbf{CH_3CH_2C^{+}HO\text{-}M\text{-}OH \rightarrow O{=}M \rightarrow CH_3CH_2CHO + HO\text{-}M} \quad \text{(Eq 4.2.19)}$$

$$\mathbf{HO\text{-}M + HO\text{-}M \rightarrow H_2O + O{=}M + M^{+}} \quad \text{(Eq 4.2.20)}$$

$$\mathbf{½\ O_2 + M^{+} \rightarrow O{=}M} \quad \text{(Eq 4.2.21)}$$

isopropanol hits the surface to form iso-propoxy (eq 4.2.22), iso-propoxy is interacts with neighbor oxygen to subtract hydrogen from the carbons that are linked to the surface via hydroxyl oxygen ($(CH_3)_2$**CH-O**-surface), which changes it to positive charged carbon (eq 4.2.23). The next step is then followed by water desorbed (eq 4.2.20), and the missing oxygen will be taken from the gas phase (eq 4.2.21).

$$\mathbf{(CH_3)_2CH\text{-}OH + O{=}M + heat \rightarrow (CH_3)_2CH\text{-}O\text{-}M\text{-}OH} \quad \text{(Eq 4.2.22)}$$

$$\mathbf{(CH_3)_2CH\text{-}O\text{-}M\text{-}OH + O{=}M \rightarrow (CH_3)_2C^{+}\text{-}O\text{-}M\text{-}OH + HO\text{-}M} \quad \text{(Eq 4.2.23)}$$

$$\mathbf{(CH_3)_2C^{+}\text{-}O\text{-}M\text{-}OH \rightarrow (CH_3)_2C{=}O + HO\text{-}M} \quad \text{(Eq 4.2.24)}$$

Propene has the same kinetics in both isomers of propanol, where in n-propanol case, n-propoxy reacted with neighboring oxygen through the carbon that is next to the hydroxyl carbon (CH_3**CH_2**CH_2O-surface) and subtracted hydrogen atom to that positively charged carbon (eq 4.2.25). Then it breaks the C-O bond and makes a double bond and leaves the oxygen bonded to the surface as hydroxyl (eq 4.2.26). iso-propanol is bonded to the surface as iso-propoxy, which interacted with neighbor oxygen that causes hydrogen subtracted from the carbon next to hydroxyl carbon (($\mathbf{CH_3}$)$_2$CH-O-surface), where consequentially, it changes to positive charge carbon (eq 4.2.27), then the product formed is propene. Where n-propanol was converted by temperature of 75 ^{o}C , and iso-propanol was converted by temperature of 100 ^{o}C, and n-propanol oxidation showed low selectivity to propanal, as it was converted to propane and propene, which is easier than the partial oxidation to propanal, where iso-propanol oxidation was converted to acetone and propene from low temperature. Likewise, propene formation leaves the catalyst with hydroxyl that reacts to form water (eq 4.2.20), finally, the missed oxygen in re-oxidation step will be taken from the gas phase (eq 4.2.21)[8-10].

$$\mathbf{CH_3CH_2CH_2O\text{-}M\text{-}OH + O{=}M \rightarrow CH_3C^{+}HCH_2O\text{-}M\text{-}OH + HO\text{-}M} \quad \text{(Eq 4.2.25)}$$

$$\mathbf{CH_3C^{+}HCH_2O\text{-}M\text{-}OH \rightarrow CH_3\,CH{=}CH_2 + HO\text{-}M} \quad \text{(Eq 4.2.26)}$$

$$\mathbf{(CH_3)_2CH\text{-}O\text{-}M\text{-}OH + O{=}M \rightarrow}$$

$$\mathbf{CH_3C(C^{+}H_2)H\text{-}O\text{-}M\text{-}OH + HO\text{-}M} \quad \text{(Eq 4.2.27)}$$

$$CH_3C(C^+H_2)H\text{-}O\text{-}M\text{-}OH \rightarrow CH_3CH{=}CH_2 + HO\text{-}M \quad \text{(Eq 4.2.28)}$$

Additionally, propane is formed by partial oxidation of both n-propoxy and iso-propoxy, in the presence of oxygen and enough heat to oxidize two molecules of propoxy. One molecule will donate hydrogen to the other propoxy molecule, and then propane desorbs, as oxidative hydrogenation (eq 4.2.29) (eq 4.2.30), which will produces a great deal of CO that will decrease with the decrease of propane selectivity as in the result section (figure 4.62 and 4.63). Here, CO was produced at a low temperature, which then decreased with increase of heat, while not a result of full combustion that normally occurs at high temperature like CO_2 in the same experiments, where with the increase of heat, all products selectivity dropped and CO_2 selectivity increased.

$$2\ CH_3CH_2CH_2O\text{-}M\text{-}OH + 0.5\ O_2 \rightarrow CH_3CH_2CH_3 + 3CO + 4H_2 \quad \text{(Eq 4.2.29)}$$
$$2\ (CH_3)_2CH\text{-}O\text{-}M\text{-}OH + 1.5\ O_2 \rightarrow CH_3CH_2CH_3 + 3CO + 4H_2 \quad \text{(Eq 4.1.30)}$$

4.3.2 Catalyst anionic activity

In Chapter 3, single oxides were tested for methanol oxidation, while more complex oxide catalysts were chosen for this chapter based on the materials in the third chapter. In the case of iron molybdate, iron oxide catalyst was tested, which showed 100% selectivity to CO_2 at any conversion. It was an active catalyst, it converts methanol by 180 ^oC. Also, molybdenum oxide catalyst was tested, and was found to be selective to formaldehyde. However, the catalyst was poor in activity, only about 50% of methanol was converted by 500 ^oC. Overall, iron molybdate catalyst is 96% selective to formaldehyde, and it converts 96% of methanol by 300 ^oC, from which can be seen that iron molybdate catalyst is selective because of the molybdenum part (cation), and the activity comes from the iron part (anion).

Iron was replaced by three other metals, copper, manganese and bismuth. However, in copper molybdate, it is well known that copper has oxidation state of $2+$[14], whereas, iron has 3+ oxidation state. However, in terms of activity, where

iron molybdate first converted (10%) methanol by temperature of 180 ^{o}C, whereas copper molybdate first converted methanol by 160 ^{o}C and manganese molybdate catalyst is more active catalyst, it is converting methanol by 110 ^{o}C, because the lower oxidation state of the catalyst is the more active. Still, vanadate catalysts are the most active catalysts in our study, the three ratio catalysts of iron vanadate converted 100% of methanol by 200 ^{o}C (table4.1) , this is because vanadium is very active oxide catalyst for methanol oxidation, many paper published[23-26] confirmed that V=O units is the reason of its high activity to adsorb methanol to methoxy, then to formaldehyde.

4.3.3 Catalyst cationic selectivity

The two parts of iron molybdate catalyst were illustrated earlier this section (4.3.2). The first part is the activity or anionic part (iron) as discussed, the second part of iron molybdate is the selectivity part (molybdenum), as molybdenum was replaced by four others metals.

In Chapter 3, it was shown that the oxidation state is a major factor for selectivity to formaldehyde. However, this showed selectivity to formaldehyde for more than 4+ catalysts. Where niobium oxide catalyst was 80% selective to formaldehyde at 50% conversion, then the catalyst turned out to be selective with higher conversion and heat to CO; and was not even active up 350 ^{o}C. In iron niobate the activity was improved converting methanol by 180 ^{o}C, and selectivity with 100% by 225 ^{o}C with methanol conversion of 30%, it is better result than niobium oxide in terms of activity and less heat for the catalyst needing to be activated, but the catalyst again is selective to CO with increase of conversion and heat, which makes it not a very selective catalyst as desired. Moreover, iron antimonite was very selective to formaldehyde, where the best result was 55% selectivity and 50% methanol conversion, then the catalyst turned out to be selective to CO and CO_2.

One 5+ metal wise chosen is selective catalyst, which is vanadium that is prepared with iron. The stoichiometry iron vanadate is fairly good, where the best point was by 225 ^{o}C with 90% formaldehyde selectivity and 60% methanol conversion, whereas, with more vanadium ratio (V/Fe=2) the catalyst is 100% selective to formaldehyde with 100% methanol conversion. Moreover,

stoichiometry iron tungstate is a selective catalyst to formaldehyde, where it is 100% selective to formaldehyde at low conversion, and then the best point was 90% selectivity and 85% conversion. However, using (W/Fe=2.2) iron tungstate has the best result, with 95% formaldehyde selectivity with 85% methanol conversion, when CO and CO_2 increased with increase of heat.

Thus, the only part changed is molybdenum, and iron stayed constant or in the structures of the four metals catalyst, where the selectivity was a great deal changed from one catalyst to another, some are selective like vanadium and tungsten, and some are poor like antimony and niobium. Thus, the selectivity is controlled by this part, which gives an ideal rule that helps to make an active and selective catalyst as desired by changing which part to reach the goaled product. This is further proof of the result discussed in Chapter 3. However, this part is usually poor in activity, where the heat needed to activate the catalyst cannot be the right heat to obtain the desired product before being full oxidized by heat.

4.3.4 Catalyst cationic segregation and active phase

The cationic part is the selective part to formaldehyde. If the surface was shared equally between the cationic part (molybdenum), and the active part (iron), the result should contain products that cation part is selected to (formaldehyde), and products that anion is selected to (CO, CO_2). Because the surface is in touch with adsorbents, it is pathway redirector to which products, but the real result is only related to cation part, like iron molybdate is selective to formaldehyde not to CO or to CO_2. In other words, the surface only is covered by cation, and underneath the surface is a mix of cation and anion. The other proof of that is when iron is changed to copper or manganese, the same is repeated. Neither copper nor manganese was involved in the adsorption reaction, and it is not a special case for iron. Another proof is in the characterization of these catalysts by XPS, it is energetic to inter within a few layers, this gives an idea that it is fully covered by layer of cations double bonded to terminal oxygen, and then those cations are bonded from underneath to a layer that is mix of cations and anions, because cations with more oxidation state are more stable for the catalyst to be on the

surface and ends by making a double bond with oxygen. That double bond relaxes the whole surface structure with low surface free energy[26].

The main problem in these systems is in their structures. If that surface cation volatized, this leaves the whole structure with less ratio of cation, and in sequence, that deactivates the catalyst as the cation is the selective part, and even more cations covering the surface results in more selectivity toward formaldehyde. In other words, if the cation ratio is increased to in excess of the stoichiometry ratio, the extra cation will be all in the surface as single oxide linked to the surface. On the other hand, anion will be further from the surface than in the stoichiometric structure, which is even further away from the whole adsorption process, and less affective on the production pathway. This leads to more selectivity than the stoichiometric catalyst, whereas activity will not be affected that much, because the anion works as electrons feeder from the bulk to a surface involved in adsorption, and has a change in its electrons structure[17-22].

In the result section (4.2) manganese molybdate catalyst is an example that has excess molybdenum as Mo/Mn=1.5 ratio, and Mo/Mn=2 ratio beside the stoichiometric ratio, where the stoichiometry manganese molybdate catalyst is 100% selective to formaldehyde at low methanol conversion up to 65% and temperature of 265 ^{o}C. Then, when the temperature increased and methanol conversion increased, the selectivity to formaldehyde decreased and CO, then CO kept increasing with increase of heat up to 50% selectivity by 400 ^{o}C with 100% methanol conversion. The ratio 1.5 manganese molybdate is also 100% selective to formaldehyde at low methanol conversion, where by 100% methanol the selectivity is 70% formaldehyde, which is better formaldehyde yield than the stoichiometry catalyst with less combustive CO. Moreover, manganese molybdate catalyst with more excessed molybdenum (Mo/Mn=2) is more selective to formaldehyde than the two previous manganese molybdate catalysts, where by 100% methanol conversion the selectivity of formaldehyde is 75%. The point is that the activity did not change much with excess molybdenum; there is a little change, as explained earlier in anionic activity section, but the change was not huge, because anion is still doing its job by enhancing activity within the bulk

while the surface is covered by cations. Furthermore, it is the same result when repeated in copper molybdate, iron vanadate and iron tungstate.

4.3.5 Selected catalysts

The mean of selected catalyst for methanol oxidation in this study is that the catalyst converts methanol to formaldehyde, where an efficient catalyst is when it converts 100% of methanol with no need of unreacted methanol recycling. That catalyst should convert every methanol molecule to formaldehyde, then the reducing heat is an honor target for a greener environment. While iron molybdate catalyst has the best result with 95% selective to formaldehyde and 94% methanol conversion by approximately 300 ^{o}C, any better yield is an achievement in this study. Iron vanadate catalyst with V/Fe =2 is a more selective catalyst than iron molybdate catalyst, as it is 100% selective to formaldehyde and converts 100% methanol by 200 ^{o}C, which is the best catalyst ever tested in this study. The right yield was achieved and even the heat was reduced. Even the active phase as ratio (V/Fe=3) and the stoichiometry iron vanadate catalysts are less efficient than ratio 2 iron vanadate catalyst.

Although good catalyst were found, they are not better than iron molybdate catalyst, which makes them interesting catalysts. These are iron tungstate catalysts, manganese molybdate catalysts and copper molybdate catalysts, but they are still selective to formaldehyde at lower percentage than iron molybdate catalyst and iron vanadate catalyst. The average of formaldehyde selectivity in these catalysts is 75% where the rest is CO. However, CO is less combustive than CO_2, which is worthy sign for future modification on these catalysts to reach better formaldehyde yields. The rule can be used to reach the active phase, like iron vanadate with ratio 2 as the selective catalyst and the active phase compared with the rest of iron vanadate catalysts that have different ratios. Iron tungstate catalyst especially was expected to be better than molybdate catalysts, because the single oxide of tungsten was 100% selective to formaldehyde but not very active.

4.4 Conclusion

In conclusion, alcohol oxidation is changed from simple alcohols to more complex in terms of which products are converted to. Such as where methanol is converted to formaldehyde, and ethanol is converted to acetaldehyde with low production to ethylene. However, this pathway to aldehyde decreased with decrease of hydrogen number that linked to hydroxyl carbon. The other pathway is alkene instead of aldehyde as in the case n-propanol oxidation, and iso-propanol oxidation on iron molybdate.

Moreover, the result above confirms that the catalyst has two important parts, the cationic part and anionic part, and each part has a special job. The anionic part is the activity responsible part, and cations are the selective part. Thus any change of two ratio more than stoichiometric ratio leads to change in the catalytic behavior: increasing the cation ratio will increase the selectivity to formaldehyde with no big change in the catalytic activity, because excess cations segregate on the surface leaving a mix of anion and cation on the bulk.

Furthermore, the targeted objectives were achieved in this chapter by finding a new selective catalyst: this catalyst is iron vanadate with ratio (V/Fe=2), which is 100% selective to formaldehyde at 100% methanol by 200 ^{o}C. However, iron tungstate, manganese molybdate and copper molybdate catalysts are also selective catalysts to formaldehyde and CO.

4.5 References

[1] K. Routray, W. Zhou, C. J. Kiely, I. E. Wachs. (2010). Catalysis science of methanol oxidation over iron vanadate catalysts: nature of the catalytic active sites. ACS: 1, 54-66.
[2] R. Haggblad, J. B. Wagner, S. Hansen, A. Andersson. (2008). Oxidation of methanol to formaldehyde over a series of $Fe_{1-x}Al_x$-V-oxide catalysts. Journal of catalysis: 258, 345-355.
[3] E. Steen, M. Schnobel, R. Walsh, T. Riedel. (1997). Time on stream behavior in the partial oxidation propene over iron antimony oxide. Applied catalysis A: General: 165, 349-356.
[4] M. D. Allen, G. J. Hutchings, M. Bowker. (2001). Iron antimony catalysts for the ammoxidation of propene to acrylonitrile: comments on the method of preparation of tellurium promoted catalysts. Applied catalysis A: General: 217, 33-39.

[5] J. Jung, H. Kim, A. Choi, Y. Chung, T. Kim, S. Lee, S. Oh, I. Song. (2006). Preparation, Characterization, and catalytic activity of bismuth molybdate catalysts for oxidative dehydrogenation of n-butene into 1,3-butadiene. Journal of molecular catalysis A: Chemical: 259, 166-170.
[6] D. Koop, M. Coon. (1985). Role of alcohol P-450-Oxygenase (APO) in microsomal ethanol oxidation. Ankho international Inc: 2, 23-26.
[7] L. Mattos, F. Noronha. (2005). Partial oxidation of ethanol on supported Pt catalysts. Journal of power source: 145, 10-15.
[8] A. Ali, F. Zaera. (2002). Kinetic study on the selective catalytic oxidation of 2-propanol to acetone over nickel foils. Journal of molecular catalysis A: Chemical: 177, 215-235.
[9] S. Liu, S. Yang. (2008). Complete oxidation of 2-propanol over gold-based catalysts supported on metal oxides. Applied catalysis A: General: 334, 92-99.
[10] L. Yerman, N. Homs, P. Piscina. (2012). Hydrogen production from oxidative steam-reforming of n-propanol over Ni/Y_2O_3-ZrO_2 catalysts. Internationl journal of hydrogen energy: 37, 7094-7100.
[11]J. Deng, J. Jiang, Y. Zhang, X. Lin, C. Du, Y. Xiong. (2008). $FeVO_4$ as a highly active heterogeneous Fenton-like catalyst towards the degradation of orange II. Applied catalysis B: Environmental: 84, 468-473.
[12]A.K. Sriraman, A.K. Tyagi. (2003). A new method of $Fe_2(WO_4)_3$ preparation and its thermal stability. Thermochimica Acta: 406, 29-33.
[13]C. Lu, Y. Wong. (1995). Fabrication of ferroelectric lead iron tungstate ceramic via a two-stage solid-state reaction. Ceramics international: 21, 413-419.
[14] R. M. Thompson, H. Yang, R. T. Downs. (2012). Packing systematics and structural relationships of the new copper molybdate markascherite and related minerals. American mineralogist: 97, 1977-1986.
[15] A. Clearfield, A. Moini, P. R. Rudolf. (1985).Preparation and Structure of Manganese Molybdates. Inorg. Chem: 24, 4606-4609
[16] Franklin D. Hardcastlet and Israel E. Wachs. (1991). Molecular Structure of Molybdenum Oxide in Bismuth Molybdates by Raman Spectroscopy. The Journal of Physical Chemistry: 95, 10763-10772.
[17] Kiennemann, A., Soares, A. P. V., Portela, M. F.(2004) *Methanol selective oxidation to formaldehyde over iron-molybdate catalysts*. Taylor & Francis. 47, 125-174.
[18] Bowker, M., Holroyd, R., House, M., Bracey, R., Bamroongowndee, C., Carley A. and Shannon M. (2008). *The Selective Oxidation of Methanol on Iron Molybdate Catalysts*. Springer science, 48, 158-165.
[19] Michael Bowker, Albert F. Carley, Matthew House. (2008). *Contrasting the Behaviour of MoO3 and MoO2 for the Oxidation of Methanol*. Catal Lett. 120, 34–39.
[20] House, M.P., Shannon, M.D. and Bowker, M.(2008). *Surface Segregation in Iron Molybdate Catalysts*. Springer science,122, 210-213.
[21] Bowker, M., Holroyd, R., Elliott, A., Morrall, P., Alouche, A., Entwistle, C. and Toerncrona, A.(2002). *The selective oxidation of methanol to formaldehyde on iron molybdate catalysts and on component oxides*. Plenum Publishing Corporation,83, 3-4.

[22] Bowker, M., Carley, A. and House, M.(2007). *Selective oxidation of methanol on iron molybdate catalysts and the effects of surface reduction*. Journal of catalysis, 252, 88-96.
[23]Nouralishahi, A. A. Khodadadi, A. M. Rashidi, Y. Mortazavi. (2013). Vanadium oxide decorated carbon nanotubes as a promising support of Pt nanoparticles for methanol electro-oxidation reaction. Journal of Colloid and Interface Science: 393, 291–299
[24]H. Golinska, P. Decyk, M. Ziolek. (2011). Vanadium and antimony supported NbSiO**x**—Characterisation and catalytic properties in methanol oxidation. Catalysis Today: 169, 242–248.
[25]T. Feng and J.M. Vohs. (2004). A TPD study of the partial oxidation of methanol to formaldehyde on CeO2-supported vanadium oxide. Journal of Catalysis: 221, 619–629.
[26] E. Lugscheider, K. Bobzin, St. B¨arwulf, Th. Hornig. (2000). Oxidation characteristics and surface energy of chromium based hardcoatings for use in semisolid forming tools. Surface and Coatings Technology 133-134, 540-547.

5. The selective oxidation of methanol on catalysts doped surface.

5.1. Introduction

Chapter 5 will illustrate doped surface of iron molybdate and other catalysts using methods of preparation like impregnation. This method was used rather than co-precipitation method, which was used for most of the previous catalysts, as it also shows the catalytic behaviour in modified surfaces.

5.2 Result

Table 1 below shows the surface areas of all catalysts that were tested.

Catalyst	Surface area $m^2.g^{-1}$
2.2 $Fe_2(MoO_4)_2$ support	6
2% $WO_3/Fe_2(MoO_4)_3$ catalyst	3
2% V_2O_5/ $Fe_2(MoO_4)_3$ catalyst	5
2% $Fe_2(WO_4)_3/Fe_2(MoO_4)_3$ catalyst	4
2% $FeVO_4$/ $Fe_2(MoO_4)_3$ catalyst	3
2% $MnMoO_4$/ $Fe_2(MoO_4)_3$ catalyst	5
2% $CuMoO_4$/ $Fe_2(MoO_4)_3$ catalyst	6
3% MoO_3/Fe_2O_3 catalyst	9
6% MoO_3/C catalyst	37
1% Nano-gold/MoO_3 catalyst	1
1% Nano-gold/$Fe_2(MoO_4)_3$ catalyst	4

Table 1 Surface area of chapter 5's catalysts

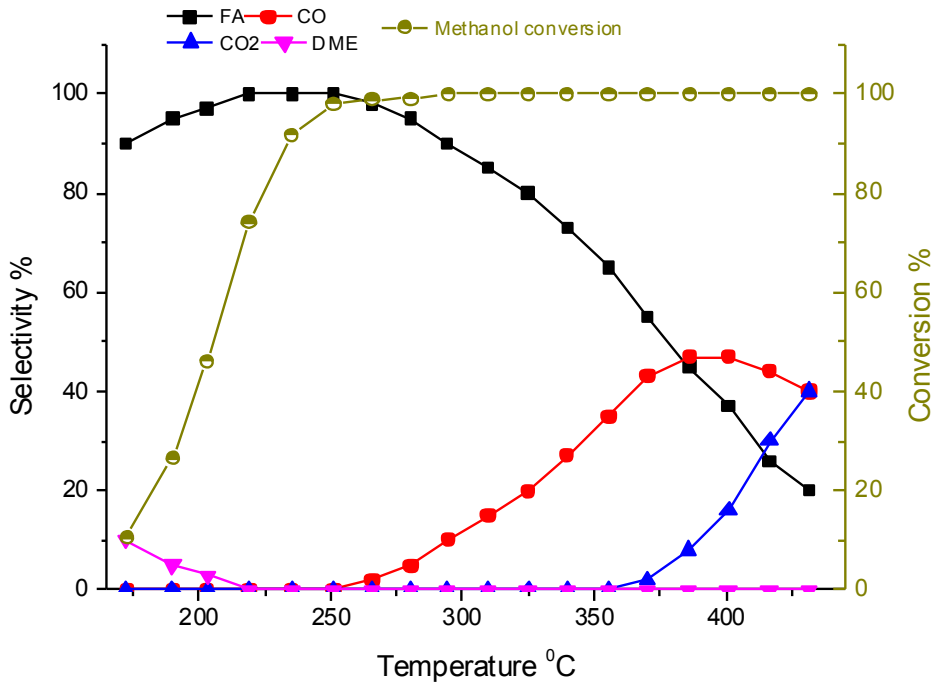

Figure 5.1 Reaction profile of 2.2 iron molybdate catalyst

5.2.1 (2%) $WO_3/Fe_2(MoO_4)_3$ catalyst

$WO_3/Fe_2(MoO_4)_3$ as shown in figure 5.2 (XPS spectra), it shows tungsten loading on the surface of 2.2 iron molybdate. The catalyst starts converting methanol by low temperature at 150 ^oC as in figure 5.3. It is more active than iron molybdate catalyst that converts methanol by 180 ^oC, and more active than tungsten oxide catalyst that converts methanol by 250 ^oC, where the selectivity toward formaldehyde is 100% at low conversion. However, with increased conversion the selectivity to formaldehyde decreased, and carbon dioxide was produced starting from temperature 175 ^oC, which is a very low temperature compared to iron molybdate catalyst, as in iron molybdate catalyst, carbon dioxide was not produced up to temperature of 350 ^oC and above, and CO was produced at 250 ^oC, which is a lower temperature than CO_2 in iron molybdate catalyst case. Tungsten oxide never produced CO and CO_2, whereas $WO_3/Fe_2(MoO_4)_3$ catalyst produces carbon dioxide at low temperatures and then CO was produced and increased in selectivity with the increase of conversion beside CO_2. CO selectivity kept increasing up to 350 ^oC, then decreased as result of full oxidation of CO to CO_2. In the TPD result, the desorption peaks that can be seen are related to formaldehyde, CO and CO_2 (figure 5.4), which is run in

anaerobic conditions. As mentioned earlier, the surface area from this catalyst is lower than iron molybdate catalyst.

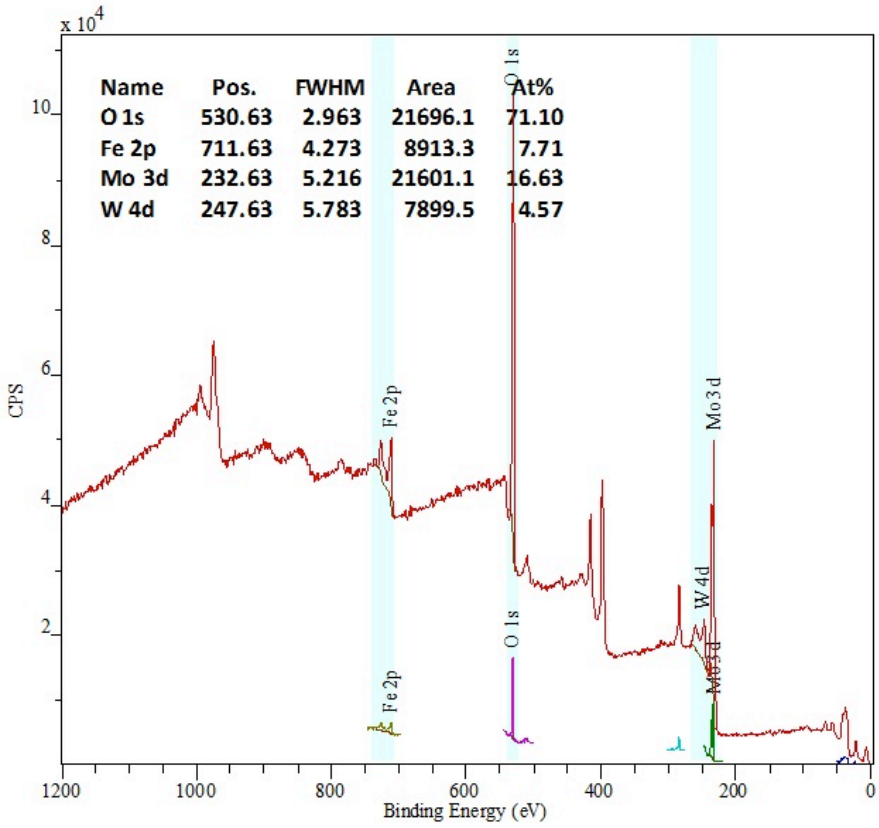

Figure 5.2 XPS spectra $WO_3/Fe_2(MoO_4)_3$ catalyst

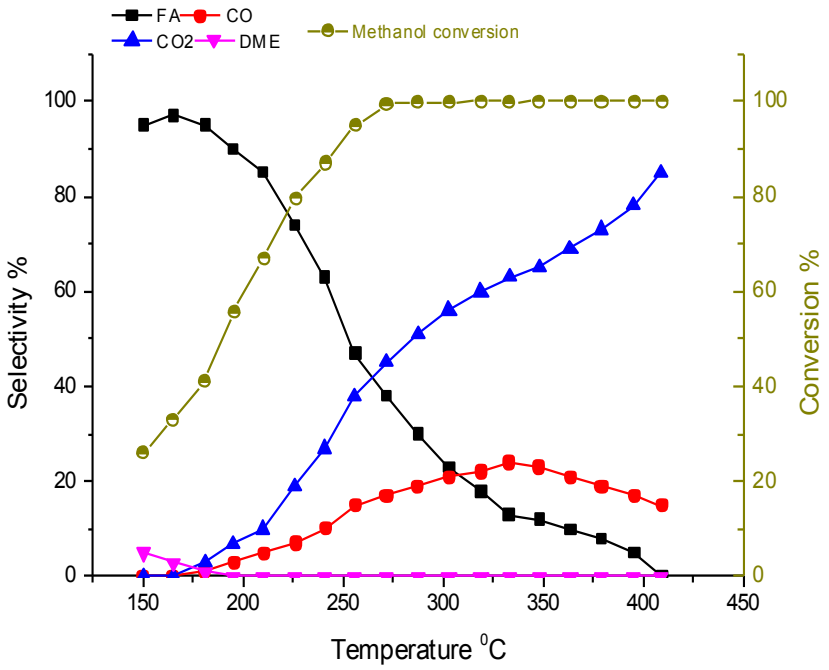

Figure 5.3 Reaction profile result of $WO_3/Fe_2(MoO_4)_3$ catalyst

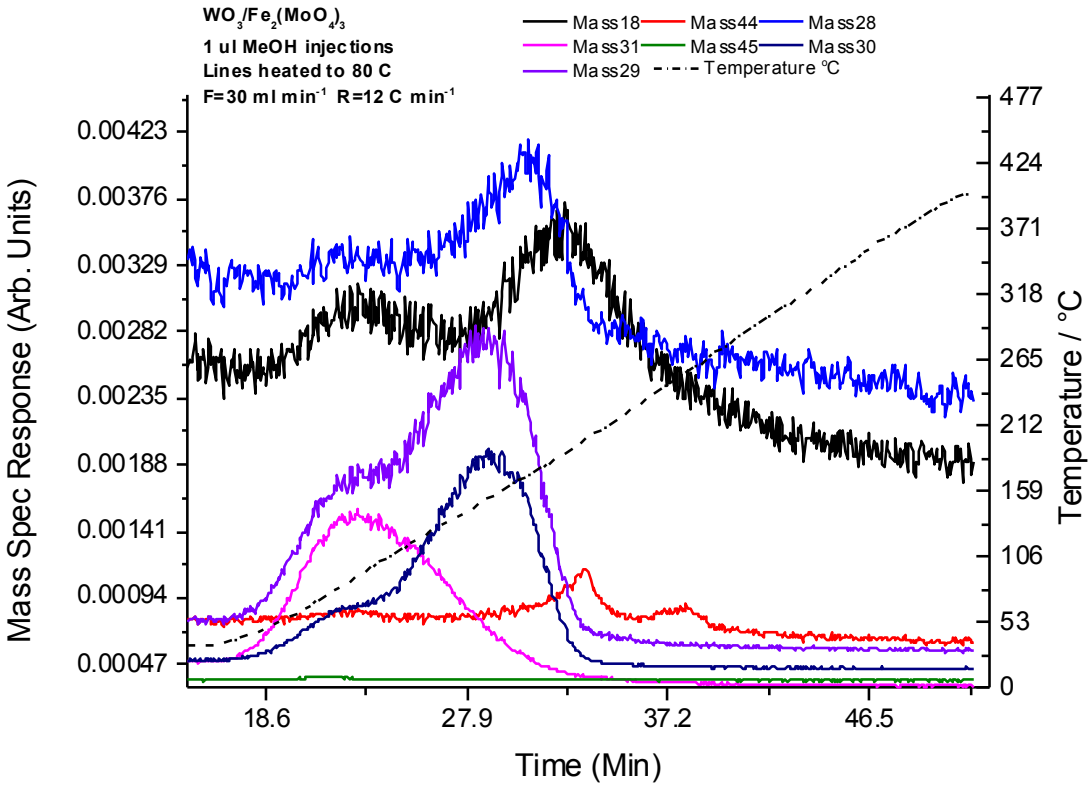

Figure 5.4 TPD result of $WO_3/Fe_2(MoO_4)_3$ catalyst

5.2.2 (2%) V_2O_5/ $Fe_2(MoO_4)_3$ catalyst

2.2 iron molybdate with 2% vanadium oxide loading (XPS spectra, figure 5.5) has a more interesting result in terms of activity. The catalyst is active by 150 ^oC (figure 5.6), Moreover, the single oxide of vanadium is also active. However, the catalyst selectivity to formaldehyde was 100% by low conversion, then formaldehyde selectivity decreased. However, the maximum formaldehyde selectivity was 80% by 250 ^oC, which is a lower yield compared to pure iron molybdate, while it is a very close result to V_2O_5 selectivity conversion, which was illustrated in Chapter 3. However the production of CO_2 is lower in this catalyst than in the case of tungsten loading, but more than in vanadium oxide catalyst itself. It is close to pure iron molybdate catalyst, which did not produce carbon dioxide up to high temperatures, which is the result of full oxidation for all products to CO_2 caused by heat. Meanwhile CO production is high using loaded vanadium on iron molybdate catalyst, where the decrease of formaldehyde

selectivity was followed by increase of CO selectivity, which makes this catalyst less selective to formaldehyde by high conversion.

However, the TPD result (figure 5.7) was compared to the results of iron molybdate catalyst and vanadium oxide in the previous chapters, and the comparison showed that vanadium oxide catalyst has the same result as vanadium loaded on iron molybdate catalyst, where iron molybdate does not show any peaks for CO and CO_2 in anaerobic conditions. However, vanadium oxide catalyst has peaks for CO, and a new peak that is related to CO_2. Neither iron molybdate nor vanadium oxide shows peaks to CO_2.

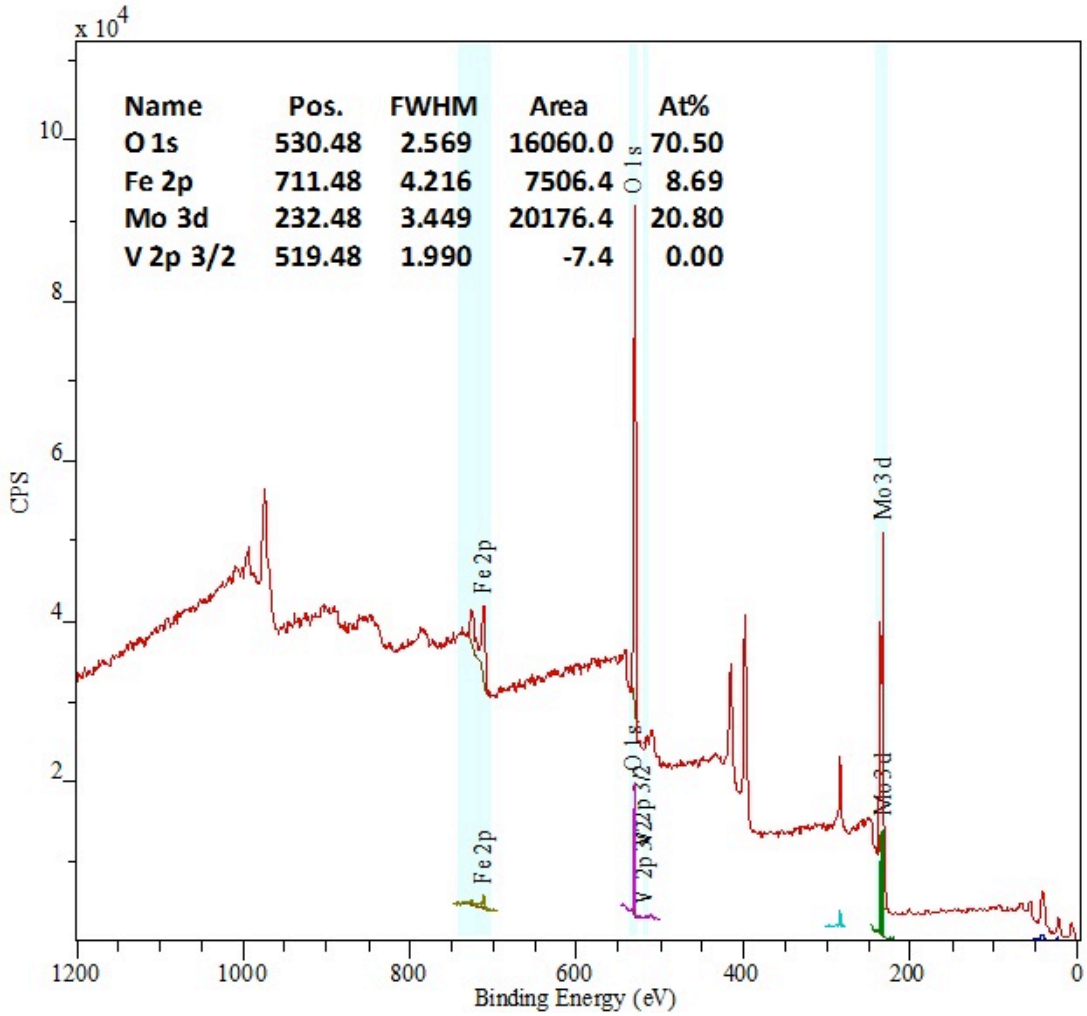

Figure 5.5 XPS spectra of V_2O_5/ $Fe_2(MoO_4)_3$ catalyst

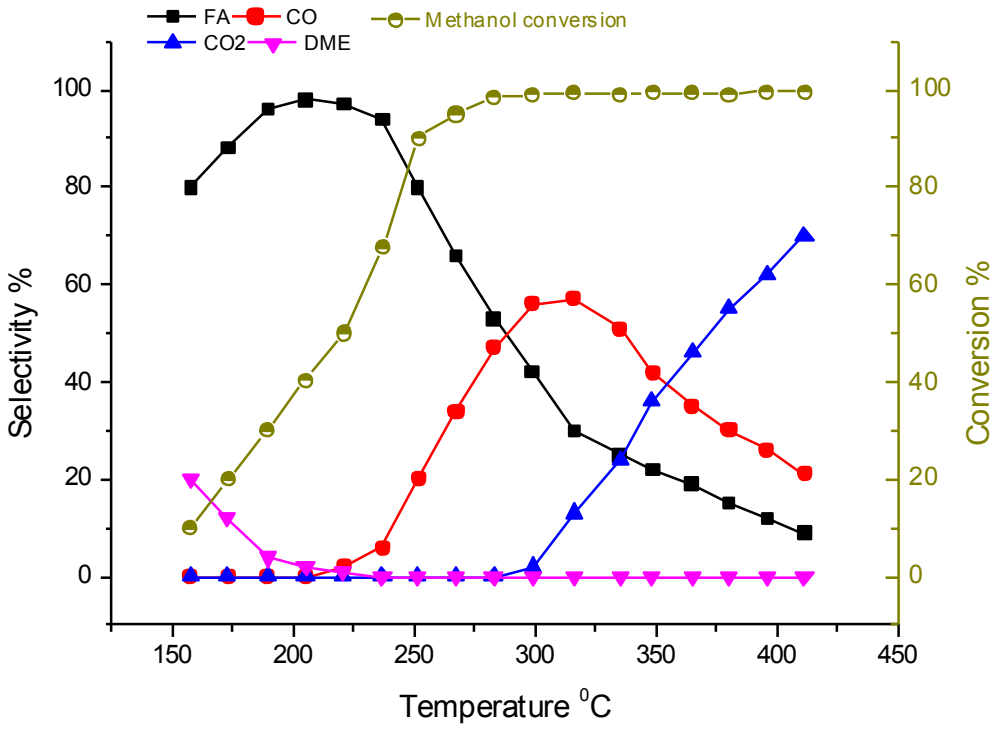

Figure 5.6 Reaction profile result of V_2O_5/ $Fe_2(MoO_4)_3$ catalyst

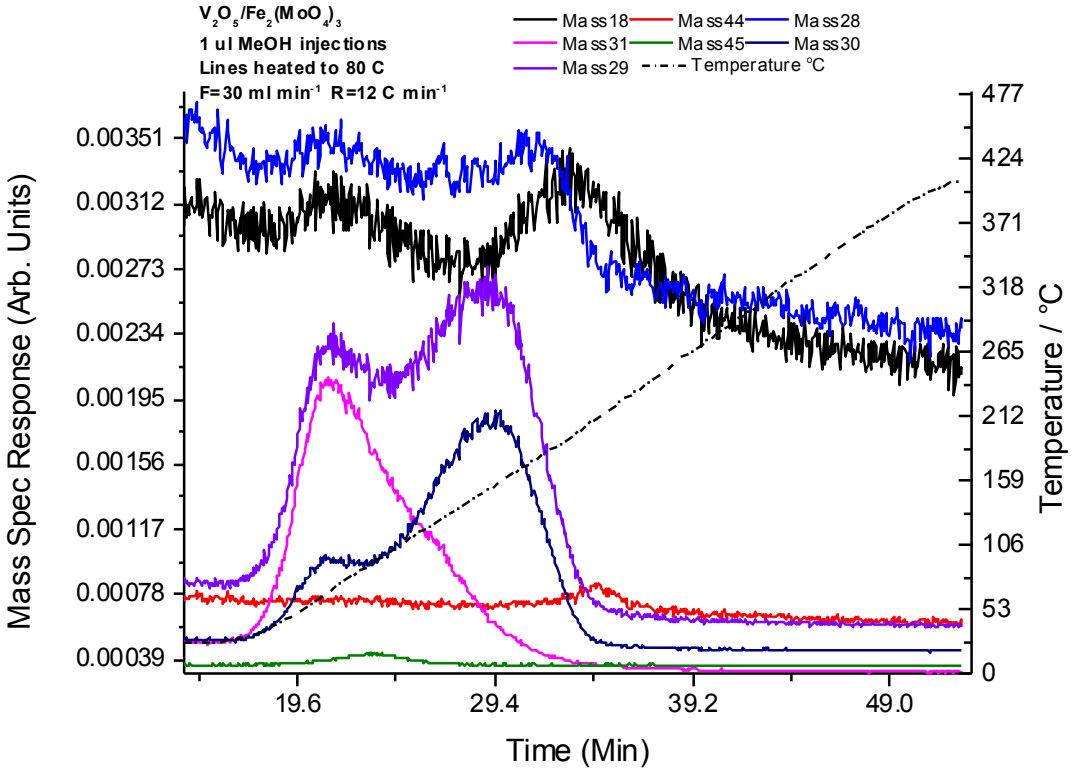

Figure 5.7 TPD result of V_2O_5/ $Fe_2(MoO_4)_3$ catalyst

5.2.3 (2%) $Fe_2(WO_4)_3/Fe_2(MoO_4)_3$ catalyst

Iron tungstate was loaded on 2.2 iron molybdate catalyst (figure 5.8), and figure 5.9 shows the catalytic behaviour of this catalyst, which shows that 100% of formaldehyde was obtained at low conversion. However, the selectivity toward formaldehyde slowly decreased with the increase of conversion and heat. However the best yield of formaldehyde was 93%, which is better than tungsten and vanadium loading, but still worse than iron molybdate catalyst. Nevertheless, the positive point is that the catalyst is more active than iron molybdate catalyst as illustrated in figure 5.1, which converts methanol by 160 ^oC (10% conversion), and converts 93% of methanol by 240 ^oC with 95% selectivity of formaldehyde. Thus it is better than iron molybdate catalyst in activity and even better than iron tungstate in activity as illustrated in Chapter Four. Moreover, the decrease formaldehyde selectivity was followed by an increase of CO selectivity and CO_2 at high temperature: the production of CO and CO_2 (at high temperature) was recorded to both catalysts iron tungstate catalyst and iron molybdate catalyst, which is associated with both catalysts.

The TPD result in figure 5.10 illustrates that peaks are related to formaldehyde (mass 30,29) , which was recorded for both iron tungstate catalyst and iron molybdate catalyst. The most interesting point is the desorption peaks, as they are sharp, which means that the surface of this catalyst is a strong adsorber. This is a better result in the case of iron molybdate and iron tungstate catalysts, while the surface area is lower than the surface area of iron molybdate and iron tungstate catalysts, as table 5.1 above shows. This catalyst has 4 $m^2.g^{-1}$, iron molybdate has 5 $m^2.g^{-1}$, and iron tungstate has 6 $m^2.g^{-1}$. However, the TPD result in figure 5.10 has peaks of CO, CO_2 and H_2 which is a sign of formate.

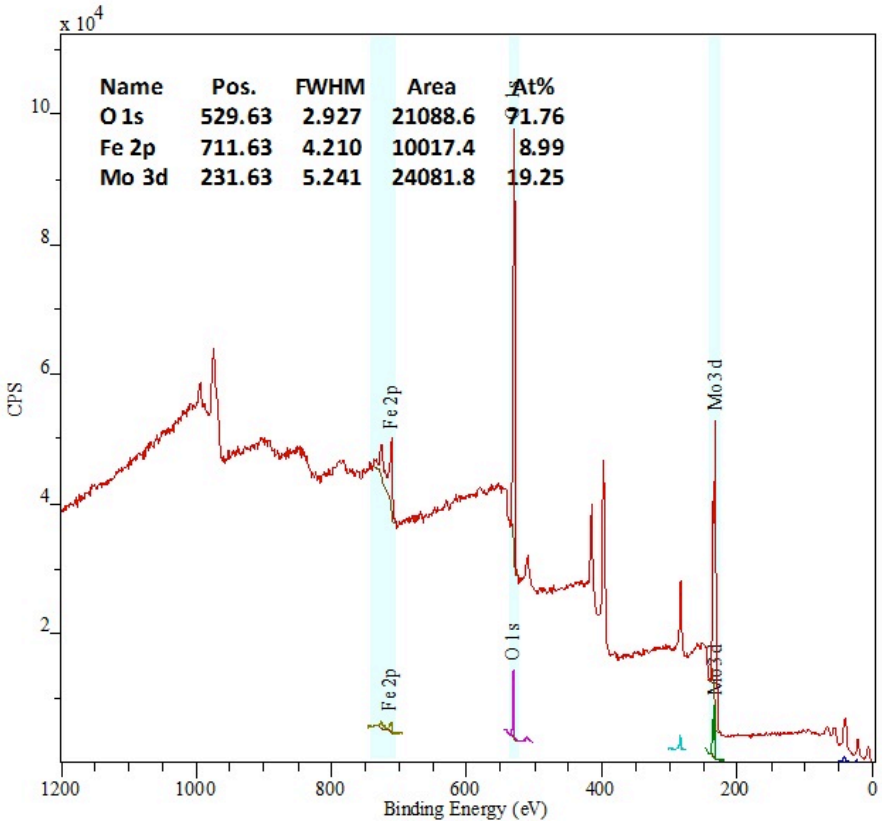

Figure 5.8 XPS spectra of (2%) $Fe_2(WO_4)_3/Fe_2(MoO_4)_3$ catalyst

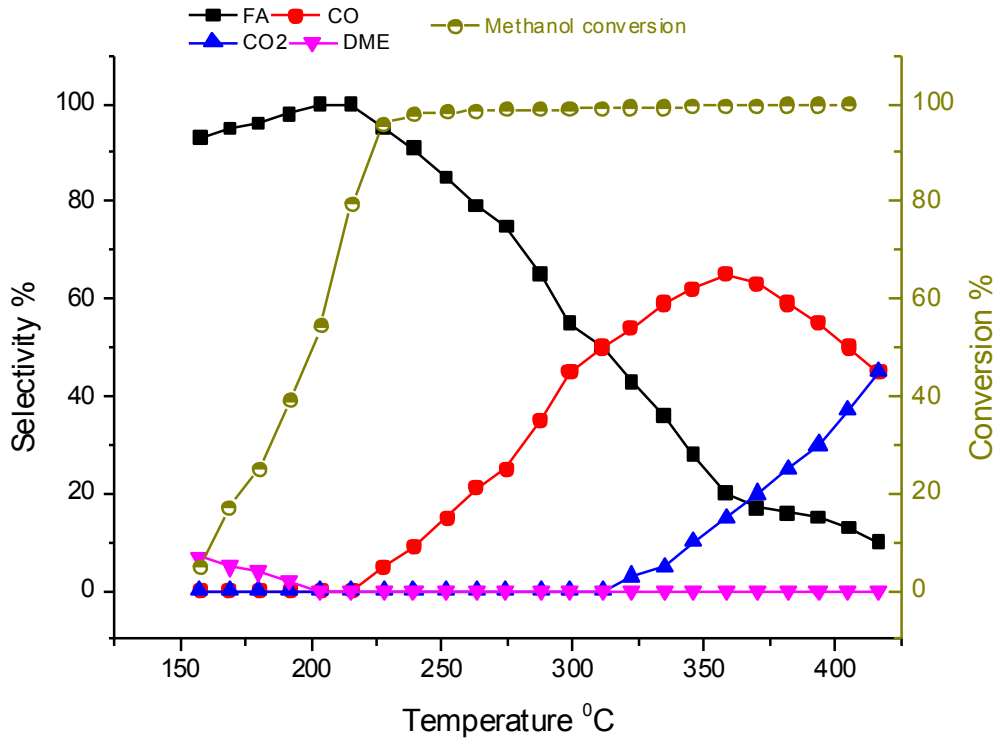

Figure 5.9 Reaction profile result of $Fe_2(WO_4)_3/Fe_2(MoO_4)_3$ catalyst

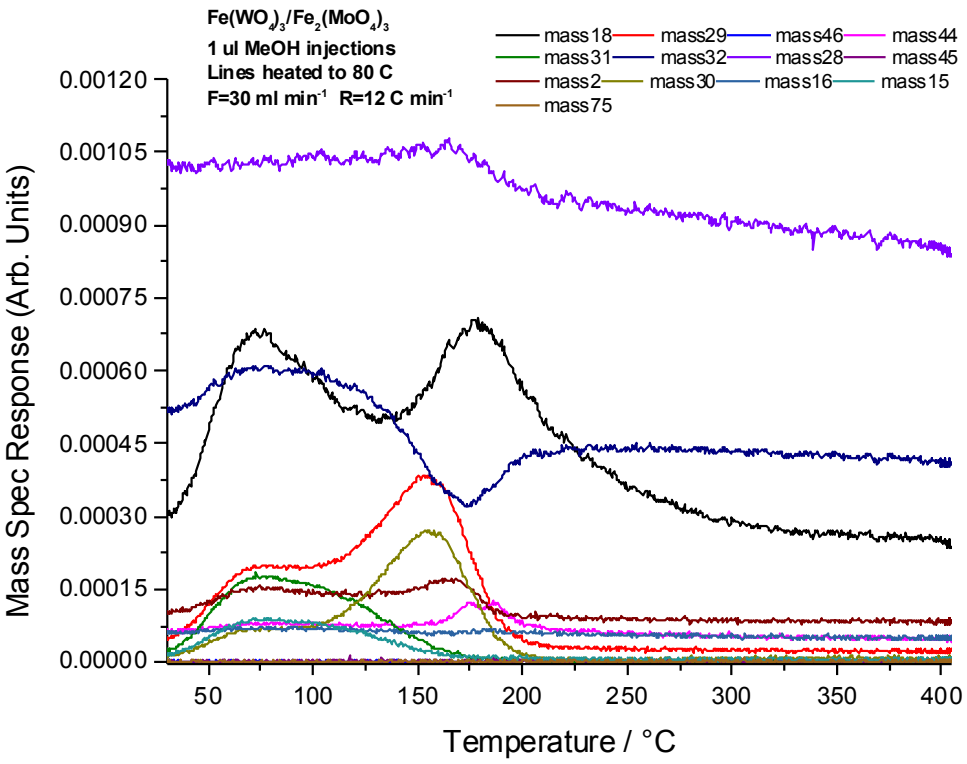

Figure 5.10 TPD result of $Fe_2(WO_4)_3/Fe_2(MoO_4)_3$ catalyst

5.2.4 (2%) $FeVO_4/Fe_2(MoO_4)_3$ catalyst

2% of Iron vanadate was loaded to 2.2 iron molybdate catalyst, as XPS spectra (figure 5.11) shows spectra for molybdenum, vanadium and iron. Figure 5.12, the reaction profile result of this catalyst, shows the selectivity and activity of the catalyst. It is less active than the previous loaded iron molybdate catalysts that were illustrated in this chapter, as it converted methanol by 165 ^{o}C compared to 150 ^{o}C for the previous catalysts. Moreover, the selectivity of iron molybdate with iron vanadate loading catalyst is 100% selective to formaldehyde at low conversion, which then decreased with the increase of temperature and conversion. The resulting product is CO, which increases to 70% selectivity by 340 ^{o}C. The point to notice is its selectivity to CO, more than all previous catalysts that were mentioned in this chapter, the selectivity of formaldehyde dropped to a very low point. However, the TPD in figure 5.13 shows that the catalyst is only selective to formaldehyde, and there are no peaks for CO or CO_2, which means the catalyst is 100% selective to formaldehyde in anaerobic conditions, where in aerobic conditions CO was highly formed.

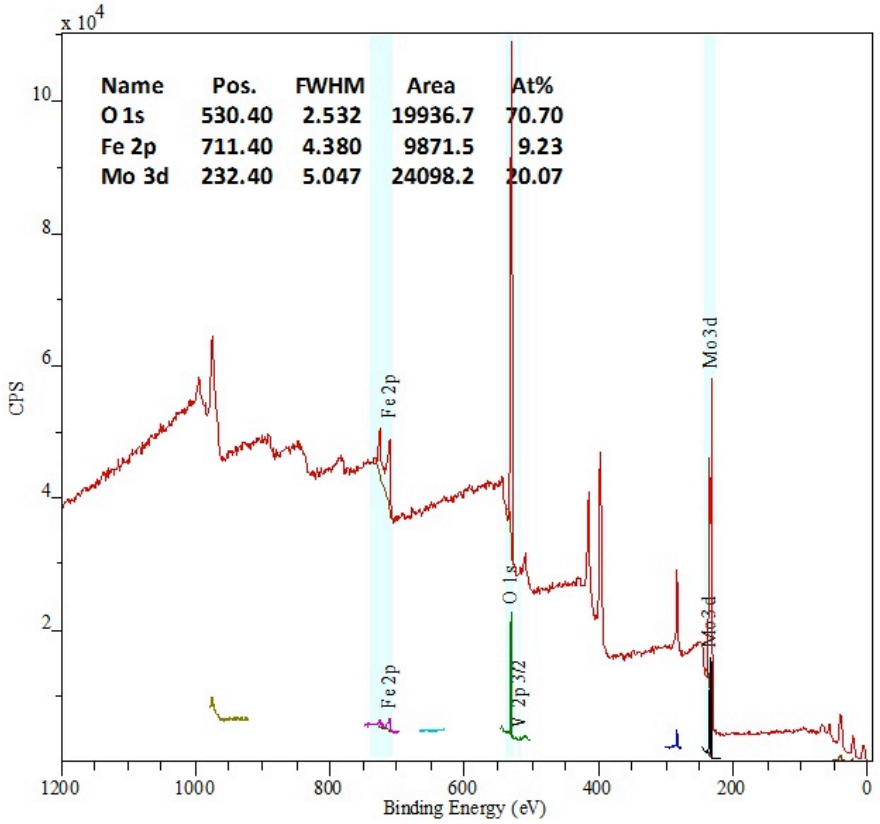

Figure 5.11 TPD result of $FeVO_4/Fe_2(MoO_4)_3$ catalyst

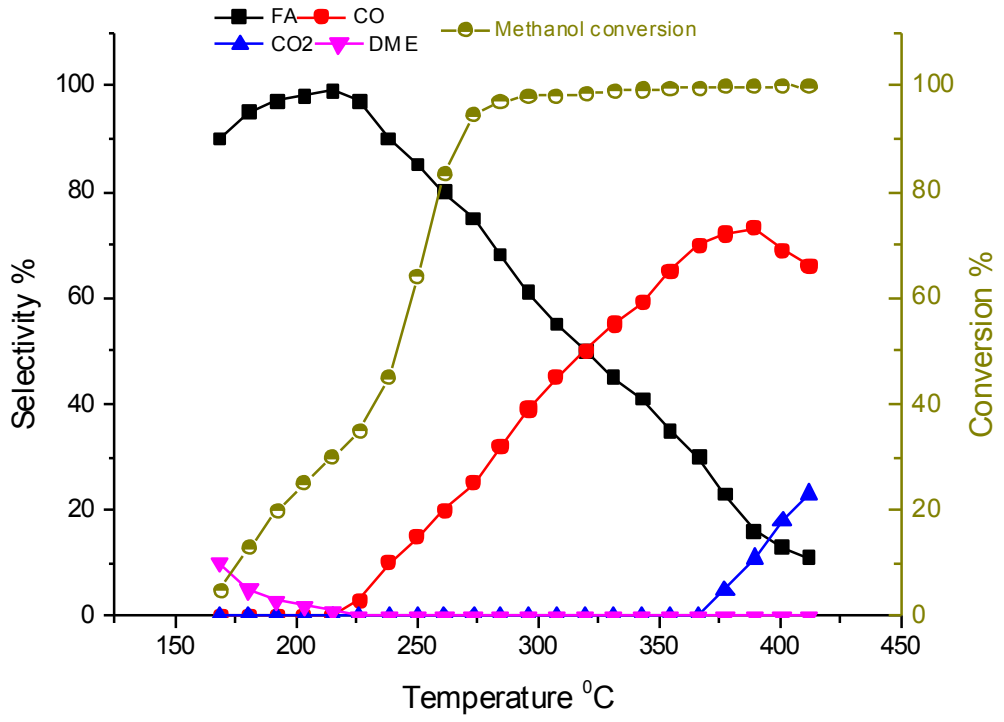

Figure 5.12 Reaction profile result of $FeVO_4/Fe_2(MoO_4)_3$ catalyst

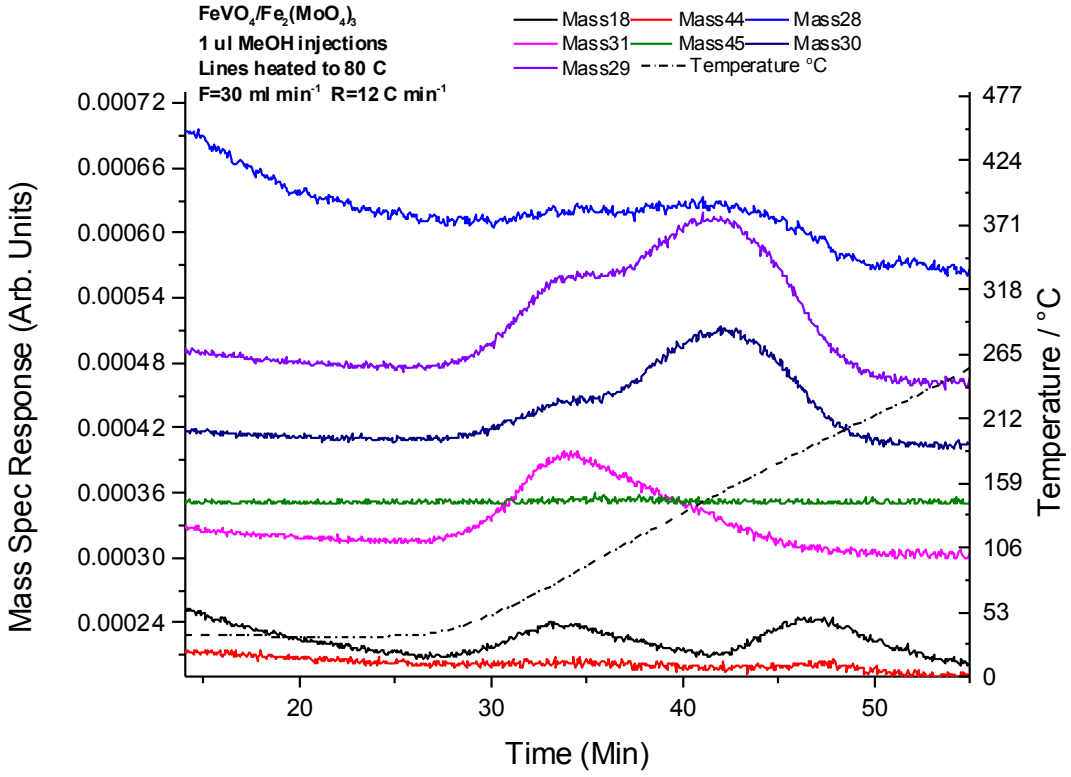

Figure 5.13 TPD result of $FeVO_4/Fe_2(MoO_4)_3$ catalyst

5.2.5 (2%) $MnMoO_4/ Fe_2(MoO_4)_3$ catalyst

Manganese molybdate catalyst was studied in Chapter Four beside 2.2 iron molybdate catalyst, and both catalysts were found to be selective to formaldehyde. However, iron molybdate was more selective: the maximum yield of iron molybdate was 96%, whereas manganese molybdate catalyst yielded 88% at a lower temperature than iron molybdate catalyst. However, when manganese molybdate was loaded on 2.2 iron molybdate (XPS spectra in figure 5.14), the new catalyst has very close yield of formaldehyde to iron molybdate catalyst as illustrated in figure 5.15. It yielded 94% formaldehyde by 275 ^{o}C, and this temperature is the same as in iron molybdate catalyst that fully converts methanol by 275 ^{o}C. Furthermore, the result of TPD (figure 5.16) is showing formaldehyde peaks similar to the result of the two catalysts when they are pure.

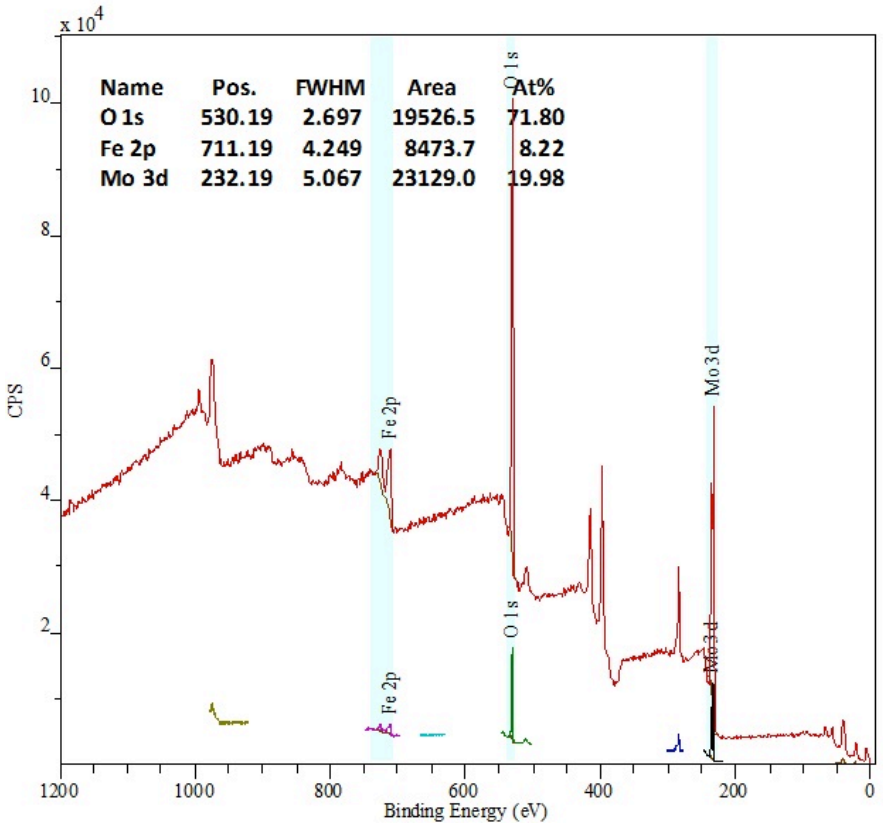

Figure 5.14 XPS spectra of (2%) $MnMoO_4$/ $Fe_2(MoO_4)_3$ catalyst

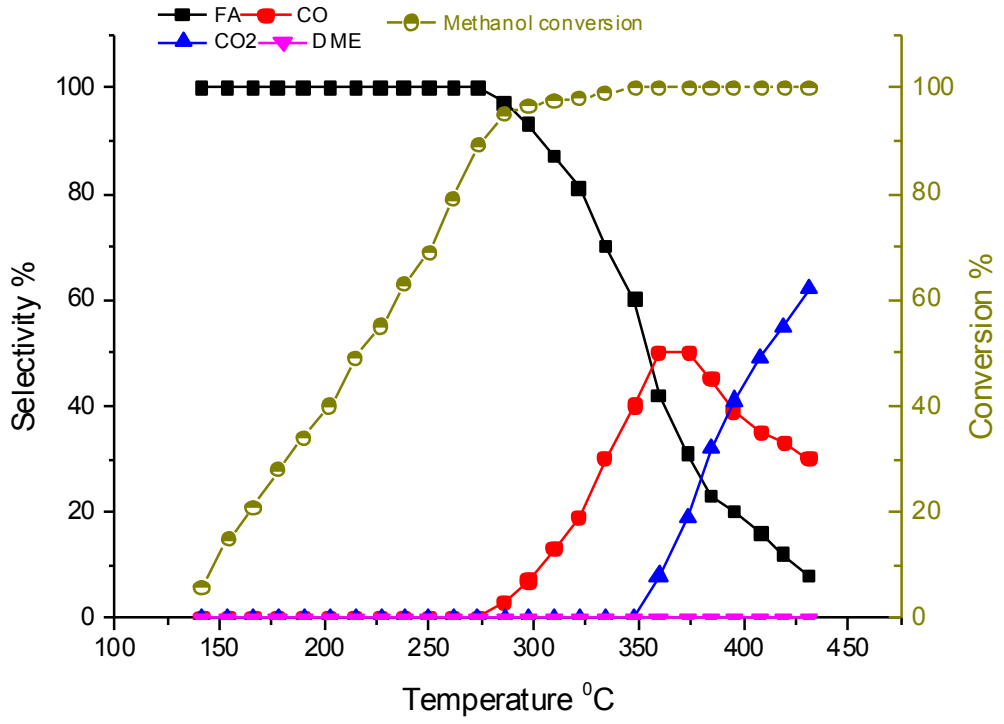

Figure 5.15 Reaction profile result of $MnMoO_4$/ $Fe_2(MoO_4)_3$ catalyst

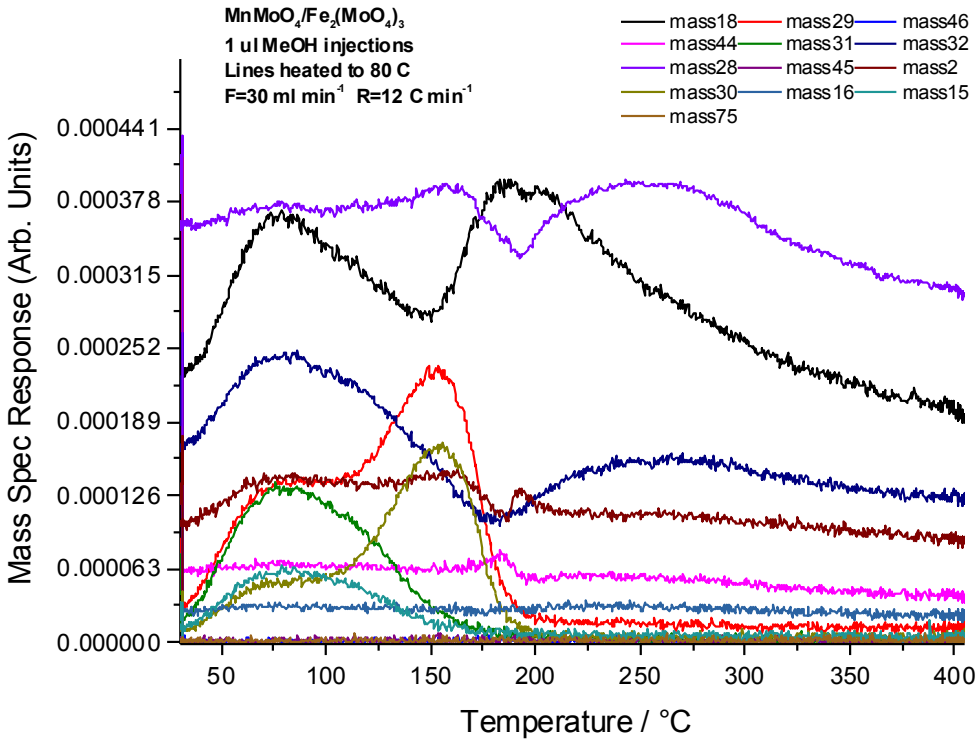

Figure 5.16 TPD result of $MnMoO_4$/ $Fe_2(MoO_4)_3$ catalyst

5.2.6 (2%) $CuMoO_4$/ $Fe_2(MoO_4)_3$ catalyst

2% of copper molybdate loaded on 2.2 iron molybdate is shown in figure 5.17 (XPS spectra), it is 100% selective to formaldehyde at low conversion (figure 5.18). However, as with the previous loaded catalysts, selectivity toward formaldehyde decreased and was then followed by an increase of carbon monoxide production, then carbon dioxide increased with the increase of temperature. In terms of activity, the catalyst is as active as other supported catalysts in this chapter that were mentioned above: it converts methanol by 150 ^{o}C, and the maximum formaldehyde yield is 96% by 210 ^{o}C. This is a better result than iron molybdate catalyst that has a yield of 96% by 275 ^{o}C, and it is better than copper molybdate that has less selectivity to formaldehyde. The reduction of heat compared to iron molybdate catalyst makes a more interesting catalyst, as it was not a very large difference but still saves energy. Moreover, the TPD result (figure 5.19) shows only desorbed peaks that related to formaldehyde, but the peaks are sharper, which is a sign of strong methanol.

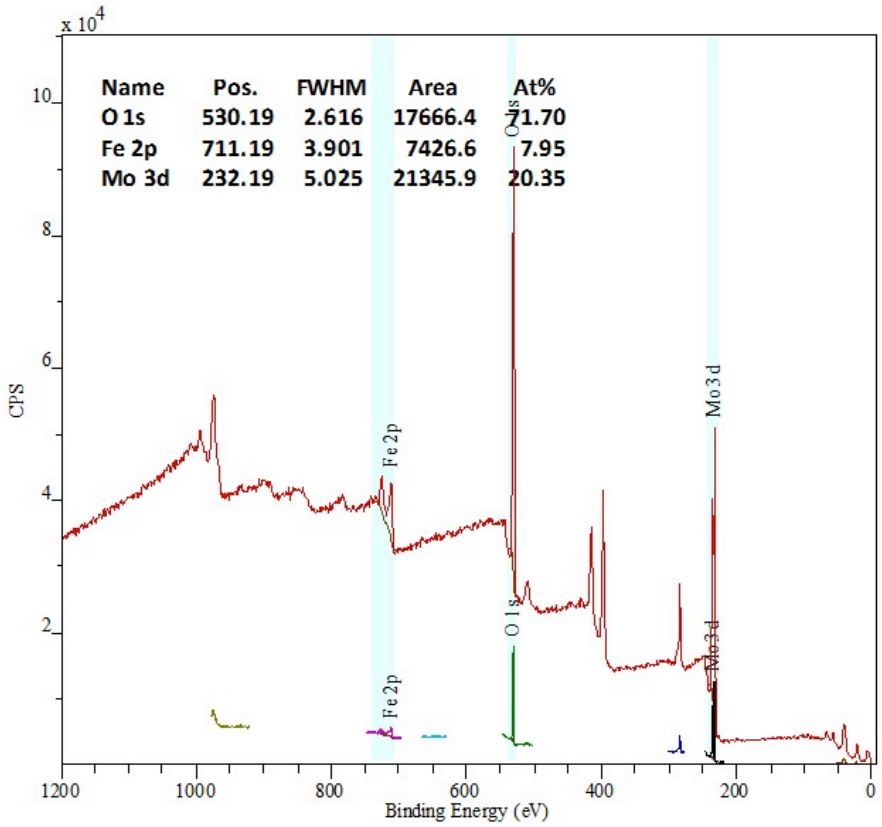

Figure 5.17 XPS spectra of (2%) $CuMoO_4$/ $Fe_2(MoO_4)_3$ catalyst

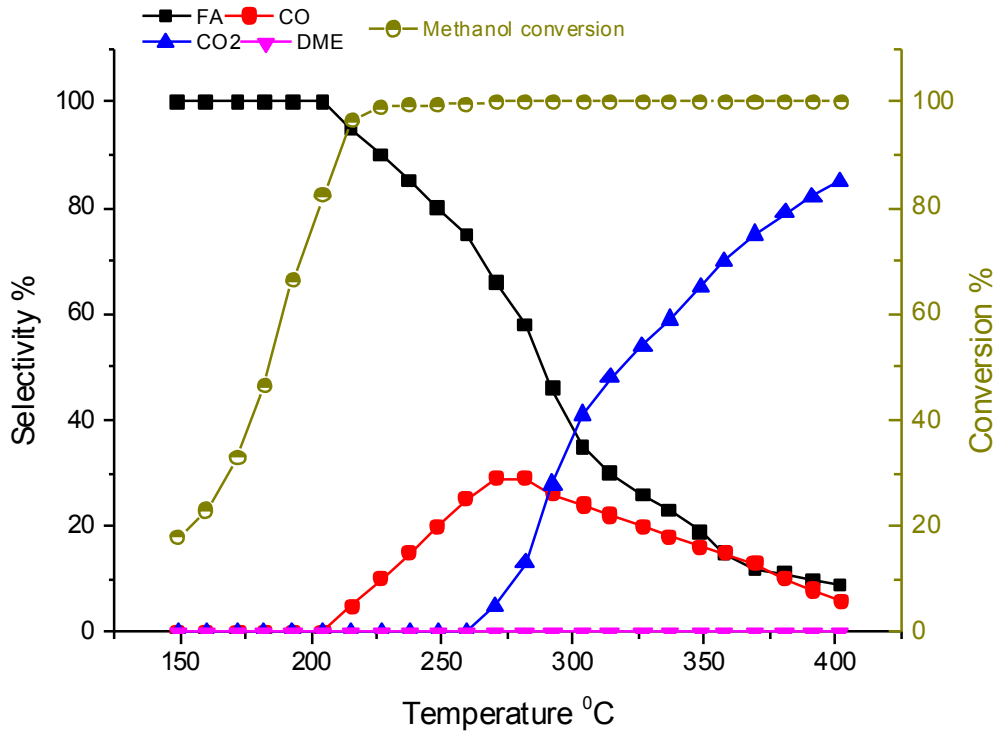

Figure 5.18 Reaction profile result of $CuMoO_4$/ $Fe_2(MoO_4)_3$ catalyst

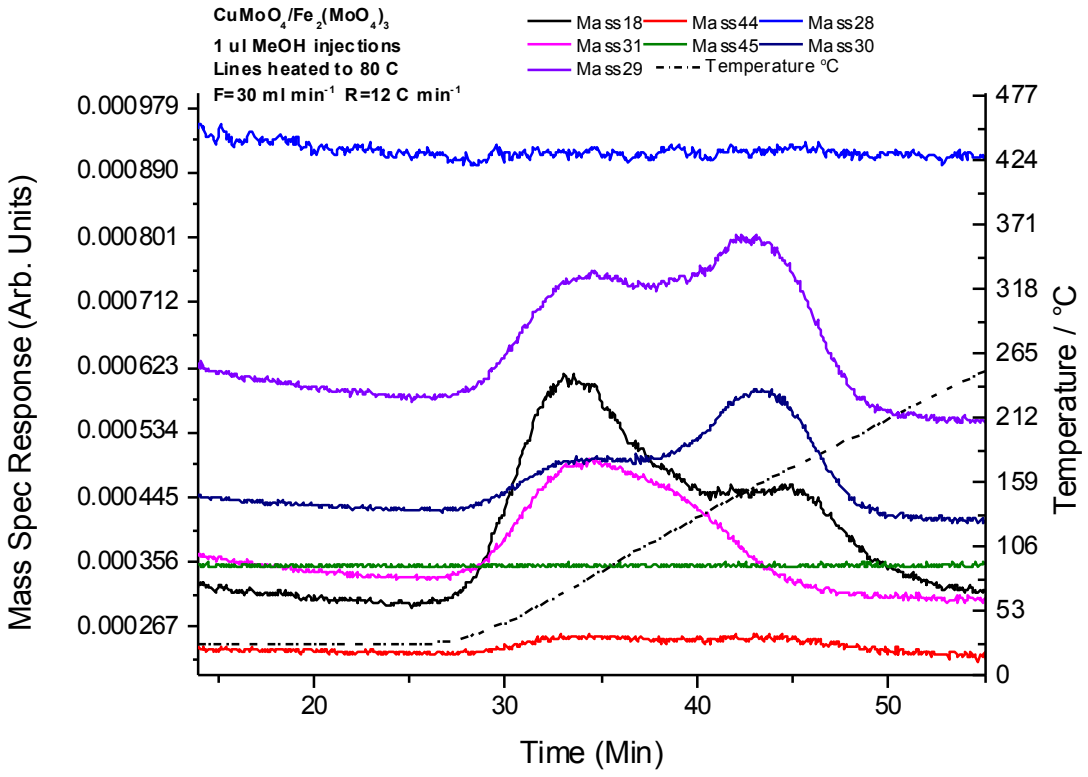

Figure 5.19 TPD result of $CuMoO_4$/ $Fe_2(MoO_4)_3$ catalyst

5.2.7 (3%) MoO_3/Fe_2O_3 catalyst

In Chapter 3, molybdenum oxide catalyst was tested for methanol oxidation. The result showed that methanol oxidation on molybdenum was mainly converted to formaldehyde, and the iron oxide catalyst was 100% selective to CO_2. However, 3% of molybdenum oxide was loaded on iron oxide catalyst, the point is in table 5.1, where the surface area is 9 $m^2.g^{-1}$. With iron oxide surface of 9 $m^2.g^{-1}$, and molybdenum oxide with surface area of 1 $m^2.g^{-1}$, from figure 5.20, the catalyst is by 120 ^oC and 100% selectivity to dimethyl ether. Then its selectivity to dimethyl ether suddenly dropped, while the selectivity to formaldehyde was very low (5% selectivity) and later decreased, when the selectivity of CO increased to replace dimethyl ether and formaldehyde production. In other words, it is a selective catalyst to CO. However, the TPD result in figure 5.21 illustrates desorption peaks of which products, and formaldehyde was desorbed beside CO and CO_2.

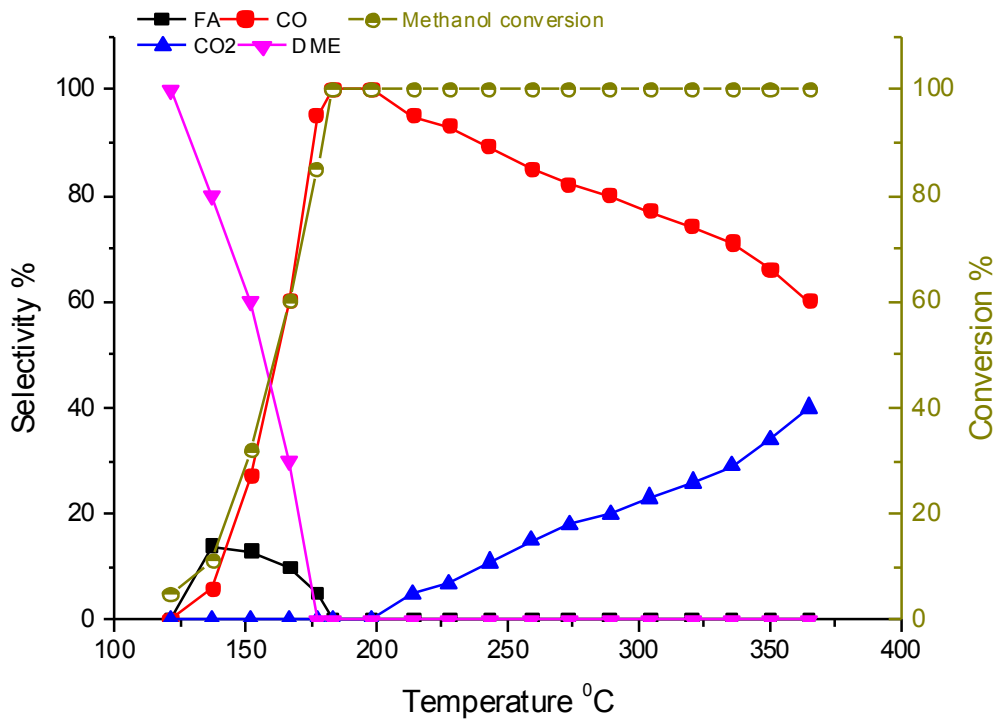

Figure 5.20 Reaction profile result of MoO_3/Fe_2O_3 catalyst

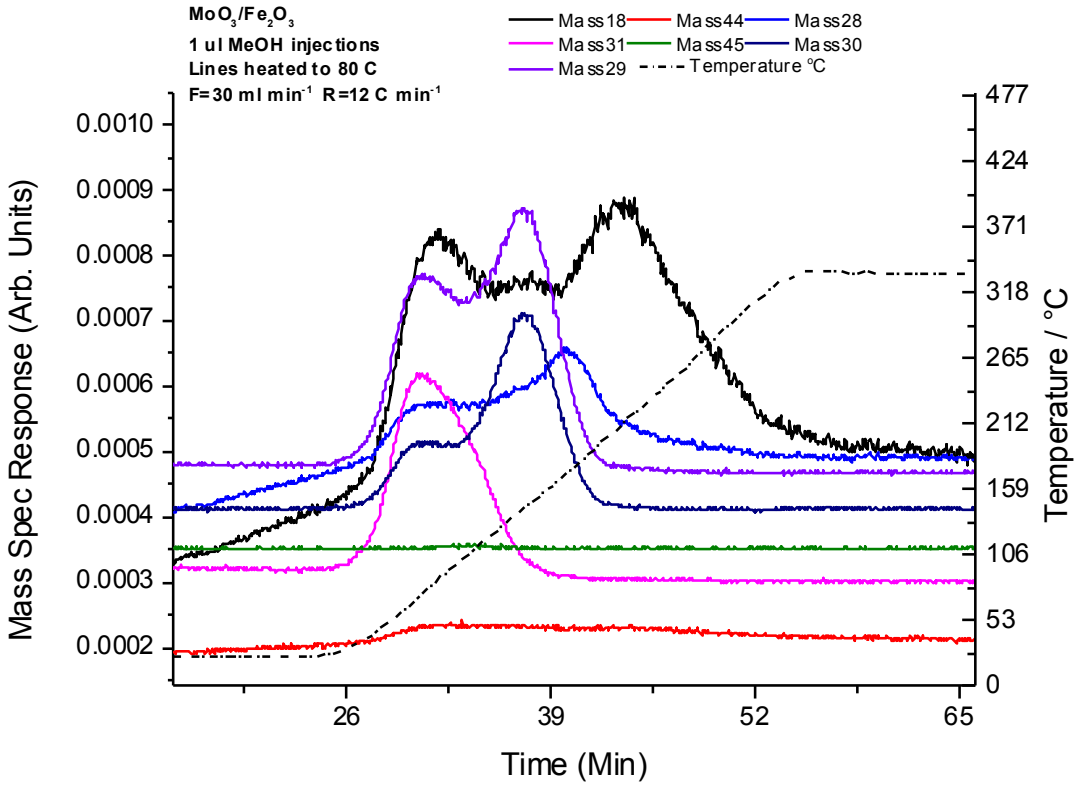

Figure 5.21 TPD result of MoO_3/Fe_2O_3 catalyst

5.2.8 (6%) MoO_3/C catalyst

Molybdenum oxide has a very poor surface area, where carbon has a very large surface. Therefore loading of molybdenum on carbon leads to having a catalyst with a very large surface, where the surface area of MoO_3/Carbon catalyst is 37 $m^2.g^{-1}$. However, the activity of this is quite poor, as shown in figure 5.22, where it converts methanol 230 ^oC. Moreover, the catalyst is selective to carbon monoxide and carbon dioxide, and just a very small amount (3% maximum selectivity) of dimethyl ether was produced. However, TPD in figure 5.23 shows peaks desorbed for formaldehyde and CO_2, where TPD are in anaerobic conditions, because carbon support reacts with oxygen and forms CO, which leads to consumption of the support its self, so, oxygen was not flowing with methanol.

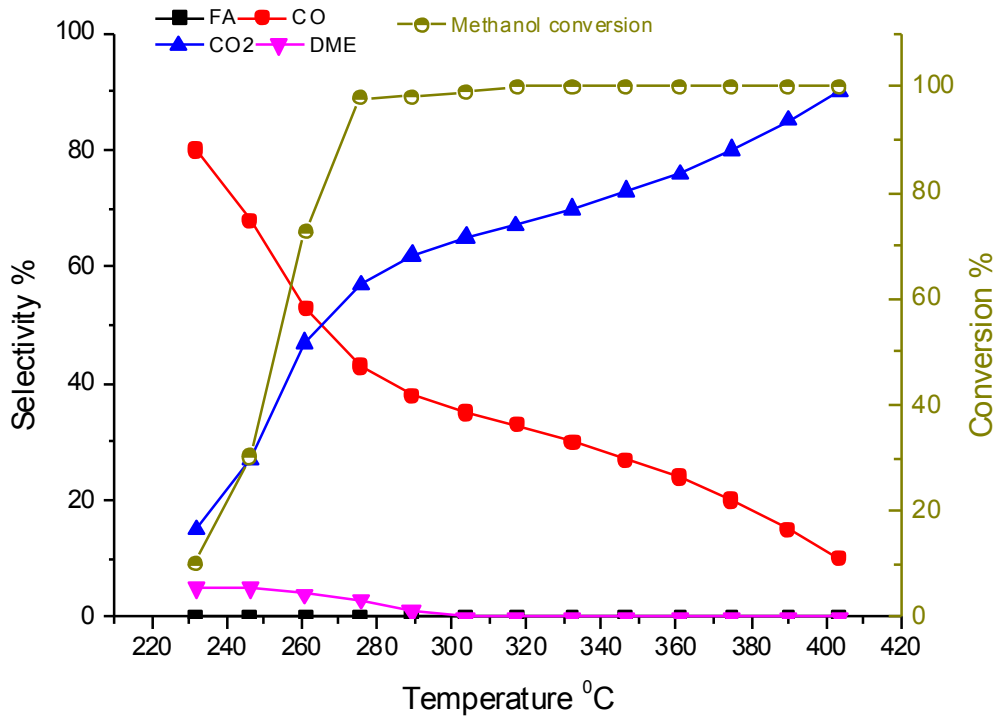

Figure 5.22 Reaction profile result of MoO_3/C catalyst

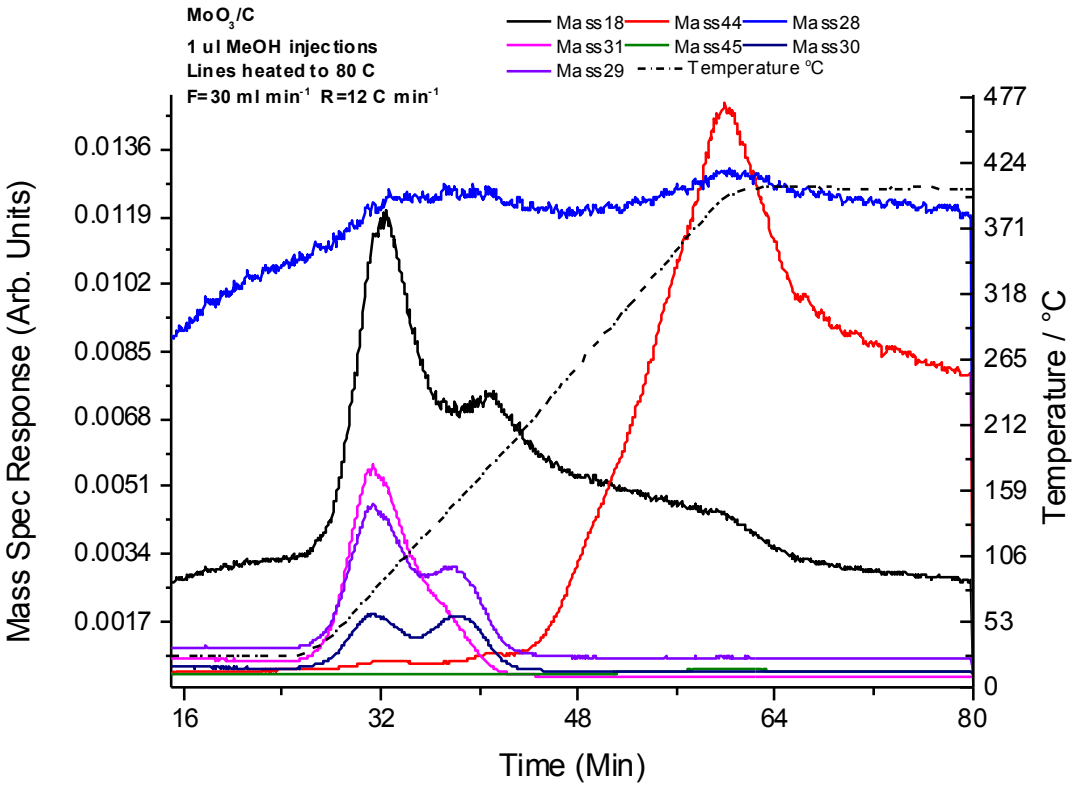

Figure 5.23 TPD result of MoO_3/C catalyst

5.2.9 (1%) Nano-gold/MoO_3 catalyst

In Chapter 3, molybdenum oxide was tested for methanol oxidation on its surface. The result was very poor, as molybdenum oxide is not active: it converts methanol by 215 ^{o}C to formaldehyde and CO, the maximum conversion was 85% by 420 ^{o}C. However, the surface has nano-gold partials loading of 1% (figure 5.24, XPS spectra), the catalytic behaviour has changed as in figure 5.25, where the catalyst is active by 150 ^{o}C with 100% selectivity to formaldehyde. However, that selectivity decreases gradually with increase of heat, while CO selectivity increases, and maximum yield of formaldehyde was 82% by 260 ^{o}C, which is close a result to iron molybdate with less yield of formaldehyde and more CO production, and even more active than iron molybdate. Furthermore, the TPD result in figure 5.26 shows the selectivity to only formaldehyde with one desorption peak, where the catalyst prefers formaldehyde.

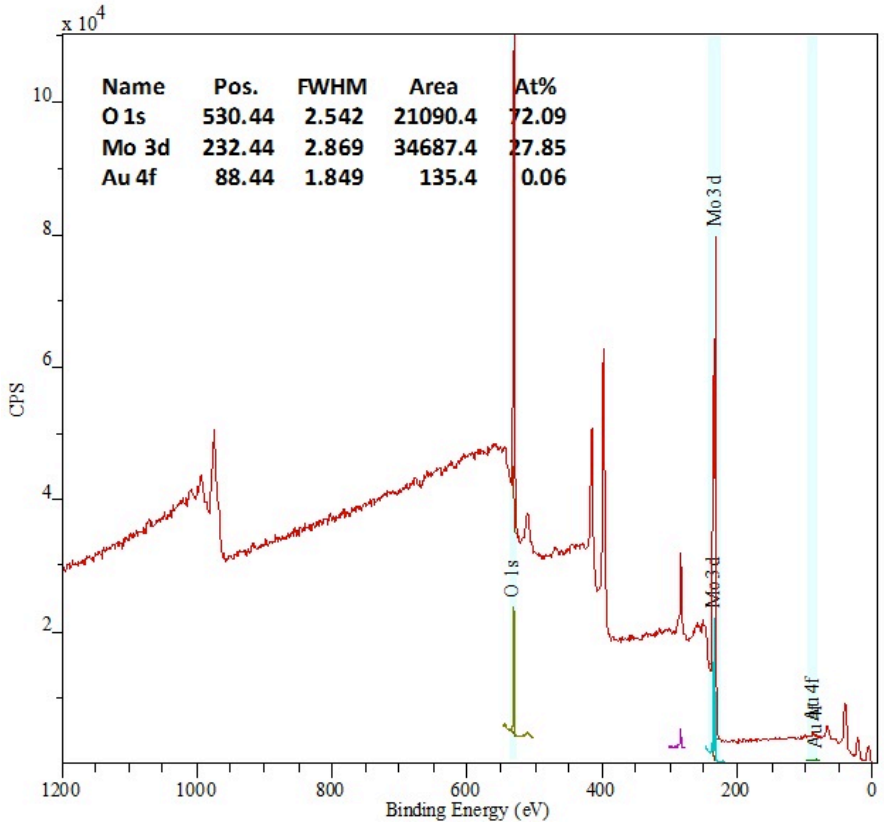

Figure 5.24 XPS spectra of (1%) nano-gold/MoO_3 catalyst

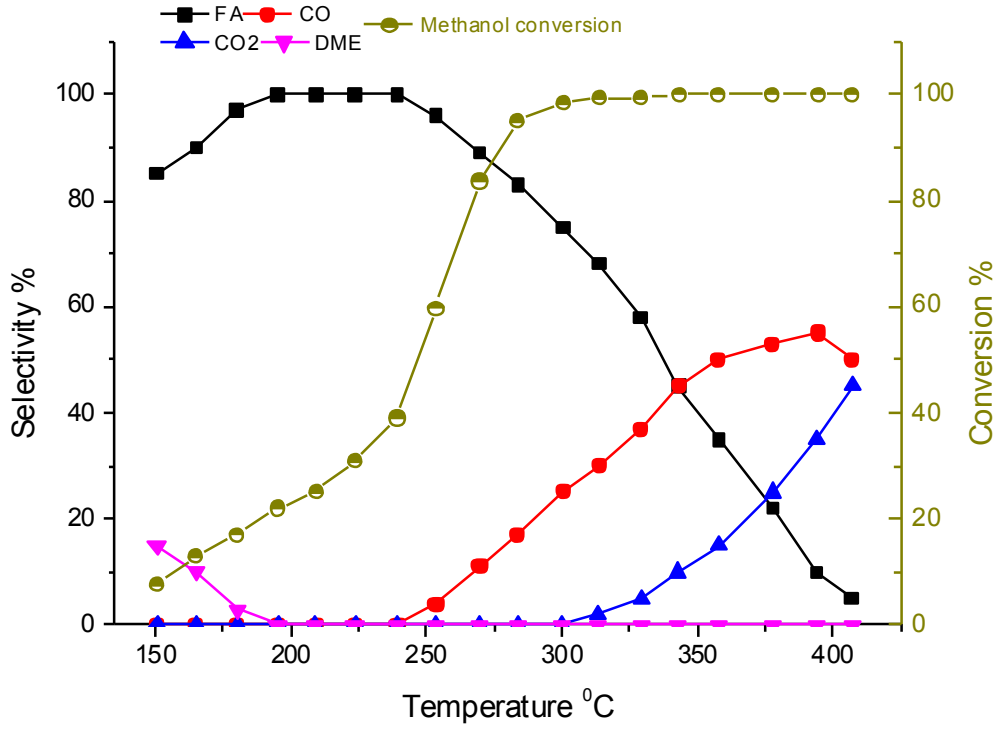

Figure 5.25 Reaction profile rsult of Nano-gold/MoO_3 catalyst

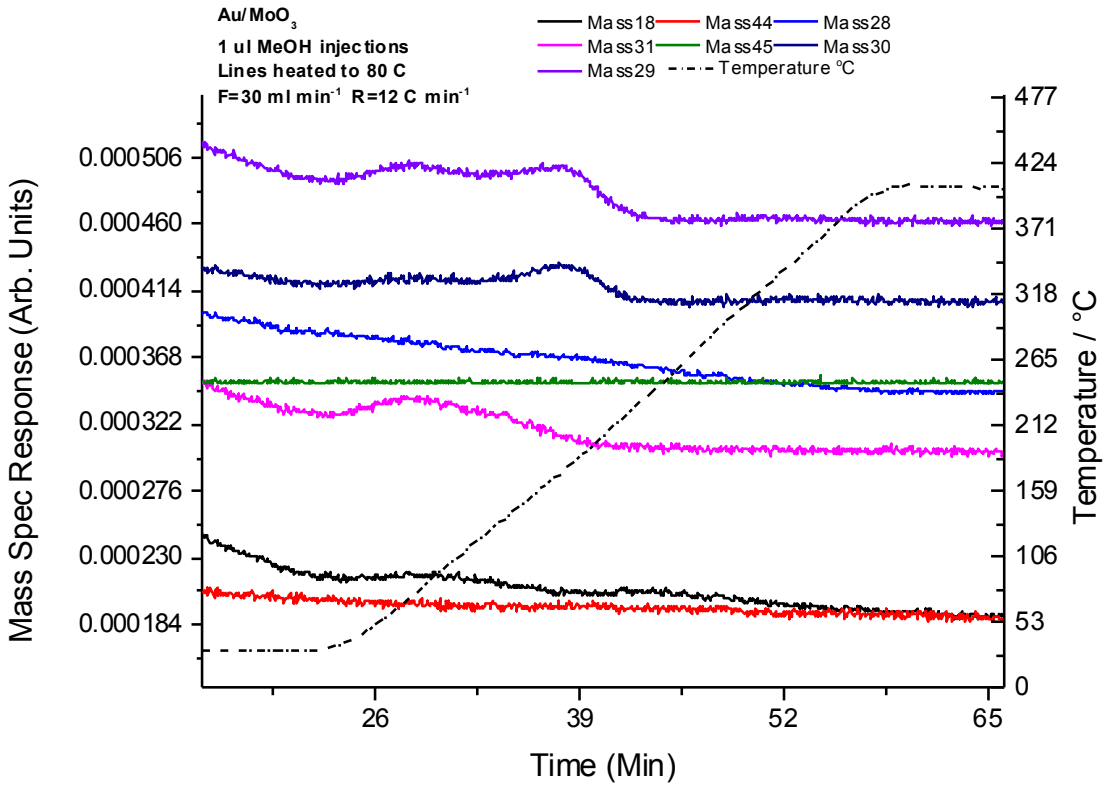

Figure 5.26 TPD result of Nano-gold/MoO_3 catalyst

5.2.10 (1%) Nano-gold/$Fe_2(MoO_4)_3$ catalyst

1% of nano-gold was loaded on the surface 2.2 iron molybdate as shown by XPS spectra (figure 5.27). However, the result is worse than pure iron molybdate catalyst in selectivity to formaldehyde (figure 5.28), because CO_2 was produced as well as formaldehyde at first conversion, then the selectivity dropped and CO_2 increased, which makes the catalyst is not selective to formaldehyde. However, in terms of activity, the catalyst is very active. It converted methanol by 150 ^oC with full conversion by 240 ^oC, making it more active than pure iron molybdate catalyst, which converted methanol by 180 ^oC, and the full conversion was by 275 ^oC as in Chapter Four. Moreover, TPD in figure 5.29 demonstrates three desorbed products: formaldehyde, CO and CO_2.

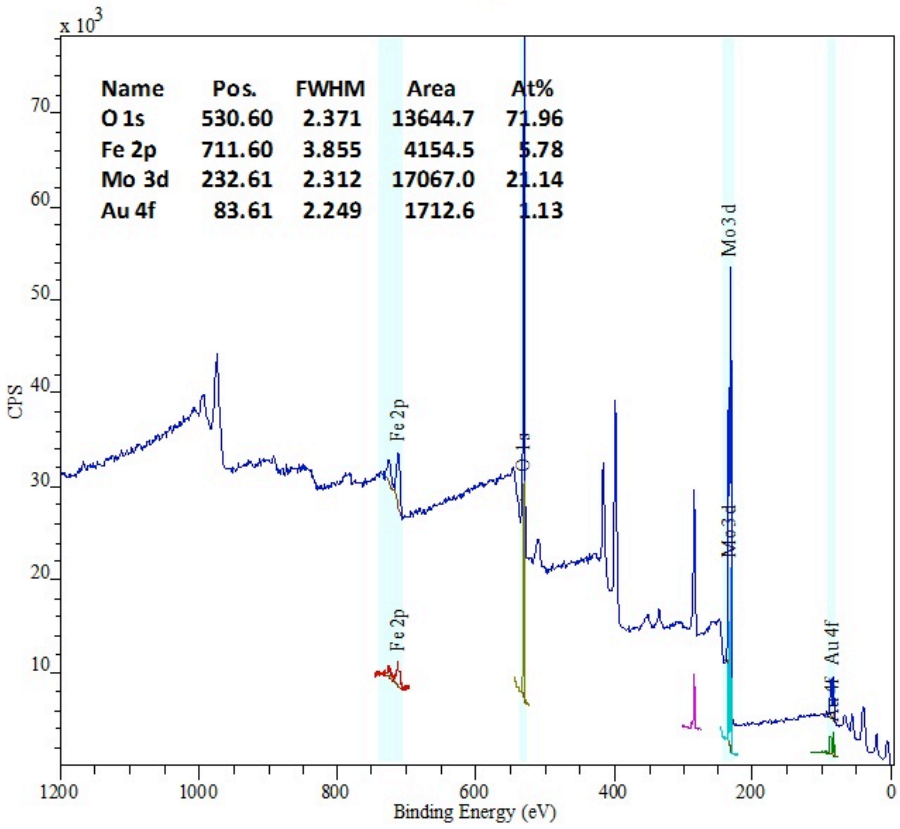

Figure 5.27 XPS spectra of (1%) nano-gold/$Fe_2(MoO_4)_3$ catalyst

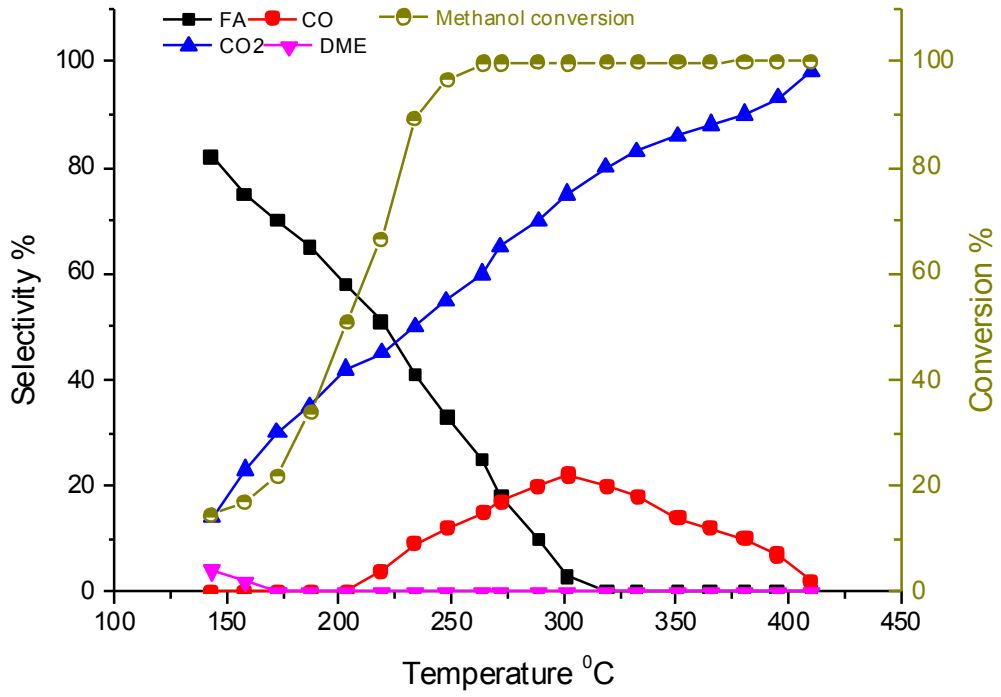

Figure 5.28 Reaction profile result of Nano-gold/$Fe_2(MoO_4)_3$ catalyst

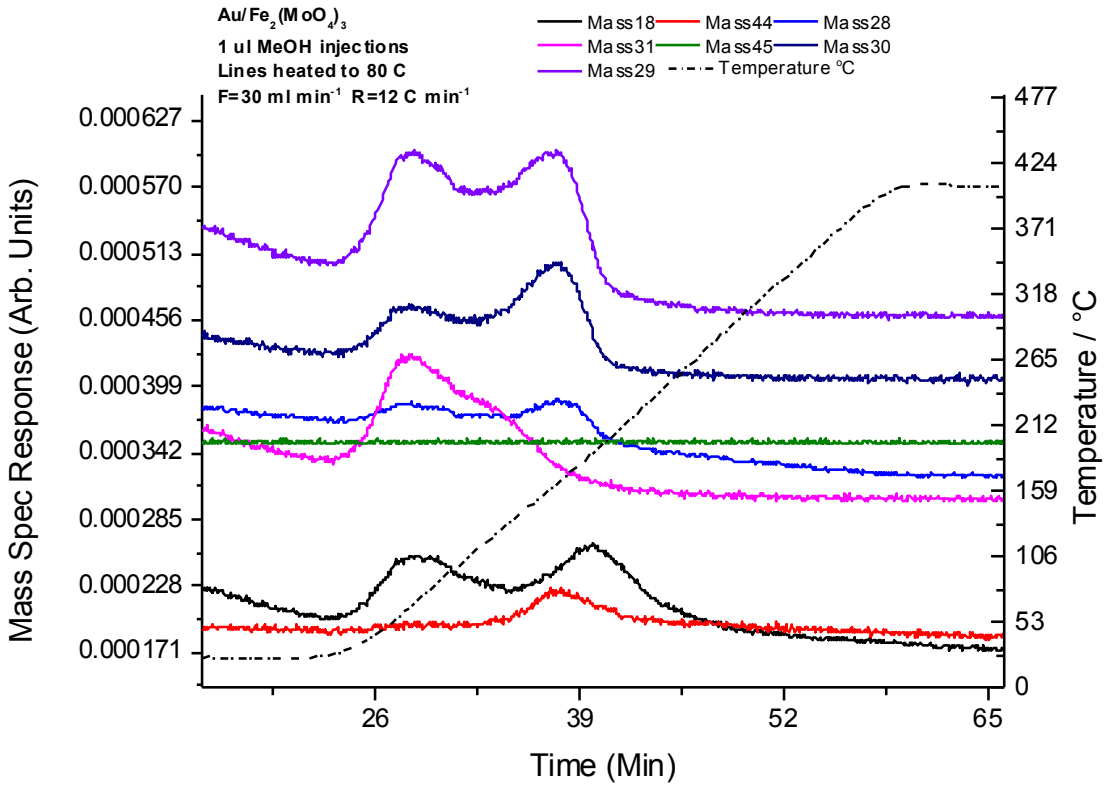

Figure 5.29 TPD result of Nano-gold/$Fe_2(MoO_4)_3$ catalyst

5.3 Discussion

5.3.1 Metal oxides loading

The results above showed great changes in the catalytic behaviour of iron molybdate catalyst when it has other materials loading on its surface. Tungsten and vanadium oxides catalysts are selective to formaldehyde. Therefore covering the surface with selective metal oxide was proposed, to improve the selectivity to formaldehyde, and increase methanol conversion by impregnation preparation method. However, the activity was increased, where iron molybdate catalysts with two loaded tungsten and vanadium are active, the two catalyst converted methanol by 150 ^{o}C, while the pure 2.2 iron molybdate catalyst converted methanol by temperature of 180 ^{o}C. However, the full conversion of methanol (100%) is by 275 ^{o}C on the pure 2.2iron molybdate catalyst and the doped surface catalysts.

However, the impregnation method increased the activity of the doped iron molybdate catalyst, because the surface is in a heterogeneous state. As the loaded tungsten and vanadium oxides are not bonded to the surface, it is the opposite case compared with molybdenum oxide in the ratio 2.2 iron molybdate catalyst, where molybdenum stoichiometry has 1.5 Mo: 1Fe, as in co-precipitation method any addition of molybdenum will cover the surface as molybdena. However, that requires high temperature treatment as for calcination (500 ^{o}C). The heat is important for molybdenum spreading [20-25], but the disadvantage is that of decreasing activity [1-5], whereas the impregnation method does not require that heat, and the doped particles are too small (1.1 to 1.5nm with calcination temperature lower than 400 ^{o}C [26]), which in turn increase the catalyst activity. In other words, tungsten and vanadium go into iron molybdate porous and fill it, which leads to an electrostatic interaction between iron molybdate and the loaded metal oxide, and that interaction causes a disorder and reduces the activation energy of iron molybdate to react at lower temperature than unloaded surface iron molybdate catalysts as seen in the result above [1-10]. Moreover, this case is applied to molybdenum oxide on iron oxide catalyst that converted methanol by 140 ^{o}C, and the pure iron oxide converted methanol by 180 ^{o}C, whereas molybdenum oxide on carbon was not very active as bar because carbon need more heat to activate it [11,19].

However, the selectivity to formaldehyde is affected by the various supports, 2.2 iron molybdate, carbon and iron oxide. In 2.2 iron molybdate support, the selectivity to formaldehyde is slightly decreased compared to the pure iron molybdate catalyst, and the reason of that decrease is the coverage of loaded metal oxide. Where 2.2 iron molybdate has excess molybdenum on its surface, that excess molybdenum is part selective with terminal oxygen, and is responsible for methanol adsorption to methoxy. The coverage of vanadium and tungsten oxide are poisoning that structure, and the loaded participates in the adsorption of methanol as well as iron molybdate and converts methoxy by its bridging oxygen to form formate [20-25] bonded to the surface, and then to CO_2. Molybdenum oxide on iron oxide catalyst is better than pure iron oxide, by making a small amount of formaldehyde at low conversion and a great deal of dimethyl ether. Then, however, both dropped to zero and CO_2 was the main

product at high conversion, whereas pure iron oxide converts methanol to carbon dioxide at any conversion. That small amount of formaldehyde and dimethyl ether confirm that loaded metal is involved in the adsorption in some way. Likewise, the same case is shown in molybdenum oxide on carbon, where it is not selective to formaldehyde at all.

Complex oxide doping was not far from single oxide doping, but the result is much closer to pure 2.2 iron molybdate catalyst for formaldehyde selectivity. Where $Fe_2(WO_4)_3$/2.2 $Fe_2(MoO_4)_3$ catalyst yielded 94% formaldehyde, which is very close yield of formaldehyde to the pure iron molybdate catalyst that yielded 96% formaldehyde, it is more interesting in terms of activity. It converted methanol (20%) by 150 ^oC, where pure 2.2 iron molybdate catalyst converted methanol by 180 ^oC, and even the full conversion of methanol was at 230 ^oC in the use of iron tungstate/iron molybdate catalyst to 275 ^oC in pure 2.2 iron molybdate.

However, iron vanadate on iron molybdate catalyst ($FeVO_4/Fe_2(MoO_4)_3$) is still converting methanol completely by 260 ^oC, which is a higher temperature compared to previously mentioned catalysts. This might, during preparation, lead to deactivation of the catalyst, and even in manganese molybdate on iron molybdate catalyst ($MnMoO_4/Fe_2(MoO_4)_3$) that fully converted methanol by 270 ^oC, both catalysts are less interesting than a catalyst with iron tungstate and copper molybdate loading. However, iron vanadate on iron molybdate catalyst is losing a great deal more selectivity to formaldehyde than the three previous catalysts with iron tungstate, manganese molybdate and copper molybdate. Overall, the doping of complex catalysts are much more selective to formaldehyde than single oxides loading. However, in terms of activity, all loadings enhance the support of converting methanol at lower temperatures than in their pure state.

5.3.2 Surface area increase

One of the issues that was studied is surface and activity, where the surface of molybdenum oxide is 1 m^2/g. However, the catalyst is not very active, where iron molybdate was very active and fully converts methanol at 275 ^oC, with a surface

area of 5 m^2/g. The question arises, if the surface area is increased, will the activity increase? For example in the iron molybdate and molybdenum oxide catalysts, the result showed that the increase of surface area is not much affected in activity: the effect is the catalytic behaviour of a catalyst within its structure. As 6% of molybdenum oxide was supported on carbon, the catalyst has 37 m^2/g. However, it first converted methanol (10%) by 230 ^oC, which is much greater heat than iron molybdate that only has 5 m^2/g, and even the full conversion of methanol on MoO_3/C was 275 ^oC, which is the same as 2.2 iron molybdate catalyst that fully converted methanol by 275 ^oC.

Furthermore, 3% MoO_3/Fe_2O_3 catalyst has a surface area of 9 m^2/g. However, it is much more active than molybdenum oxide on carbon catalyst. It first converted methanol by 140 ^oC, and it fully converted methanol by 175 ^oC. Iron oxide is also very active, it fully converted methanol by 180 ^oC, so the catalytic activity does not depend solely on the surface area, the activity depends on the surface structure and the nature of adsorbed methanol. Here, methanol was fully mainly converted to carbon dioxide, as published earlier by Michael Bowker et al and other [20-25], methanol adsorbed on the surface, then was converted to formate bonded to the surface, which later desorbed as carbon dioxide, TPD in result section showed the pathway reaction of methanol oxidation to CO_2.

5.3.3 Nanoparticles affects

1% of nano-gold particles were loaded on the surface of molybdenum oxide and iron molybdate supports. It is well known that molybdenum oxide is a poorly active catalyst, but the loading of nano-gold in its surface increased its activity to convert methanol by 150 ^oC, and full conversion by 275 ^oC. The catalyst was 100% selective to formaldehyde at low conversion, then selectivity to formaldehyde gradually decreased and the increase was for CO production, where the maximum yield of formaldehyde was 82% by 260 ^oC, However, the results of selectivity to CO and formaldehyde are related to molybdenum oxide, as the pure molybdenum oxide catalyst has the same selectivity to formaldehyde and CO, but the point of improvement that makes nano-gold loading more interesting is the increase in activity with no change in selectivity.

Furthermore, when gold nanoparticles were loaded on 2.2 iron molybdate, the activity changed: the catalyst is active by 150 ^{o}C, and even reached full methanol conversion by 250 ^{o}C, which is better than 275 ^{o}C in pure 2.2 iron molybdate catalyst. However, the selectivity to CO_2 has increased from the pure catalyst, which can be explained as iron molybdate is covered by molybdenum oxide on its surface, where the bulk is built by molybdenum and iron, but during gold doping from $HAuCl_4$, chloride caused iron sintering and changed the whole support structure (2.2 iron molybdate) from its pure state [53], this is a poising of iron molybdate surface during preparation, which illustrated that the surfaces of complex supports are not stable during sol-immobilization preparation method within acidic solution and pH affect [54], and the support has a change in its structure. Consequently, loading nanoparticles of gold is more efficient on single oxide than on complex oxide supports using sol-immobilization method.

5.4 Conclusion

In conclusion, doping metal oxides has a great effect on a 2.2 iron molybdate catalyst: the catalytic activity is increased, while the selectivity to formaldehyde has a negative change. However, complex oxides loading has better results for formaldehyde selectivity than single oxides.

Moreover, the surface area has little change in activity, where MoO_3/Fe_2O_3 catalyst has 9 $m^2.g^{-1}$, and is much more active than MoO_3/C catalyst, which has 37 $m^2.g^{-1}$. The main target is catalytic behaviour in terms of catalyst structure by adsorbing methanol to methoxy, like vanadium oxide catalyst, which has high oxygen mobility.

Additionally, loading of nanoparticles of gold activated molybdenum oxide, which was poorly active as a pure catalyst, and the selectivity to formaldehyde is still as high as the pure catalyst in single oxide support. However, complex oxide support for nano-gold loading did have a good result, the support may change by chloride during preparation method, causing change in the support structure and decreasing the selectivity of formaldehyde, then increasing the selectivity of CO_2.

5.5 References

[1]. ALAYON, E. M. C., SINGH, J., NACHTEGAAL, M., HARFOUCHE, M. & VAN BOKHOVEN, J. A. 2009. On highly active partially oxidized platinum in carbon monoxide oxidation over supported platinum catalysts. *Journal of Catalysis,* 263**,** 228-238.

[2]. BASHA, S. J. S., VIJAYAN, P., SURESH, C., SANTHANARAJ, D. & SHANTHI, K. 2009. Effect of Order of Impregnation of Mo and Ni on the Hydrodenitrogenation Activity of NiO-MoO3/AlMCM-41 Catalyst. *Ind. Eng. Chem. Res.,* 48**,** 2774–2780.

[3]. BOUKHA, Z., FITIAN, L., LÓPEZ-HARO, M., MORA, M., RUIZ, J. R., JIMÉNEZ-SANCHIDRIÁN, C., BLANCO, G., CALVINO, J. J., CIFREDO, G. A. & TRASOBARES, S. 2010. Influence of the calcination temperature on the nano-structural properties, surface basicity, and catalytic behavior of alumina-supported lanthana samples. *Journal of Catalysis,* 272**,** 121-130.

[4]. BOWKER, M., NUHU, A. & SOARES, J. 2007. High activity supported gold catalysts by incipient wetness impregnation. *Catalysis Today,* 122**,** 245-247.

[5]. CHUMBHALE, V. R. & AWASARKAR, P. A. 2001. Oxidative dehydrogenation of ethylene glycol into glyoxal over phosphorus-doped ferric molybdate catalyst. *Applied Catalysis A: General,* 205**,** 109-115.

[6]. DERAZ, N.-A. M. 2001. Effect of Ag2O doping on surface and catalytic properties of cobalt–magnesia catalysts. *Materials Letters,* 51**,** 470-477.

[7]. DORADO, F., DE LUCAS-CONSUEGRA, A., JIMÉNEZ, C. & VALVERDE, J. L. 2007. Influence of the reaction temperature on the electrochemical promoted catalytic behaviour of platinum impregnated catalysts for the reduction of nitrogen oxides under lean burn conditions. *Applied Catalysis A: General,* 321**,** 86-92.

[8]. EGGENHUISEN, T. M., STEENBERGEN, M. J. V., TALSMA, H., JONGH, P. E. D. & KRIJN P. DE JONG* 2009. Impregnation of Mesoporous Silica for Catalyst Preparation Studied with Differential Scanning Calorimetry. *J. Phys. Chem. C* 113**,** 16785–16791.

[9]. GODEFROY, A., PATIENCE, G. S., CENNI, R. & DUBOIS, J.-L. 2010. Regeneration studies of redox catalysts. *Chemical Engineering Science,* 65**,** 261-266.

[10]. HANDZLIK, J., OGONOWSKI, J., STOCH, J. & MIKOŁAJCZYK, M. 2004. Anchored and impregnated molybdena-alumina metathesis catalysts—a comparative study. *Applied Catalysis A: General,* 273**,** 99-104.

[11]. HAO, X., BARNES, S. & REGALBUTO, J. R. 2011. A fundamental study of Pt impregnation of carbon: Adsorption equilibrium and particle synthesis. *Journal of Catalysis,* 279**,** 48-65.

[12]. HU, Y. H. & RUCKENSTEIN, E. 1998. Catalyst Temperature Oscillations during Partial Oxidation of Methane. *nd. Eng. Chem. Res.,* 37**,** 2333-2335.

[13]. IVANOV, K., KRUSTEV, S. & LITCHEVA, P. 1998. methanol on sodium modified chromium molybdenum catalysts. *Journal of Alloys and Compounds,* 279**,** 132-135.

[14]. JIA, M., BAI, H., ZHAORIGETU, SHEN, Y. & LI, Y. 2008. Preparation of Au/CeO2 catalyst and its catalytic performance for HCHO oxidation. *Journal of Rare Earths,* 26**,** 528-531.

[15]. KUMAR, A., MUKASYAN, A. S. & WOLF, E. E. 2010. Impregnated layer combustion synthesis method for preparation of multicomponent catalysts for the production of hydrogen from oxidative reforming of methanol. *Applied Catalysis A: General,* 372**,** 175-183.
[16]. LAI, C. W. & SREEKANTAN, S. 2013. Incorporation of WO3 species into TiO2 nanotubes via wet impregnation and their water-splitting performance. *Electrochimica Acta,* 87**,** 294-302.
[17]. LARSSON, E. M., MILLET, J., GUSTAFSSON, S., SKOGLUNDH, M., ZHDANOV, V. P. & LANGHAMMER, C. 2012. Real Time Indirect Nanoplasmonic in Situ Spectroscopy of Catalyst Nanoparticle Sintering. *ACS Catalysis,* 2**,** 238-245.
[18]. LI, J. L., TAKEGUCHI, T. & INUI, T. 1996. Doping effect of potassium permanganate on the performance of a copper/zinc oxide/alumina catalyst for methanol formation. *Applied Catalysis A: General,* 139**,** 97-106.
[19]. LIU, W., VIDIC, R. D. & BROWN, T. D. 2000. Optimization of High Temperature Sulfur Impregnation on Activated Carbon for Permanent Sequestration of Elemental Mercury Vapors. *Environ. Sci. Technol. ,* 34**,** 483-488.
[20]. Kiennemann, A., Soares, A. P. V., Portela, M. F.(2004) *Methanol selective oxidation to formaldehyde over iron-molybdate catalysts*. Taylor & Francis. 47, 125-174.
[21]. Bowker, M., Holroyd, R., House, M., Bracey, R., Bamroongowndee, C., Carley A. and Shannon M. (2008). *The Selective Oxidation of Methanol on Iron Molybdate Catalysts*. Springer science, 48, 158-165.
[22]. Michael Bowker, Albert F. Carley, Matthew House. (2008). *Contrasting the Behaviour of MoO3 and MoO2 for the Oxidation of Methanol*. Catal Lett. 120, 34–39.
[23]. House, M.P., Shannon, M.D. and Bowker, M.(2008). *Surface Segregation in Iron Molybdate Catalysts*. Springer science,122, 210-213.
[24]. Bowker, M., Holroyd, R., Elliott, A., Morrall, P., Alouche, A., Entwistle, C. and Toerncrona, A.(2002). *The selective oxidation of methanol to formaldehyde on iron molybdate catalysts and on component oxides*. Plenum Publishing Corporation,83, 3-4.
[25]. Bowker, M., Carley, A. and House, M.(2007). *Selective oxidation of methanol on iron molybdate catalysts and the effects of surface reduction*. Journal of catalysis, 252, 88-96.
[26]. MA, X., GONG, J., YANG, X. & WANG, S. 2005. A comparative study of supported MoO3 catalysts prepared by the new “slurry” impregnation method and by the conventional method: their activity in transesterification of dimethyl oxalate and phenol. *Applied Catalysis A: General,* 280**,** 215-223.
[27]. MI, W., SU, Q., FENG, J. & DANG, Y. 2012. Effect of Preparation Conditions on the Performance of CO Preferential Methanation Catalyst*. *Physics Procedia,* 25**,** 1285-1291.
[28]. MORI, M., IWAMOTO, Y., ASAMOTO, M., ITAGAKI, Y., YAHIRO, H., SADAOKA, Y., TAKASE, S., SHIMIZU, Y., YUASA, M., SHIMANOE, K., KUSABA, H. & TERAOKA, Y. 2008. Effect of preparation routes on the catalytic activity over SmFeO3 oxide. *Catalysis Today,* 139**,** 125-129.
[29]. NISHIDA, K., LI, D., ZHAN, Y., SHISHIDO, T., OUMI, Y., SANO, T. & TAKEHIRA, K. 2009. Effective MgO surface doping of Cu/Zn/Al oxides as water–gas shift catalysts. *Applied Clay Science,* 44**,** 211-217.

[30]. PANG, Y. L. & ABDULLAH, A. Z. 2012. Effect of low Fe3+ doping on characteristics, sonocatalytic activity and reusability of TiO2 nanotubes catalysts for removal of Rhodamine B from water. *J Hazard Mater,* 235-236**,** 326-35.
[31]. RADWAN, N. R. E., FAGAL, G. A. & EL-SHOBAKY, G. A. 2001. Effects of CeO2-doping on surface and catalytic properties of CuO/Al2O3 solids. *Colloids and Surfaces A: Physicochemical and Engineering Aspects,* 178**,** 277-286.
[32]. RANE, V. H., CHAUDHARI, S. T. & CHOUDHARY, V. R. 2008. Influence of alkali metal doping on surface properties and catalytic activity/selectivity of CaO catalysts in oxidative coupling of methane. *Journal of Natural Gas Chemistry* 17**,** 313-320.
[33]. REGALBUTO, J. 2007. *Catalyst Prepparation Science and Engineering,* Boca Raton, USA, CRC press: Taylor & Francis Group.
[34]. RICHTER, M., FAIT, M. J. G., ECKELT, R., SCHREIER, E., SCHNEIDER, M., POHL, M. M. & FRICKE, R. 2007. Oxidative gas phase carbonylation of methanol to dimethyl carbonate over chloride-free Cu-impregnated zeolite Y catalysts at elevated pressure. *Applied Catalysis B: Environmental,* 73**,** 269-281.
[35]. RIDA, K., BENABBAS, A., BOUREMMAD, F., PEÑA, M. A., SASTRE, E. & MARTÍNEZ-ARIAS, A. 2007. Effect of calcination temperature on the structural characteristics and catalytic activity for propene combustion of sol–gel derived lanthanum chromite perovskite. *Applied Catalysis A: General,* 327**,** 173-179.
[36]. ROSSMEDGAARDEN, E., KNOWLES, W., KIM, T., WONG, M., ZHOU, W., KIELY, C. & WACHS, I. 2008. New insights into the nature of the acidic catalytic active sites present in ZrO2-supported tungsten oxide catalysts. *Journal of Catalysis,* 256**,** 108-125.
[37]. ROY, B., MARTINEZ, U., LOGANATHAN, K., DATYE, A. K. & LECLERC, C. A. 2012. Effect of preparation methods on the performance of Ni/Al2O3 catalysts for aqueous-phase reforming of ethanol: Part I-catalytic activity. *International Journal of Hydrogen Energy,* 37**,** 8143-8153.
[38]. SHAN, W., GUO, H., LIU, C. & WANG, X. 2012. Controllable preparation of CeO2 nanostructure materials and their catalytic activity. *Journal of Rare Earths,* 30**,** 665-669.
[39]. TABAKOVA, T., BOCCUZZI, F., MANZOLI, M., SOBCZAK, J. W., IDAKIEV, V. & ANDREEVA, D. 2004. Effect of synthesis procedure on the low-temperature WGS activity of Au/ceria catalysts. *Applied Catalysis B: Environmental,* 49**,** 73-81.
[40]. UHLRICH, J. J., SAINIO, J., LEI, Y., EDWARDS, D., DAVIES, R., BOWKER, M., SHAIKHUTDINOV, S. & FREUND, H. J. 2011. Preparation and characterization of iron–molybdate thin films. *Surface Science,* 605**,** 1550-1555.
[41]. WANG, Y., DU, W. & XU, Y. 2009. Effect of Sintering Temperature on the Photocatalytic Activities and Stabilities of Hematite and Silica-Dispersed Hematite Particles for Organic Degradation in Aqueous Suspensions. *Langmuir,* 25**,** 2895-2899.
[42]. XIAO-MENG, L., JUN, L., HUI, Z., JIAN-LIN, D. & JI-MIN, X. 2009. Structure and property of mesoporous molybdenum/carbon co-doped brookite titania *Trans. Nonferrous Met. Soc. China,* 19**,** 669-673.
[43]. XIE, Y., LI, Y. & ZHAO, X. 2007. Low-temperature preparation and visible-light-induced catalytic activity of anatase F–N-codoped TiO2. *Journal of Molecular Catalysis A: Chemical,* 277**,** 119-126.

[44]. XING, X., LIU, Z. & YANG, J. 2008. Mo and Co doped V2O5/AC catalyst-sorbents for flue gas SO2 removal and elemental sulfur production. *Fuel,* 87**,** 1705-1710.
[45]. XUE, B., LI, H., XU, J., LIU, P., ZHANG, Y. & LI, Y. 2012. A novel method to prepare shape-selective catalysts by complexation–impregnation. *Catalysis Communications,* 29**,** 153-157.
[46]. YANG, F., CHEN, M. S. & GOODMAN, D. W. 2009. Sintering of Au Particles Supported on TiO2(110) during CO Oxidation. *J. Phys. Chem. C* 113**,** 254-260.
[47]. YANG, G., TSUBAKI, N., SHAMOTO, J., YONEYAMA, Y. & ZHANG†, Y. 2010. Confinement Effect and Synergistic Function of H-ZSM-5/ Cu-ZnO-Al2O3 Capsule Catalyst for One-Step Controlled Synthesis. *AM.CHEM. SOC,* 132**,** 8129-8136.
[48]. YU, J.-P., GUAN, Y.-X., YAO, S.-J. & ZHU, Z.-Q. 2011. Preparation of Roxithromycin-Loaded Poly(l-lactic Acid) Films with Supercritical Solution Impregnation. *Industrial & Engineering Chemistry Research,* 50**,** 13813-13818.
[49]. ZAHRAN, A. A., SHAHEEN, W. M. & EL-SHOBAKY, G. A. 2005. Surface and catalytic properties of MoO3/Al2O3 system doped with Co3O4. *Materials Research Bulletin,* 40**,** 1065-1080.
[50]. ZDRAŽIL, M. 2001. Supported MoO3 catalysts- preparation by the new "slurry impregnation" method and activity in hydrodesulphurization. *Catalysis Today* 65**,** 301–306.
[51]. ZHANG, R., LIN, W., MOON, K. S. & WONG, C. P. 2010. Fast preparation of printable highly conductive polymer nanocomposites by thermal decomposition of silver carboxylate and sintering of silver nanoparticles. *ACS Appl Mater Interfaces,* 2**,** 2637-45.
[52]. ZHAO, Y., QIU, X. & BURDA, C. 2008. The Effects of Sintering on the Photocatalytic Activity of N-Doped TiO2 Nanoparticles. *Chem. Mater. ,* 20**,** 2629–2636.
[53]. OLEVSKY, E. A., WANG, X., BRUCE, E., STERN, M. B., WILDHACK, S. & ALDINGER, F. 2007. Synthesis of gold micro- and nano-wires by infiltration and thermolysis. *Scripta Materialia,* 56**,** 867-869.
[54]. ARAKI, H., FUKUOKA, A., SAKAMOTO, Y., INAGAKI, S., SUGIMOTO, N., FUKUSHIMA, Y. & ICHIKAWA, M. 2003. Template synthesis and characterization of gold nano-wires and -particles in mesoporous channels of FSM-16. *Journal of Molecular Catalysis A: Chemical,* 199**,** 95-102.